U.S. Department
of Commerce

Volume 116
Number 1
January 2018

Fishery Bulletin

Pacific Islands Fisheries
Science Center Library

Received on: 2/9/18

U.S. Department of Commerce

Wilbur L. Ross Jr.
Secretary

National Oceanic and Atmospheric Administration

Timothy Gallaudet
Deputy Administrator
of NOAA

National Marine Fisheries Service

Chris Oliver
Assistant Administrator
for Fisheries

Fishery Bulletin

Scientific Editor
Jose Castro

National Marine Fisheries Service, NOAA
263 13th Avenue South
Saint Petersburg, FL 33701

Managing Editor
Sharyn Matriotti

National Marine Fisheries Service
Scientific Publications Office
7600 Sand Point Way NE
Seattle, Washington 98115-0070

Associate Editor
Kathryn Dennis

National Marine Fisheries Service
Office of Science and Technology
1845 Wasp Blvd., Bldg. 176
Honolulu, Hawaii 96818

Editorial Committee

Richard Brodeur	National Marine Fisheries Service, Newport, Oregon
John Carlson	National Marine Fisheries Service, Panama City, Florida
Kevin Craig	National Marine Fisheries Service, Beaufort, North Carolina
John Graves	Virginia Institute of Marine Science, Gloucester Point, Virginia
Rich McBride	National Marine Fisheries Service, Woods Hole, Massachusetts
Rick Methot	National Marine Fisheries Service, Seattle, Washington
Bruce Mundy	National Marine Fisheries Service, Honolulu, Hawaii
David Sampson	Oregon State University, Newport, Oregon
Michael Simpkins	National Marine Fisheries Service, Woods Hole, Massachusetts
Dave Somerton	National Marine Fisheries Service, Seattle, Washington
Mary Yoklavich	National Marine Fisheries Service, Santa Cruz, California

***Fishery Bulletin* web site: www.fisherybulletin.noaa.gov**

The *Fishery Bulletin* (ISSN 0090-0656) is published quarterly by the Scientific Publications Office, National Marine Fisheries Service, NOAA, 7600 Sand Point Way NE, Seattle, WA 98115-0070.

Although the contents of this publication have not been copyrighted and may be reprinted entirely, reference to source is appreciated.

The Secretary of Commerce has determined that the publication of this periodical is necessary according to law for the transaction of public business of this Department. Use of funds for printing of this periodical has been approved by the Director of the Office of Management and Budget.

For Sale by the Superintendent of Documents, U.S. Government Printing Office, Washington, DC 20402. Subscription price per year: $32.00 domestic and $44.80 foreign. Cost per single issue: $19.00 domestic and $26.60 foreign. **See back for order form.**

The *Fishery Bulletin* carries original research reports on investigations in fishery science, engineering, and economics. It began as the Bulletin of the United States Fish Commission in 1881; it became the Bulletin of the Bureau of Fisheries in 1904 and the *Fishery Bulletin* of the Fish and Wildlife Service in 1941. Separates were issued as documents through volume 46; the last document was no. 1103. Beginning with volume 47 in 1931 and continuing through volume 62 in 1963, each separate appeared as a numbered bulletin. A new system began in 1963 with volume 63 in which papers are bound together in a single issue. Beginning with volume 70, number 1, January 1972, *Fishery Bulletin* became a periodical, issued quarterly. In this form, it is available by subscription from the Superintendent of Documents, U.S. Government Printing Office, Washington, DC 20402. It is also available free in limited numbers to libraries, research institutions, state and federal agencies, and in exchange for other scientific publications.

U.S. Department of Commerce
Seattle, Washington

Volume 116
Number 1
January 2018

Fishery Bulletin

Contents

Short Conribution

1–8 **Julián Olaya-Restrepo, Karim Erzini, and Mercedes González-Wangüemert**

Estimation of growth parameters for the exploited sea cucumber *Holothuria arguinensis* from South Portugal

Articles

9–20 **Emigdio Marín-Enríquez and Arturo Muhlia-Melo**

Environmental and spatial preferences of dolphinfish (*Coryphaena* spp.) in the eastern Pacific Ocean off the coast of Mexico

21–33 **David Somerton, Kenneth Weinberg, Peter Munro, Louis Rugolo, and Thomas Wilderbuer**

The effects of wave-induced vessel motion on the geometry of a bottom survey trawl and the herding of yellowfin sole (*Limanda aspera*)

34–49 **Margarita M. Rincón, Ignacio A. Catalán, Samu Mäntyniemi, Diego Macías, and Javier Ruiz**

Embedding the effect of environmental conditions on recruitment and survival of the European anchovy (*Engraulis encrasicolus*): a Bayesian model with dual-time resolution

Short contributions

50–59 **Yi Gong, Xinjun Chen, Yunkai Li, and Zhou Fang**

Geographic variations of jumbo squid (*Dosidicus gigas*) based on gladius morphology

The National Marine Fisheries Service (NMFS) does not approve, recommend, or endorse any proprietary product or proprietary material mentioned in this publication. No reference shall be made to NMFS, or to this publication furnished by NMFS, in any advertising or sales promotion which would indicate or imply that NMFS approves, recommends, or endorses any proprietary product or proprietary material mentioned herein, or which has as its purpose an intent to cause directly or indirectly the advertised product to be used or purchased because of this NMFS publication.

The NMFS Scientific Publications Office is not responsible for the contents of the articles.

60–68 **Noel Sme, Sarah Lyon, Michael Canino, Natalia Chernova, Jason O'Bryhim, Stacey Lance, Kenneth Jones, Franz Mueter, and Anthony Gharrett**

Distinction of saffron cod (*Eleginus gracilis*) from several other gadid species by using microsatellite markers

69–74 **Laura M. Lee and Jason E. Rock**

The forgotten need for spatial persistence in catch data from fixed-station surveys

75–80 **Kevin R. Piner, Hui-Hua Lee, and Lennon R. Thomas**

Bias in estimates of growth when selectivity in models includes effects of gear and availability of fish

Articles

81–92 **Joana Vasconcelos, Ana R. Vieira, Vera Sequeira, José A. González, Manfred Kaufmann, and Leonel Serrano Gordo**

Identifying populations of the blue jack mackerel (*Trachurus picturatus*) in the Northeast Atlantic by using geometric morphometrics and otolith shape analysis

93–106 **Guillermo Sanchez-Rubio, Harriet Perry, James S. Franks, and Donald R. Johnson**

Occurrence of pelagic *Sargassum* in waters of the U.S. Gulf of Mexico in response to weather-related hydrographic regimes associated with decadal and interannual variability in global climate

107–110 **Guidelines for authors**

National Marine Fisheries Service
NOAA

Fishery Bulletin
established in 1881

Spencer F. Baird
First U.S. Commissioner of Fisheries and founder of *Fishery Bulletin*

Estimation of growth parameters for the exploited sea cucumber *Holothuria arguinensis* from South Portugal

Julián Olaya-Restrepo[1,2]
Karim Erzini[1]
Mercedes González-Wangüemert (contact author)[1]

Email address for contact author: mwanguemert@ualg.pt

[1] Centro de Ciências do Mar
Universidade do Algarve
Campus de Gambelas
8005-139 Faro, Portugal

[2] Departamento de Zoologia
Setor de Ciências Biológicas
Universidade Federal do Paraná
Avenida Coronel Francisco H. dos Santos, 100
19020 Curitiba, Brazil

Abstract—Understanding how species grow is critical for choosing appropriate fisheries management strategies. Sea cucumbers shrink during periods of aestivation and have naturally flaccid bodies that make measuring growth difficult. In this study, we obtained length-frequency data on *Holothuria arguinensis*, measuring undisturbed animals in situ, because it is one of the new target species of the NE Atlantic and Southwestern Mediterranean fisheries. Growth parameters were estimated for individuals inhabiting the Ria Formosa lagoon (Portugal). Length-frequency data were collected between November 2012 and March 2014 by using a visual census augmented with random sampling in 2014. To estimate the asymptotic length (L_∞) and growth coefficient (K), 2 different growth models were fitted to the length frequency data for 1198 sea cucumbers: the nonseasonal von Bertalanffy and Hoenig seasonal von Bertalanffy models. A L_∞ of 69.9 cm and K of 0.88 were estimated by using the Hoenig function for seasonal growth. The value of 1.0 obtained for the parameter C of this function indicates reduction in growth during winter. The relatively high growth rate (K) of this species may have important implications for its survival, mainly in environments where conditions cause biological stress and oceanic disturbances but may also increase its potential as a candidate for aquaculture.

Manuscript submitted 18 January 2017.
Manuscript accepted 21 September 2017.
Fish. Bull. 116:1–8 (2018).
Online publication date: 10 October 2017.
doi: 10.7755/FB.116.1.1

The views and opinions expressed or implied in this article are those of the author (or authors) and do not necessarily reflect the position of the National Marine Fisheries Service, NOAA.

The economic value of sea cucumbers is well known and at least 66 species have been harvested in more than 70 countries (Purcell et al., 2012), but these fisheries usually follow a boom and bust pattern (Eriksson et al., 2012; Purcell et al., 2013; González-Wangüemert et al., 2014; González-Wangüemert et al., 2015). The rapid expansion of sea cucumber fisheries over the past several decades has overshadowed efforts to implement effective management, leading to overexploitation of sea cucumbers by the majority of fisheries worldwide (Purcell et al., 2013; González-Wangüemert et al., 2016). This inadequate management is primarily due to insufficient biological and ecological knowledge of target species (Lovatelli et al., 2004; Purcell, 2010). Knowledge of growth parameters not only is essential for conservation and management of a target species but also for reducing fishing pressure on wild populations. One common fisheries management measure, for example, has been the implementation of a minimum size at capture, which is species-specific and often based on size at first maturity (Bruckner, 2006; Purcell, 2010). This management measure is important because of its applicability in the field, and together with information on the time to reach maturity, can be used to implement seasonal closures, as well as be used in guidelines for rebuilding hatchery stocks.

Estimation of growth rates of sea cucumbers is difficult because of their ability to shrink (negative growth), their flaccid body, and their propensity to shed physical tags (Conand, 1983; Uthicke et al., 2004; Purcell et al., 2008). Until recently, external tagging methods have been unsuitable for estimating growth owing to biological factors such as evisceration, necrosis, skin sloughing, changes in sea cucumber behavior, and even increases in natural mortality and predation rates (Conand, 1991; Purcell et al., 2006). The use of passive inductive transponder (PIT) tags in sea cucumbers is also problematic because of the different results obtained with different sea cucumber

species. Some studies have, for example, reported poor retention of PIT tags in 2 tropical sea cucumbers, *Holothuria whitmaei* and *Actinopyga miliaris* (Purcell et al., 2008). In fact, only 8 d after release in suitable reef habitats, just one-quarter of *H. whitmaei* individuals tagged by Purcell et al. (2008) retained PIT tags and no *A. miliaris* individuals retained them. Similar results were found for the gray sea cucumber (*Holothuria grisea*), where the retention of the PIT tag was low, with 100% being lost by week 9 (Rodríguez-Barreras et al., 2016), but in the case of *Cucumaria frondosa*, results on tag retention were much improved (Gianasi et al., 2015). Implanting the tag in an oral tentacle of *C. frondosa* to reach the hydrovascular system of the aquapharyngeal bulb resulted in the best retention rates in full-size individuals: from a maximum of 92% after 30 d to 68% at the end of the experimental period (300 d). Efficacy was lower in smaller individuals (84% after 30 d and 42% after 300 d).

In a pioneer work, Ebert (1978) studied growth of the sea cucumber known as the lolly fish (*Holothuria atra*) by tagging the plates of their calcareous rings with tetracycline. The growth of the plates was used to estimate growth parameters for the Brody–Bertalanffy growth equation. Subsequently, other methods based on weight and size data have been undertaken to study growth in both wild and cultured sea cucumber populations. For example, Battaglene et al. (1999) calculated sea cucumber length from wet weight measurements, using a polynomial regression. Measurements of specific growth rates and relative weight increase have also been obtained for sea cucumbers (Yang et al., 2005; Dong et al., 2008), while other studies have adapted different growth models like Francis's model and the von Bertalanffy model to calculate weight and length data (Conand, 1988; Herrero-Pérezrul et al., 1999; de la Fuente-Betancourt et al., 2001; Uthicke et al., 2004; Sulardiono and Prayitno, 2012). Interestingly, some consistent differences in growth rates have been observed between tropical species of sea cucumber, such as *Stichopus vastus*, the Florida sea cucumber (*Holothuria floridana*), the lolly fish, and the mammy fish (*Actinopyga nobilis*), exhibite slow growth rates (Ebert, 1978; de la Fuente-Betancourt et al., 2001; Uthicke et al., 2004; Sulardiono and Prayitno, 2012) and some temperate species, such as *Australostichopus mollis* and *C. frondosa,* that grow faster than the previously mentioned tropical species but also show some seasonal variation (Hamel and Mercier, 1996; Slater and Jeffs, 2010).

Holothuria (*Rowethuria*) *arguinensis* has a restricted distribution in the northeast Atlantic Ocean, from Portugal to the Canary Islands and Mauritania in northwestern Africa, although recently, it was recorded in the Southwestern Mediterranean Sea (Alicante, Spain) and in Algerian waters, implying that it is colonizing the Mediterranean Sea (González-Wangüemert and Borrero-Pérez, 2012; Mezali and Thandar, 2014). *Holothuria arguinensis* is one of the new target species of NE Atlantic and Southwestern Mediterranean fisheries, where catches driven by its high commercial value, are increasing (González-Wangüemert and Godino, 2016; González-Wangüemert et al., 2016; Roggatz et al., 2016). Illegal harvest of this species in Portugal and Spain, is a threat to the sustainability of the fishery, especially in the Ria Formosa lagoon, at Portimão and Albufeira (South Portugal), and at the coast of Cadiz (South Spain) (González-Wangüemert and Godino, 2016). Also, this species is targeted for aquaculture development for both commercial production and restocking (Domínguez-Godino et al., 2015).

The species has been linked to the presence of seaweed and seagrass meadows of *Cymodocea nodosa* and *Zostera noltii*, with reported densities up to 563 individuals/ha (Faro, South Portugal) (González-Wangüemert et al., 2013; Siegenthaler et al., 2015). The home range of *H. arguinensis* individuals has been estimated to average 35 m^2, and individual movements are close to 10 m/d (Siegenthaler et al., 2015).

An average size of 255 mm was reported for this species in Gran Canaria (Canary Islands, Spain) and a maximum size of 370 mm (Navarro et al., 2013). In Ria Formosa (South Portugal), González-Wangüemert et al. (2013) found individuals ranging between 70 to 360 mm, and having an average size of 221 mm and a multimodal size-frequency distribution. Three years later, González-Wangüemert et al. (2016), considering *H. arguinensis* populations throughout the geographical range of this species, estimated a positive allometric growth. In that study, individuals ranged from 90 to 360 mm in length and had significant differences in mean size between sampled areas, such that individuals from Sagres (SW Portugal) were significantly longer than those from Ria Formosa.

Our aim was to obtain growth parameters from length-frequency data of the species *H. arguinensis* inhabiting the Ria Formosa (South Portugal), by fitting different growth models: the nonseasonal von Bertalanffy and the Hoenig seasonal von Bertalanffy models.

Material and methods

Study area

Ria Formosa is a coastal lagoon located in the Algarve region (South Portugal) (Fig. 1). Its area is approximately 105 km^2, half of which is intertidal and covered by sand, mud and marshes (Duarte et al., 2007). It is composed of a system of barrier islands with small ponds, inlet deltas, and barrier platforms (Pacheco et al., 2010). The water temperature varies between 12°C and 13°C in winter and 27°C and 28°C in summer. Variations in salinity are small due to the low freshwater input into the lagoon, ranging between 35.5 and 36.9 throughout the year (Ribeiro et al., 2008), with the exception of surface waters for brief periods after heavy winter rainfall (Ribeiro et al., 2008; Rodrigues et al., 2015).

Ria Formosa, was declared a Natural Park in 1987 (Decreto-Lei No. 373/87, available from website) and it

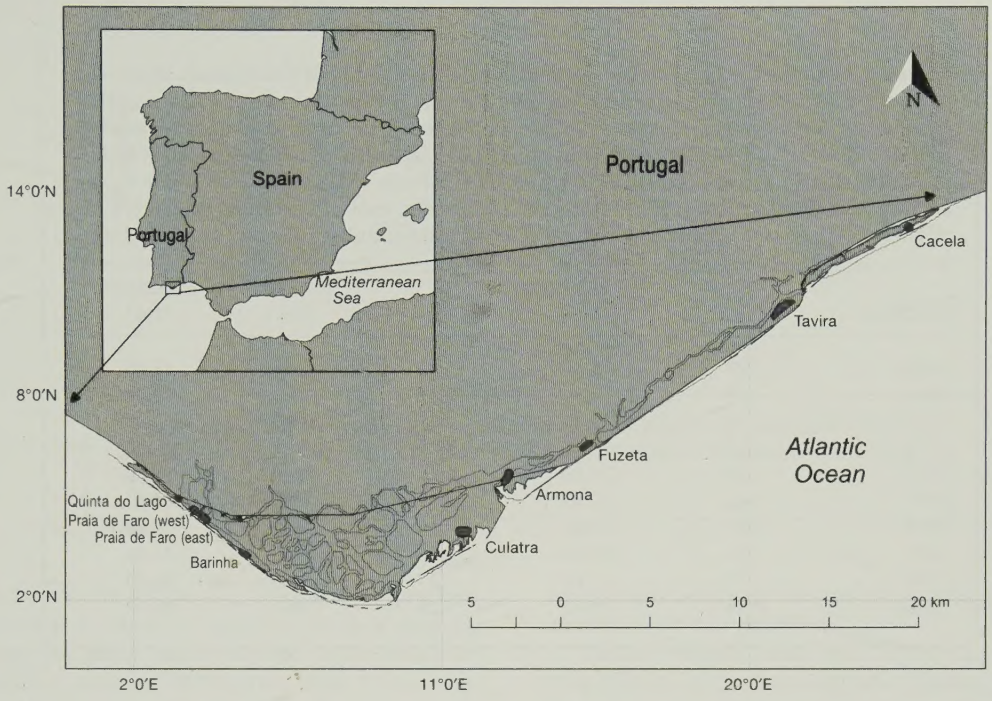

Figure 1

Map of the study area showing the 9 locations, indicated by areas shaded in black, where *Holothuria arguinensis* were sampled between November 2012 and March 2014 inside the Ria Formosa, a coastal lagoon in southern Portugal. Sampling was conducted by visual census at 3 sites: Praia de Faro to the west of the main bridge (PFW), Praia de Faro to the east of the main bridge (PFE), and Fuzeta (FUZ). Random sampling was conducted at 6 sites: Quinta do Lago (QTL), Barinha (BAR), CUL (Culatra), Armona (ARM), Tavira (TAV), and Cacela (CAC).

plays an important role in the local economy by supporting commercial fisheries, bait harvesting, tourism, aquaculture, port activities, and providing a recreational fishing area near human settlements. The lagoon is classified as coastal waters within the scope of the European Water Framework Directive (EC/2000/60, available from website).

Data collection

The data were collected by 2 methods: visual census and random sampling. During the volunteer program linked with the research project "Sea cucumbers: the new resources for a hungry fishery" (CUMFISH) conducted by the Centro de Ciências do Mar, Universidade do Algarve, monthly visual censuses of sea cucumbers were carried out in the Ria Formosa lagoon during low tides from November 2012 to March 2014 in 3 locations: 2 sites (west and east) at Praia do Faro and 1 site at Fuzeta (Fig. 1). In each locality, 6 transects (each 100×2 m) were surveyed. Three transects were surveyed by walking along the coast "outside" the water and 3 transects were surveyed by snorkeling "inside" sea water and by following the edge of the low tide level. All sea cucumber individuals were identified to species and their total length registered to the nearest 0.1 cm. Measurements of length were recorded in situ without disturbing the animals, which were not touched or removed from the water. More details of the methods can be found in González-Wangüemert et al. (2013).The random sampling was conducted in 6 different locations inside the Ria Formosa—Quinta do Lago, Barinha, Armona, Tavira, Culatra, and Cacela (Fig. 1)—during February and March 2014. Presence (in absolute geographical coordinates [datum: World Geodetic System 1984]) and total length (in centimeters) of all sea cucumbers were recorded by 2 researchers walking along the intertidal zone during low tide and following a route with registered geographical coordinates. Again, sea cucumbers were measured in situ. In this way, it was possible to sample over a wide area and later to calculate the area sampled. The sampling was undertaken during tides lower than 0.7 m, when the seagrass meadows were always exposed in the sampling locations.

Data analysis

All length data obtained from visual census and random sampling were pooled together and grouped in 4-cm classes. Two different growth models—the non-

Table 1

Number and mean lengths (with standard deviations [SD]) for individuals of the sea cucumber *Holothuria arguinensis* sampled by visual census and random sampling inside the Ria Formosa, a coastal lagoon in southern Portugal, between November 2012 and March 2014. The 9 localities sampled (see Fig. 1) were Armona (ARM), Barinha (BAR), Cacela (CAC), Culatra (CUL), Fuzeta (FUZ), Praia de Faro to the west of the main bridge (PFW), Praia de Faro to the east of the main bridge (PFE), Quinta do Lago (QTL), and Tavira (TAV). N signifies number of sampled individuals.

Locality	N	Mean length (cm)	SD	Minimum (cm)	Maximum (cm)
ARM	222	26.51	6.42	10.00	45.00
BAR	78	17.54	3.31	12.00	23.00
CAC	1	23.00	-	23.00	23.00
CUL	12	23.42	5.47	13.00	34.00
FUZ	78	23.38	6.29	10.00	38.00
PFE	433	22.46	6.27	4.00	35.00
PFW	332	21.63	5.18	10.00	48.00
QTL	25	17.48	4.78	15.00	25.00
TAV	17	17.18	6.27	9.00	30.00
Total	1198	23.10	6.28	4.00	48.00

seasonal von Bertalanffy growth model (Pauly, 1987) and the Hoenig seasonal von Bertalanffy model (Hoenig and Hanumara, 1982)—were fitted to the length-frequency data by using the electronic length frequency analysis (ELEFAN) system implemented in the length frequency distribution analysis (LFDA) software, vers. 5.0 (Kirkwood[1]). The best estimators of asymptotic length (L_∞) and the growth coefficient (K) were selected on the basis of maximum value of the score function and the best fit of the curve to the observed data (Kirkwood[1]).

The ELEFAN method is based on fitting the von Bertalanffy model to length- frequency data (Pauly, 1987). It works by restructuring the length-frequency data, emphasizing the peaks and troughs in the data set, and calculating score functions for growth curves generated for different combinations of von Bertalanffy growth parameters. Every time the growth curves passed through the peaks in the restructured data it accumulates points, resulting in a score function for each curve. The Hoenig function takes into account seasonality in growth, including a parameter that fits the beginning of the sinusoidal function (Ts), and the parameter C that expresses the relative amplitude of the seasonal oscillation in growth (Pauly et al., 1992).

Results

Length data of 1198 individuals of *H. arguinensis* from 9 different localities inside the Ria Formosa were used for length-frequency analysis (Table 1).

For the nonseasonal growth model, estimates of K=1.99 and L_∞=40 cm were obtained with a score function of 0.460. However, the growth curve does not adequately fit the data (Suppl. Fig.) (online only).

Considering these results, we then fitted the Hoenig model for seasonal growth. This provided estimates of K=0.88 and L_∞= 69.9 cm, and a score function of 0.565. The average length was 23.1 cm, sizes ranged from 4 to 48 cm, and approximately 98% of the individuals ranged from 11 to 35 cm (Fig. 2). The growth curve showed a higher score function than that of the nonseasonal growth model (Fig. 3). The value of C=1 indicates the existence of a period of no growth during the year for the species.

Discussion

The L_∞ and K for *H. arguinensis* were estimated by using 2 different functions. The first function, the nonseasonal von Bertalanffy model, did not provide realistic results. However, when seasonality was included (with the Hoenig model), more reliable values were obtained, which confirmed the seasonality in the growth of *H. arguinensis*. The observed growth rate (K=0.88) indicates that this species achieves asymptotic size quickly, even faster than tropical commercially valuable holothurians, such as the lolly fish (K=0.11), *Thelenota ananas* (K=0.20), *Stichopus chloronotus* (K=0.45), or *Isostichopus fuscus* (K=0.18) (Ebert, 1978; Conand, 1988; Herrero-Pérezrul et al., 1999). Herrero-Pérezrul et al. (1999) discussed the difficulties of comparing growth parameters derived from von Bertalanffy-like models of different sea cucumbers species because not all model assumptions are fulfilled. The 3 general assumptions

[1] Kirkwood, G. 2001. Enhancement and support of computer aids for fisheries management. Final technical report, 65 p. MRAG, Ltd., London. [Available from website.]

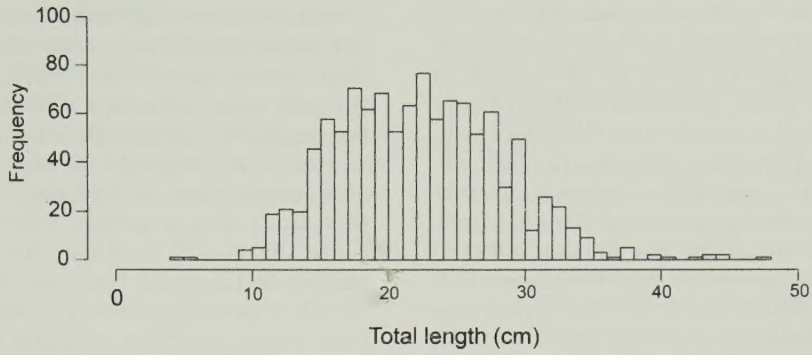

Figure 2

Length-frequency distribution of *Holothuria arguinensis* sampled inside the Ria Formosa lagoon in southern Portugal between November 2012 and March 2014.

for these models are the following: 1) species reproduce and recruit once per year; 2) species reach a specific size; and 3) species grow isometrically. Most commercial sea cucumber species fulfill the first 2 assumptions, but usually they do not exhibit isometric growth. In the case of *H. arguinensis*, allometric growth has also been reported (González-Wangüemert et al., 2016). For this reason, comparisons of growth rates from different commercial species must be regarded with caution; most of them do not show the isometric growth assumed by the model.

Faster growth rates may have important and positive effects on the survival of a species, primarily under high stress conditions and in disturbed environments (Morgan, 2012). Achieving a larger size rapidly could be an adaptive advantage: larger sea cucumbers would be capable of moving and stabilizing themselves in more mobile sediments, such as sandy substrates, and

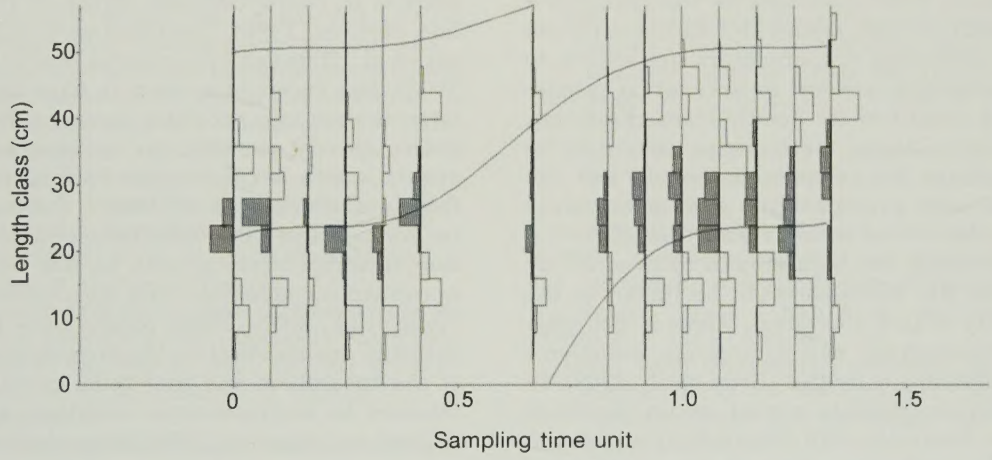

Figure 3

Growth curve from a von Bertalanffy model with a Hoening function for seasonal growth fitted, by using electronic length-frequency analysis (ELEFAN), to length-frequency data of *Holothuria arguinensis* sampled inside the Ria Formosa lagoon in southern Portugal between November 2012 and March 2014. The gray bars indicate running average frequencies (Pauly, 1987). Results for parameters of the Hoenig seasonal von Bertalanffy growth model were 0.88 for the growth coefficient (K), −0.30 for the time when the average length was zero (T_0), 1.00 for parameter C, which expresses the relative amplitude of the seasonal oscillation in growth, and 70.00 for the asymptotic length (L_∞). Sampling time units are the relative time units (months) during data collection. A time unit of 0 represents the month in which sampling started (November 2012), and a value of 1 corresponds with the 12th month of sampling.

they would also be more likely to escape predation (Wiedemeyer, 1993). In the Salomon Islands, the growth rate, as well as the daily distance covered by the sand fish (*Holothuria scabra*), was found to be related to substrate type, and the sandy areas were occupied only when individuals reached a specific size (Mercier et al., 2000). Inside the Ria Formosa, individuals of *H. arguinensis* move through a patchy environment; despite the relatively large percent coverage of *Z. noltii* (46% of the intertidal area) within the Ria Formosa, distribution of this seagrass species is highly fragmented, dominated by small patches from 0 to 5 ha (Guimarães et al., 2012). These seagrass patches are separated by sand, mud, and marshes that sea cucumbers must pass through when searching for more suitable feeding areas, or probably for areas where they can avoid direct sunlight and desiccation (González-Wangüemert et al., 2013). However, the results obtained by Siegenthaler et al. (2015) in a small-scale capture-recapture experiment with *H. arguinensis* in the Ria Formosa, revealed that mean length was not a significant factor in determining the distribution of this species, and its movement was independent of habitat type (sand and seagrass). In fact, movement of *H. arguinensis* was better explained by the need of specimens for shelter against UV-radiation, when individuals remain outside water during low tides (Siegenthaler et al., 2015). Further studies should be considered to evaluate whether the same pattern exists at larger spatial and temporal scales than those considered by Siegenthaler et al. (2015), and also including a greater size range of animals for the experiment.

A faster growth rate could also be the result of a decrease in predation rate, mainly during the early life history stages. Although few predators are known to feed on sea cucumbers, several antipredation mechanisms has been described for holothurians (Francour, 1997) and some of these mechanisms seems to be linked to animal size. For example, in the lolly fish, the strength of the toxin present on its skin significantly increases with the size of an individual (Castillo[2]).

On the other hand, the high growth rates of *H. arguinensis* in the Ria Formosa could be linked to the high productivity of this ecosystem, where a rich phytobenthos, of macrophytic and microphytic organisms (seagrass and diatoms) is located (Brito et al., 2009). In some mesoscosm experiments carried out on the Great Barrier Reef in Australia with lolly fish, it was found that higher food availability per individual increased growth rate (Lee et al., 2008). Therefore, further studies of individuals from areas outside Ria Formosa, and with varying levels of natural productivity, should be carried out to confirm the growth rates we have reported here.

The value obtained for the parameter C (Hoenig model) indicates a seasonal cycle of growth for *H. arguinensis*, which may cease at least during part of the year. According to Pauly (1987), $Ts + 0.5$ is the time of the year when growth is slower, and where Ts denotes the beginning of the sinusoidal growth oscillation. This winter point, suggests a reduction in the growth rate of *H. arguinensis* at 0.19 time units (the time unit for this study was a month, where a 0 time unit represents the month in which the sampling started [November 2012] and 1 time unit corresponds to the 12th month of sampling) from the beginning of the sampling year, which coincides with the months of January and February, when waters may have brackish conditions and the lowest temperatures occur in Ria Formosa (Newton and Mudge, 2003). Feeding experiments on *H. arguinensis*, in laboratory tanks, could confirm this reduction in growth rate during winter months because under rearing conditions, the species is stationary and decreases feeding rate when water temperature is lower than 14°C (Domínguez-Godino and González-Wangüemert[3]). These low temperatures are common during winter months in Ria Formosa (Ramos et al., 2013). Another temperate sea cucumber species inhabiting the Aegean Sea, *Holothuria tubulosa*, exhibits similar behavior, with a negative specific growth rate at 15°C. At this temperature, individuals enter a hibernation phase and have a corresponding drop in metabolic rate, which directly affects their feeding activity (Günay et al., 2015).

This pattern of a complete shutdown in growth during winter is also found in other temperate species such as *A. mollis* (Morgan, 2012), *C. frondosa* (Hamel and Mercier, 1996), *Parastichopus californicus* (Paltzat et al., 2008) and *Holothuria theeli* (Sonnenholzner, 2003). Sea cucumbers, seem to have failed to adapt to large fluctuations in water temperature (Dong et al., 2008), clearly showing an optimal temperature for growth which is close to the optimal temperature for food intake (Yang et al., 2005). Conversely, high water temperatures can also induce aestivation in some sea cucumber species, such as has been observed in *Apostichopus japonicus* and *Australostichopus mollis* (Yang et al., 2005). These results show that water temperature has an effect on the physiological performance of sea cucumbers and that their growth is largely influenced by environmental conditions and food supply (Hamel and Mercier, 1996; Sonnenholzner, 2003).

Acknowledgments

This research was supported by the CUMFISH (PTDC/MAR/119363/2010) and "Sea cucumber as new marine resource: potential for aquaculture" (CUMARSUR) (PTDC/MAR-BIO/5948/2014) projects funded by Funda-

[2] Castillo, J. A. 2006. Predator defense mechanisms in shallow water sea cucumbers (Holothuroidea). UCB Moorea Class: Biol. Geomorphol. Trop. Isl., Univ. Calif. Berkeley, Berkeley, CA. [Available from website.]

[3] Domínguez-Godino, J., and M. González-Wangüemert. In review. Centro de Ciências do Mar, Universidade do Algarve, Campus de Gambelas, 8005-139 Faro, Portugal.

ção para a Ciência e a Tecnologia (FCT, Portugal), and was performed as a dissertation for the International Master in Marine Biodiversity and Conservation. Authors thank the field support of all volunteers implementing and carrying out the visual censuses. The first author was supported by Fundación para el Futuro de Colombia (Colfuturo) and M. González-Wangüemert by FCT Investigator Programme-Career Development (IF/00998/2014).

Literature cited

Battaglene, S. C., J. E. Seymour, and C. Ramofafia.
1999. Survival and growth of cultured juvenile sea cucumbers, *Holothuria scabra*. Aquaculture 178:293–322.

Brito, A., A. Newton, P. Tett, and T. F. Fernandes.
2009. Temporal and spatial variability of microphytobenthos in a shallow lagoon: Ria Formosa (Portugal). Est. Coast. Shelf Sci. 83:67–76.

Bruckner, A. W. (ed.).
2006. Proceedings of the CITES workshop on the conservation of sea cucumbers in the families Holothuriidae and Stichopodidae. NOAA Tech. Memo. NMFS-OPR-34, 244 p.

Conand, C.
1983. Methods of studying growth in holothurians (beche-de-mer), and preliminary results from a beche-de-mer tagging experiment in New Caledonia. SPC Fish. Newsl. 26:31–38.
1988. Comparison between estimations of growth and mortality of two stichopodid holothurians: *Thelenota ananas* and *Stichopus chloronotus* (Echinodermata: Holothuroidea). *In* Proceedings of the 6th International Coral Reef Symposium, vol. 2; Townsville, Australia, 8–12 August (J. H. Choat and D. Barnes, eds.), p. 661–665. 6th Int. Coral Reef Symp. Exec. Comm., Townsville, Australia.
1991. Long-term movements and mortality of some tropical sea-cucumbers monitored by tagging and recapture. *In* Biology of Echinodermata: Proceedings of the 7th International Echinoderm Conference; Atami, Japan, 9–14 September 1990 (T. Yanagisawa I. Yasumasu, C. Oguro, N. Suzuki, and T. Motokawa, eds.), p. 169–175.. A.A. Balkema Publishers, Rotterdam, Netherlands.

de la Fuente-Betancourt, M. G., A. de Jesús-Navarrete, E. Sosa-Cordero, and M. D. Herrero-Perezrul.
2001. Assessment of the sea cucumber (Echinodermata: Holothuroidea) as potential fishery resource in Banco Chinchorro, Quintana roo, Mexico. Bull. Mar. Sci. 68:59–67.

Domínguez-Godino, J. A., M. J. Slater, C. Hannon, and M. González-Wangüermert.
2015. A new species for sea cucumber ranching and aquaculture: breeding and rearing of *Holothuria arguinensis*. Aquaculture 438:122–128.

Dong, Y., S. Dong, and T. Ji.
2008. Effect of different thermal regimes on growth and physiological performance of the sea cucumber *Apostichopus japonicus* Selenka. Aquaculture 275:329–334.

Duarte, P., B. Azevedo, C., Ribeiro, A., Pereira, M., Falcão, D., Serpa R. Bandeira, and J. Reia.
2007. Management oriented mathematical modelling of Ria Formosa (South Portugal). Transitional Waters Monogr. 1:13–51.

Ebert, T. A.
1978. Growth and size of the tropical sea cucumber *Holothuria (Halodeima) atra* Jager at Enewetak Atoll, Marshall Islands. Pac. Sci. 32:183–191.

Eriksson, H., M. de la Torre Castro, and P. Olsson.
2012. Mobility, expansion and management of a multi-species scuba diving fishery in East Africa. PLoS ONE 7(4): e35504.

Francour, P.
1997. Predation on holothurians: a literature review. Invertebr. Biol. 116:52–60.

Gianasi, B. L., K. Verkaik, J.-F. Hamel, and A. Mercier.
2015. Novel use of PIT tags in sea cucumbers: promising results with the commercial species *Cucumaria frondosa*. PLoS ONE 10(5):e0127884.

González-Wangüemert, M., and G. Borrero-Pérez.
2012. A new record of *Holothuria arguinensis* colonizing the Mediterranean Sea. Mar. Biodivers. Rec. 5:e105.

González-Wangüemert, M., and J. A. D. Godino.
2016. Sea cucumbers as new marine resource in Europe. Front. Mar. Sci. Conf. Abstr.: IMMR | International Meeting on Marine Research 2016.

González-Wangüemert, M., T. Braga, M. Silva, S. Valente, F. Rodriguez, and E. Serrao.
2013. Volunteer programme assesses the *Holothuria arguinensis* populations in Ria Formosa (southern Portugal). SPC Beche-de-mer Inf. Bull. 33:44–48.

González-Wangüemert, M., M. Aydin, and C. Chantal.
2014. Assessment of sea cucumber populations from the Aegean Sea (Turkey): first insights to sustainable management of new fisheries. Ocean Coast. Manage. 92:87–94.

González-Wangüemert, M., S. Valente, and M. Aydin.
2015. Effects of fishery protection on biometry and genetic structure of two target sea cucumber species from the Mediterranean Sea. Hydrobiologia 743:65–74.

González-Wangüemert, M., S. Valente, F. Henriques, J. A. Domínguez-Godino, and E. A. Serrão.
2016. Setting preliminary biometric baselines for new target sea cucumbers species of the NE Atlantic and Mediterranean fisheries. Fish. Res. 179:57–66.

Guimarães, M. H. M. E., A. H. Cunha, R. L. Nzinga, and J. F. Marques.
2012. The distribution of seagrass (*Zostera noltii*) in the Ria Formosa lagoon system and the implications of clam farming on its conservation. J. Nat. Conserv. 20:30–40.

Günay, D., D. Emiroğlu, T. Tolon, O. Özden, and H. Saygi.
2015. Growth and survival rate of juvenile sea cucumbers (*Holothuria tubulosa*, Gmelin, 1788) at various temperatures. Turkish J. Fish. Aquat. Sci. 15:533–541.

Hamel, J.-F. and A. Mercier.
1996. Early development, settlement, growth, and spatial distribution of the sea cucumber *Cucumaria frondosa* (Echinodermata: Holothuroidea). Can. J. Fish. Aquat. Sci. 53:253–271.

Herrero-Pérezrul, M. D., H. Reyes Bonilla, F. García-domínguez, and C. Cintra-Buenrostro.
1999. Reproduction and growth of *Isostichopus fuscus* (Echinodermata:Holothuroidea) in the southern Gulf of California, México. Mar. Biol. 135:521–532.

Hoenig, J. M., and R. C. Hanumara.
1982. A statistical study of a seasonal growth model for fishes, 91 p. Tech. Rep., Dep. Comp. Sci. Stat., Univ. Rhode Isl., Narragansett, RI.

Lee, J., M. Byrne, and S. Uthicke.
2008. The influence of population density on fission and growth of *Holothuria atra* in natural mesocosms. J. Exp. Mar. Biol. Ecol. 365:126–135.

Lovatelli, A., C. Conand, S. Purcell, S. Uthicke, J.-F. Hamel, and A. Mercier (eds.).
2004. Advances in sea cucumber aquaculture and management. FAO Fish. Tech. Pap. 463, 425 p. FAO, Rome.

Mercier, A., S. C. Battaglene, and J.-F. Hamel.
2000. Periodic movement, recruitment and size-related distribution of the sea cucumber *Holothuria scabra* in Solomon Islands. Hydrobiologia 440:81–100.

Mezali, K., and A. S. Thandar.
2014. First record of *Holothuria (Roweothuria) arguinensis* (Echinodermata: Holothuroidea: Aspidochirotida: Holothuriidae) from the Algerian coastal waters. Mar. Biodivers. Rec. 7:e40.

Morgan, A. D.
2012. Use of a growth model to estimate size at age in the temperate sea cucumber *Australostichopus mollis*. SPC Beche-de-mer Inf. Bull. 32:24–32.

Navarro, P. G., S. García-Sanz, and F. Tuya.
2013. Patrones de abundancia y talla de *Holothuria sanctori*, *Holothuria mammata* y *Holothuria arguinensis* (Echinodermata: Holoturoidea) en la isla de Gran Canaria, Atlántico oriental. Rev. Biol. Mar. Oceanogr. 48:273–284.

Newton, A., and S. M. Mudge.
2003. Temperature and salinity regimes in a shallow, mesotidal lagoon, the Ria Formosa, Portugal. Est. Coast. Shelf Sci. 57:73–85.

Pacheco, A., Ó. Ferreira, J. J. Williams, E. Garel, A. Vila-Concejo, and J. A. Dias.
2010. Hydrodynamics and equilibrium of a multiple-inlet system. Mar. Geol. 274:32–42.

Paltzat, D. L., C. M. Pearce, P. A. Barnes, and R. S. McKinley.
2008. Growth and production of California sea cucumbers (*Parastichopus californicus* Stimpson) co-cultured with suspended Pacific oysters (*Crassostrea gigas* Thunberg). Aquaculture 275:124–137.

Pauly, D.
1987. A review of the ELEFAN system for analysis of length-frequency data in fish and aquatic invertebrates. *In* Length-based methods in fisheries research. ICLARM Conf. Proc. 13 (D. Pauly and G. R. Morgan, eds.), p. 7–34. Int. Cent. Living Aquat. Resour. Manage., Manila, Philippines, and Inst. Sci. Res., Safat, Kuwait.

Pauly, D., M. Soriano-Bartz, J. Moreau, and A. Jarre-Teichmann.
1992. A new model accounting for seasonal cessation of growth in fishes. Aust. J. Mar. Freshw. Res. 43:1151–1156.

Purcell, S. W.
2010. Managing sea cucumber fisheries with an ecosystem approach. FAO Fish. Aquacult. Tech. Pap. 520, 157 p. FAO, Rome.

Purcell, S. W., B. F. Blockmans, and W. J. Nash.
2006. Efficacy of chemical markers and physical tags for large-scale release of an exploited holothurian. J. Exp. Mar. Biol. Ecol. 334:283–293.

Purcell, S. W., N. S. Agudo, and H. Gossuin.
2008. Poor retention of passive induced transponder (PIT) tags for mark-recapture studies on tropical sea cucumbers. SPC Beche-de-mer Inf. Bull. 28:53–55.

Purcell, S. W., Y. Samyn, and C. Conand.
2012. Commercially important sea cucumbers of the world. FAO Species Catalogue for Fishery Purposes 6, 150 p. FAO, Rome.

Purcell, S. W., A. Mercier, C. Conand, J.-F. Hamel, M. V. Toral-Granda, A. Lovatelli, and S. Uthicke.
2013. Sea cucumber fisheries: global analysis of stocks, management measures and drivers of overfishing. Fish Fish. 14:34–59.

Ramos, J. A., P. Pedro, A. Matos, and V. H. Paiva.
2013. Relation between climatic factors, diet and reproductive parameters of Little Terns over a decade. Acta Oecol. 53:56–62.

Ribeiro, J., C. C. Monteiro, P. Monteiro, L. Bentes, R. Coelho, J. M. S. Gonçalves, P. G. Lino, and K. Erzini.
2008. Long-term changes in fish communities of the Ria Formosa coastal lagoon (southern Portugal) based on two studies made 20 years apart. Est. Coast. Shelf Sci. 76:57–68.

Rodrigues, F., S. Valente, and M. González-Wangüemert.
2015. Genetic diversity across geographical scales in marine coastal ecosystems: *Holothuria arguinensis* a model species. J. Exp. Mar. Biol. Ecol. 463:158–167.

Rodríguez-Barreras, R., J. López-Morell, and A. M. Sabat.
2016. Effectiveness of two tagging devices in the sea cucumber *Holothuria* (*Halodeima*) *grisea*. Mar. Freshw. Res. 68:563–567.

Roggatz, C. C., M. González-Wangüemert, H. Pereira, M. J. Rodrigues, M. M. da Silva, L. Barreira, J. Varela, and L. Custódio.
2016. First report of the nutritional profile and antioxidant potential of *Holothuria arguinensis*, a new resource for aquaculture in Europe. Nat. Prod. Res. J. 30:2034–2040.

Siegenthaler, A., F. Cánovas, and M. González-Wangüemert.
2015. Spatial distribution patterns and movements of *Holothuria arguinensis* in the Ria Formosa (Portugal). J. Sea Res. 102:33–40.

Slater, M. J., and A. G. Jeffs.
2010. Do benthic sediment characteristics explain the distribution of juveniles of the deposit-feeding sea cucumber *Australostichopus mollis*? J. Sea Res. 64:241–249.

Sonnenholzner, J.
2003. Seasonal variation in the food composition of *Holothuria theeli* (Holothuroidea: Aspidochirotida) with observations on density and distribution patterns at the central coast of Ecuador. Bull. Mar. Sci. 73:527–543.

Sulardiono, B., S. B. Prayitno, and I. B. Hendrarto.
2012. The growth analysis of *Stichopus vastus* (Echinodermata: Stichopodidae) in Karimunjawa waters. J. Coast. Dev. 15:315–323.

Uthicke, S., D. Welch, and J. A. H. Benzie.
2004. Slow growth and lack of recovery in overfished holothurians on the Great Barrier Reef: evidence from DNA fingerprints and repeated large-scale surveys. Conserv. Biol. 18:1395–1404.

Wiedemeyer, W. L.
1993. Feeding behavior of two tropical Holothurians *Holothuria (Metriatyla) scabra* (Jager 1833) and *H. (Halodeima) atra* (Jager 1833), from Okinawa, Japan. *In* Proceedings of the 7th International Coral Reef Symposium, vol. 2; Guam, 22–27 June 1992 (R. H. Richmond, ed.), p. 853–860. Univ. Guam Press, Mangilao, Guam.

Yang, H., X. Yuan, Y. Zhou, Y. Mao, T. Zhang, and Y. Liu.
2005. Effects of body size and water temperature on food consumption and growth in the sea cucumber *Apostichopus japonicus* (Selenka) with special reference to aestivation. Aquacult. Res. 36:1085–1092.

National Marine
Fisheries Service
NOAA

Fishery Bulletin
established in 1881

Spencer F. Baird
First U.S. Commissioner
of Fisheries and founder
of *Fishery Bulletin*

Environmental and spatial preferences of dolphinfish (*Coryphaena* spp.) in the eastern Pacific Ocean off the coast of Mexico

Emigdio Marín-Enríquez
Arturo Muhlia-Melo (contact author)

Email address for contact author: amuhlia04@cibnor.mx

Centro de Investigaciones Biológicas del Noroeste, Sociedad Civil
Avenida Instituto Politécnico Nacional 195
Colonia Playa Palo de Santa Rita
23096 La Paz, Baja California Sur, Mexico

Abstract—The main objective for this study was to provide information on the relationship between dolphinfish (*Coryphaena* spp.) catches and the environmental conditions, which could help to explain dolphinfish movements in the eastern tropical Pacific Ocean off the coast of Mexico—a topic that is still under debate. We analyzed a 10-year (2004–2013) database of estimated incidental catch from the Inter-American Tropical Tuna Commission, reported by observers on board tuna purse-seine ships. Significant seasonal and interannual differences were found in the incidental catch. No segregation due to size was apparent. Two areas of high catch were present in the study zone: one near the Baja California Peninsula that is especially productive during summer, and a second in an oceanic area (~15°N, 120°W), which is present all year long but becomes more important during May–June. Using satellite images, we found that the 2 species of dolphinfish preferred warm waters (24–28°C) with low concentrations of chlorophyll-*a* (<0.02 mg/m^3), and mainly positive values of sea-surface height, all of which suggested that dolphinfish spp. associate with oceanographic features, such as anticyclonic eddies. There was a seasonal SE–NW–NE movement of high incidental catch across survey quadrants (1°×1°), movement that is closely related to the latitudinal displacement of the 25°C isotherm.

Manuscript submitted 25 January 2017.
Manuscript accepted 18 October 2017.
Fish. Bull. 116:9–20 (2018).
Online publication date: 7 November 2017.
doi: 10.7755/FB.116.1.2

The views and opinions expressed or implied in this article are those of the author (or authors) and do not necessarily reflect the position of the National Marine Fisheries Service, NOAA.

Fish commonly known as dolphinfish are members of the family Coryphaenidae, which represents only one genus, *Coryphaena*, but 2 species, the common dolphinfish (*Coryphaena hippurus*) and the pompano dolphinfish (*C. equiselis*) (Gibbs and Collette, 1959).

Dolphinfish, or both species of dolphinfish (hereafter "dolphinfish"), inhabit the tropical and subtropical waters of the world and can be found from 40°N to 40°S (Palko et al., 1982); they are fast-swimming, fast-growing voracious predators, capable of making considerable migrations (Alejo-Plata et al., 2011) and of passing through different fishery management zones within short periods of time (Farrell, 2009). Their distribution is limited by the 20°C isotherm (Palko et al., 1982), and seasonal and interannual changes in sea-surface temperature (SST) influence their local catch rate and abundance (Kraul, 1999; Norton, 1999; Zúñiga-Flores et al., 2008); additionally, their distribution seems to be influenced by prey availability and metabolic needs for sustaining their rapid growth (Schwenke, 2004). These fish are opportunistic predators and feed on a wide spectrum of prey, which includes several species of bony fish, cephalopods, and crustaceans (Aguilar-Palomino et al., 1998; Massutí et al., 1998; Oxenford, 1999; Sakamoto and Kojima; 1999; Tripp-Valdez et al., 2010).

Despite dolphinfish having been reserved for the recreational fishery within 92.6 km (50 nmi) from the coastline since 1986 (Sosa-Nishizaki, 1998), they are the primary species caught by the artisanal shark fleet in some states of central and south Mexico, where dolphinfish alone can contribute to more than 50% of the total catch (Madrid and Beltrán, 2001; Damián-Guillén et al., 2010; Miranda-Carrillo et al., 2010). Dolphinfish are also caught incidentally by the tuna purse-seine (Arenas et al., 1999) and longline fleets (Santana-Hernández, 2001), in both coastal and offshore waters off Mexico.

Because of its circumtropical and subtropical distribution and its biological characteristics (fast growth, early maturity, and high fecundity), high catch rates of dolphinfish are reported all over the world, where they are targeted by commercial and recreational fisheries (Martínez-Rincón

et al., 2009; Farrell et al., 2014). In the Mediterranean Sea, dolphinfish are caught by using a special type of net (called *llampuguera*) around fish-aggregating devices (Massutí and Morales-Nin, 1997), and in the western Atlantic Ocean, they are caught commercially by using pelagic longlines, and recreationally by rod and reel (Farrell et al., 2014). In South America, it is fished industrially in the Pacific Ocean waters by using surface nets at night near Colombia and Venezuela (Lasso and Zapata, 1999) and by the longline fleets of Ecuador and Costa Rica (Patterson and Martinez, 1991; Campos et al., 1993). In the Pacific Ocean, it is targeted mainly by the Japanese longline fleet (Kojima, 1961).

There are few published works on catch rates and abundance of dolphinfish in relation to environmental parameters. Norton (1999) found, for example, that dolphinfish habitat expanded poleward in the eastern tropical Pacific Ocean, owing to increase in downwelling forced by a long-distance wave transmission along the coast and a decrease in upwelling off the coast of northwestern Mexico, which causes an increase in SST. Zúñiga-Flores et al. (2008) studied seasonal and interannual variation in dolphinfish catch rates in the Cabo San Lucas, Mexico sport fishery. They found a high correlation (~0.78, with 1-month delay) between monthly mean SST and their catch rate time series. Zúñiga-Flores et al. (2008) reported that dolphinfish catch rates increase toward the second half of the year, when values of SST range between 26°C and 29°C.

Martínez-Rincón et al. (2009) found that most (~79%) dolphinfish caught incidentally by the purse-seine tuna fleet in the eastern tropical Pacific Ocean were caught when SST values ranged between 25°C and 28°C, and that no seasonal or interannual spatial pattern was observed. In contrast, Farrell et al. (2014) suggest that chlorophyll-*a* (chl-*a*) concentration and SST are the 2 environmental variables that explain the variations in dolphinfish catch from both the commercial longline and the recreational fisheries in the northwestern Atlantic Ocean. Higher catches occurred in waters with SST between 22°C and 27°C and chl-*a* concentrations <0.2 mg/m^3. Farrell et al. (2014) concluded that dolphinfish are highly sensitive to changes in the biophysical environment because a large number of variables was retained in the statistical model fitted to catch data. Apart from SST and chl-*a* concentration, another variable that could influence dolphinfish abundance is sea-surface height (SSH), which can be used as an indicator of some mesoscale oceanographic features, such as eddies; moreover, some SSH features have elucidated the preference of certain species for particular water masses, such as cyclonic eddies or currents (Zainuddin et al., 2006; Theo and Block, 2010).

Our main objective was to assess environmental and spatial preferences of dolphinfish in the Pacific Ocean off the coast of Mexico by using 1) estimated incidental catch per unit of effort (ICPUE) data from the purse-seine tuna fleet and 2) SST, chl-*a* concentration, and SSH from remote sensing databases.

Materials and methods

Fishery database

We analyzed a 10-year database of estimated dolphinfish caught incidentally, reported by scientific observers of the Inter-American Tropical Tuna Commission on board class 6 (>425 m^3 storage capacity; IATTC[1]) tuna purse-seine ships that operated from 2004 to 2013 in the Pacific Ocean off the coast of Mexico from 10° to 33°N and from 90° to 125°W. The database included the estimated number of dolphinfish caught monthly in 1°×1° latitude–longitude survey quadrants, the number of purse-seine sets that resulted in that estimated number of fish for each quadrant, the number of fish caught per size class of fish (small: <30 cm in total length (TL), medium: 30–60 cm TL, and large: >60 cm TL), the coordinates of latitude and longitude at the center of the quadrants, for each month and year. The following equation was used to calculate ICPUE:

$$ICPUE_i = \frac{DC_i}{NS_i},$$

where DC_i = estimated catch (total number of dolphinfish); and

NS_i = the number of positive purse-seine sets (with at least one dolphinfish) that resulted in the estimated catch, all for ith quadrant.

Environmental database

Monthly means for 3 environmental variables over the same 10-year period were used in the analysis: SST, chl-*a* concentration, and SSH. Both SST and concentration of chl-*a* were obtained from BloomWatch360, a product of the NOAA CoastWatch West Coast Regional Node (available from website). With this product, each database has a unique 7-letter code. For the SST database, the code is TBssta, has a 0.1°×0.1° spatial resolution, and represents a multimission (sent from different sensors) database. The data for chl-*a* concentration (with a database code of TMHchla) have a 0.05°×0.05° resolution, and include data up to September 2013. Data for chl-*a* concentration for the last 3 months of 2013 were obtained from NOAA's ERDAPP data server (available from website), have a 0.025°×0.025° resolution (code erdMBChlamday). Both chl-*a* concentration data sets come from the Aqua-MODIS satellite. SSH data were obtained from the AVISO website (available from Copernicus at website), with a temporal resolution of 1 d, and a spatial resolution of 0.125°. Monthly averages were then calculated from January 2004 to De-

[1] IATTC (Inter-American Tropical Tuna Commission). 2009. Agreement on the International Dolphin Conservation Program. 21st meeting of the parties. Vessel capacity class definitions related to the requirement for carrying an onboard observer. Doc. MOP-21-07, 2 p. IATTC, La Jolla, CA. [Available from website.]

cember 2013. All environmental data were downscaled to 1°×1° in order to match the spatial resolution of the fishery database.

Analysis of incidental catch

Kolmogorov–Smirnov D test and Bartlett's B test were conducted to assess normality and homoscedasticity of the data. Depending on the results, parametric or nonparametric (Kruskal–Wallis H test) analyses of variance were conducted to evaluate significant seasonal and interannual differences in dolphinfish ICPUE.

Quadrants with catches higher than the lower limit of the upper quartile of ICPUE were considered high catch quadrants (Andrade and Garcia, 1999). Results from these analyses were used to evaluate possible dolphinfish migration patterns.

Relation of dolphinfish incidental catch to environmental and spatial variables

To assess the relationship of ICPUE to environmental variables, and because of their apparent nonlinear relationship, a 3rd degree polynomial linear model was fitted for each one of the variables in relation to the log-transformed ICPUE. We fitted a model for each different size class, in order to highlight differences in environmental preferences at different dolphinfish life stages. Standard validation techniques (residuals vs. fitted values, histogram of residuals) were used to assess the relevance of the fitted models to the data (Zuur et al., 2009, p. 23). *F*-tests were then conducted to evaluate the significance of model fit.

With the purpose of evaluating possible segregation due to size, we created histogram-like figures for the estimated number of fish caught per size class of fish and each spatial and environmental variable at the 1°×1° resolution. Spatial distribution maps were created with R, vers. 3.0.1 (R Core Team, 2013), and its maptools package, vers. 0.8-34.

The monthly latitude of the 25°C isotherm at 120°W was extracted from the monthly mean SST data from the satellite imagery by using the contourLines and convCP functions of the R PBSmapping package, vers. 2.68.68. Possible relation between mean latitude of high catch quadrants and mean latitude of the isotherm was explored by using the Pearson correlation coefficient (r).

All calculations were performed with R and with a significance of 0.05 for all statistical tests.

Results

Spatiotemporal variation of incidental catch

A total of 627 positive sets were reported in the 10-year fishery database, which resulted in a total of 55,406 fish caught, and a per-quadrant maximum, minimum, mean, and standard deviation (SD) of 3527, 1, 88.36, and 269.76 fish, respectively. Maximum and minimum ICPUE values were 3527 fish/set, with a mean of 55.32 fish/set (SD 189.47). The monthly maximum and mean number of positive sets per quadrant was 46 sets and 1.81 sets (SD 3.09).

Data of ICPUE was nonnormally distributed (D_1=0.38, P<0.05) and nonhomoscedastic for monthly ($B_{(11, 627)}$=817.41, P<0.05) and year-to-year variation ($B_{(9, 627)}$=706.81, P<0.05). With the exception of December, all months had at least one set with 1 fish/set. The highest value of 3527 fish/set was found during July 2004. Significant differences were found in monthly ICPUE ($H_{(11, 627)}$=58.85, P<0.05): in general, maximum values occurred during June and October, and minimum values occurred during January and November (Fig. 1A).

Yearly, maximum values of ICPUE were found during 2004, and minimum values were reported for 2008 (Fig. 1B). Year-to-year variation was also statistically significant ($H_{(9, 627)}$=26.72, P<0.05).

Two areas with high dolphinfish concentration (>300 fish/set) were found, one in the open ocean around, 10–20°N and 115–125°W, and a second one near the Baja California Peninsula (BCP), around 20–27°N and 113–116°W. Catches around 100–300 fish/set were found in the northern coastal part of the study area (~33°N, 117°W) and in the entrance of the Gulf of California, around 23°N and 107°W. In the southern part of the study area, scattered quadrants with high estimated ICPUE were also present, especially west of 110°W (Fig. 2).

Analysis of size classes

A total of 5306 dolphinfish (9.50% of total fish) of the small-size class were caught; 21,387 (38.60%) belonged to the medium-size class, and 28,713 (51.82%) belonged to the large-size class. Number of fish caught by size class was nonnormal (D_1=0.41, P<0.05) and nonhomoscedastic ($B_{(2, 1881)}$=347.83, P<0.05). Significant differences were found between fish caught for different size classes ($H_{(2, 1881)}$=449.25, P<0.05). An average of 8.50 fish (SD 74.30) in the small-size class (min. 0, max. 1706) were caught per quadrant per month. Mean for the medium- and large-size classes were 34.10 fish (SD 151.03; min. 0, max. 2185) and 45.80 fish (SD 153.44; min.0, max. 1689) per quadrant per month, respectively.

No apparent well-defined spatial pattern due to size class was observed. Dolphinfish of all size classes were caught both on coastal and offshore waters throughout the study area (results not shown).

For the small-size class, most fish were caught during July (45% of total fish for that size class, 2428 fish), and 0 fish were caught during December. July was also the month when most incidental catch of fish in the mid-size class occurred (30.50% of total fish [6521 fish for the size class]). Only 0.03% (8 fish) of total fish of the medium-size class were caught during December. For the large-size class, most fish were caught during October (32.22% of total fish for the size class, 9522 fish), and a monthly minimum of 0.08% of total fish

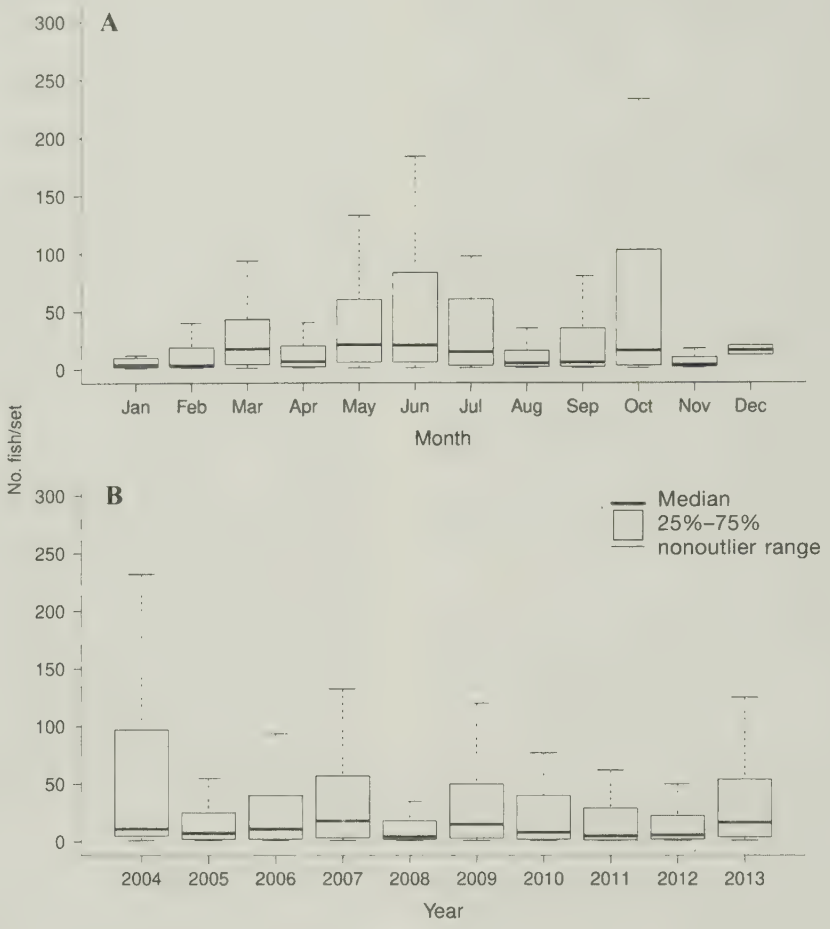

Figure 1

Variation between (**A**) months and (**B**) years in estimated incidental catch per unit of effort of common dolphinfish (*Coryphaena hippurus*) and pompano dolphinfish (*C. equiselis*) in the eastern Pacific Ocean off Mexico during 2004–2013. The thick black line is the median, the box displays the 25% and 75% quartiles, and the whiskers extend 1.5 times beyond the interquartile range.

(24 fish) were reported during December for this size class (Fig. 3A).

Highest incidental catch occurred during 2004, where 40% (2121), 28% (5977), and 22.50% (6453) of total fish for the 10-year period were caught for the small-, medium-, and large-size classes, respectively. Lowest annual incidental catch occurred during 2008 for the small-size class (0.50% of total fish for this size class, 26 fish) and the medium-size class (2.40% of total fish for this size class, 507 fish), and during 2011 for the large-size class (2.70%, 782 fish) (Fig. 3B).

Summary of environmental variables

A wide range of SST, chl-*a* concentration, and SSH values was found in the study area, during the 10-year period. Maximum, minimum, and mean values for SST were 33.12°C, 12.54°C, and 24.54°C (SD 4.28). Chl-*a* concentration ranged from 0.02 to 38.76 mg/m^3, with a mean of 0.51 mg/m^3 (SD 1.47). Lowest SSH value for the study period was –0.30 m, with a maximum of 0.39 m, and a mean of 0.02 m (SD 0.07).

Environmental and spatial preferences per class size

Residuals vs. fitted values in scatter plots for fitted polynomial models showed no clear pattern for any of the environmental variables, and the histograms of the residuals were apparently normal (results not shown) in all cases, which suggests good fits (Zuur et al., 2009). Large and small dolphinfish incidental catch per unit of effort (ICPUE) peaked at ~24°C, whereas medium-size fish ICPUE peaked at ~26°C (Fig. 4A). Most fish were caught in waters with low (<0.15 mg/m^3) chl-*a* concentrations, but 2 interesting peaks in catch occurred for small- and medium-size fish in wa-

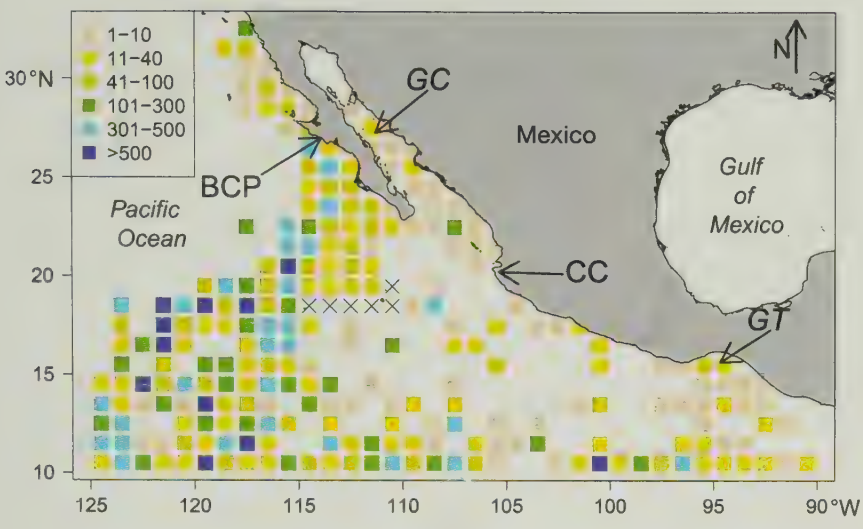

Figure 2

Map of the spatial distribution of estimated incidental catch per unit of effort (ICPUE) of common dolphinfish (*Coryphaena hippurus*) and pompano dolphinfish (*C. equiselis*) for the period 2004–2013 in the eastern Pacific Ocean off Mexico. The scale indicates ICPUE measured in number of fish caught per set. An × indicates areas where fishing is prohibited. Arrows indicate the Gulf of California (GC), Baja California Peninsula (BCP), Cabo Corrientes (CC), and Gulf of Tehuantepec (GT).

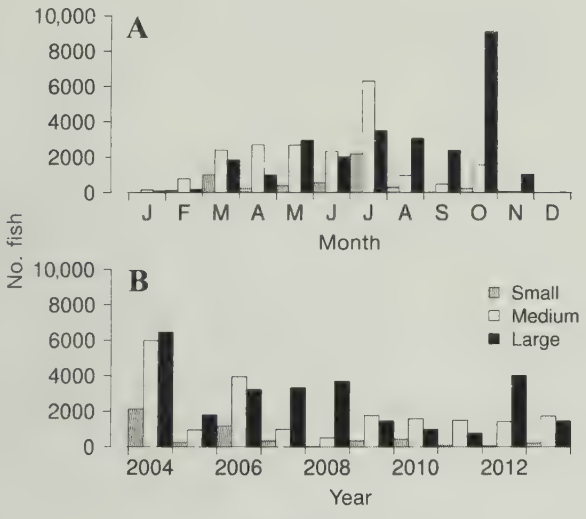

Figure 3

Temporal variation in estimated number of dolphinfish (*Coryphaena* spp.) caught per size class of fish by the purse-seine fleet for the period 2004–2013, (**A**) by month and (**B**) year. The 3 size classes are small (<30 cm in total length [TL]), medium (30–60 cm TL), and large (>60 cm TL).

ters with high (>1 mg/m^3) chl-*a* concentrations (Fig. 4B). A similar result was found in respect to SSH preferences for the 3 size classes, with higher catch in waters with positive SSH values (Fig 4C). Relationship between logarithm of ICPUE and SST was significant only for medium- and large-size dolphinfish ($F_{(4, 306)}$=7.52, P<0.05 and $F_{(4, 423)}$=16.02, P<0.05), whereas chl-*a* concentration and ICPUE were significant of all 3 size classes ($F_{(4, 92)}$=13.71, P<0.05, $F_{(4, 304)}$=22.78, P<0.05 and $F_{(4, 423)}$=46.68, P<0.05 for small, medium-size, and large fish). Relationship of catch and SSH was not as clear (F=~1; P>0.22 for all 3 size classes).

No apparent spatial segregation due to size was observed, but some spatial patterns arose when an analysis per latitudinal bands was applied. Of the total fish in the small-size class, 33.39% (1719 fish) were caught between 20°N and 22°N. On the other hand, for the medium-size class, 24.30 % of total fish (4893 fish) were caught between 10°N and 12°N. For the large-size class, there was a prominent mode at the southernmost latitudinal band (10–12°N), where 27.30% of total fish (7177 fish) were caught (Fig. 5A).

A total of 2090 fish (41.50% of total fish) in the small-size class were caught between 114° W and 116°W. Fish for the medium-size class were distributed west of 113°W and the maximum number of fish (4708, 23.50% of total fish) were caught between 117°W and 120°W. The most important mode for the large-size fish (6242, 24% of total fish) was found between 114°W and 117°W (Fig. 5B).

The maximum and minimum SST values from quadrants where at least one dolphinfish was caught were 31.10° and 18.50°C. Despite this wide range, dolphinfish showed a clear preference for warm waters. Almost 40% (38.20%, 1926 fish) of total fish belonging to the small-size class were caught between 25°C and 26°C. The main mode for the incidental catch of fish in the medium- and large-size classes was found between 27°C and 28°C, with 38.60% (7755) and 36.82% (9711) of total fish caught for the medium- and large-size class, respectively (Fig. 5C).

Chl-*a* concentration also showed a wide range (0.05–2.61 mg/m3) for those quadrants with positive sets. However, 82.90% of total fish, in all 3 size classes was caught in waters with concentrations of chl-*a* between 0.05 and 0.25 mg/m^3 (3877, 75% of total fish, for the small-size class, 16,092, 80% of total fish for the medium-size class, and 22,764, 86% of total fish for the large-size class; Fig. 5D).

Dolphinfish were caught incidentally in SSH values ranging from –0.13 to 0.32 m. Of total fish (2047) of the small-size class, 40% were caught in waters with SSHs from 0.05 to 0.1 m. For the medium-size class,

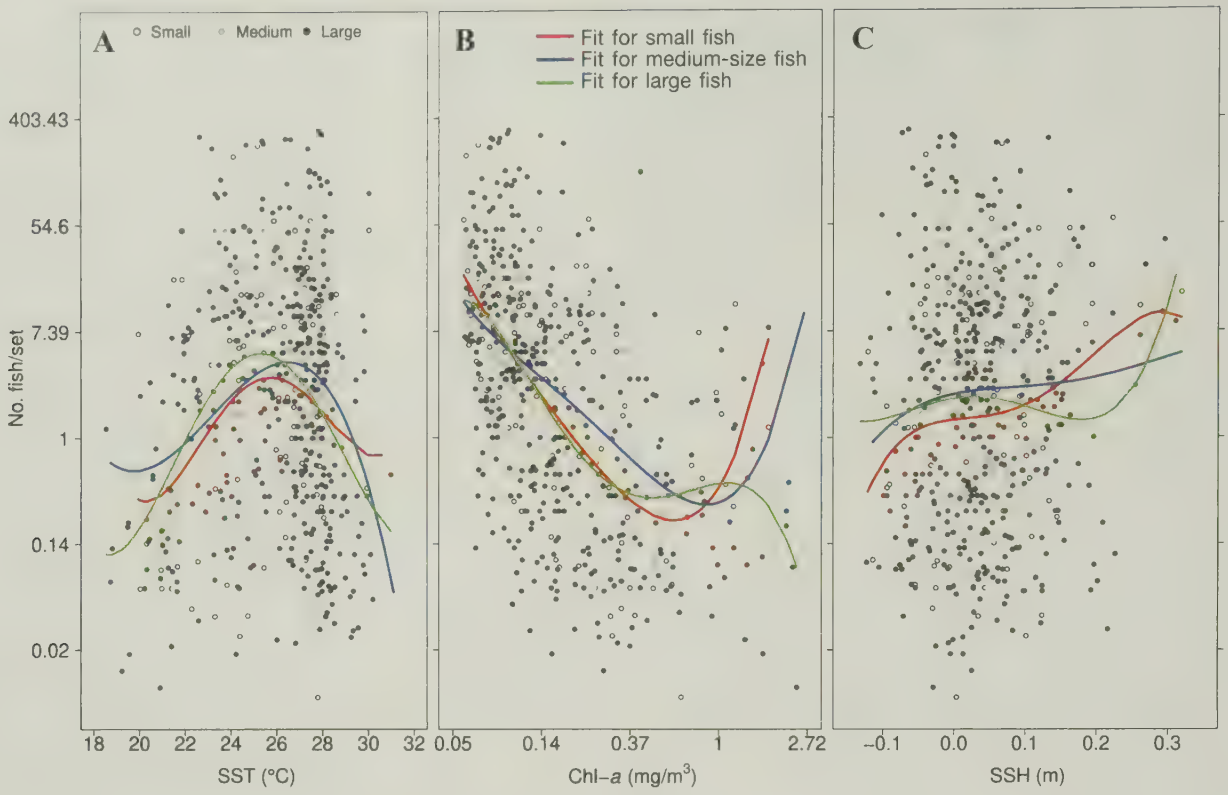

Figure 4

Scatter plots of the relationship between incidental catch per unit of effort (in logarithmic scale) for each size class of dolphinfish (*Coryphaena* spp.) and (**A**) sea-surface temperature (SST), (**B**) chlorophyll-*a* concentration (chl-*a*), and (**C**) sea-surface height (SSH) in the eastern Pacific Ocean off Mexico during 2004–2013. Points indicate observed values, and the colored lines were generated by fitting the polynomial linear models to the data.

7674 fish (38% of total fish in this class) were caught in waters with SSH from 0.05 to 0.1 m, and 5149 fish (25% of total fish in this class) for this size class were caught in SSH values from −0.05 to 0 m. Fish in the large-size class showed SSH preferences similar to those in the medium-size class, with 27% (7229 fish for this class) and 23% (6059 fish) of total fish caught in SSH ranges from −0.05 to 0 m and from 0.05 to 0.1 m, respectively (Fig. 5E).

Figure 6 shows the spatial distribution of total estimated ICPUE and (**A**) mean SST, (**B**) chl-*a* concentration, and (**C**) SSH values for the whole study area.

In general, most dolphinfish catches occurred south of the 21°C isotherm, especially around the 25°C isotherm, and few catches occurred in waters with SSTs over 28°C. The 10-year average SST values higher than 21°C and lower than 28°C occurred both in the oceanic zone and near the coast of the BCP, especially in the central portion of the study area, and in the Gulf of California. Values higher than 28°C occurred near the coast, south of 18°N and east of 110°W.

The vast majority of dolphinfish ICPUE occurred, for the 10-year average, west of the 0.20 mg/m^3 isoline. This area with values of chl-*a* concentration lower than 0.20 mg/m^3 represented most of the oceanic zone, with the exception of an area east of ~104°W. High (>1 mg/m^3) values were found in coastal zones, especially in the upper Gulf of California, the west coast of the BCP, the Cabo Corrientes area (~21°N, 105°W), and the Gulf of Tehuantepec, in the southern portion of the study area.

The 10-year average for SSH resulted in positive values for the study area. Most dolphinfish were caught in or near the 0.02 m SSH isoline, which was located mainly in an oceanic area around 11–18°N and 125–110°W. In the west coast of the BCP, high ICPUE occurred where SSH values were greater than 0.03 m.

Analysis of high-catch quadrants and their relationship with the 25°C isotherm

The lower limit of the upper quartile of the ICPUE vector was 42.62 fish/set; hence, all the quadrants with catches higher than this value were considered high-catch quadrants. Mean monthly latitude for these quadrants increased from January through August and then decreased from August to November, and no high catch quadrants were observed during December. The opposite was observed in the monthly mean longitude for these quadrants: a decrease from January to August and an increase from August to November (results not shown). When visualized in latitude and longitude

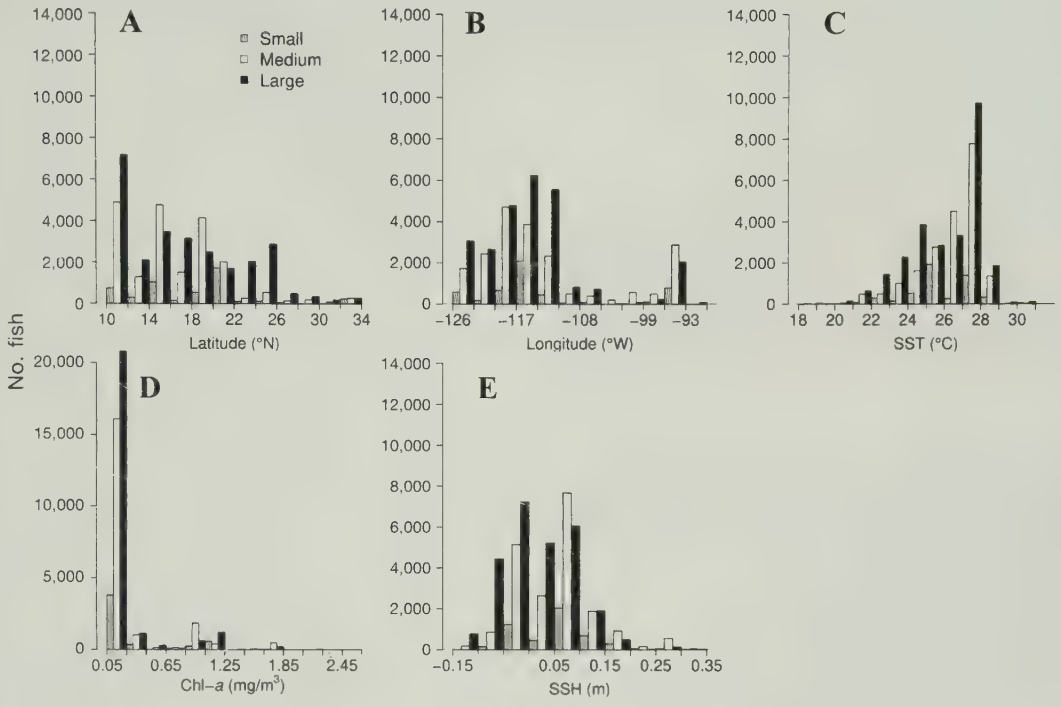

Figure 5

Spatial and environmental preferences of dolphinfish (*Coryphaena* spp.) caught by the purse-seine fleet off Mexico in the Pacific Ocean from January 2004 to June 2013: (**A**) latitude; (**B**) longitude; (**C**) sea-surface temperature (SST); (**D**) chlorophyll-*a* concentration (chl-*a*); and (**E**) sea-surface height (SSH). Note the difference in the scale of the *y*-axis in graph D.

coordinates on a map (i.e., "centroids"), areas with high dolphinfish ICPUE moved north westward during the months of April–May, and from south eastward during September–October (Fig. 7).

Mean monthly latitudes of high catch quadrants and position of 25°C isotherm at 120°W showed a similar pattern, although a 1-month lag was visible for the peaks of the 2 curves: maximum latitude for the isotherm occurs 1 month later than the maximum mean latitude of the quadrants (Suppl. Fig. 1) (online only). A high r of 0.84 was found, which was significantly different from 0 ($P<0.05$).

Discussion

Two areas of high dolphinfish ICPUE were present in the study area, one on the west coast of the BCP, where practically all ICPUE occurs during August (20–27°N and 113–116°W), and a second one in an oceanic zone (around 10–20°N and 115–125°W), where higher ICPUE occurs during May–June. July seems to be a month of transition between areas of high catch because a large area of relatively high abundance is observed, which covers the northern portion of the oceanic area and the southern portion of the BCP high catch area (Suppl. Fig. 2) (online only). Two of the potential factors that determine dolphinfish presence are the occurrence of floating objects and variations in SST; unfortunately, the relationship of ICPUE with floating objects could not be explored because of limited data. In terms of environmental factors, such as SST, it is well known that the upwelling of subsurface cool waters favors the development of the oceanic food web by bringing nutrients into the photic upper ocean layer (Reilly, 1990). Along the western coast of the BCP, wind blows parallel to the coast and causes intense upwelling (Zaytzev et al., 2003) during March–June because of the Ekman transport; these upwelling events can last up to 10 d (Walsh et al., 1977; Cervantes-Duarte et al., 1993) and are capable of concentrating plankton feeders such as the red pelagic crab (*Pleuroncodes planipes*), one of the main sources of food for dolphinfish and other large pelagic fish in this area (Aguilar-Palomino et al., 1998; Tripp-Valdez, 2005; Martínez-Rincón et al., 2009). Ortega-García and Lluch-Cota (1996) found a 3-month lag between spatial chlorophyll fronts (with peak chl-*a* concentration) and peaks in high abundance of yellowfin tuna (*Thunnus albacares*). Because yellowfin tuna and dolphinfish share habitat to some extent, the same ~3 month lag could also help to explain high dolphinfish abundance in the BCP during August–September,

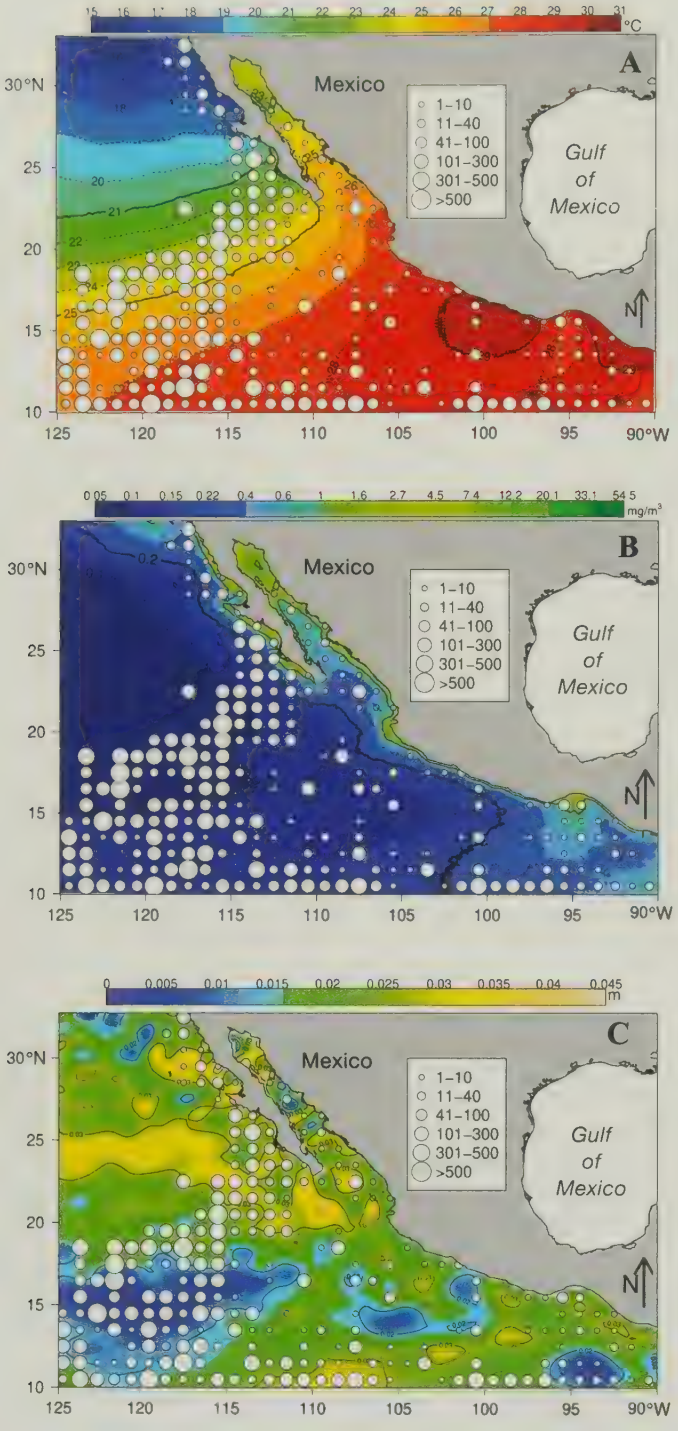

Figure 6

Maps of the spatial distribution of total estimated incidental catch per unit of effort in the eastern Pacific Ocean off Mexico, the number of fish per set indicated by the size of the white circles, and mean values of (**A**) sea-surface temperature (measured in degrees Celsius), (**B**) chlorophyll-*a* concentration (measured in milligrams per cubic meter) and (**C**) sea-surface height (measured in meters) for the 10-year period 2004–2013. The scale at the top of each panel indicates levels for 1 of the 3 environmental parameters.

~2–4 months after the conclusion of the upwelling season along the west coast of BCP, when the food web is fully "mature" for large pelagic pray, and SST is optimal for dolphinfish.

In the ocean zone where a high ICPUE is reported, there is also a current pattern that seasonally optimizes the SST for dolphinfish. The California Current System is the eastern part of the North Pacific Subtropical Gyre, which reaches the BCP (Badan, 1997). Part of the California Current turns westward, at around 15°N, 112°W, as evident by the curvature of the isotherms, and becomes the North Equatorial Current (Karl, 1999; Fiedler and Talley, 2006). In this area thermal fronts occur when the cold California Current meets the Eastern Pacific Warm Pool, an area in the central Pacific Ocean off the coast of Mexico, characterized by temperatures > 27.5°C all year long (Fiedler and Talley, 2006; Kessler, 2006), as a result of large net heat flux and poor wind mixing (Wang and Enfield, 2001, cited by Fiedler and Talley, 2006). Additionally, the North Pacific Subtropical Gyre is anticyclonic and characterized by low productivity and a high pressure center (Lalli and Parsons, 1997), both of which suggest that low production areas occur on both sides of the branch of the California Current that joins the Equatorial Current System; a branch that spatially agrees with the oceanic area of high ICPUE.

The direction and intensity of the California Current has a pattern similar to that of oceanic wind (Pantoja et al., 2012), and both are strongest during winter (Martínez-Rincón et al., 2009; Marín-Enríquez, 2012). Assuming that the 3-month lag hypothesis of Ortega-García and Lluch-Cota (1996) also applies to this oceanic area, because dolphinfish arrive during May–June, ~3–4 months after the winter season, the California Current enters a dormant state, and tropical water masses, with high temperature and low salinity (Torres-Orozco, 1993) move northwards, bringing the preferred SST values to the high ICPUE zone for dolphinfish.

Survey quadrants with high ICPUE were scattered throughout the southernmost part of the study area, especially from February through April (Suppl. Fig. 1) (online only). This zone (0°–10°N) is under the influence of the Equatorial Current System and is a highly productive zone because of the upwelling caused by the trade winds (Martínez-Rincón et al., 2009). In the zone of the equatorial cold-upwelled water tongue, trade winds, and upwelling are more intense during winter months (Kessler, 2006, fig. 9). Mann and Lazier (1996) suggested that high trophic level predators, such as sharks, tunas, and other fish use this area as feeding grounds because of the high prey abundance resulting from the nutrient-rich upwelling process. Bocanegra Castillo (2007) suggested that billfish, sharks, and dolphinfish feed on a wide variety of prey in this area, such as crustaceans, small fish, and squid. The relatively high ICPUE in this zone could then be explained by the time lag that it takes the trophic web to "climb" up to the trophic levels of the prey that dolphinfish

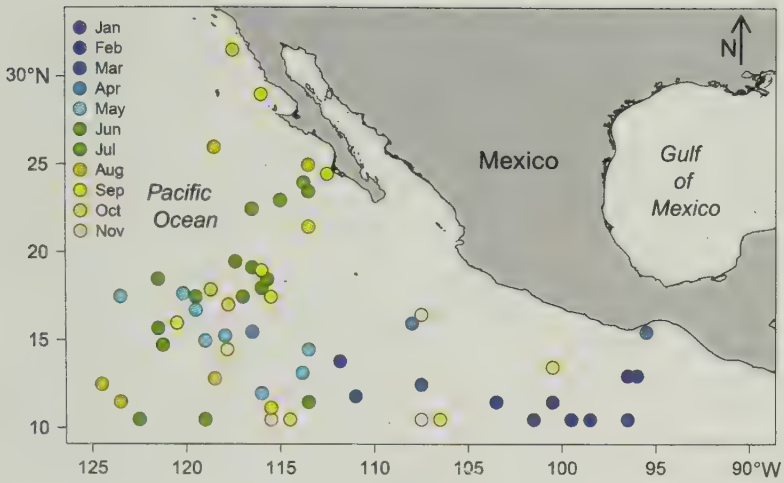

Figure 7

Mean geographic locations (centroids) of survey quadrants (1°×1°) with high (>42.62 fish/set) monthly mean incidental catch per unit of effort for dolphinfish (*Coryphaena* spp.) in the Pacific Ocean off Mexico during 2004–2013

feed on—a climb that occurs ~4–5 months after the peak in trade winds and upwelling activity.

Year-to-year variation in ICPUE was also quite variable. During our study period, higher ICPUE occurred during 2004, one of the years with higher SST values (results not shown); according to NOAA's Oceanic Niño Index (ONI, available from website), there was a moderate to strong warm episode during 2004. Lower ICPUE was recorded during 2008, a year with low SST and negative (i.e., "cold period") ONI values. Another period of low ICPUE occurred during 2011–2012, a period dominated by negative ONI values; however, during 2013 a high ICPUE peak agreed with a year of negative ONI values, and therefore year-to-year variability of ICPUE has a week correlation with ONI and indicates that biotic and abiotic factors other than SST may influence relative abundance of dolphinfish.

To the best of our knowledge, this study provides the first approach to assess ontogenetic variations in dolphinfish habitat preferences. For both small and large fish, ICPUE showed a peak at ~25°C, nearly 2°C lower than the peak for medium-size fish (~27°C). Kraul (1999) suggested that dolphinfish growth rate is very sensitive to temperature, which would imply larger discrepancies in thermal preferences for small and large fish and is opposite to what we observed. One explanation might be that medium-size fish have different metabolic needs than small and large fish, perhaps because they are reaching size at first maturity (Alejo-Plata et al., 2011). However, this hypothesis needs to be validated, perhaps with a controlled experimental design, such as those designed for aquaculture purposes.

Fitted models show that there was 2 interesting peaks of ICPUE at relatively high (>1 mg/m^3) chl-*a* concentrations for small and medium-size fish. Kitchens and Rooker (2014) found that dolphinfish larvae density increases with higher concentrations of chl-*a*—a finding that suggests that fast-growing larvae survive in areas of enhanced food availability, such as cold-core eddies and fronts. The fact that some fish <60 cm TL are caught in these "high" chl-*a* concentrations might be explained by the energetic needs that dolphinfish require in their early, fast-growth life stage (Zúñiga-Flores, 2009). Additionally, Olson and Galván-Magaña (2002) found that dolphinfish body and prey size are positively correlated, and therefore smaller dolphinfish might explore areas of high productivity, where smaller prey are expected to be more abundant. Olson and Galván-Magaña (2002) also found that dolphinfish food consumption rates are different for males and females in early life stages, and therefore sex could also be playing an important role in the differences presented in our study.

Overall, dolphinfish shows a clear preference for SSTs between 23°C and 28°C, chl-*a* concentration < 0.2 mg/m^3, and SSH values from −0.05 to 0.05 m. Dolphinfish thermal preferences have been reported by other authors, such as Martínez-Rincón et al. (2009), who suggest that temperatures below 20°C may limit the metabolism and growth of this species. Norton (1999) reports that dolphinfish move to warmer waters when a decrease in SST occurs, and that fish habitat expands northwards during events of extreme increase in SST. In addition to the 2 areas with high catch that were mentioned earlier, low ICPUE occurred in an area around 11–18°N and 97–110°W, in the zone of the Eastern Pacific Warm Pool. As stated before, some authors suggest that dolphinfish abundance increases with high temperatures (Zúñiga-Flores et al., 2008); however, our findings suggest that optimal temperatures for dolphinfish are between 25°C and 28°C (with an important decrease in ICPUE at temperatures >28°C), which could explain the low ICPUE area in the Eastern Pacific Warm Pool, an area that is characterized by high (>27.5°C) SST values all year long (Fiedler and Talley, 2006).

A wide range of SSH values were found in the study area, although high ICPUE occurred only over a narrow range of both positive and negative values. Positive SSH values indicate a zone of convergence (anticyclonic activity) in the Northern Hemisphere (Lalli and Parsons, 1997) and indicate that dolphinfish associate with anticyclonic structures—a behavior that has been reported for other large pelagic fish, such as the albacore (*Thunnus alalunga*) (Zainuddin et al., 2006).

Additionally, in respect to the possible effect of migrations during the seasonality of dolphinfish catch, Kraul (1999) suggested that dolphinfish can spawn several times a year, that some cohorts are "stronger" than others, and that the survivors of those strong

cohorts could also influence the seasonal analysis of catch. Given the growth curve proposed by Zúñiga-Flores (2009), dolphinfish of the small-size class would be less than 3 months old, the medium-size individuals would be between 3 and 6 months old, and the large fish would be more than 6 months old. Substantial differences have been found in size at first maturity for one of the species in our study for *Coryphaena hippurus*, dolphinfish, in the southern part of our study area (Gulf of Tehuantepec); the dolphinfish matures at ~50 cm in fork length (FL) (Alejo-Plata et al., 2011), and in the central part (southern tip of the BCP), at around 80 cm FL (Zúñiga-Flores et al., 2011). Dolphinfish of the small-size class would then probably be all immature individuals; the medium- and large-size class of fish could be a mixture of mature and immature fish. If we assume that large-size class of fish are mature fish, a large number of potential spawners should have been present during October in the study area. Following the hypothesis of Kraul (1999), we could expect a high abundance of juveniles for the first months of the following year—a pattern that was not fully clear and needs to be investigated; it is worth noting that all these published works refer mainly to only one species, the common dolphinfish, and therefore these inferences are made for that particular species.

Literature cited

Aguilar-Palomino, B., F. Galván-Magaña, L. A. Abitia-Cárdenas, A. F. Muhlia-Melo, and J. Rodríguez-Romero.
1998. Feeding aspects of the dolphin *Cmyphaena hippurus* Linnaeus, 1758 in Cabo San Lucas, Baja California Sur, Mexico. Cienc. Mar. 24:253–265.

Alejo-Plata, C., P. Díaz-Jaimes, and I. H. Salgado-Ugarte.
2011. Sex ratios, size at sexual maturity, and spawning seasonality of dolphinfish (*Coryphaena hippurus*) captured in the Gulf of Tehuantepec, Mexico. Fish. Res. 110:207–216.

Andrade, H. A., and C. A. E. Garcia.
1999. Skipjack tuna in relation to sea surface temperature off the southern Brazilian coast. Fish. Oceanogr. 8:245–254.

Arenas, P., M. Hall, and M. García.
1999. Association of fauna with floating objects in the eastern Pacific Ocean. In Proceedings of the international workshop on the ecology and fisheries for tunas associated with floating objects. IATTC Spec. Rep. 11; 11–13 February 1992, p. 285–326. Inter-Am. Trop. Tuna Comm., La Jolla, CA.

Badan, A.
1997. La corriente costera de Costa Rica en el Pacífico Mexicano. *In* Contribuciones a la oceanografía física en México. Monografía 3 (M. F. Lavín, ed.), p. 99–112. Unión Geofísica Mexicana, Ensenada, Mexico.

Bocanegra Castillo, N.
2007. Relaciones tróficas de los peces pelágicos asociados a la pesquería del atún en el Océano Pacífico oriental. Ph.D. diss., 178 p. Cent. Interdiscip. Cienc. Mar., Inst. Politéc. Nac., La Paz, Mexico.

Campos, J. A., A. Segura, O. Lizano, and E. Madrigal.
1993. Ecología básica de *Coryphaena hippurus* (Pisces: Coryphaenidae) y abundancia de otros grandes pelágicos en el Pacifico de Costa Rica. Rev. Biol. Trop. 41:783–790.

Cervantes-Duarte, R., S. Aguíñiga-Garcia, and S. Hernández-Trujillo.
1993. Upwelling conditions associated to the distribution of zooplankton in San Hipolito, B.C.S. Cienc. Mar. 19:117–135.

Damián-Guillén, M., S. R. Soriano-Velázquez, C. E. Ramírez-Santiago, and D. E. Acal-Sánchez.
2010. Captura incidental de la flota artesanal tiburonera del puerto de Zihuatanejo, Guerrero. *In* Proceedings of the symposium: V foro científico de pesca ribereña; Boca del Río, Mexico, 7–9 September (E. Espino-Barr, M. A. Carrasco-Águila, E. Romero-Hernández, H. Aguirre-Villaseñor, and O. Miranda-Carrillo, eds), p. 45–46. Inst. Nac. Pesca, Mexico City, Mexico.

Farrell, E. R.
2009. The habitat, movements, and management of dolphin, *Coryphaena hippurus*, in the western North Atlantic, Caribbean, and Gulf of Mexico. M.S. thesis, 55 p. Nicholas School Environ., Duke Univ., Durham, NC.

Farrell, E. R., A. M. Boustany, P. N. Halpin, and D. L Hammond.
2014. Dolphinfish (*Coryphaena hippurus*) distribution in relation to biophysical ocean conditions in the northwest Atlantic. Fish. Res. 151:177–190.

Fiedler, P. C., and L. D. Talley.
2006. Hydrography of the eastern tropical Pacific: a review. Prog. Oceanogr. 69:143–180.

Gibbs, R. H., Jr., and B. B Collette.
1959. On the identification, distribution, and biology of dolphins, *Coryphaena hippurus* and *C. equiselis* of The Gulf and Caribean. Bull. Mar. Sci. 9:117–152.

Karl, D. M.
1999. A sea of change: biogeochemical variability in the North Pacific Subtropical Gyre. Ecosystems 2:181–214.

Kessler, W. S.
2006. The circulation of the eastern tropical Pacific: a review. Prog. Oceanogr. 69:181–217.

Kitchens, L. L., and J. R. Rooker.
2014. Habitat associations of dolphinfish larvae in the Gulf of Mexico. Fish. Oceanogr. 23:460–471.

Kojima, S.
1961. Studies of fishing conditions of dolphin, *Coryphaene hippurus*, in the western region of the Sea of Japan. III. On food contents of dolphin. Bull. Jpn. Soc. Sci. Fish. 27:625–629.

Kraul, S.
1999. Seasonal abundance of dolphinfish, *Coryphaena hippurus*, in Hawaii and the tropical Pacific Ocean. Sci. Mar. 63:261–266.

Lalli, C. M., and T. R. Parsons.
1997. Biological oceanograpy: an introduction, 2nd ed., 324 p. Elsevier Butterworth-Heinemann, Oxford, UK.

Lasso, J., and L. Zapata.
1999. Fisheries and biology of *Coryphaena hippurus* (Pisces: Coryphaenideae) in the Pacific coast of Colombia and Panama. Sci. Mar. 63:387–399.

Madrid, J. V., and R. Beltrán-Pimienta.
2001. Longitud, peso y sexo del dorado *Coryphaena hippurus* (Perciformes: Coryphaenidae), del litoral de Sinaloa, Nayarit y Baja California Sur, México. Rev. Biol. Trop. 49:931–938.

Mann, K. H., and J. R. N. Lazier.
1996. Dynamics of marine ecosystems: biological–physical interactions in the oceans, 2nd ed., 394 p. Wiley-Blackwell, Inc., Hoboken, NJ.

Marín-Enríquez, E.
2012. Variabilidad de las tasas de captura de Marlin Azul (*Makaira nigricans*) en la entrada del Golfo de California, y su relación con algunas variables oceanográficas. M.S. thesis, 67 p. Cent. Interdiscip. Cienc. Mar., Inst. Politéc. Nac. La Paz, Mexico.

Martínez-Rincón, R. O., S. Ortega-García, and J. G. Vaca-Rodríguez.
2009. Incidental catch of dolphinfish (*Coryphaena* spp.) reported by the Mexican tuna purse seiners in the eastern Pacific Ocean. Fish. Res. 96:296–302.

Massutí, E., and B. Morales-Nin.
1997. Reproductive biology of dolphin-fish (*Coryphaena hippurus* L.) off the island of Majorca (Western Mediterranean). Fish. Res. 30:57–65.

Massutí, E., S. Deudero, P. Sánchez, and B. Morales-Nin.
1998. Diet and Feeding of dolphin (*Coryphaena hippurus*) in western Mediterranean waters. Bull. Mar Sci. 63:329–341.

Miranda-Carrillo, O., E. Espino-Barr, E. Cabral-Solís, M. Puente-Gómez, A. García-Boa, and F. J. De La Cruz-Gonzáles.
2010. Aspectos de la pesca ribereña en la Bahía de Barra de Navidad, Jalisco, 2007 a 2009. *In* Proceedings of the symposium: V foro científico de pesca ribereña, Boca del Río, Mexico, 7–9 September (E. Espino-Barr, M. A. Carrasco-Águila, E. Romero-Hernández, H. Aguirre-Villaseñor, and O. Miranda-Carrillo, eds.), p. 147–148. Inst. Nac. Pesca, Mexico City, Mexico.

Norton, J. G.
1999. Apparent habitat extensions of dolphinfish (*Coryphaena hippurus*) in response to climate transients in the California Current. Sci. Mar. 63: 239–260.

Olson, R. J., and F. Galván-Magaña.
2002. Food habits and consumption rates of common dolphinfish (*Coryphaena hippurus*) in the Eastern Pacific Ocean. Fish. Bull. 100:279–298.

Ortega-García, S., and S. Lluch-Cota.
1996. Distribución de la abundancia de atún aleta amarilla (*Thunnus albacares*) y su relación con la concentración de pigmentos fotosintéticos medidos por satélite en aguas al sur de México. Invest. Geogr. 4:85–93.

Oxenford, H. A.
1999. Biology of the dolphinfish (*Coryphaena hippurus*) in the western central Atlantic: a review. Sci. Mar. 63:277–301.

Palko, B. J., G. L. Beardsley, and W. J. Richards.
1982. Synopsis on the biological data of dolphin-fishes, *Coryphaena hippurus* Linnaeus and *Coryphaena equiselis* Linnaeus. NOAA Tech. Rep. NMFS. Circ. 443, 28 p.

Pantoja, D. A., S. G. Marinone, A. Parés-Sierra, and F. Gómez-Valdivia.
2012. Numerical modeling of seasonal and mesoscale hydrography and circulation in the Mexican Central Pacific. Cienc. Mar. 38:363–379.

Patterson, K. R., and J. Martinez.
1991. Explotation of the dolphin-fish *Coryphaena hippurus*. L. off Ecuador: analysis by length-based virtual population analysis. Fishbyte 9:21–23.

R Core Team.
2013. R: a language and environment for statistical computing. R Foundation for Statistical Computing. Vienna, Austria. [Available from website, accessed September 2013]

Reilly, S. B.
1990. Seasonal changes in distribution and habitat differences among dolphins in the eastern tropical Pacific. Mar. Ecol. Prog. Ser. 66:1–11.

Sakamoto, R., and S. Kojima.
1999. Review of dolphinfish biological and fishing data in Japanese waters. Sci. Mar. 63:375–385.

Santana-Hernández, H.
2001. Estructura de la comunidad de pelágicos mayores capturados con palangre en el Pacífico Mexicano (1983–1996) y su relación la temperatura superficial del mar. Ph.D. diss., 122 p. Univ. Colima, Manzanillo, Mexico.

Schwenke, K. L.
2004. Age, growth and reproduction of dolphin (*Coryphaena hippurus*) caught off the coast of North Carolina. M.S. thesis, 62 p. North Carolina State Univ., Raleigh, NC.

Sosa-Nishizaki, O.
1998. Historical review of the billfish management in the Mexican Pacific. Cienc. Mar. 24:95–111.

Theo, S., and L. B. A. Block.
2010. Comparative influence of ocean conditions on yellowfin and Atlantic bluefin tuna catch from longlines in the Gulf of Mexico. PLoS ONE 5:e10756.

Torres-Orozco, E.
1993. Analisis volumetrico de las masas de agua del Golfo de California. M.S. thesis, 92 p. Cent. Invest. Cient. Educ. Super. Ensenada. Ensenada, Mexico.

Tripp-Valdez, M. A.
2005. Ecología trófica del dorado *Coryphaena hippurus* (Linnaeus, 1758) en dos áreas del sur del Golfo de California. M.S. thesis, 125 p. Cent. Interdiscip. Cienc. Mar., Inst. Politéc. Nac., La Paz, Mexico.

Tripp-Valdez, M. A., F. J. García de León, S. Ortega-García, D. Lluch-Cota, J. López-Martínez, and P. Cruz.
2010. Population genetic structure of dolphinfish (*Coryphaena hippurus*) in the Gulf of California, using microsatellite loci. Fish. Res. 105:172–177.

Walsh, J. J., T. E. Whitledge, J. C. Kelley, S. A. Huntsman, and R. D. Pillsbury.
1977. Further transition states of Baja California upwelling ecosystem. Limnol. Oceanogr. 22:264–280.

Wang, C., and D. B. Enfield.
2001. The tropical Western Hemisphere warm pool. Geophys. Res. Lett. 28:1635–1638.

Zainuddin, M., H. Kiyofuji, K. Saitoh, and S. I. Saitoh.
2006. Using multi-sensor satellite remote sensing and catch data to detect ocean hot spots for albacore (*Thunnus alalunga*) in the northwestern North Pacific. Deep Sea Res., II 53:419–431.

Zaytzev, O., R. Cervantes-Duarte, O. Montanate, and A. Gallegos-García.
2003. Coastal upwelling activity on the Pacific shelf of the Baja California Peninsula. J. Oceanogr. 59:489–502.

Zúñiga-Flores, M. S.
2009. Dinámica poblacional del dorado (*Coryphaena hippurus*) en Baja California Sur, México: implicaciones para su manejo. Ph.D. diss., 203 p. Cent. Interdiscip. Cienc. Mar., Inst. Politéc. Nac., La Paz, Mexico.

Zúñiga-Flores, M. S., S. Ortega-García and A. Klett-Trauslen.
2008. Interannual and seasonal variation of dolphinfish (*Coryphaena hippurus*) catch rates in the southern Gulf of California, Mexico. Fish. Res. 94:13–17.

Zúñiga-Flores, M. S., S. Ortega-García, M. D. C. Rodríguez-Jaramillo, and J. López-Martínez.
2011. Reproductive dynamics of common dolphinfish *Coryphaena hippurus* in the Southern Gulf of California. Mar. Biol. Res. 7:677–689.

Zuur, A., E. N. Ieno, N. J. Walker, A. A. Saveliev, and G. M. Smith.
2009. Mixed effect models and extensions with R, 574 p. Springer-Verlag, New York.

National Marine
Fisheries Service
NOAA

Fishery Bulletin
established in 1881

Spencer F. Baird
First U.S. Commissioner
of Fisheries and founder
of *Fishery Bulletin*

The effects of wave-induced vessel motion on the geometry of a bottom survey trawl and the herding of yellowfin sole (*Limanda aspera*)

David Somerton (contact author)
Kenneth Weinberg
Peter Munro
Louis Rugolo
Thomas Wilderbuer

Email address for contact author: dsomerton4@gmail.com

Resource Assessment and Conservation Engineering Division
Alaska Fisheries Science Center
National Marine Fisheries Service, NOAA
7600 Sand Point Way NE, Building 4
Seattle, Washington 98115-6349

Abstract—Bottom trawl surveys need constant catchability over time to produce estimates of relative abundance that are most informative for stock assessment modeling. However, environmental conditions during surveys can potentially produce both interannual and long-term changes in catchability. Here we consider the effects of one environmental variable, sea state, on vessel motion, trawl performance, and, presumably, catchability. We present the results of 2 field experiments performed on chartered commercial trawlers typical of those used by the National Marine Fisheries Service for conducting its eastern Bering Sea bottom trawl survey. The first experiment shows that wave-induced vessel motion is transmitted down the towing warps, creating vertical oscillation in both trawl bridles and the footrope, which potentially influence both the herding and footrope escapement of fish. The second experiment shows that the herding of yellowfin sole (*Limanda aspera*) by the survey trawl decreases with an increase in wave height. A proposed mathematical model of flatfish herding is used to provide a hypothetical mechanism describing the effect of surface waves on flatfish herding. In addition, the annual biomass estimates of yellowfin sole determined from the bottom trawl survey data are shown to decrease with increasing wave height. The potential impacts of these relationships on the yellowfin sole assessment model are then considered.

Manuscript submitted 9 May 2017.
Manuscript accepted 18 October 2017.
Fish. Bull. 116:21–33 (2018).
Online publication date: 9 November 2017.
doi: 10.7755/FB.116.1.3

The views and opinions expressed or implied in this article are those of the author (or authors) and do not necessarily reflect the position of the National Marine Fisheries Service, NOAA.

Uncertainty in estimates of relative stock abundance determined from bottom trawl survey data has long been recognized to be a function of sample size, survey design, and species patchiness (Kimura and Somerton, 2006). However, the relative-abundance estimate at each sampling location depends on trawl sampling efficiency (i.e., the proportion of animals that are captured within the trawl path); consequently, uncertainty in survey-wide estimates of relative abundance must also reflect spatial and temporal variability in sampling efficiency. Despite efforts to reduce the influence of this variability on NOAA bottom trawl surveys through the standardization of survey gear and operational protocols (Stauffer, 2004), biotic and abiotic factors remain that cannot be controlled. We examined the influence of one such factor: that is, surface waves, which affect, in turn, vessel motion, trawl geometry, and sampling efficiency (Politis et al., 2012). Here we consider the effects of wave height on the performance of the bottom trawl used by the Alaska Fisheries Science Center, National Marine Fisheries Service, to conduct its annual eastern Bering Sea (EBS) trawl survey (henceforth referred to as "the survey trawl"; Conner and Lauth, 2016).

Although the connection between surface waves and vessel motion is readily apparent, the connection between vessel motion and trawl performance is not. Previous studies, however, have shown that effects of vessel motion can be pronounced. For example, O'Neill et al. (2003) considered the increase in size selectivity observed by trawl fishermen during stormy periods, focused on the oscillation in trawl speed caused by vessel motion, and investigated its consequent effects on the opening of codend meshes and fish escapement. Likewise, Politis et al. (2012) examined how vessel motion can be transmitted down the towing warps to impact many aspects of trawl performance, especially bottom contact of the trawl bridles (which influences fish herding) and bottom contact of the footrope (which influences fish escapement) (Dickson, 1993; Somerton et al., 2007).

In this study, we consider several related topics connected to the potential effects of surface waves on sampling efficiency of the survey trawl. First, we describe a field experiment that we conducted, which was similar to those of O'Neill et al. (2003) and Politis et al. (2012), to estimate the effects of vessel motion on the bottom contact of the bridles and footrope of the survey trawl. Second, we describe another field experiment that we conducted to estimate the effects of wave height on the herding of yellowfin sole (*Limanda aspera*). The experimental design focused on the trawl bridles, which has been shown to be the primary trawl component determining sampling efficiency of flatfishes (Somerton and Munro, 2001; Munro and Somerton, 2002). Third, we use the results of these 2 experiments to develop a mathematical model describing the effect of wave height on the herding of yellowfin sole. Fourth, we examine how the annual biomass estimates of yellowfin sole determined from EBS trawl survey data, and the deviations between these estimates and those produced by the yellowfin sole stock assessment model (Wilderbuer et al.[1]), are correlated with wave heights that the vessels encountered during the surveys. Finally, we consider the significance of these findings in terms of fisheries stock assessments.

Materials and methods

Description of the EBS survey trawl

The EBS survey trawl, known as the 83-112 Eastern trawl, is a low-rise, 2-seam flatfish trawl designed for use on a smooth, soft sea bottom. A detailed description is of its design and construction is presented in Stauffer (2004), however several aspects of its design are important for this study and are considered below (Fig. 1). The nylon net has a 25.5-m headrope and 34.1-m footrope which is 5.2 cm in diameter and constructed of wire rope with a single wrap of both polypropylene line and split rubber hose, but without bobbins or rollers to allow it to better conform to the smooth bottom in the EBS. The net is attached to a pair of 55-m wire bridles that are joined together and attached to a single 12.2-m wire door leg extension, which, in turn, is connected to two, 3-m chain door legs attached to 816-kg steel "V" doors (Fig. 1). Although this length of door leg extension is typical for many EBS survey vessels, door legs are custom built for each charter vessel and can vary from 8 to15 m. Henceforth, when bridle measurements are specified aft of the doors, they include the length of the door extension for a specific vessel but exclude the lengths of the tail chains, which are standard for all vessels.

Wave height and vessel motion

Experimental design An experiment to estimate the performance of the survey trawl at various levels of wave height was conducted in the EBS from 14 through 25 September 2003 aboard the chartered 38-m commercial stern trawler FV *Vesteraalen*. Because wave heights cannot be predicted sufficiently far in advance to plan a study of wave height, the experimental tows were completed opportunistically, in 2 parts, while the vessel was engaged in other studies. The first part, located near 55°58′N, 162°55′W at a depth of 82 m, consisted of repetitive trawl tows that were 5 min in duration, measured from the time the trawl first contacted the bottom to the time the footrope left the bottom by using a bottom contact sensor (BCS; Weinberg and Somerton, 2006). The second part, located near 55°10′N, 166°15′W at a depth of 115 m, consisted of repetitive tows that were 15 min in duration. During both parts, all operating procedures, except tow duration (standard survey tow duration is 30 min) and the use of open codends, were consistent with EBS trawl survey sampling protocols (Stauffer, 2004).

Various aspects of trawl geometry were measured on all tows. Along the footrope, the distance between the footrope and the seafloor (off-bottom distance) was measured to the nearest centimeter, at 1.5-s intervals and at 5 positions by placing BCS units at the center of the footrope, at 3 m to both sides of the center (the footrope corners), and on each wing 1 m behind the wing tip (Fig. 1). Along the bridles, off-bottom distance was measured at 6 positions by placing BCS units on the lower bridle at distances of 25, 40, and 50 m forward of the wing tip on both port and starboard sides of the trawl (Fig 1; measurements were made at all 11 positions simultaneously). The BCS units measure the tilt angle between their points of bottom contact and their points of attachment to the trawl and were individually calibrated to allow prediction of off-bottom distance from tilt angle. Description of the BCS units and the methods for attaching them to the footrope and bridles are described in Weinberg and Somerton (2006).

Heave (vertical movement in centimeters), pitch (angular motion on the along-vessel axis to the nearest 0.1°), and roll (angular motion on the across vessel axis to the nearest 0.1°) were measured with a heave, pitch, and roll sensor (Teledyne TSS Ltd.,[2] Watford, UK) at 1-s intervals. The sensor, which was positioned near the center of motion of the vessel, allowed prediction of heave at one remote position on the vessel based on the x, y, and z coordinates of this position in relation to the sensor. We chose this position as the location where the starboard warp passed over the stern trawl

[1] Wilderbuer, T. K., D. G. Nichol, and J. Ianelli. 2015. Assessment of the yellowfin sole stock in the Bering Sea and Aleutian Islands. *In* Stock assessment and fishery evaluation report for the groundfish resources of the Bering Sea/Aleutian Islands regions, p. 733–820. North Pacific Fishery Management Council, Anchorage, AK. [Available from website.]

[2] Mention of trade names or commercial companies is for identification purposes only and does not imply endorsement by the National Marine Fisheries Service, NOAA.

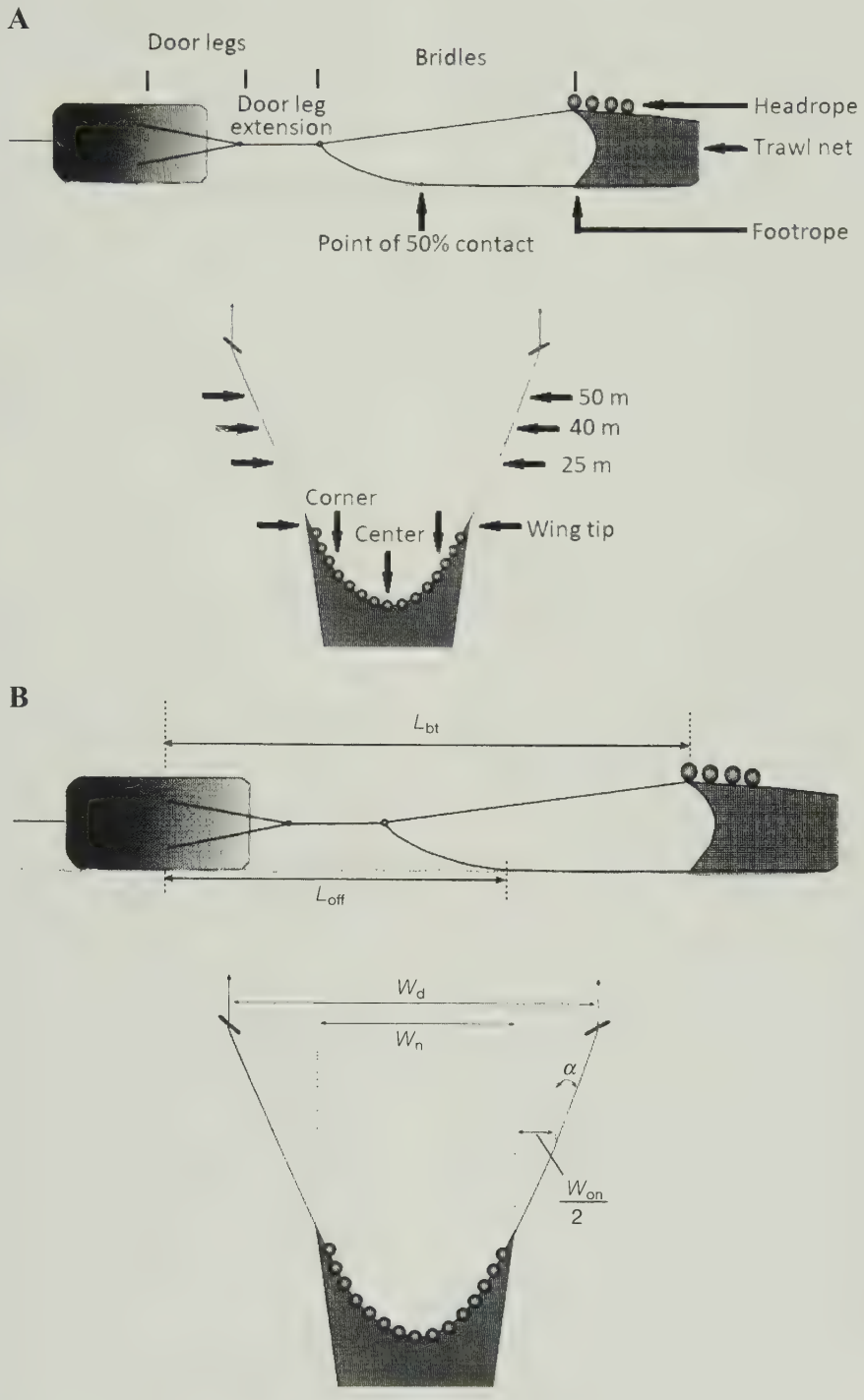

Figure 1

(**A**) Schematic diagram of the 83-112 Eastern survey trawl used in an experiment conducted in the eastern Bering Sea during September 2003, shown from the side (upper diagram) and from above (lower diagram). Various trawl components referred to in the text are identified in the upper diagram. Placement locations of bottom contact sensors along the lower bridles and footrope are indicated by arrows in the lower diagram. (**B**) Diagram showing the trawl dimension variables used in the catch ratio model to describe how wave height can influence herding of yellowfin sole (*Limanda aspera*).

block (i.e., the last point of contact between the vessel and the warp) and measured its coordinates relative to the heave sensor with a surveyor's tape. In addition, 2 measures of sea state, swell height and wave height, were estimated by the vessel captain during each tow. Recognizing that these are subjective estimates, we did not try to disentangle the exact meanings of the 2 values, but instead followed the approach of Stewart et al. (2010) and simply added them together to create a composite value of sea state, henceforth referred to as wave height. In addition, the captain estimated the wave direction and determined the angular difference between wave direction and vessel heading. This directional difference was recorded both as a numeric value (i.e., the absolute value of the cosine of the angle between the 2 directions) and as a relative value (i.e., the vessel heading either toward or away from the wave direction).

Analysis of wave height, vessel motion, and trawl motion data The data for each tow consisted of 1) wave height and the difference between wave direction and vessel heading, 2) remote heave at the trawl block, and 3) off-bottom distances at each of the 11 positions along the lower bridles and footrope. Mean and standard deviation of the heave and off-bottom measurements were computed for each of the 62 tows but the number of off-bottom values varied among the measurement positions because of occasional malfunction of some BCS units. Henceforth, the standard deviation of the heave at the trawl block (SDH) will be used as a measure of vessel motion.

We examined whether SDH is influenced by variables other than wave height, in particular, the numeric and relative differences between vessel heading and the wave direction, by including both variables, along with wave height, in a linear model (using the function lm in R, vers. 2.0.0; R Development Core Team, 2004) of SDH. Analysis of variance was used to test for the significance of the terms. Nonsignificant variables were removed and the model was re-fit sequentially until all remaining variables were significant. In addition, we used linear models to examine whether the mean and standard deviation of off-bottom measurements at each BCS position were influenced by SDH, using analysis of variance to test the significance of SDH.

Because the driving variable for movement of the vessel, and potentially the trawl, was surface waves, the time series of vertical measurements from each trawl location can display periodic oscillations. As did O'Neill et al. (2003) and Politis et al. (2012), we assumed that coherence in the period of oscillations between the vessel and the various measurement locations on the trawl indicated that surface waves were the causative agent of trawl motion. Therefore, for some tows, measurements of heave and off-bottom distance were subjected to spectral analysis (spectrum function in statistical software S+, vers. 6.2, TIBCO Software, Inc., Palo Alto, CA; Venables and Ripley, 1994) to determine the major period of oscillation. The period was estimated as the inverse of the frequency at the spectral peak, multiplied by the sampling interval (the sampling interval differed among the various types of data).

Wave height and herding of yellowfin sole

Experimental design Flatfish are typically herded into the net path by direct contact with or close approach of the lower bridles. The proportion of the fish within the bridle contact area (i.e., area of the bottom contacted by the bridles) that are herded into the net path can be determined by using a herding experiment (Engås and Godø,1989) in which the size of the bridle contact area is varied by repeatedly conducting trawl hauls with varying bridle lengths. In previous experiments with a survey trawl, this species was strongly herded (~60% of fish within the contact area were herded into the trawl path; Somerton and Munro, 2001), therefore yellowfin sole was considered a good candidate species for examining the influence of surface waves on herding.

An experiment to examine the effects of surface waves on the herding of yellowfin sole, patterned after the experiments described in Somerton and Munro (2001), was conducted aboard the 56.7 m stern trawler FV Cape Flattery during 11–16 August 2016 in the EBS near 60°33′N and 170°29′W. On each day of the experiment, 3 paired tows were completed according to all EBS survey operating protocols (Stauffer, 2004), except that for one tow of each pair, 27.4-m bridles were used, and for the other tow of the pair, 82.3-m bridles were used, instead of the standard 54.9-m bridles. The tow order of each bridle length was alternated in successive pairs to help reduce the potential for a tow order effect. Although the tow direction of each pair could vary with wind and wave direction, tow direction within each pair was always identical. During each tow, net and door spread was measured to the nearest 0.1 m with an acoustic mensuration system (Marport Deep Sea Technologies Inc., Saint John's, Canada) and tow length was measured with GPS from the first to last bottom contact of the footrope, determined by using a BCS. Yellowfin sole were sorted from each catch and collectively weighed but not counted. Catch weight in each tow was later standardized by dividing by the swept area of the net (i.e., net width multiplied by tow length). Swell and wave heights were also estimated for each tow and, as in the previous experiment, were summed together and referred to as "wave height." However, unlike the earlier sea-state experiment, we did not have a heave recorder and therefore wave height was used as the descriptor of sea state. Over the 6 d of the experiment, 18 pairs of tows were completed.

Analysis of the herding data An index of the strength of herding for each pair of tows was calculated as the catch ratio (i.e., the standardized catch from the long bridle tow divided by that of the short bridle tow in each tow pair). Because the 2 bridle lengths result in a strong contrast in bridle contact area, any factor that

reduces either the size of the bridle contact area or the effectiveness of herding within the area will have a greater impact on the catch from the longer bridle and should result in a decrease in catch ratio. Thus, to determine whether herding is influenced by wave height, we used linear modeling (function lm in R) to examine whether the catch ratio was significantly related to wave height.

Modeling the mechanism of wave influence on catch ratios of yellowfin sole

We propose the following model to describe how the catch ratio could vary with wave height. Starting with the trawl catch model presented in Somerton et al. (2007), a trawl catch can be expressed as a function of trawl measurements (see Fig. 1B for definitions) and other variables:

$$C = k_n(w_n + h(w_{on}))DL, \quad (1)$$

where C = catch in weight;
w_n = net path width;
w_{on} = width of the path contacted by the bridle;
D = fish density;
L = tow length;
k_n = proportion of fish within the net path width that are captured; and
h = proportion of fish within the bridle contact area that are herded into the net path.

However, to better describe how sea state may affect the catch, it is simpler to express the relationship in terms of the bridle lengths and the bridle angle of attack (α). To do this, w_{on} is redefined as

$$w_{on} = 2sin(\alpha)\ (L_{bt} - L_{off})\ , \quad (2)$$

where L_{bt} = bridle length including the length of the tail chain extensions connecting the doors to the bridles. The tail chain extensions used in the herding experiment were 12 m.
L_{off} = distance between the door and the point along the bridle where bottom contact is maintained 50% of the time; and
α = bridle angle of attack.

The angle of attack can be calculated for each tow as

$$\alpha = \sin^{-1}\left(\frac{w_d - w_n}{2L_{bt}}\right). \quad (3)$$

Assuming that D and k_n are approximately constant for each pair of tows, then the catch ratio (R) can be expressed as

$$R = \frac{C^l}{C^s} = \frac{w_n + h(2\sin(\alpha)(L^l_{bt} - L_{off}))}{w_n + h(2\sin(\alpha)(L^s_{bt} - L_{off}))} \quad (4)$$

where the superscripts l and s represent the long and short bridles.

In this expression C^l, C^s, w_n, α, L^l_{bt} and L^s_{bt} are measured for every pair of tows, however h and L_{off} need to be estimated by using data from separate experiments. Estimates of these parameters are available from previous studies of the survey trawl and its operation on yellowfin sole (Somerton and Munro, 2001); these are h=0.58 and L_{off}=36 m. However, the estimate of L_{off} is available only for standard length bridles, not the 2 lengths used in our herding study. Consequently, as in the original study, we assumed L_{off} is constant at all experimental bridle lengths, but only at zero wave height. At wave heights >0, we assumed that L_{off} increases linearly with wave height, but at a rate that differs between bridle lengths. With these changes the wave-height–dependent herding model becomes

$$R = \frac{C^l}{C^s} = \frac{w_n + 0.58(2\sin(\alpha)(L^l_{bt} - (36 + k^l H)))}{w_n + 0.58(2\sin(\alpha)(L^s_{bt} - (36 + k^s H)))}, \quad (5)$$

where H = the estimated wave height; and
k^l, k^s = coefficients regulating the influence of wave height on L_{off} for the long and short bridles.

With this formulation, we are assuming that the only influence of wave height on herding is that of decreasing the length of the bridle in contact with the bottom, which happens differently for the long and short bridles. The choice in the form of the wave height effect was, in part, guided by the results of the sea state and trawl performance study, which will be considered later. Note that when H=0, L_{off} becomes identical to the experimentally measured value and is identical for long and short bridle lengths. Therefore, the model has 2 unknown parameters; that is, k^l and k^s. To estimate these parameters we considered the right side of the above equation as a predicted value of the catch ratio and minimized the sum of the squared differences between the observed and predicted catch ratios over the 18 paired tows, using nonlinear minimization (R function nlm).

Variation in survey abundances of yellowfin sole with wave height

The abundance of yellowfin sole in the EBS survey area is estimated annually with the EBS survey by using the swept-area method applied to each of the 356 stations located at the centers of a rectangular sampling grid (Conner and Lauth, 2016). Annual abundance is estimated by multiplying the estimates of local density (i.e., catch/trawl swept area) by the area of each grid square and then summing over all grid squares. A variety of environmental parameters are also measured at each sampling site, including swell and wave heights estimated by the vessel captain, which again were summed and referred to as wave height. Although the survey time series began in 1982, the wave height data have only been available since 2005. For each year of data, wave height was averaged over all sampling sites where yellowfin sole were caught.

To determine whether the abundance estimates from the yellowfin sole survey were influenced by variation in wave height, perhaps because wave height influenced trawl sampling efficiency, we modeled the survey abundance estimates as a linear function of mean

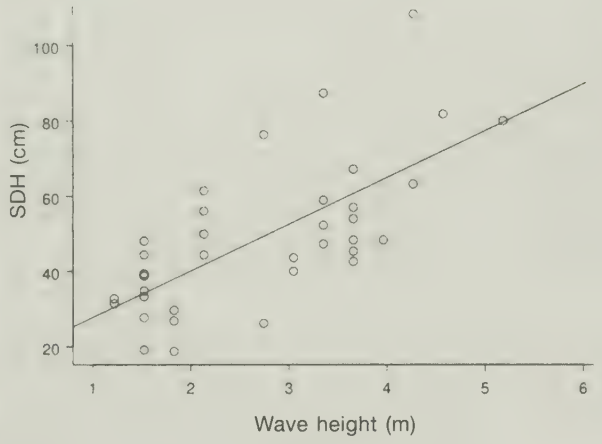

Figure 2

Standard deviation of vessel heave (SDH), in centimeters, at the starboard trawl block, plotted against wave height, in meters, estimated by the captain of FV *Vesteraalen*. Data were obtained from an experiment conducted in the eastern Bering Sea during September 2003. The solid line shows the regression of SDH on wave height, excluding consideration of vessel heading relative to wave direction.

wave height (R function lm) and tested the significance of the slope, using standard methods. However, it is possible that factors, such as a temporal change in population structure, could influence this relationship. Therefore, to better isolate interannual changes due to waves from more gradual changes, we calculated the deviations between the survey abundance estimates and the abundance estimates produced by the yellowfin sole stock assessment model (Wilderbuer et al.[1]), then modeled the deviations as a linear function of mean wave height. The estimates of abundance from the models we used are slightly different from those reported in Wilderbuer et al.[1] because the version of the model used for stock assessment included an environmental correlate (mean bottom temperature). Because we were examining the influence of another environmental correlate, we fitted the model without the temperature effect to produce the model estimates of survey abundances used in our analysis.

Results

Vessel motion and wave height

Vessel motion, expressed as the SDH, increased significantly with the estimated wave height (Fig. 2, Table 1). However, SDH was not significantly related to either the numeric or the binary measure of the alignment of vessel heading and wave direction.

Table 1

The relationship between the standard deviation of vessel heave at the trawl block with the 3 predictor variables from results of an experiment conducted in the eastern Bering Sea during September 2003. The predictor variables are 1) wave height (summed values of wave and swell heights estimated by the vessel captain), 2) alignment (alignment of vessel course and wave direction, i.e., absolute value of the cosine of the angle between the 2 directions) and 3) relative direction (vessel course either away from, ±180°, or into the direction of wave travel).

	Coefficient	*P*-value
Intercept	14.10	0.071
Wave height	11.98	<0.001
Alignment	–2.86	0.259
Relative direction	0.07	0.500

Bridle and footrope distances off bottom

Off-bottom distance measurements along the lower bridles and footrope oscillated with a period nearly identical to that of vessel motion. For example, on one haul, which had a wave height of 5.3 m, the heave oscillation period (5.13 s) was nearly identical to that for the periods measured at all trawl positions, both along the bridles (50 m, 5.16 s; 40 m, 5.12 s; 25 m, 5.12 s) and along the footrope (wing, 5.16 s; corner, 5.16 s; center, 5.16 s). At low levels of SDH, however, spectral peaks were harder to identify, and the variability among positions increased. This finding indicates that, at least for relatively high waves, vessel motion is detectable throughout the trawl and substantiates the notion that surface waves influence trawl performance.

The magnitude of the trawl oscillatory movement, expressed as the standard deviation of off-bottom distance, increased significantly with SDH at all trawl positions, except at the wings. The magnitude of the increase (slope of the regression line) varied with position (Fig. 3, Table 2). The smallest increase in SDH occurs at the wings, consistent with the design of the survey trawl that produces the maximum bottom contact, and presumably strongest downward force at the wing tips. Away from the point of maximum bottom contact, both forward along the bridles and aft along the footrope, the standard deviation of off-bottom distance increases as the constraints on vertical motion, such as tension and bottom contact, lessen. At the 50-m bridle position, where the bridle rarely contacts the bottom, the oscillations were the largest (Table 2).

The mean distance off bottom also varied among trawl positions; however, its increase with SDH was only significant at the 40-m bridle position (Fig. 4, Table 3). At the wing and the 25-m bridle positions, the downward forces keep the mean off-bottom distance

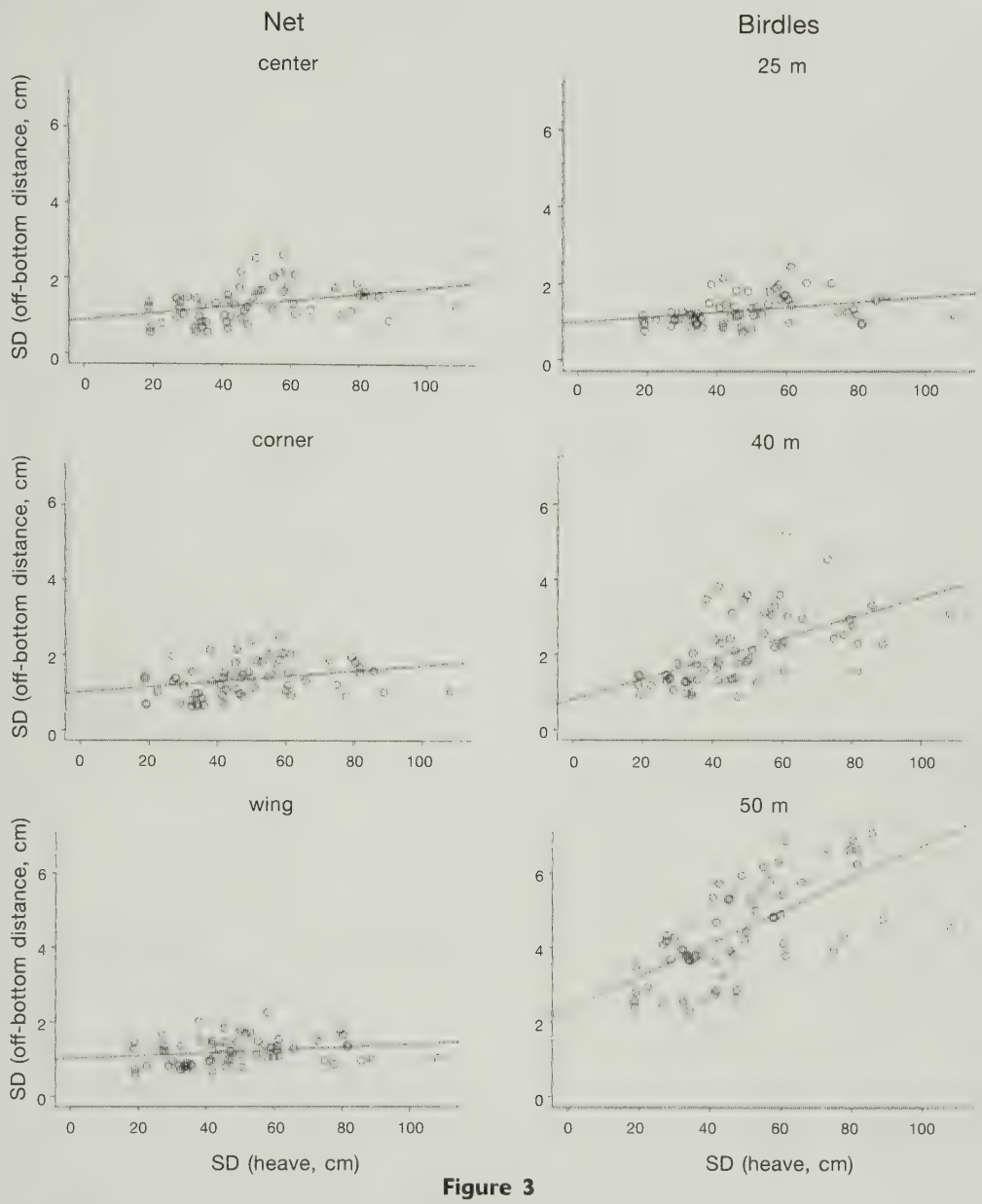

Figure 3

The standard deviation of off-bottom distance, in centimeters, plotted against the standard deviation of vessel heave, in centimeters, at the starboard trawl block for each of 6 positions along the lower bridles and footrope, from the footrope center to the 50-m bridle position, from an experiment conducted in the eastern Bering Sea during September 2003. The line on each plot is the regression of the standard deviation of off-bottom distance on the standard deviation of heave. Slope of the line indicates the relative sensitivity to vessel motion of the footrope and bridles at each position.

relatively insensitive to changes in SDH; however at the 40-m bridle position the constraints on vertical motion are less and the mean off-bottom distance increases with wave height. At the 50-m bridle position, the vertical oscillations are apparently unconstrained by the bottom, so that the mean off-bottom distance is independent of SDH.

One consequence of the progressive sensitivity of mean off-bottom distance to SDH with increasing distance from the wing tips (at least out to 40 m) is that the length of the bridle in contact with the bottom must decrease with SDH. To show this, we evaluated equations predicting off-bottom distance (Table 3) at the wing, and at the 25 m, 40 m, and 50 m bridle posi-

Table 2

Slope, intercept, and *P*-value for linear regressions of vertical motion, expressed as the standard deviation of off-bottom distance (in centimeters) at various positions along the lower bridles and footrope, against vessel motion, expressed as standard deviation of vessel heave at the trawl block from an experiment conducted in the eastern Bering Sea during September 2003.

Position	Intercept	Slope	*P*-value
Center	0.893	0.0087	0.005
Corner	1.016	0.0071	0.019
Wing	1.022	0.0038	0.103
Bridle—25 m	0.997	0.0066	0.0073
Bridle—40 m	0.803	0.0274	<0.001
Bridle—50 m	2.349	0.0439	<0.001

tions at 5 levels of SDH (0, 20, 40, 60, 80 cm) and then plotted the predicted off-bottom distances as a function of SDH (Fig. 5). Comparing the off-bottom distances in this way emphasizes that, in terms of a mean response, the primary influence of SDH on off-bottom distance occurs in the region between the 25- and 40-m positions, which is near the point where the bridle leaves the bottom in calm conditions (~31 m from the wing; Somerton and Munro, 2001). If a value of off-bottom distance is specified as a critical value for herding (e.g., in Fig. 5 a value of 2.5 cm is used), then as SDH increases, the bridle position at the critical value of off-bottom distance moves toward the wing tip, reducing the area exposed to herding.

Although the change in the mean off-bottom distance at the center and corner positions on the footrope are not significant, the slopes of the regressions are nearly as large as those at the 40-m bridle positions (Table 3), but there is more haul-to-haul variability. This relationship indicates that the oscillations are also likely to impact escapement along the footrope.

Influence of wave height on the herding of yellowfin sole

In the yellowfin sole herding experiment, the catch ratio declined significantly with increasing wave height (R=1.96 – (0.51×wave height), P=0.038, coefficient of determination [r^2]=0.24; Fig. 6). Because the catch ratio was based on pairs of tows taken near each other, in the same direction, and in quick succession, essentially all influences on catch were kept constant, except that of bridle length. Therefore, the decrease in catch ratio with increasing wave height indicates that herding was decreased.

Our hypothesized model expressing the influence of wave height on catch ratio is shown below with the estimated values of k^l and k^s:

$$R = \frac{w_n + 0.58(2\sin(\alpha)(L_{bt}^{l} - (36 + 2.29H))}{w_n + 0.58(2\sin(\alpha)(L_{bt}^{S} - (36 + 0.042H))}.$$

The estimated value of k^l is considerably larger than k^s, confirming the notion that the impact of wave height would be stronger for the long bridles. However, the fit of the model to the catch ratios was poorer (r^2=0.12) than the fit of the wave height data itself to the catch ratios (r^2=0.24). This result indicates that either the model was incorrectly specified, perhaps lacking other important factors influenced by wave height, or that the fixed parameter estimates (i.e., h and L_{off}) obtained from previous studies were biased.

Influence of wave height on annual estimates of yellowfin sole abundance

The biomass of yellowfin sole estimated by the EBS bottom trawl survey, during the period 2005–2016, declined significantly with an increase in the mean wave height (biomass=3.37 – (0.67×wave height), P=0.028, r^2=0.40; Fig. 7). The deviations between the survey biomass estimates and those produced by the yellowfin sole stock assessment model, during the same time period, also declined significantly with an increase in the mean wave height (deviation=1.11 – (0.19 ×wave height), P=0.044, r^2=0.35; Fig. 7). This result indicates that wave height, perhaps through its apparent effect on herding, may produce a detectable bias in the annual estimates of yellowfin sole abundance in the EBS.

Discussion

Wave height and vessel motion

It is clear that wave height influences vessel motion. This was shown by the strong correlation of SDH with estimated wave height. However, SDH was insensitive to vessel heading relative to wave direction, which is counterintuitive to most observers standing on the deck of a vessel. An alternate measure of vessel motion proposed by Politis et al. (2012) divides heave by time to create a measure of vertical speed, which is sensitive to vessel heading relative to the waves. We chose SDH as a measure of vessel motion because it is consistent with the subjective estimates of wave heights now provided by vessel captains and which are the basis of our time series of sea states encountered during trawl surveys.

An objective, repeatable, measure of wave height obtained with a vessel heave sensor is definitely preferred to the subjective estimates now provided by vessel captains. Although heave sensors are nearly always included in the instrument suite on fishery research vessels, all NOAA bottom trawl surveys conducted by chartered fishing vessels along the U.S. West Coast do not use heave sensors (Stauffer, 2004); therefore the only available information on sea-state is the wave and swell heights estimated by the vessel captains. Such estimates are inadequate because they are subjective, likely to vary among vessel captains, and do not capture variability in vessel motion introduced by factors

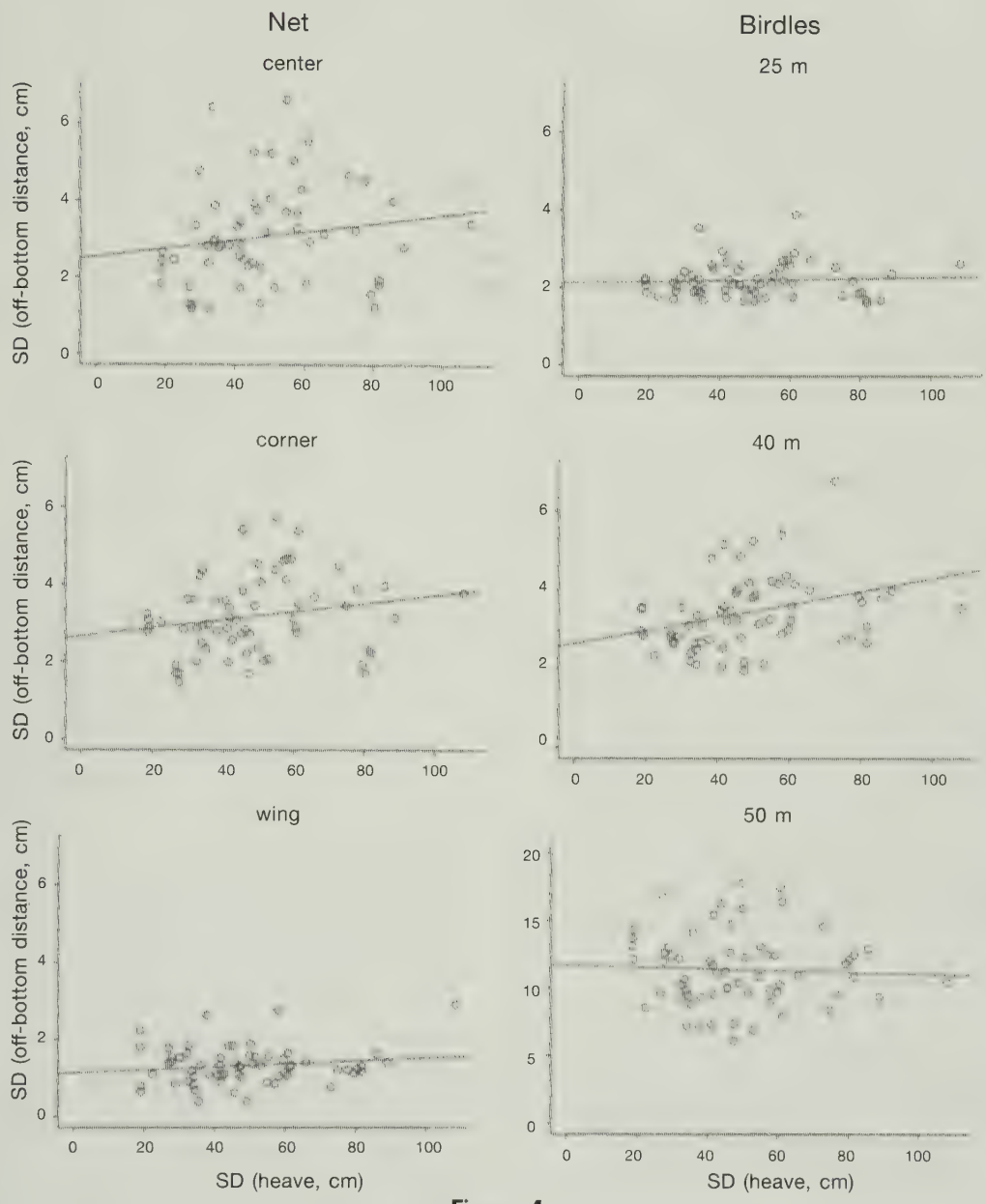

Figure 4

Mean off-bottom distance, in centimeters, plotted against the standard deviation of vessel heave, in centimeters, at the starboard trawl block for each position along the lower bridles and footrope, from the footrope center to the 50-m bridle position, from an experiment conducted in the eastern Bering Sea during September 2003. The line on each plot is the regression of the mean off-bottom distance on the standard deviation of heave. Slope of the line indicates the relative sensitivity to vessel motion of the footrope and bridles at each position.

such as vessel size and trawling procedures. As in previous studies of the influence of sea-state on bottom trawl surveys (Stewart et al., 2010; Politis et al., 2012), we emphasize the need to measure vessel motion directly on all trawl survey vessels.

The coherence between the vertical oscillations of the vessel and the vertical oscillations at all measured positions along the bridles and footrope of the trawl indicate that, at least in high waves, vessel motion is transmitted down the warps and throughout the trawl. O'Neill et al. (2003) and Politis et al. (2012) used similar methods to ours and obtained similar results. For bottom trawl surveys, however, the important question is how these oscillations influence sampling efficiency.

Table 3

Slope, intercept, and *P*-value for linear regressions of the mean distance off-bottom, in centimeters at various positions along the lower bridles and footrope, against vessel motion expressed as the standard deviation of vessel heave at the trawl block from an experiment conducted in the eastern Bering Sea during September 2003.

Position	Intercept	Slope	*P*-value
Center	2.537	0.0111	0.197
Corner	2.664	0.0106	0.101
Wing	1.136	0.0039	0.223
Bridle—25 m	2.133	0.0013	0.665
Bridle—40 m	2.642	0.0165	0.017
Bridle—50 m	11.661	-0.0063	0.722

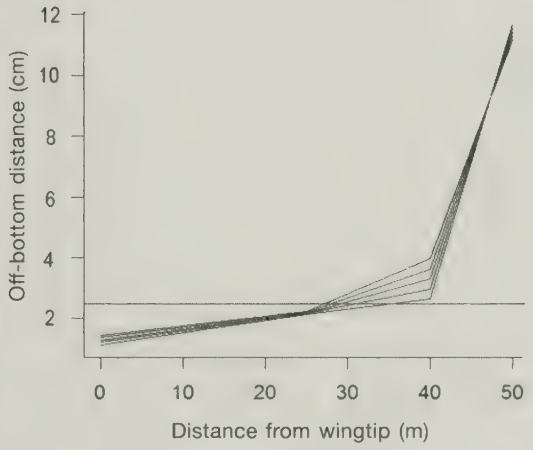

Figure 5

Predicted off-bottom distance at the 0-, 25-, 40-, and 50-m positions on the lower bridles by using the parameters in Table 3. Predictions were made at 5 levels of vessel motion (standard deviation of vessel heave [SDH] at the starboard trawl block: 0, 20, 40, 60, 80 cm) spanning the values observed during the experiment conducted in August 2016 to examine the effect of wave height on herding of yellowfin sole (*Limanda aspera*). In the region between 25 and 40 m, the top line corresponds with an SDH of 80 cm, and the bottom- line corresponds with an SDH of 0. The horizontal line represents a hypothetical reference level of off-bottom distance, 2.5 cm, above which the bridle no longer elicits herding of yellowfin sole. As SDH increases, the point along the bridle where herding ceases (i.e., the intersection point of the horizontal and diagonal lines) moves progressively toward the wings.

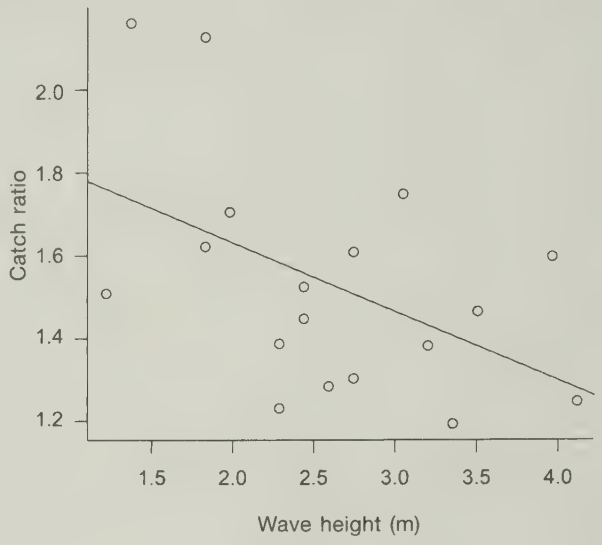

Figure 6

Ratio of the standardized catch from the long bridle tow to that from the short bridle tow in the experiment conducted in August 2016 to examine the effect of wave height on herding of yellowfin sole (*Limanda aspera*), plotted against the sum of the estimated wave and swell heights in meters. The slope of the regression line is significant (P=0.038).

For the 83-112 Eastern trawl, one important effect of the oscillations is that they result in an increase in the mean off-bottom distance at the bridle position that is most influential in determining the size of the bridle contact area. Prior studies of herding by the survey trawl conducted in calm conditions indicate that the off-bottom distance of the lower bridle increases forward of the wing tips and at ~31 m reaches an off-bottom distance sufficiently large that the bridle no longer elicits herding behavior of flatfish (Somerton and Munro, 2001). Our study on the change in mean off-bottom distance with SDH along the lower bridles indicates that at 25 m the downward forces are sufficient to inhibit a change in off-bottom distance with increasing SDH; however at 40 m the change is the highest of all measured positions. As a consequence, the length of the bridle in contact with the bottom, and the size of the area exposed to herding stimuli, will decrease with increasing SDH (Fig. 5).

Another likely effect of SDH is on escapement under the footrope. Studies show that the central portion of the footrope is the aggregation point of herded flatfish and where most escapement occurs (Main and Sangster, 1981). In addition, escapement of flatfishes under the footrope of the survey trawl has been shown to increase as the off-bottom distance increases at the center of the footrope (Weinberg et al., 2002). Consequently, any factor that increases footrope off-bottom distance should increase escapement, and although not

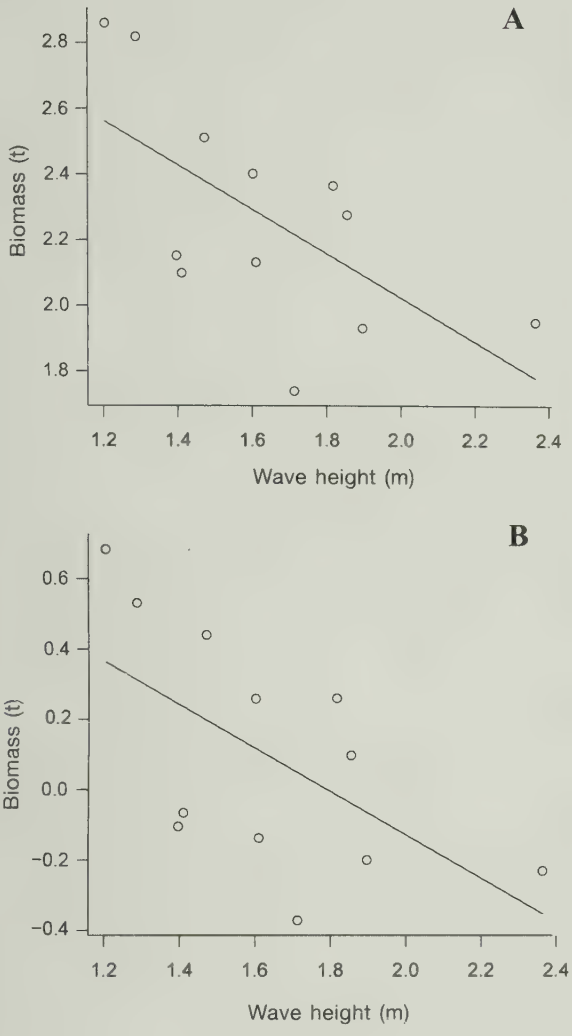

Figure 7

(**A**) Swept-area biomass, in metric tons (t), of yellowfin sole (*Limanda aspera*) estimated by the bottom trawl survey conducted in the eastern Bering Sea by the National Marine Fisheries Service during 2005–2016, plotted against the sum of the estimated wave and swell heights, in meters, averaged over all stations where yellowfin sole were caught. The slope of this regression line is significant (P=0.028). (**B**) Deviations between the swept-area biomass estimates and the biomass predicted by the stock assessment model for yellowfin sole in relation to wave height. The slope of the regression line is significant (P=0.044).

significant, the increase in the off-bottom distance at the center and corner portions of the footrope indicate that escapement is likely also affected by sea state.

Besides their effect of changing mean distance off-bottom, the vertical oscillations undoubtedly have a pronounced effect on fish escapement and herding behaviors. The studies of both O'Neill et al. (2003) and Politis et al. (2012) show that the oscillations we measured in terms of off-bottom distance also produce oscillations in trawl speed. Such oscillations were shown to be the principal mechanism for the increase in escapement from the codend mesh with increased sea-state, both by changing mesh geometry and by altering fish behavior (O'Neill et al., 2003). However, we have no direct evidence of how either the vertical oscillations of the footrope and bridles on the survey trawl or the likely oscillations in speed influence the escapement or herding behavior of yellowfin sole.

Influence of wave height on the herding of yellowfin sole

Based on the results of the yellowfin sole herding experiment, the ratio of the standardized catches from long and short bridle tows clearly declined with increasing wave height. Because the paired design of the bridle experiment was intended to minimize all influences other than bridle length, the decline in catch ratio shows that sampling efficiency declined with increasing wave height. We suspect this result is due to diminished herding.

We proposed a model to predict how catch ratio could vary as a function of wave height to explore possible mechanisms to explain the observed change in catch ratio. This model focuses on the change in bridle contact area with increasing SDH described earlier. Although the model does predict a decrease in catch ratio with increasing SDH, it explains only half of the variability in catch ratio that is explained by a simple linear regression on SDH. One reason for the poor fit is that the model considers herding to be a product of the bridle contact area and the efficiency of herding within this area. Therefore, parameters affecting the bridle area (L_{off}) are confounded with parameters affecting the efficiency of herding (h) within the bridle contact area, and a priori estimates of at least one is needed to obtain a tractable solution. The values we used for these two parameters were obtained from an experiment conducted in relatively calm conditions (Somerton and Munro, 2001) and may well be biased when applied to rougher sea-state conditions. Furthermore, the estimate of L_{off} was obtained from an experiment in which only standard length bridles were considered (Somerton and Munro, 2001). We applied this value to bridles both longer and shorter than the standard length with some hesitancy, although in a similar study in which off-bottom distances were measured along 3 lengths of bridle on a bottom trawl, this value was found to be reasonable (Somerton, 2003). In addition to these issues, we were concerned that the herding process during high waves may be fundamentally different from that in calm water. For example, when the bridle experiences increased tension and lifts off the bottom, we assumed in our model, that the effect is to momentarily shorten the length of the bridle in contact with the bottom and thereby decrease the area of herding. However, the vertical motion itself

may create a greater herding stimulus than a similar length of bridle in calm water. If so, then the efficiency of herding within the bridle contact area, which was assumed to be constant, would also be influenced by wave height. Further research is needed to better define these parameters and determine how they might change at higher sea states.

Estimated abundance of yellowfin sole and its relation to wave height

The abundance of yellowfin sole estimated by the annual bottom trawl survey clearly declines with an increase in mean wave height (Fig. 7)—a finding that is consistent with wave height effects reported for the NOAA West Coast bottom trawl survey (Stewart et al., 2010). In addition, the deviations between the survey estimates and assessment model estimates of abundance also decline with an increase in mean wave height (Fig. 7). The question is whether these associations establish causation. We have shown that increased wave height results in a reduction in the bridle contact area, which should reduce the herding of flatfish. We also confirmed this notion by providing evidence that increased wave height reduces the sampling efficiency of yellowfin sole, presumably owing to the reduction in herding. However, a decrease in herding by itself may not exert a sufficiently strong effect to account for the observed decline in estimated yellowfin sole biomass because during normal survey conditions only ~30% of a flatfish catch comprises herded fish (Somerton et al., 2007). However, the potential effects of wave height on sampling efficiency could be much larger if escapement under the footrope is considered.

Although our experimental evidence showed that the mean off-bottom distance at all points on the footrope did not increase significantly with SDH, the magnitude of the change was still strong enough to potentially allow greater escapement. Coupled with both the oscillations in off-bottom distance and, likely, trawl speed, we suspect that footrope escapement increases with SDH, but we have no experimental evidence to prove this.

Exactly how the vertical and horizontal oscillatory motion of the footrope and bridles influences fish behavior is unknown. However, the study of O'Neill et al. (2003) on codend mesh escapement has shown that oscillations in trawl speed produce changes in fish behavior, as well as changes in net geometry. Consequently, footrope escapement and bridle herding may be quite different in an elevated sea state from what has been reported for relatively calm water (Somerton et al., 2007) and this difference may be the primary reason why we obtained such a poor fit of our model to the experimental catch ratio data.

Even with the potential for increased footrope escapement to compound the apparent influence wave height has on sampling efficiency of the survey trawl, the observed decrease in yellowfin sole biomass estimates with increased wave height may also reflect other influences. Wilderbuer et al.[1], in a stock assessment model for EBS yellowfin sole, determined that the trawl survey catchability function is temperature dependent and that the estimated stock abundance declines at colder temperatures. Two hypotheses were proposed for this: 1) sampling efficiency of the survey trawl is temperature dependent (i.e., yellowfin sole herd less or escape more in cold water) and 2) availability of this species to the survey is temperature dependent (i.e., more yellowfin sole remain in their shallow spawning areas, which are outside the survey area, during colder years). To complicate these hypotheses further, annual mean wave height and bottom temperatures in yellowfin sole areas are negatively correlated (Nichol[3]), and therefore perhaps both sampling efficiency and availability are involved. Regardless of which mechanism is ultimately responsible for the correlation between yellowfin sole abundance and wave height, the inclusion of either variable in the survey catchability function used in the yellowfin sole assessment model of the National Marine Fisheries Service will have a significant effect on the estimates of total allowable catch for this species. Therefore further research to clarify this issue is critically needed.

Acknowledgments

We thank B. Lauth, D. Nichol, and W. Palsson for reviewing the manuscript, D. Nichol for providing the EBS survey wave height and yellowfin catch data, and the captains and crew of the FV *Vesteraalen* and FV *Cape Flattery* for their help and expertise during the experiments. This research was funded, in part, by NOAA, National Marine Fisheries Service, Office of Sustainable Fisheries from their National Catch Share and Magnuson-Steven Act Implementation Funds.

Literature cited

Conner, J., and R. R. Lauth.
2016. Results of the 2013 eastern Bering Sea continental shelf bottom trawl survey of groundfish and invertebrate resources. NOAA Tech. Memo. NMFS-AFSC-331, 153 p. Tech. Memo.

Dickson, W.
1993. Estimation of the capture efficiency of trawl gear. I: Development of a theoretical model. Fish. Res. 16:239–253.

Engås, A., and O. R. Godø.
1989. The effect of different sweep lengths on the length composition of bottom-sampling trawl catches. ICES J. Mar. Sci. 45: 263–268.

Kimura, D. K., and D. A. Somerton.
2006. Review of statistical aspects of survey sampling for marine fisheries. Rev. Fish. Sci. 14:245–283.

[3] Nichol, D. 2016. Personal commun. Resour. Assess. Conserv. Eng. Div., Alaska Fish. Sci. Cent., Natl. Mar. Fish. Serv., 7600 Sand Point Way NE, Bldg. 4, Seattle, WA 98115-6349.

Main, J., and G. I. Sangster.
1981. A study of the fish capture process in a bottom trawl by direct observations from a towed underwater vehicle. Scott. Fish. Res. Rep. 23, 23 p.
Munro, P. T., and D. A. Somerton.
2002. Estimating net efficiency of a survey trawl for flatfishes. Fish. Res. 55:267–279.
O'Neill, F. G., S. J. McKay, J. N. Ward, A. Strickland, R. J. Kynoch, and A. F Zuur
2003. An investigation of the relationship between sea state induced vessel motion and cod-end selection. Fish. Res. 60:107–130.
Politis, P. J., J. T. DeAlteris, R. W. Brown, and A. T. Morrison III.
2012. Effects of sea-state on the physical performance of a survey bottom trawl. Fish. Res. 123:26–36.
R Development Core Team.
2004. R: a language and environment for statistical computing. R Foundation for Statistical Computing, Vienna, Austria. [Available from website, accessed October 2004.]
Somerton, D. A.
2003. Bridle efficiency of a survey trawl for flatfish: measuring the length of the bridles in contact with the bottom. Fish. Res. 60:273–279.
Somerton, D. A., and P. T. Munro.
2001. Bridle efficiency of a survey trawl for flatfish. Fish. Bull. 99:641–652.
Somerton, D. A., P. T. Munro, and K. L. Weinberg.
2007. Whole-gear efficiency of a benthic survey trawl for flatfish. Fish. Bull. 105:278–291.
Stauffer, G. (compiler).
2004. NOAA protocols for groundfish bottom trawl surveys of the nation's fishery resources. NOAA Tech. Memo. NMFS-SPO-65, 205 p.
Stewart, I. J., A. A. Keller, E. L. Fruh, V. H. Simon, and B. H. Horness.
2010. Throwing in the towel: when do adverse conditions dictate a weather day during a bottom trawl survey? Fish. Res. 102:130–140.
Venables, W. N., and B. D. Ripley.
1994. Modern applied statistics with S-plus, 462 p. Springer-Verlag, New York.
Weinberg, K. L., and D. A. Somerton.
2006. Variation in trawl geometry due to unequal warp length. Fish. Bull. 104:21–34.
Weinberg, K. L., D. A. Somerton, and P. T. Munro.
2002. The effect of trawl speed on the footrope capture efficiency of a survey trawl. Fish. Res. 58:303–313.

National Marine
Fisheries Service
NOAA

Fishery Bulletin
established in 1881

Spencer F. Baird
First U.S. Commissioner
of Fisheries and founder
of *Fishery Bulletin*

Embedding the effect of environmental conditions on recruitment and survival of the European anchovy (*Engraulis encrasicolus*): a Bayesian model with dual-time resolution

Margarita M. Rincón (contact author)[1]
Ignacio A. Catalán[2]
Samu Mäntyniemi[3]
Diego Macías[4]
Javier Ruiz[1]

Email address for contact author: margarita.rincon@icman.csic.es

[1] Department of Coastal Ecology and Management
Instituto de Ciencias Marinas de Andalucía (ICMAN)
Consejo Superior de Investigaciones Científicas (CSIC)
Campus Universitario Río San Pedro
11519 Puerto Real, Cádiz, Spain

[2] Institut Mediterrani d'Estudis Avançats (IMEDEA)
CSIC/Universitat de les Illes Balears (UIB)
Carrer de Miquel Marquès 21
07190 Esporles, Balearic Islands, Spain

[3] Fisheries and Environmental Management Group
Department of Environmental Sciences
University of Helsinki
P.O. Box 65
Viikinkaari 1
00014 Helsinki, Finland

[4] Sustainable Resources Directorate
Joint Research Centre
European Commission
Via Enrico Fermi 2749
21027 Ispra, Italy

Abstract—Many studies underscore the importance of incorporating the effect of environmental data within a life-history-stage–specific framework for determining the recruitment and survival of small pelagic fish. The recruitment of anchovy (*Engraulis encrasicolus*) in the Gulf of Cádiz (NE Atlantic) is sensitive to the effect of intense easterlies, stratification of the water column, and discharges from the Guadalquivir River on early life stages. As a proof of concept, we have developed the basis for a new Bayesian model with a dual time step resolution: monthly for juveniles and adults, and weekly for earlier life stages. This dual time step resolution resolves environmental effects on prerecruits while simulating the effect of fishing on recruits. Our estimates for juvenile abundances are validated with field data. The Bayesian framework accounts for the uncertainty, thus providing consistent length-frequency estimates and a plausible environmentally driven stock-recruitment relationship.

Manuscript submitted 19 January 2017.
Manuscript accepted 2 November 2017.
Fish. Bull. 116:34–49 (2018).
Online publication date: 13 December 2017.
doi: 10.7755/FB.116.1.4

The views and opinions expressed or implied in this article are those of the author (or authors) and do not necessarily reflect the position of the National Marine Fisheries Service, NOAA.

The physical and trophic environment affects fish stocks and landings (Lloret et al., 2001; Erzini, 2005), particularly for short-lived small pelagic species (Nakata et al., 2000; Guisande et al., 2004; Basilone et al., 2006; Lindegren et al., 2013). This effect is observed at different time scales (Fréon et al., 2005). Short-term synoptic events that last a few days and affect a relatively large area affect mostly the early life stages of fish. For small pelagic fish, stock dynamics are often more dependent on recruitment failure from mortality at early life stages than on variations in fishing effort (Cingolani et al., 1996; Dimmlich et al., 2004). Variability and instability characterize the dynamics of small pelagic fish (Fréon et al., 2005). Their position in the food web and the prominent role of recruitment in population dynamics partly explain the aforementioned dynamics. The inclusion of environmental drivers in predictive recruitment models for these (and other) species has been advocated in the past and is increasing (Barange[1];

[1] Barange, M. 2001. Report of the first meeting of the SPACC/IOC study group on "use of environmental indices in the management of pelagic fish populations"

Durant et al., 2013), but the adoption of these drivers for management is not widespread (Fréon et al., 2005; Fréon et al., 2009).

Intense easterlies, stratification of the water column, and the influence of the Guadalquivir river have been identified as the main environmental factors influencing early life stages of the European anchovy (*Engraulis encrasicolus*) (Ruiz et al., 2006) in the Gulf of Cádiz. The synoptic time-scales of these environmental forcing variables and the nature of the spawning process, with clear, spatially explicit components, suggest that egg and larval abundances can change drastically within a time scale of days (Catalán et al., 2006). Because many environmental databases are structured on a weekly basis, both the natural scale of the environmentally controlled recruitment process and the availability of data suggest that it is sensible to model these early stages at a weekly resolution.

However, for small pelagic fish, fishing-induced mortality may become a dominant element of population dynamics after recruitment (Pinsky et al., 2011; Lindegren et al., 2013). Fisheries data are frequently structured as monthly statistics in publicly available databases. Moreover, the availability of landing data or catch per unit of effort (CPUE) data and the decreased sensitivity of individual fish to short-term synoptic events suggest that it is sensible to model postrecruit processes with a time resolution longer than a week. The change of time scale for the natural processes governing the dynamics of clupeoids during ontogenetic development poses significant challenges for modeling purposes. Restricting the whole model to a resolution that is suitable only for postrecruits (e.g., monthly) would result in a model that misses the impact of oceanographic synoptic events on recruitment. These synoptic events have a time scale of the order of days but their potential impact can be devastating on the survival of eggs and larvae. Ruiz et al. (2009) parameterized the impact of synoptic events through the implementation of monthly averages. However, these averages may hide the real impact of synoptic events. For instance, in spring or summer, a period of several days of calm and sunny weather in the Gulf of Cádiz will result in a warming of the sea surface, thereby triggering spawning of species like anchovy. If this event is followed by days of intense easterlies, spawning will be lost by the advection of eggs by oceanic currents (Ruiz et al., 2006). The time-scale of these synoptic events (several days) cannot be resolved by the monthly averages implemented in Ruiz et al. (2009). A trivial option would be to select the maximum resolution (e.g., weekly) for the whole life cycle. However, this option may render the model numerically intractable owing to the large number of time steps involved. A dual resolution model, with shorter time steps for earlier stages, offers a compromise between the need to resolve the synoptic scale that forces both eggs and larvae and the need to keep the numerical burden tractable.

A dual resolution model should be able to encompass the change in time scales inherent with ontogenic development. However, the suitability of such a model does not imply the ability to resolve the intrinsic uncertainty that characterizes ecosystem dynamics. This uncertainty demands a probabilistic rather than a deterministic approach (Ruiz and Kuikka, 2012). In fishery research, state–space models, a kind of probabilistic model that describes the probabilistic dependence between the latent state variables and the observed measurements, coupled with Bayesian Markov Chain Monte Carlo (MCMC) methods, provide estimates of abundance while measuring the uncertainty pervasive throughout the life-cycle of individuals. State–space models separate the problem into two stochastic models (Meyer and Millar, 1999; Rivot et al., 2004). The first one, the process model, accounts for the unobservable stochastic variations that govern internal population dynamics. The second one, the observation model describes how the population state is observed and with what uncertainty. The linking of these two stochastic models provides consistent simulation of stock dynamics and computes uncertainty as a natural output (Punt and Hilborn, 1997; Millar and Meyer, 2000).

We describe the implementation of a state–space, size-structured population dynamics model for anchovy in the Gulf of Cádiz. For this model, it is assumed that the environment affects early stages of the life cycle at different time scales, and a von Bertalanffy growth process provides consistent recruitment and length-frequency estimates. The first section of this article is devoted to the description of the conceptual framework necessary to accommodate a dual resolution and environmentally forced formulation into the general population dynamics model (GPDM) described in Mäntyniemi et al. (2015). The second section describes the model outputs, and the third section presents a discussion regarding the validation of our hypothesis and the effectiveness of the proposed tool.

Materials and methods

For this study, we implemented a Bayesian state–space size-structured population dynamics model. This state–space model included 2 stochastic models, a process model and an observation model. The process model has two modules in order to integrate both environmentally forced recruitment and size-structured stock dynamics. The first one is applied in this study to the environmental conditions in the Gulf of Cádiz but could be extended to model the dynamics of other small pelagic fish species whose recruitment is mainly forced by the environment during their earliest life stages. The second module describes mainly growth and mortality processes. The observation model requires data on catch in numbers, CPUE, and acoustic surveys. The notation for data and model parameters is summarized in

(3–5 September 2001, Cape Town, South Africa). GLOBEC Spec. Contrib. 5, 122 p. [Available from website.]

Table 1

List of symbols used in the specification of the Bayesian state-space model, a kind of probabilistic model that describes the probabilistic dependence between latent state variables and the observed measurements, used to incorporate an environmentally forced recruitment for European anchovy (*Engraulis encrasicolus*) in the Gulf of Cádiz, Spain. TL=total length.

Symbol	Description
Indexes	
k and l	Size class, k,l=1,...,6
t	Month, t=1,...,222
j	Week, j=1,...,4
i	Age (months), specified only for individuals between 3 and 5 months old
Data	
T_t^j	Sea-surface temperature during week j in month t (°C)
W_t^j	Number of days that strong easterlies have blown during week j in month t
D_t	Discharges from Alcalá del Río dam at month t (hm^3)
$CPUE_t$	Catch per unit of effort at month t (tons/fishing trip)
A_t	Stock abundance from acoustic surveys in month t (numbers)
C_t	Catch in numbers at month t
Parameters	
λ	Parameter for the effect of easterlies
ρ	Parameter for the effect of discharges
C_R	Coefficient of variation of recruitment process
Q	Monthly catchability (*fish caught per unit of effort*)
L_∞	Asymptotic length (cm TL)
σ_{L_∞}	Standard deviation for the size of large individuals (cm TL)
g	Monthly somatic growth rate
F	Monthly fishing mortality
M	Monthly natural mortality
N^*	Initial population (numbers)
η^{**}	Inverse of the number of fish in a school (numbers/s)
σ_A	Standard deviation for acoustic surveys
$\mathbf{l}_t$	Column vector of size-class frequencies after recruitment at time t
Fixed parameters	
minLinf, *maxLinf*	Bounds for L_∞ in cm TL (see Table 2)
minsdLinf, *maxsdLinf*	Bounds for σ_{L_∞} in cm TL (see Table 2)
ming, *maxg*	Bounds for the expected somatic growth rate (see Table 2)
W_k	Weight (g) for a fish in size class k (a=00029, b=3.3438)
fec	Number of eggs per gram spawned by a female *fec*=450 eggs/g
sexr	Proportion of females in the population, *sexr*=0.5
mat_k	Maturity at length k. If fish in size class k is mature (>11.2 cm TL) is equal to 1, or, 0 otherwise
Other parameters	
$B_t(i)$	Number of anchovies between i and i+1 months old at time t
N_t	Population of individuals more than 5 months old (numbers) in the stock at month t
R_t	Recruits at month t (numbers)
d_t	Death of fish at month t (numbers)
s_t	Proportion of the population that survives to the next month t+1
p_t	Survival probability
q_t	Proportion of caught fish to dead fish at month t

Table 1 and a formal graphical representation is provided in Figure 1 (an informal and illustrative diagram is available from the following website).

Process model

We present below a weekly resolution model to explain mathematically the dynamics of anchovy eggs and larvae in the Gulf of Cádiz. The model includes the effect of the environment on these early life history stages and it is designed to be embedded in a GPDM that runs with longer time steps.

Environmentally forced recruitment According to the anchovy spawning dynamics described in Motos et al. (1996) and García and Palomera (1996), it is reasonable to consider that the production of anchovy eggs in the Gulf of Cádiz occurs when there is a sea-surface temperature (SST) increase of at least one degree (°C) between consecutive months and the temperature

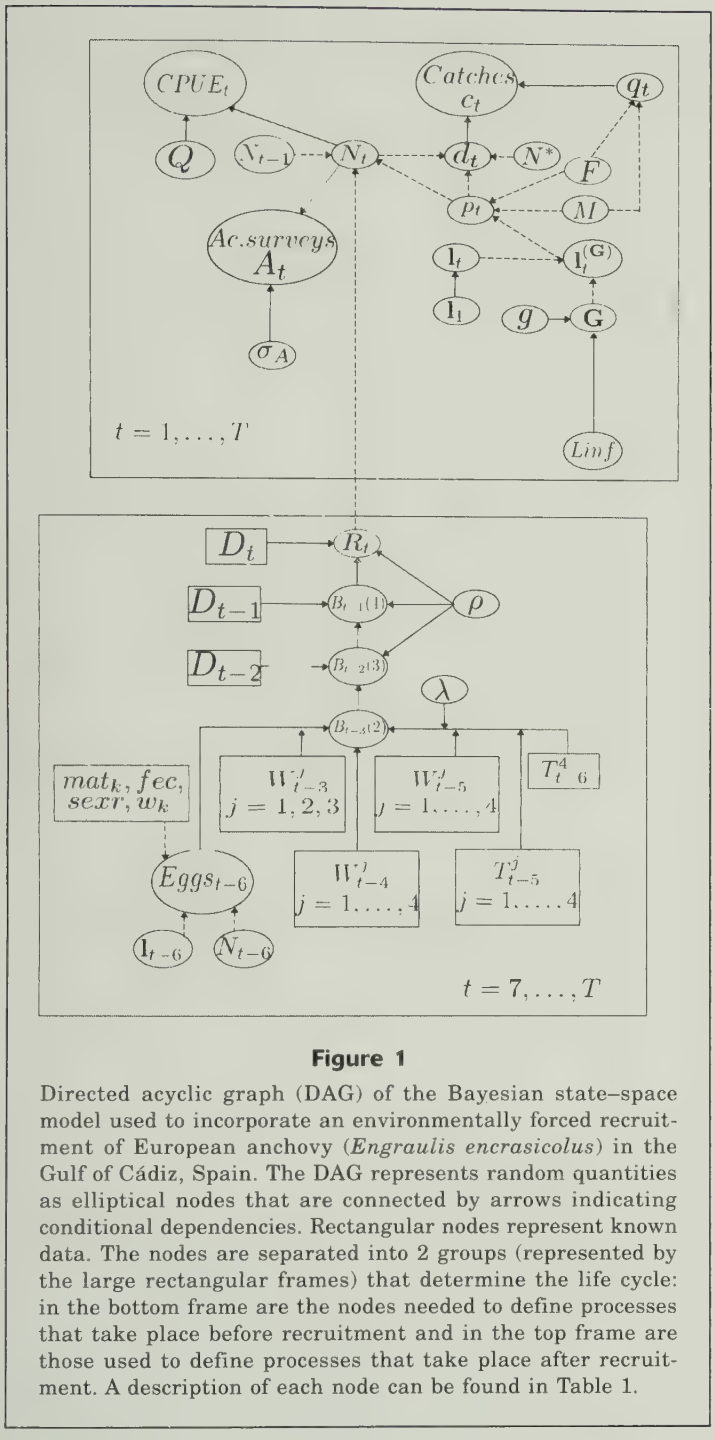

Figure 1

Directed acyclic graph (DAG) of the Bayesian state–space model used to incorporate an environmentally forced recruitment of European anchovy (*Engraulis encrasicolus*) in the Gulf of Cádiz, Spain. The DAG represents random quantities as elliptical nodes that are connected by arrows indicating conditional dependencies. Rectangular nodes represent known data. The nodes are separated into 2 groups (represented by the large rectangular frames) that determine the life cycle: in the bottom frame are the nodes needed to define processes that take place before recruitment and in the top frame are those used to define processes that take place after recruitment. A description of each node can be found in Table 1.

is above 16°C (Ruiz et al., 2006, 2009). To resolve the weekly heat-triggered egg production we assume that it occurs when there is an increment of at least a quarter degree in a week, and therefore consistent with the proposal of a degree per month in Ruiz et al. (2009). Empirical data from other areas suggest that females may spawn on average every three days under suitable temperature conditions (Somarakis et al., 2004). After spawning, strong currents created by easterlies can advect eggs and larvae away from favorable conditions (Catalán et al., 2006). Hence, the number of individuals that survive is negatively influenced by the occurrence of easterlies during the following two months after spawning. After these two months, individuals are better able to control their position in the water and are less vulnerable to currents.

The model resolves the triggering of spawning by SST and egg and larval survival that depend on easterlies through weekly time steps over two months (see Eq.1). Juvenile and adult stages are modeled by using monthly time steps that adequately resolve the dynamics of the population (see Ruiz et al. [2009] for a detailed description of anchovy life stages). Therefore the model resolution changes from weekly to monthly time steps as the development of anchovy individuals moves from egg and larval toward juvenile and recruit stages. This coupling between two different time resolutions is achieved by converting the eggs produced in the first, second, third, and fourth week to juveniles at the 9th, 10th, 11th and 12th week, respectively. Consequently, B_t (2), defined as the number of individuals that are two months old in month t (first juveniles), is modeled by following a truncated normal distribution and using data from weekly SST at the times of spawning (9, 10, 11 or 12 weeks before) and the weekly effect of easterlies in the preceding 2 months, as follows:

$$B_t(2) \sim N\left(\overline{B_t(2)}, 200000^2\right)\mathbf{I}\left\{B_t(2) \geq 0\right\},$$

where **I** = an indicator variable; and $\overline{B_t(2)}$ is defined as follows:

$$\overline{B_t(2)} = Eggs_{t-3}\left(M_t^1 + M_t^2 + M_t^3 + M_t^4\right), \qquad (1)$$

where

$$M_t^1 = \begin{cases} e^{-\lambda(W_{t-1}^4 + \ldots + W_{t-1}^1 + W_{t-2}^4 + \ldots + W_{t-2}^1)} & \text{if } T_{t-2}^1 > 16, T_{t-2}^1 - T_{t-3}^4 > 0.25, \\ 0 & \text{otherwise} \end{cases}$$

$$M_t^2 = \begin{cases} e^{-\lambda(W_t^1 + W_{t-1}^4 + \ldots + W_{t-1}^1 + W_{t-2}^4 + \ldots + W_{t-2}^2)} & \text{if } T_{t-2}^2 > 16, T_{t-2}^2 - T_{t-2}^1 > 0.25, \\ 0 & \text{otherwise} \end{cases}$$

$$M_t^3 = \begin{cases} e^{\lambda(W_t^2 + W_{t-1}^1 + W_{t-1}^4 + \ldots + W_{t-1}^1 + W_{t-2}^4 + W_{t-2}^3)} & \text{if } T_{t-2}^3 > 16, T_{t-2}^3 - T_{t-2}^1 > 0.25, \\ 0 & \text{otherwise} \end{cases}$$

and

$$M_t^4 = \begin{cases} e^{-\lambda(W_t^3 + W_t^2 + W_t^1 + W_{t-2}^4 + \ldots + W_{t-1}^1 + W_{t-2}^4)} & \text{if } T_{t-2}^4 > 16, T_{t-2}^4 - T_{t-2}^1 > 0.25, \\ 0 & \text{otherwise} \end{cases}$$

where T_t^j and W_t^j = the temperature and the number of days that strong easterlies (>30 km/h) have blown, respectively, during week j in month t.

Parameter λ accounts for the effect of strong winds and $Eggs_{t-3}$ is the number of eggs at time $t-3$ in relation to the population size at the first time step (N^*), whose

calculation will be explained in the second part of the model. The variance is large enough to avoid any constraint on parameters while the Gibbs sampling algorithm explores the space of possible values for the parameters. Note that corresponds with the assumption of birth in the *j*th week of month *t*–2.

The regulation of freshwater in the dam of Alcalá del Río has a significant impact on the survival of juveniles at their second (3–4 months old), third (4–5 months old) and fourth (5–6 months old) stages (Ruiz et al., 2009). A lack of discharge, D_t, implies low fertilization of the water, and excessive discharges cause individuals to leave the estuary and cause a loss of the protection it provides. The concentration of anchovy as a function of discharges can be described by the standardized normal density function as $\varphi(\ln(D_t) - 4.6052)$ and by taking the maximum value when D_t=100 hm^3 (Ruiz et al., 2009); consequently, the model for second-, third-, and fourth-stage juveniles (3-, 4-, and 5-month-old fish, respectively, at time t+1, t+2, and t+3, respectively $B_{t+1}(3)$, $B_{t+2}(4)$ and $B_{t+3}(5)$ is formulated as

$$B_{t+1\ 2}(\mathrm{i}) \sim N\left(\overline{B_{t+1\ 2}(\mathrm{i})}, 2000^2\right)\mathbf{I}\left\{0 \le B_{t+\mathrm{i}\ 2}(\mathrm{i}) \le B_{t+1\ 3}(i-1)\right\}$$

with

$$\overline{B_{t+\mathrm{i}\ 2}(\mathrm{i})} = B_{t+\mathrm{i}-3}(i-1)\rho\varphi\left(\ln(D_t) - 4.6052\right) \quad i=3,4,5, \quad (2)$$

where parameter ρ accounts for the effect of monthly discharges D_t. The variance chosen (2000^2) is large enough not to constrain the model while the model searches for appropriate parameter values and keeps the population within sensible limits.

The number of individuals in age group 5 ($B_{t+3}(5)$) could be considered as a function of the number of eggs.

According to Maunder and Deriso (2003), and Mäntyniemi et al. (2013), recruitment process error is accounted with a lognormal process:

$$\ln(R_{t+3}) \sim N(\ln(\overline{B_{t+3}(5)}) - 0.5\sigma_R^2, \sigma_R^2),$$

where $\sigma_R^2 = \ln(C_R^2 + 1)$, and C_R is a parameter representing the coefficient of variation of $B_{t+3}(5)$.

Therefore, R_t acts as the link between the environmental forcing of anchovy life stages (Ruiz et al., 2009) and the dynamics of the stock as modeled in Mäntyniemi et al. (2013), where the change in total population size equation is defined as

$$N_{t+1} = s_t N_t + R_{t+1}, \quad (3)$$

where s_t = the proportion of the population that survives to the next time step (see supplementary text (online only) for the formal definition of the survival process error);

N_t = the stock population size (individuals with more than 5 months of age) in relation to the population size at the beginning of the first time step, N^*, i.e., N_t = 1 and absolute population size is calculated as $N_t N^*$; and

R_{t+1} = the number of recruits at time t+1 in relation to N^*

Size-structured stock dynamics Population of the stock, whose length range is herein defined as 10–22 cm in total length (TL) according to the ICES reports (see for example ICES[2,3,4,5,6]), was assumed to be gathered in 6 length intervals of 2 cm TL each, $J_k = [I_k, I_{k+1})$, k=1,..., 6, where I_k and I_{k+1} are the size class limits.

Spawning As an approximation for the three days of spawning frequency, and in order to keep computational time reasonable, the female population is assumed to spawn once each week if suitable conditions exist. They are supposed to produce a number of eggs computed with the following dot product:

$$Eggs_t = (\mathbf{l}_t \cdot N_t \mathbf{e}),$$

where $\mathbf{l}_t$ and $\mathbf{e}$ are column vectors with 6 components.

The first column vector denotes the size class frequencies after recruitment, allocating the relative population N_t in the 6 length intervals defined above. The second column vector represents the number of eggs per gram spawned by a mature female in each length class. Each component of column vector $\mathbf{e}$ is calculated as the product of the fixed parameters *fec*, mat_k, *sexr*, and w_k, defined in Table 1. Note that this number of eggs only becomes effective if spawning conditions settled in Equation 1 are satisfied.

Growth The growth of individuals is assumed to take place instantly at the beginning of each month. The length of individuals at time t (individuals that at time t–1 were in length class k (L_k)), is assumed normally distributed with an expected value and standard deviation calculated as follows:

$$\mu_{L_k} = L_\infty(1 - e^{-g}) + \frac{I_{k+1} + I_k}{2} e^{-g} \quad (4)$$

and

$$\sigma_{L_k} = \sigma_{L_\infty}\sqrt{1 - e^{-2g}}, \quad (5)$$

---

[2] ICES (International Council for the Exploration of the Sea). 2005. Report of the working group on the assessment of mackerel, horse mackerel, sardine and anchovy (WGMHSA), 6–15 September 2005, Vigo, Spain. ICES CM 2006/ACFM:08, 615 p. [Available from website.]

[3] ICES (International Council for the Exploration of the Sea). 2010. Report of the working group on anchovy and sardine (WGANSA), 24–28 June 2010, Vigo, Spain. ICES CM 2010/ACOM:16, 289 p. [Available from website.]

[4] ICES (International Council for the Exploration of the Sea). 2012. Report of the working group on southern horse mackerel, anchovy and sardine (WGHANSA), 23–28 June 2012, Azores (Horta), Portugal. ICES CM 2012/ACOM:16, 544 p. [Available from website.]

[5] ICES (International Council for the Exploration of the Sea). 2014. Report of the working group on southern horse mackerel, anchovy and sardine (WGHANSA), 20–25 June 2014. Copenhagen, Denmark. ICES CM 2014/ACOM:16, 599 p. [Available from website.]

[6] ICES (International Council for the Exploration of the Sea). 2016. Report of the working group on southern horse mackerel, anchovy and sardine (WGHANSA), 24–29 June 2014, Lorient, France. ICES CM 2016/ACOM:17, 588 p. [Available from website.]

where L_∞ and σ_{L_∞} = the asymptotic expected value and standard deviation, respectively, for the length distribution and g is somatic growth rate.

The mean value of L_k is an application of the von Bertalanffy growth equation (Quinn and Deriso, 1998) starting from $\frac{l_{k+1}+l_k}{2}$. Each individual has the possibility to stay in the same length class or move to a larger length class. This transfer is modeled through a transition matrix $\mathbf{G} = (g_{k,l})_{6\times6}$, where $g_{k,l}$ denotes the probability that an individual in class J_k grows enough in a month to move to class J_l.

The size distribution at month t after growth is given by $\mathbf{l}_t^{(G)} = \mathbf{G}\mathbf{l}_t$.

Calculation of σ_{L_k} and $g_{k,l}$ is described in Appendix 2 of Mäntyniemi et al. (2015).

Mortality and survival A fish in length class k after growth has been completed has three possibilities: to die naturally, be caught, or to survive ($\rho_{t,k}$, $\gamma_{t,k}$, and $p_{t,k}$, respectively), with respective probabilities given by Baranov (Baranov, 1976; Quinn and Deriso, 1998) as follows:

$$\rho_{t,k} = \tfrac{M}{F+M}(1-e^{-(F+M)})l_{t,k}^{(G)}, \quad (6)$$

$$\gamma_{t,k} = \tfrac{F}{F+M}(1-e^{-(F+M)})l_{t,k}^{(G)}, \quad (7)$$

$$p_{t,k} = e^{-(F+M)}l_{t,k}^{(G)}, \quad (8)$$

with F and M denoting fishing-induced and natural mortality, respectively (where M and F are assumed as constant in time for all individuals available to the fishery, i.e., bigger than 10 cm TL). Then the proportion of caught fish in length class k from all dead fish is computed as

$$q_{t,k} = \frac{\gamma_{t,k}}{1-p_{t,k}}.$$

The number of surviving anchovies at time t determined by the probability $p_t = \sum_{k=1}^{6} p_{t,k}$ given in Equation 8, together with the environmentally forced recruits at time t+1 computed in the first part, constitute the population available to fisheries in the stock for time t+1 (Eq. 3). The procedure is repeated for each time step.

Length distribution Accordingly, the length distribution in the next time step will be defined as the weighted sum of the known length distribution of recruits (between 10 and 12 cm TL) and the length distribution of surviving individuals ($\mathbf{l}_t^{(S)}$), as follows:

$$\mathbf{l}_{t+1} = (1-\frac{R_{t+1}}{N_{t+1}})\mathbf{l}_t^{(S)} + \frac{R_{t+1}}{N_{t+1}} * (1,0,0,0,0,0)^T,$$

where $\mathbf{l}_t^{(S)} = p_t\mathbf{l}_t^{(G)}$.

Observation model

Catch in numbers Anchovy catches at time t, c_t, are assumed to follow a beta-binomial distribution, as follows:

$$c_t|q_t,d_t \sim Betabin(q_t\eta_t,(1-q_t)\eta_t,d_t) \quad t=1,\ldots,222, \quad (9)$$

where $q_t = \sum_{k=1}^{6} q_{t,k}$, $d_t = N^* N_t(1-s_t)$ representing all dead individuals (by natural and fishing-induced mortality) at time t and η_t as defined in the supplementary text (online only).

This choice corresponds to an overdispersed alternative to a binomial distribution (Gelman et al., 2013). A binomial distribution is too restrictive, considering the schooling and clustering behavior of anchovy (Mäntyniemi and Romakkaniemi, 2002), and a beta-binomial distribution reflects the fact that all individuals do not have the same probability of being captured. Note that the expected value of the distribution ($q_t d_t$) corresponds to Baranov's catch equation.

CPUE The catch per unit of effort at time t, $CPUE_t$ is applied only for the spawning times, i.e when the mean SST of the month is higher than 16°C and it has increased at least 1°C from the mean temperature of the last month. As extensively discussed in Ruiz et al. (2009), this value is reported yearly but most of the CPUE signal is produced during the spawning period. $CPUE_t$ is normally distributed with a mean proportional to the stock size at time t (N_t,) and a very high variance that reflects a vague knowledge about this variable, as follows:

$$CPUE_t \,|\, Q, N_t \sim N(QN_t, 10^5), \quad (10)$$

where Q, = the catchability coefficient.

Acoustic surveys Estimations of the population size by means of acoustic surveys are available for two specific months: June 1993 and June 2004, as in Ruiz et al. (2009). These acoustic data for stock size, A_t, t = 71,215, provide abundance estimates. They are assumed to follow a normal distribution with unknown variance σ_A^2, that is transformed to a lognormal distribution as follows:

$$A_t \,|\, N_t, \sigma_A \sim LN(\log(\overline{N_t}) - 0.5\sigma_A^2, \log(1+CV^2)) \quad t = 71,215,$$

where CV = the coefficient of variation of N_t.

Those acoustic surveys are the only "contact" of the model with nonfishery estimates of stock size. We decided to let variance be a nonfixed parameter to be determined a posteriori by the Gibbs sampler. This decision imposes an additional numerical burden on the exercise, but not an excessive one owing to the low number of estimates, and is justified given the important role of this fishery-independent source of data.

Directed acyclic graph (DAG)

Figure 1 shows the directed acyclic graph (DAG) for the model. The DAG represents random quantities as elliptical nodes connected by arrows that indicate conditional dependencies. Data are introduced as rectangles and the arrows could be dotted or solid lines that

Table 2

Prior probability density functions assigned to the parameters to reflect previous knowledge for the Bayesian state–space model used to incorporate environmentally forced recruitment of European anchovy (*Engraulis encrasicolus*) in the Gulf of Cádiz, Spain. When the reliability of previous information was considered weak, large variance distributions were selected; such a situation is known as a vague prior, and parameters with a vague prior received a label of "vague" in this table. If there was enough information in the literature, the prior selected is more informative and the literature source is given in this table. The parameter *pLinf* is such that L_∞=*minLinf* +(*maxLinf* – *minLinf*)*pLinf*, and analogously *g*=*ming*+(*maxg*-*ming*)*pg* and σ_{L_∞} = *minsdLinf*+(*maxsdLinf* – *minsdLinf*)*psdLinf*

Parameters	Prior probability density function	Comments
λ	~*Unif*(0,2)	Vague
ρ	~*N*(0.1,0.1)	Ruiz et al. (2009)
C_R	~*Unif*(0,3)	Vague, Mäntyniemi et al. (2009)
η^{**}	~*Beta*(1,1)	
$1/\sigma_A^2$	~*Gamma*(0.001,0.001)	
ln(*F*)	~*N*(ln(0.09),0.04)**1**{*F*>0.05}	Giráldez et al. (2009)
ln(*M*)	~*N*(ln(0.035),0.05)**1**{*M*<0.08}	Giráldez et al. (2009)
N^*	~*N*(ln(1),10000)	Vague
pLinf	~Logitnorm(0,1)	
maxLinf=20		Bellido et al. (2000)
minLinf=18		Bellido et al. (2000)
pg	~Logitnorm(0,1)	
maxg=0.08		Bellido et al. (2000)
ming=0.05		Bellido et al. (2000)
psdLinf	~Logitnorm(0,1)	
maxsdLinf=3		
minsdLinf=0.1		
ln(*Q*)	~*N*(ln(2000000),500)	
$\mathbf{l}_1$	~*Dirich*([1/1,2/2,...,*K*/*K*])	

correspond to logical and stochastic dependencies, respectively. If parameter A follows a distribution dependent on parameter B, there is a solid arrow pointing from B to A. If parameter A is a function of parameter B, there is a dotted arrow pointing from B to A (Meyer and Millar, 1999). For example, in Figure 1, the relationship of catches (c_t) with dead individuals (d_t) and the total probability of being caught (q_t) is detailed in Equation 9.

Priors

After an extensive literature search on parameter values for this particular species and area, the data were filtered, preprocessed, and interpreted in terms of reliability by those with an expert knowledge. This method implied an initial inspection of the data distribution and the metadata. If, for example, the age structure from one particular data set was markedly different with respect to that from the Gulf of Cádiz, those data were excluded. Secondly, if the final filtered available data were of poor quality (e.g., produced with a dubious method), the probability density functions (PDFs) were built in a conservative way and at a level of reliability that determines the amount of information provided by the prior distributions (Table 2). When the reliability of previous information was considered weak, large variance distributions were selected. In general, the use of the lognormal distribution was considered adequate for informative priors given the underlying variability and the scarcity of such data. The source of information to derive biological and exploitation-related data was anchovy stocks from European waters and expert-knowledge on those stocks. All parameters were restricted to positive values that were consistent with the processes described. For some parameters (e.g., ρ), the PDF was modeled according to previous research, whereas for others, such as natural and fishing-induced mortality (F and M), no reliable information was available for the area; hence selected information from similar stocks was used.

Identical monthly distributions for F were chosen on the assumption of a mean annual F of 1.1 corresponding to age-1 fish in the close-by Alborán Sea stock (Giráldez et al.[7]). The genetic structure of Alborán Sea

[7] Giráldez, A., P. Torres, L. F. Quintanilla-Hervás, J. M. Bellido-Millán, F. Alemany, and M. Iglesias. 2009. Anchovy (*Engraulis encrasicolus*) stock assessment in the GFCM geographical sub-area GSA 01, Northern Alborán Sea, 18 p.

stock is very similar to that of the Gulf of Cádiz stock (Zarraonaindia et al., 2012). Further, age 1 reflects the average age of most close-by stocks (Pertierra and Lleonart, 1996). A large standard deviation was supplied, so that maximum (annual) F values might reach the maximum F values reported in the literature for the aforementioned stocks (approximately F=2/year). The prior distribution was constrained at the lower end to 0.05/month, which corresponds to approximately 50% of the selected average F value for age 1. The PDF for M, for which even less data exist, was based on the age-specific M estimates for age-1 anchovy in the near Alborán Sea (Giráldez et al.[7]). Those authors estimated M according to the ProdBiom method (Abella et al., 1997) that is based on Caddy (1991). The large variance assigned to M had an upper boundary of 0.08, which would yield theoretical annual mortality rates close to M=1/year, which is 15% higher than the M value for age-0 anchovy reported from 5 years of surveys of an unfished anchovy stock (Gulf of Biscay; ICES[3]).

The bounds for growth parameters L_∞, σ_{L_∞}, and g (logitnorm function) were constructed on the basis of a single work performed in the Gulf of Cádiz (Table 2) during which biological data were collected fortnightly for 4 years on individuals ranging in size from 4 cm TL to maximum length. L_∞, and g extremes were estimated directly from that series, whereas bounds for σ_{L_∞} were considered uninformative and embraced the mean of the standard deviation of L_∞ also approximated from that series.

The lower bound for λ was chosen by considering the negative effect of winds on recruitment (Ruiz et al., 2006), and the upper bound was chosen on the basis of a preliminary analysis, in which extreme windy conditions from a historical series were considered and that would allow a replacement rate of at least one recruit per female. This assumption prevents collapse in the absence of fishing and adverse environmental conditions.

Constant values used in the model were taken from the literature and were based on expert knowledge, namely the consensus of two experts, and with the assumption that if data were not available from the same stock, they should be taken from the closest (genetically and geographically) stock that experiences a similar exploitation pattern. Using data collected during 4 years in the Gulf of Cádiz (Millán, 1999), we extracted constant parameter values including a 1/1 sex ratio ($sexr$=0.5), an average length of maturity equal to 11.2 cm TL (for females) to define maturity at length class k (mat_k) (see Table 1), and a=0029 and b=3.3438 for the power length–weight relationship, $w_k = a(\frac{l_{k+1}+l_k}{2})^b$. The number of eggs spawned per gram fec=450 eggs/g was approximated from a review on spawning traits of 22 anchovy stocks in European waters (Somarakis et al., 2004).

Data

The observation model is defined by using quarterly data on catch (in numbers of fish) and yearly CPUE from January 1988 to December 2004 extracted from ICES reports (ICES[2,8,9,10]). CPUE data were transformed to monthly data with the knowledge that most of the anchovy landings occur during the spawning season. Therefore, it was assumed that CPUE is known only for spawning months and is equal to the CPUE in the corresponding year. Acoustic estimates were provided by ICES (ICES[2]) for June of years 1993 and 2004. Length frequency of the catches for the same years from ICES annual reports (ICES[2,8,9,10]) was used for validation. Monthly catch (in numbers) and monthly length frequency of the catch data resulted from the assumption that the same amount of fish is landed every month of the quarter and that the third quarter has four months. This assumption results in months of 28 days, 13 months per year approximately, and that the 204 months from January 1988 to December 2004 become 222 months in the process model (T=222).

The environmental covariates SST, discharges from the Alcalá del Río dam, and wind were obtained as follows: SST was extracted from the advanced very high resolution radiometer (AVHRR) sensor data. The nighttime AVHRR PATHFINDER SST v5 weekly means with 4-km^2 pixel resolution were taken from NASA Physical Oceanography Distributed Active Archive Center (available from website). The region of interest was acquired from the global image, and the arithmetic mean was calculated from the SST of all pixels within this region. Discharges were provided by Confederación Hidrográfica del Guadalquivir (data available from website). The data correspond to the monthly accumulated cubic hectometers that are discharged from the dam each month. Wind data represent the weekly accumulated time (in days) that easterlies faster than 30 km/h have been recorded at the meteorological station of Cádiz.

Working paper of the GFCM-SAC-SCSA working group on stock assessment of small pelagic species. Centro Oceanográfico de Málaga, Málaga, Spain. [Available from Centro Oceanográfico de Málaga, Instituto Español de Oceanografia, Puerto Pesquero, s/n Apdo. 285 29640, Fuengirola (Málaga), Spain.]

[8] ICES (International Council for the Exploration of the Sea). 1990. Report of the working group on the assessment of the stocks of sardine, horse mackerel and anchovy, Copenhagen, 20–29 June 1990. ICES CM 1990/Assess:24, 176 p. [Available from ICES, H. C. Andersens Blvd. 44-46, 1553 Copenhagen, Denmark.]

[9] ICES (International Council for the Exploration of the Sea). 1995. Report of the working group on the assessment of mackerel, horse mackerel, sardine and anchovy, ICES Headquarters, 21 June–1 July 1994. ICES CM 1995/Assess:2, 329 p. [Available from ICES, H. C. Andersens Blvd. 44-46, 1553 Copenhagen, Denmark.]

[10] ICES (International Council for the Exploration of the Sea). 2000. Report of the working group on the assessment of mackerel, horse mackerel, sardine and anchovy, ICES Headquarters, 14–23 September 2000. ICES CM 2001/ACFM:06, 456 p. [Available from website.]

Model implementation and posterior analysis

The model was run in the Centre of Supercomputing of Galicia (CESGA) by using the Galician virtual supercomputer (SVG) cluster with an Ivy Bridge microarchitecture (Intel Corp., Santa Clara, CA). The software used was R, vers. 3.2.0 (R Core Team, 2015) and JAGS 4.2.0 (Just Another Gibbs Sampler) (Plummer, 2012a). The R package rjags links the R code with the MCMC sampler (Plummer, 2012b; see the supplementary text (online only) for the JAGS code used in this study). The cluster required 311.28 hours for 170,000 iterations of two chains running in different cores. The first 10,000 iterations were for adaptation without thinning, and then a thinning of 100 iterations was applied. After a burn-in period of 80,000 iterations, potential scale-reduction factors (Gelman et al., 2013) and the Heidelberg and Welch convergence diagnostic (Heidelberger and Welch, 1981, 1983) were calculated for all monitored parameters by using the coda package (Plummer et al., 2006). The potential-scale reduction factor remained below 1.05 for all of them. Heidelberg and Welch tests were passed for both chains and all parameters.

We used the Kullback–Leibler (KL) divergence (Kullback and Leibler, 1951) as a measure of statistical distance between the obtained distributions. The KL divergence measures the loss of information when the predicted distribution is used instead of the real one. It is also considered as a basis for valid inference in ecological Bayesian approaches (Burnham and Anderson, 2001). It was calculated by using the KLdiv function from the R package flexmix (Grün and Leisch, 2008). In order to compare the estimated time series with available data, the expected value of the quadratic loss and its square root, i.e., mean squared error and root mean-squared error (MSE and RMSE) were calculated. Standardization was necessary to compare yearly model outputs and in situ data for juveniles because they express juvenile abundance at different scales.

Results

Posterior distributions and the joint posterior of the parameters are displayed in Figure 2 and Supplementary Figure 1 (online only), respectively. The posterior for initial population N^* is coherent with the initial modeled population in Ruiz et al. (2009), where an uninformative prior was also implemented. The annual fishing-induced mortality mode is higher than the annual natural mortality mode; that finding is consistent with the restrictions placed on the priors, but natural mortality values are very close to the boundary. The mode for parameters L_∞, and growth rate g for the von Berttalanfy growth model are close to the middle point of the limits established by the priors according to Bellido et al. (2000). The easterlies parameter (λ) is concentrated in values between one and two, and the discharge parameter (ρ) remains in low values with 0.005 as the mode of the distribution.

In Figure 3A, a temporary decay in the modeled recruitment time series from 1992 to 1995 is observed together with a sudden recovery in the next year. Figure 3B shows a consistent evolution of catches compared with the modeled stock population size, a result that is coherent with the assumption of catches proportional to abundance. This proportionality is derived by considering a constant mortality in Baranov's catch equation which is equivalent to the expected value of c_t in Equation 9.

A detailed representation of the juvenile population is presented in Figure 4 to assess the performance of the higher temporal resolution for the first life stages. The dual-time resolution results in a consistent relation between the model output for the juvenile population ($B_t(3)+B_t(4)$, $t=1,\ldots, T$) and in situ data (Drake et al., 2007) and offers a smoother version of the former, although the way these data are recorded is prone to sampling noise. There are also some differences between both time series—the most remarkable in year 2000, which shows a smaller estimated number of juveniles than the number reported from in situ data, as detailed in Table 3.

The model seems to offer a smoother version of the in situ data although the way these data were recorded (Drake et al., 2007) is prone to sampling noise.

An additional contrast between the output and the data not used in the model formulation or parametrization comes from the length structure of the population. The growth module, included through the matrix $\mathbf{G}$, allows the simulation of the length frequency in the stock for each month ($\mathbf{l}_t$). The KL divergence between model outputs and ICES data was smaller than 2 in 80.63 of the months considered (Fig. 5), showing that a von Berttalanfy-based matrix could model the length frequency of the population without a significant loss of information in many cases. A lower KL divergence was obtained in the later years, where the sensitivity to initial values was reduced. Main differences are in the first two length classes, as can be seen in the comparison between modeled and observed length distributions for each month in Supplementary Figure 2 (online only). The lengths reported by ICES are in the rank of the estimated length (between the 5th and 95th percentiles) for the first and second length classes in the 62% and 59% of all the 222 months, respectively, compared with 63%, 63%, 81%, and 97% for the other length classes.

Discussion

Bayesian models have proven their value for assessing the underlying stock-recruitment relationship of exploited species, along with the associated uncertainty (Dorn, 2002; Mäntyniemi and Romakkaniemi, 2002; Michielsens and McAllister, 2004). In many stocks and particularly in small pelagic fish, the sensitivity of recruitment to the environment impedes the use of traditional stock-recruitment relationships (e.g., Ricker or Beverton-Holt curves) as the unique driver of

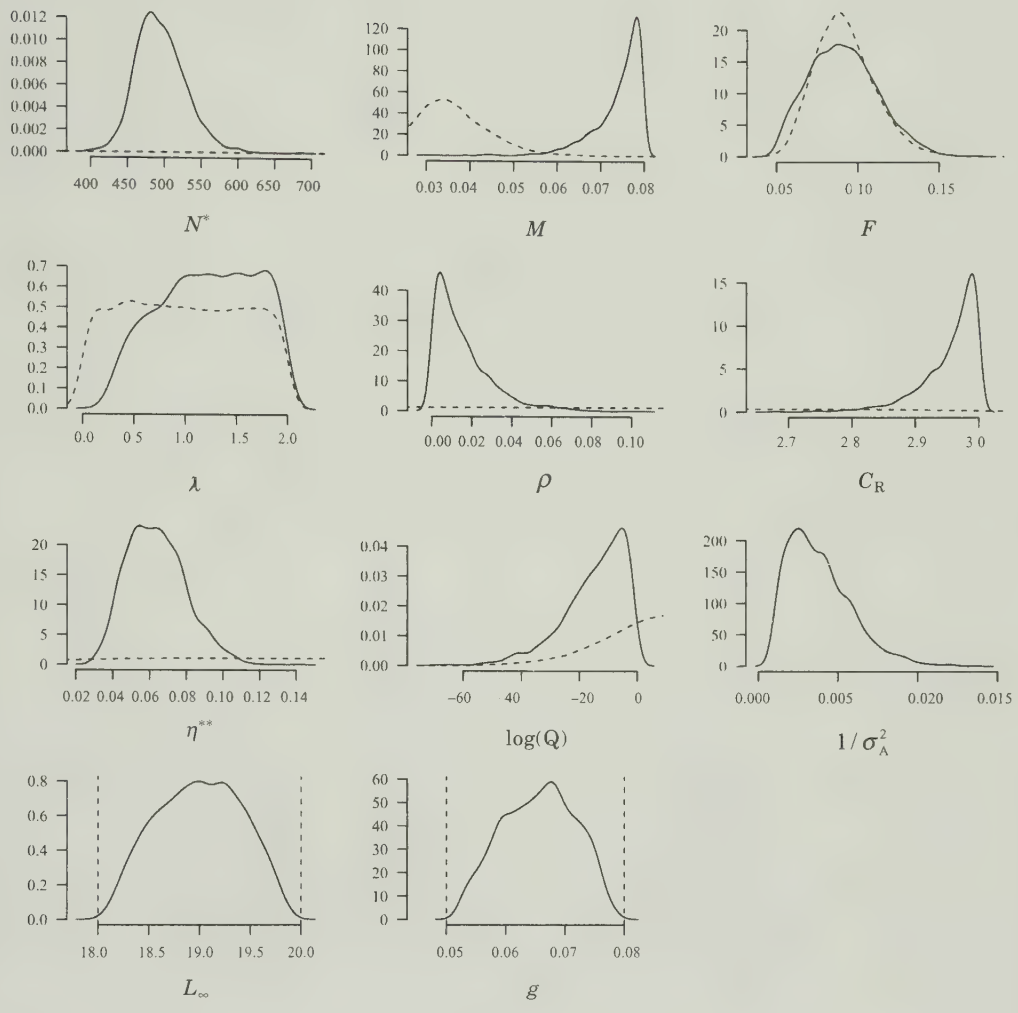

Figure 2

Posterior distributions (solid lines) for the parameters of the model used to incorporate an environmentally forced recruitment of European anchovy (*Engraulis encrasicolus*) in the Gulf of Cádiz, Spain. Parameters were the following: population size at the first time step (N^*), natural mortality (M), fishing-induced mortality (F), effect of strong winds (λ), effect of monthly discharges (ρ), coefficient of variation of recruits (C_R), inverse of the number of fish in a school (η^{**}), Naperian logarithm of monthly catchability log(Q), inverse of the variance for acoustic surveys $1/\sigma_A^2$, asymptotic length (L_∞), and somatic growth rate (g). Dotted lines indicate the prior distributions, except for parameters L_∞ and g, for which they represent upper and lower bounds.

small pelagic populations (Erzini, 2005; Fréon et al., 2005). However, attempts to include the environment in Bayesian models of recruitment (Ruiz et al., 2009) are hampered by the short time-scale response of early stages to environmental forcing.

The dual-time resolution implemented in this study overcomes this handicap. We were able to integrate within the same model the traditional formulations and parameters of fishery management (e.g., von Bertalanffy growth function, Baranov catch equation, M, F) with advanced tools in oceanographic research (e.g., remote sensing) and to perform this merging in a consistent manner with existing data from observations made in the field (e.g., CPUE, landings,or acoustic data).

The proposed dual time resolution does not create a significant numerical burden for the computational effort demanded by a model fully formulated under monthly resolution. The weekly forcing of early stages is implicitly resolved through the M_t^l terms (Eq. 1) and the whole MCMC sampling is resolved at monthly time steps. The computational time required by a monthly resolved model is already very high (311 hours in our case with a super-computing center, see also Ruiz et

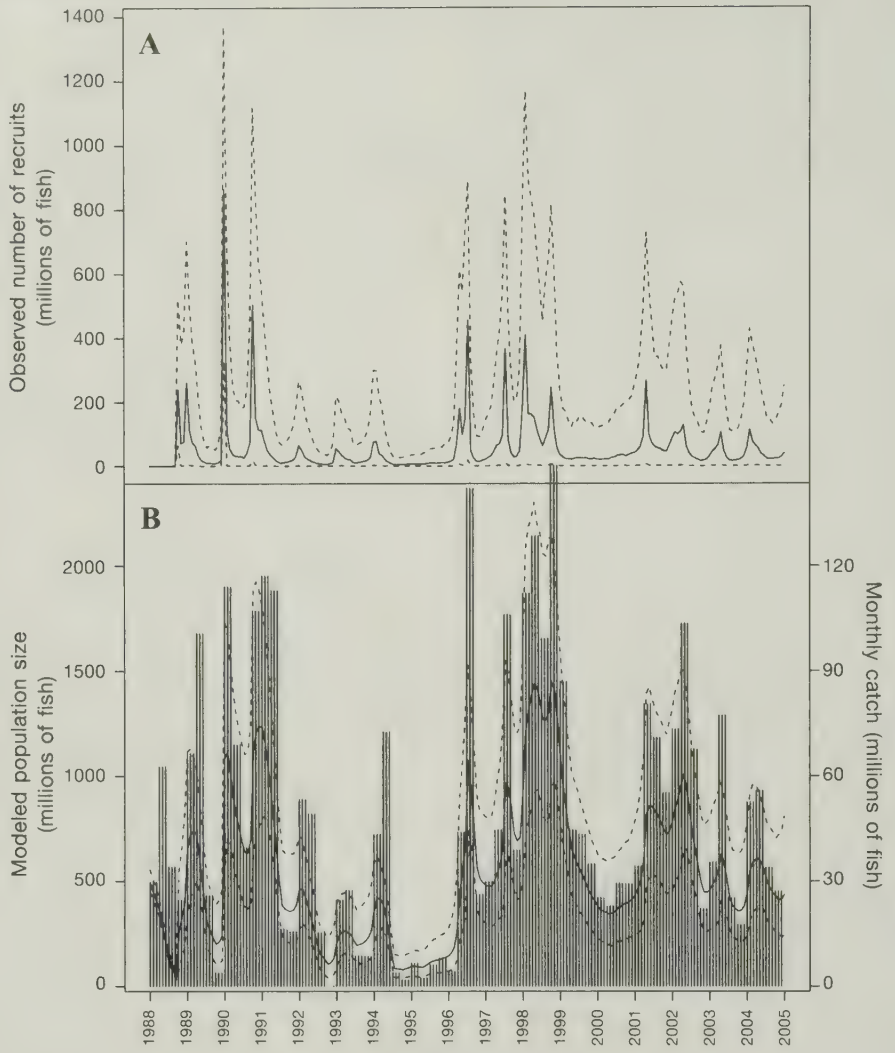

Figure 3

(**A**) Estimates of the number of recruits (individuals between 5 and 6 months old) of European anchovy (*Engraulis encrasicolus*) in the Gulf of Cádiz, Spain, during 1988–2004, determined from the study model. (**B**) Population size (lines) versus catches reported by the International Council for the Exploration of the Sea (bars) for European anchovy in the Gulf of Cádiz. Dotted lines indicate the 5 and 95 percentiles, and the solid line indicates the median of the posterior distribution. Quarterly reported catches were transformed to preserve the monthly scale.

al. (2009). Therefore, the numerical burden necessary to approach convergence would render intractable if we had formulated this model with weekly time steps. Although our computational time demanded by our approach is still large, it is tractable. In particular, with the advances in parallelization and computing power available for research, this tractability can be used with this new approach in the coming years as a tool to run models that resolve fine scales at short operational times.

Admittedly, it would have been more precise to use monthly varying F values, but constant F was chosen for our study to achieve convergence of parameters in reasonable time. In spite of constant $\boldsymbol{F}$, the model resulted in a better coherence between modeled and observed abundances: Figure 4 of this article, in contrast to Figure 7 of Ruiz et al. (2009), illustrates this fact for the seasonal variations and interannual tendencies of juveniles in the Gulf of Cádiz. This improvement is evident if we assess the performance of Ruiz et al. (2009) versus the present model as shown in Tables 3 and 4. These tables synthesize deviations between model outputs and all available data. These data include those that are incorporated in the modeling exercise (catch,

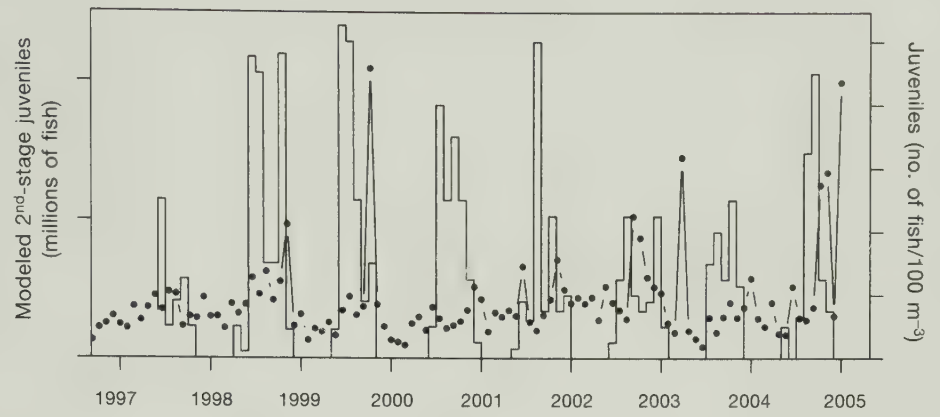

Figure 4

Modeled mean population size of second-stage juveniles (number of individuals that are 3 months old in month t, $B_t(3)$), divided by the size of the initial population (i.e., $B_t(3)/N^*$) of European anchovy (*Engraulis encrasicolus*) in the Gulf of Cádiz, Spain, during 1996–2004 (black circles) and juvenile data from Drake et al. (2007) that were not used in the model of our study (solid lines).

CPUE, and acoustics), as well as those that are not (juveniles and length frequencies). Table 3 shows the capacity of the models to reproduce the yearly evolution of juveniles. The dual-resolution performs better than the monthly model to estimate juvenile abundance in five out of the 8 years and the overall MSE is also better (1.57 vs. 1.83, respectively). In addition, the difference between CPUE residuals for both models is very small and can be thought of as an improvement of the current model over the former, considering that CPUE is the main source of data of the model in Ruiz et al. (2009) and the high variance defined in Equation 10. This high variance is permissible with some data imperfections such as those identified by ICES, for example, for CPUE in year 1998. These data imperfections are assimilated by this Bayesian exercise with greater flexibility than would have been achieved through deterministic modeling. Another difference between the present model and the Ruiz et al. (2009) model is the intimate connection between landings and N_t defined by Equation 9. This connection decreases the role of CPUE in abundance estimation when compared with the Ruiz et al. (2009) model, a model that does not include reported landings data in the observation model and relies mainly on CPUE.

Another enhancement of the current model is the possibility of calculating catches as a model output which is a preliminary condition for constructing a forecast model for management purposes. Albeit the small RMSE for observed and estimated catches (5 million corresponding to 3.84% of the maximum value of observed catches) can be a consequence of the process simplification induced by the assumption of constant fishing-induced mortality, it shows the goodness of fit of the model in a plausible "What if" scenario: What if catches are proportional to the population, and that scenario is not far from reality according to the results from the previously developed Bayesian model. Although a proportionality between catches and abundance is not necessarily observed and is the subject of hot debate (Pauly et al., 2013), this proportionality is frequently observed in short-lived small pelagic fish (Lloret et al., 2004).

Table 3

Seasonal performance of 2 models used to incorporate an environmentally forced recruitment of European anchovy (*Engraulis encrasicolus*) in the Gulf of Cádiz, Spain: the dual-time resolution model of this study and the monthly resolution model of Ruiz et al. (2009). Values are the expected value of the quadratic loss (mean squared error [MSE]) between predicted and observed juvenile abundance for each of the years when the latter available. Predictions and observations were standardized with the mean and variance of the yearly model outputs (for 8 years) before MSE was calculated.

Year	Current model	Model from Ruiz et al.(2009)	Difference
1997	3.3099	9.4143	−6.1044
1998	0.0721	0.2029	−0.1309
1999	4.0713	2.7520	1.3193
2000	2.7627	0.3107	2.4520
2001	1.2112	0.0184	1.1928
2002	0.9918	1.1475	−0.1557
2003	0.2155	1.4419	−1.2264
2004	0.0016	0.1662	−0.1646

Table 4

Interannual performance of 2 models used to incorporate an environmentally forced recruitment of European anchovy (*Engraulis encrasicolus*) in the Gulf of Cádiz, Spain: the dual-time resolution model of this study and the monthly resolution model of Ruiz et al. (2009). Values are the root mean squared errors between monthly means of estimations from the models and observations from available data (1988–2004). The model of Ruiz et al. (2009) did not estimate catches. Maximum and minimum values for observed catches are 0 and 136 millions of fish, respectively, and maximum and minimum values for observed catch per unit of effort (CPUE) are 0.138 and 1.148 tons/fishing trip, respectively.

	Current model	Model from Ruiz et al. (2009)	Difference
Catch (millions of fish)	5.235		
CPUE (tons/fishing trip)	0.276	0.2734	0.0028
Acoustic survey 1993 (millions of fish)	572.9414	185.3100	387.6314
Acoustic survey 2004 (millions of of fish)	107.4575	180.7900	−73.3325

The dual resolution also facilitates the embedding of environmental forcing into generalist models, such as the GPDM for fishery management (Mäntyniemi et al., 2015). This integration results in coherence between the model outputs and observed data beyond the initial stages of the life cycle, see for instance Figures 5 and Supplementary Figure 2 (online only) that show coherence between the size structures produced by the model and those reported by ICES. The coherence seems to indicate the suitability of the von Bertalanffy model used for Equations 4 and 5, and the bounds settled on for growth parameters provided by Bellido et al. (2000) (see Table 2). Other features observed in the population size-structure also seem to be well reproduced by the model. Therefore, the absence of large sizes and the high concentration of individuals between 10 and 14 cm TL are consistent with the suggestion that fishing pressure hampers adult survival beyond a year and the population relies on the youngest fish (BOTTOP control, Ruiz et al. (2007)). Nevertheless, discrepancies between model and data frequently occur in the first two length classes (10–12 cm TL and 12–14 cm TL, Suppl. Fig. 2) (online only). This result probably reflects the need to ameliorate the transition matrix **G** in future versions of the model. In this respect, the inclusion of another length class in the model (e.g., 8–10 cm TL, representing mostly immature fish) seems reasonable according to the recent report of landings data (ICES[6]). Further, the use of a seasonal growth model incorporating temperature effects may improve the observed results.

It is worth underscoring that the model did not previously use any of the in situ data for estimates of early-stage abundance presented in Figure 4 or with the population size structure reported by ICES (and used in the contrast of model versus observation in Figure 5 and Supplementary Figure 2) (online only). Therefore, the Bayesian integration of environmental forcing in traditional formulations of fishery management results in outputs that are coherent with field observations. This coherence holds over the whole life cycle, even when the observational data have not being previously used in the configuration of the model.

The main feature of the time series, the collapse and recovery between 1994 and 1996, is described in previous works and points to the combined effect of wind and discharges over recruitment (Ruiz et al., 2006, 2009). The resulting drastic variation in landings is also well resolved by the model. The posteriors of λ and ρ in Figure 2 indicate, nevertheless, a higher role of the wind regime in driving the dynamics of the population, consistent with the analysis presented by Rincón et al. (2016). Consistent with a recruitment-driven fishery, the model transfers these major changes in recruits (Fig. 3A) into large fluctuations of landings (Fig. 3B).

These types of dynamics can be reproduced only by models incorporating the mechanics of environmental forcing on recruitment. Classic models, such as virtual population analysis or extended survivor analysis, may be valid for assessing species with longer life spans. The impact the environment may have on these species results in abundance or size-structure changes that are slow enough to be detected by the models used in yearly evaluations of the stock, even when those models do not incorporate environmental forcings. However, these models are not valid for recruitment-dependent fisheries such as that targeting the European anchovy in the Gulf of Cádiz because stock changes are too fast. Moreover, knowledge of the cause and effect of environment on recruitment (beyond simple statistical correlations) is necessary to reach some degree of predictability in cases where severe and quick changes in recruitment pose heavy challenges for modeling.

The model presented here confirms the critical role of the environment in shaping recruitment and landings of the European anchovy in the Gulf of Cádiz. Compared with previous models, its dual-time resolution

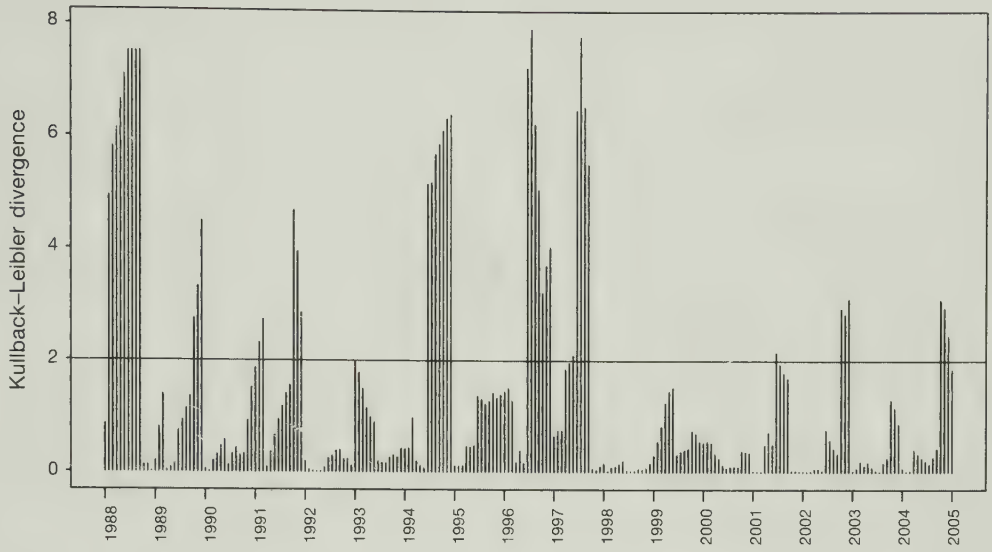

Figure 5

Kullback–Leibler divergence between the modeled and real length-frequency distributions of the population of European anchovy (*Engraulis encrasicolus*) in the Gulf of Cádiz, Spain, during 1988–2004 grouped into 6 length classes of 2 cm each from 10 cm to 22 cm total length.

improves coherence between model output and field observations throughout the life cycle of this fish, including independent observations that represent a genuine validation of the approach (Pauly et al., 2013). Environment clearly influences future recruitment of this species very early in life. For management purposes this fact implies that the concept developed here could be the basis of a tool to estimate recruitment based on data on wind, temperature, and discharge conditions before the fishing season has started. It would then be feasible to define a harvest control rule incorporating this knowledge to reduce risks of a fishery collapse. It must be remarked that in order to have that predictive tool, there is considerable room for improvement in the current model configuration (e.g., varying F, etc), but we have proved in this study that even with simpler assumptions, the model can yield useful results.

Finally, although the implementation of our model is designed for the European anchovy in the Gulf of Cádiz, the fact that Equations 1 and 2 can easily be modified for other species and stocks allows the model to be easily adapted and applied to other small pelagic species for which recruitment is key to explain the surplus or collapse of a fishery.

Acknowledgments

The research leading to these results has received funding from the European Union's Seventh Framework Programme (FP7/ 2007-2013) under grant agreement 244706/ ECOKNOWS project and M. Rincón was funded by P09-RNM-5358 of the Junta de Andalucía. However, the article does not necessarily reflect European Commission (EC) views and in no way anticipates future policy of the EU in the area. We gratefully thank CESGA (Galician Supercomputing Center) for computational time at the SVG supercomputer and technical assistance.

Literature cited

Abella, A. J., J. F. Caddy, and F. Serena.
1997. Do natural mortality and availability decline with age? An alternative yield paradigm for juvenile fisheries, illustrated by the hake *Merluccius merluccius* fishery in the Mediterranean. Aquat. Living Resour. 10:257–269.

Baranov, F. I.
1976. Selected works on fishing gear. Vol. 1: Commercial fishing techniques, 631 p. Israel Program for Scientific Translations, Jerusalem.

Basilone, G., C. Guisande, B. Patti, S. Mazzola, A. Cuttitta, A. Bonanno, A. R. Vergara, and I. Maneiro.
2006. Effect of habitat conditions on reproduction of the European anchovy (*Engraulis encrasicolus*) in the Strait of Sicily. Fish. Oceanogr. 15:271–280.

Bellido, J. M., G. J. Pierce, J. L. Romero, and M. Millán.
2000. Use of frequency analysis methods to estimate growth of anchovy (*Engraulis encrasicolus* L. 1758) in the Gulf of Cádiz (SW Spain). Fish. Res. 48:107–115.

Burnham, K.P. and D. R. Anderson.
2001. Kullback-Leibler information as a basis for strong inference in ecological studies. Wildl. Res. 28: 111–119.

Caddy, J.F.
1991. Death rates and time intervals: is there an alternative to the constant natural mortality axiom? Rev. Fish Biol. Fish. 1:109–138.
Catalán, I. A., J. P. Rubín, G. Navarro, and L. Prieto.
2006. Larval fish distribution in two different hydrographic situations in the Gulf of Cádiz. Deep-Sea Res., II 53:1377–1390.
Cingolani, N., G. Giannetti, and E. Arneri.
1996. Anchovy fisheries in the Adriatic Sea. Sci. Mar. 60 (suppl. 2):269–277.
Dimmlich, W.F.,W. G. Breed, M. Geddes, and T. M. Ward.
2004. Relative importance of gulf and shelf waters for spawning and recruitment of Australian anchovy, *Engraulis australis*, in South Australia. Fish. Oceanogr. 13:310–323.
Dorn, M.W.
2002. Advice on West Coast rockfish harvest rates from Bayesian meta-analysis of stock–recruit relationships. North Am. J. Fish. Manage. 22(1):280–300.
Drake, P., A. Borlán, E. González-Ortegón, F. Baldó, C. Vilas, and C. Fernández-Delgado.
2007. Spatio-temporal distribution of early life stages of the European anchovy *Engraulis encrasicolus* L. within a European temperate estuary with regulated freshwater inflow: effects of environmental variables. J. Fish Biol. 70:1689–1709.
Durant, J.M., G. Ottersen, and N. C. Stenseth.
2013. Impact of climate and fisheries on sub-Arctic stocks. Mar. Ecol. Prog. Ser. 480:199–203.
Erzini, K.
2005. Trends in NE Atlantic landings (southern Portugal): identifying the relative importance of fisheries and environmental variables. Fish. Oceanogr. 14(3):195–209.
Fréon, P., P. Cury,, L. Shannon, and C. Roy.
2005. Sustainable exploitation of small pelagic fish stocks challenged by environmental and ecosystem changes: a review. Bull. Mar. Sci. 76:385–462.
Fréon, P., F. Werner, and F. P. Chavez.
2009. Conjectures on future climate effects on marine ecosystems dominated by small pelagic fish. *In* Climate change and small pelagic fish (D. M. Checkley Jr., J. Alheit, Y. Oozeki, and C. Roy, eds.), p. 312–343. Cambridge Univ. Press, New York.
García, A. and I. Palomera.
1996. Anchovy early life history and its relation to its surrounding environment in the western Mediterranean basin. Sci. Mar. 60 (suppl. 2):155–166.
Gelman, A., J. B. Carlin, H. S. Stern, D. B. Dunson, A. Vehtari, and D. B. Rubin.
2013. Bayesian data analysis, 3rd ed., 667 p. CRC Press, Boca Raton, FL.
Grün, B. and F. Leisch.
2008. FlexMix version 2: finite mixtures with concomitant variables and varying and constant parameters. J. Stat. Softw. 28(4):1–35.
Guisande, C., A. R. Vergara, I. Riveiro, and J. M. Cabanas.
2004. Climate change and abundance of the Atlantic-Iberian sardine (*Sardina pilchardus*). Fish. Oceanogr. 13:91–101.
Heidelberger, P. and P. D. Welch.
1981. A spectral method for confidence interval generation and run length control in simulations. Commun. ACM 24:233–245.
1983. Simulation run length control in the presence of an initial transient. Oper. Res. 31:1109–1144.
Kullback, S. and R.A.Leibler.
1951. On information and sufficiency. Ann. Math. Stat. 22:79–86.
Lindegren, M., D. M. Checkley Jr., T. Rouyer, A. D. MacCall, and N. C. Stenseth.
2013. Climate, fishing, and fluctuations of sardine and anchovy in the California Current. Proc. Natl. Acad. Sci. U.S.A. 100:13672–13677.
Lloret, J., Lleonart, J., Solé, I., and J.-M. Fromentin.
2001. Fluctuations of landings and environmental conditions in the north-western Mediterranean Sea. Fish. Oceanogr. 10:33–50.
Lloret, J., I. Palomera, J. Salat and J. Sole.
2004. Impact of freshwater input and wind on landings of anchovy (*Engraulis encrasicolus*) and sardine (*Sardina pilchardus*) in shelf waters surrounding the Ebre (Ebro) River delta (north-western Mediterranean). Fish. Oceanogr. 13:102–110.
Mäntyniemi, S., and A. Romakkaniemi.
2002. Bayesian mark-recapture estimation with an application to a salmonid smolt population. Can. J. Fish. Aquat. Sci. 59:1748–1758.
Mäntyniemi, S., S. Kuikka, M. Rahikainen, L. T. Kell and V. Kaitala.
2009. The value of information in fisheries management: North Sea herring as an example. ICES J. Mar. Sci. 66:2278–2283.
Mäntyniemi, S., L. Uusitalo, H. Peltonen, P. Haapasaari and S. Kuikka.
2013. Integrated, age-structured, length-based stock assessment model with uncertain process variances, structural uncertainty, and environmental covariates: case of Central Baltic herring. Can. J. Fish. Aquat. Sci. 70:1317–1326.
Mäntyniemi, S. H. P., R. E.Whitlock, T. A. Perälä, P. A. Blomstedt, J. P. Vanhatalo, M. M. Rincón, A. K. Kuparinen, H. P. Pulkkinen and S. Kuikka.
2015. General state–space population dynamics model for Bayesian stock assessment. ICES J. Mar. Sci. 72:2209–2222.
Maunder, M. N. and R. B. Deriso.
2003. Estimation of recruitment in catch-at-age models. Can. J. Fish. Aquat. Sci. 60:1204–1216.
Meyer, R. and R. B. Millar.
1999. BUGS in Bayesian stock assessments. Can. J. Fish. Aquat. Sci. 56:1078–1087.
Michielsens, C. G. J., and M. K. McAllister.
2004. A Bayesian hierarchical analysis of stock-recruit data: quantifying structural and parameter uncertainties. Can. J. Fish. Aquat. Sci. 61:1032–1047.
Millán, M.
1999. Reproductive characteristics and condition status of anchovy *Engraulis encrasicolus* L. from the Bay of Cadiz (SW Spain). Fish. Res. 41:73–86.
Millar, R. B. and R. Meyer.
2000. Bayesian state-space modeling of age-structured data: fitting a model is just the beginning. Can. J. Fish. Aquat. Sci. 57:43–50.
Motos, L., A. Uriarte and V. Valencia.
1996. The spawning environment of the Bay of Biscay anchovy (*Engraulis encrasicolus* L.). Sci. Mar. 60 (suppl. 2):117–140.
Nakata, H., S. Funakoshi and M. Nakamura.
2000. Alternating dominance of postlarval sardine and

anchovy caught by coastal fishery in relation to the Kuroshio meander in the Enshu-nada Sea. Fish. Oceanogr. 9(3):248–258.

Pauly, D., R. Hilborn and T. A. Branch.
2013. Fisheries: Does catch reflect abundance? Nature 494(7437):303–306.

Pertierra, J.P. and J. Lleonart.
1996. NW Mediterranean anchovy fisheries. Sci. Mar. 60 (suppl. 2):257–267.

Pinsky, M.L., O.P. Jensen, D. Ricard and S.R. Palumbi.
2011. Unexpected patterns of fisheries collapse in the world's oceans. Proc. Natl. Acad. Sci. U.S.A. 108: 8317–8322.

Plummer, M.
2012a. JAGS version 3.3.0 user manual, 41 p. Int. Agency Res. Cancer, Lyon, France.
2012b. rjags: Bayesian graphical models using MCMC. R package, vers. 3–9. [Available from website.]

Plummer, M., N. Best, K. Cowles, and K.Vines.
2006. CODA: Convergence diagnosis and output analysis for mcmc. R News 6(1):7–11. [Available from website.]

Punt, A. E. and R. Hilborn.
1997. Fisheries stock assessment and decision analysis: the Bayesian approach. Rev. Fish Biol. Fish. 7:35–63.

Quinn, T .J. and R .B. Deriso.
1998. Quantitative fish dynamics. Oxford Univ. Press, Oxford, UK.

R Core Team.
2015. R: a language and environment for statistical computing. R Foundation for Statistical Computing, Vienna, Austria. [Available from website, accessed August 2015.]

Rincón, M.M., J.D. Mumford, P. Levontin, A.W. Leach and J. Ruiz.
2016. The economic value of environmental data: a notional insurance scheme for the European anchovy. ICES J. Mar. Sci. 73:1033–1041.

Rivot, E., E. Prévost, E. Parent and J. L. Baglinière.
2004. A Bayesian state-space modelling framework for fitting a salmon stage-structured population dynamic model to multiple time series of field data. Ecol. Model. 179:463–485.

Ruiz, J. and S. Kuikka.
2012. Tangled ecosystem models: the temptation of siren songs and silence. Sci. Mar. 76:191–194.

Ruiz, J., E. Garcia-Isarch, I. E. Huertas, L. Prieto, A. Juárez, J. L. Muñoz, A. Sánchez-Lamadrid, S. Rodríguez-Gálvez, J. M. Naranjo and F. Baldó.
2006. Meteorological and oceanographic factors influencing *Engraulis encrasicolus* early life stages and catches in the Gulf of Cádiz. Deep-Sea Res., II 53:1363–1376.

Ruiz, J., R. González-Quirós, L. Prieto, and J. García-Lafuente.
2007. Anchovy in the Gulf of Cádiz: a case of BOTTOP control. GLOBEC International Newsletter 13(2):22–24. [Available from Article]

Ruiz, J., R. González-Quirós, L. Prieto and G. Navarro.
2009. A Bayesian model for anchovy (*Engraulis encrasicolus*): the combined forcing of man and environment. Fish. Oceanogr. 18:62–76.

Somarakis, S., I. Palomera, A. Garcia, L. Quintanilla, C. Koutsikopoulos, A. Uriarte and L. Motos.
2004. Daily egg production of anchovy in European waters. ICES J. Mar. Sci. 61:944–958.

Zarraonaindia, I., M. Iriondo, A. Albaina, M.A. Pardo, C. Manzano, W.S. Grant, X. Irigoien and A. Estonba.
2012. Multiple SNP markers reveal fine-scale population and deep phylogeographic structure in European anchovy (*Engraulis encrasicolus* L.). PLoS ONE 7(7):e42201.

National Marine
Fisheries Service
NOAA

Fishery Bulletin
established in 1881

Spencer F. Baird
First U.S. Commissioner
of Fisheries and founder
of *Fishery Bulletin*

Geographic variations of jumbo squid (*Dosidicus gigas*) based on gladius morphology

Yi Gong[1]
Xinjun Chen[1,2,3,4]
Yunkai Li (contact author)[1,2,3,4]
Zhou Fang[1]

Email address for contact author: ykli@shou.edu.cn

[1] College of Marine Sciences
Shanghai Ocean University
999 Huchenghuan Road
Shanghai, 201306, China

[2] The Key Laboratory of Sustainable Exploitation of Oceanic Fisheries Resources
Ministry of Education
999 Huchenghuan Road
Shanghai 201306, China

[3] National Engineering Research Centre for Oceanic Fisheries
Shanghai Ocean University
999 Huchenghuan Road
Shanghai 201306, China

[4] National Demonstration Center for Experimental Fisheries Science Education
Shanghai Ocean University
999 Huchenghuan Road
Shanghai 201306, China

Abstract—The jumbo flying squid (*Dosidicus gigas*) is widely distributed in the eastern Pacific Ocean and its population structure is complex. Morphometric analysis of hard structures of cephalopods is frequently employed to explore the geographic variation within discreet population units. In this study, 8 morphometric characteristics of the gladius, or pen, were measured and compared from 562 jumbo squid specimens collected off Peru, the Costa Rica Dome, and from the equatorial central eastern Pacific. The growth rate of the gladius was evaluated by comparing it with the ages determined from statoliths. Results showed significant differences in gladii morphology between sexes and geographic populations. Stepwise discriminant analysis indicated that gladius morphometric characteristics were suitable discriminatory variables with an overall correct classification rate of 78.6% for distinguishing different populations. Higher daily growth rates were found in the proostracum than in the conus, possibly because of the different biological functions of these anatomical parts. These results support our general hypothesis that gladius morphology provides an alternative way to distinguish potential geographic populations of *D. gigas* and it adds new information regarding the gladius of the Ommastrephidae.

Manuscript submitted 3 March 2017.
Manuscript accepted 7 November 2017.
Fish. Bull. 116:50–59 (2018).
Online publication date: 7 December 2017.
doi: 10.7755/FB.116.1.5

The views and opinions expressed or implied in this article are those of the author (or authors) and do not necessarily reflect the position of the National Marine Fisheries Service, NOAA.

Morphometric analysis has been an accepted method for studying the geographic variation of population units within species of cephalopods (Nesis, 1993; Crespi-Abril et al., 2010; Liu et al., 2015a; van der Vyver et al., 2016). Cephalopods show high phenotypic plasticity in both soft and hard structures owing to their biological characteristics, such as rapid growth, short life span, and highly migratory activity (Crespi-Abril et al., 2010; Arkhipkin et al., 2015; van der Vyver et al., 2016). Therefore, morphometric analysis may be a useful approach for studying geographic variations in pelagic cephalopods that have an extensive distribution range.

The jumbo flying squid (*Dosidicus gigas*) is widely distributed in the eastern Pacific Ocean, extending from Alaska (60°N) to Chile (46°S) and stretching to the west (125°–140°W) at the Equator (Nigmatullin et al., 2001; Ibáñez and Cubillos, 2007). As a pelagic cephalopod, *D. gigas* has an important ecological function in marine ecosystems, not only as a voracious predator but also as a valuable source of prey (Field et al., 2007; Alegre et al., 2014). It also supports an important commercial fishery, and in 2014 the annual catch exceeded 1,000,000 metric tons (FAO, 2016). The main fishing regions are located off the coasts of Chile and Peru, off the Costa Rica Dome and within the Gulf of California.

Throughout its geographic range, the population structure of *D. gigas* is complicated and often debated. In the past, three distinguishable groups with a different size-at-ma-

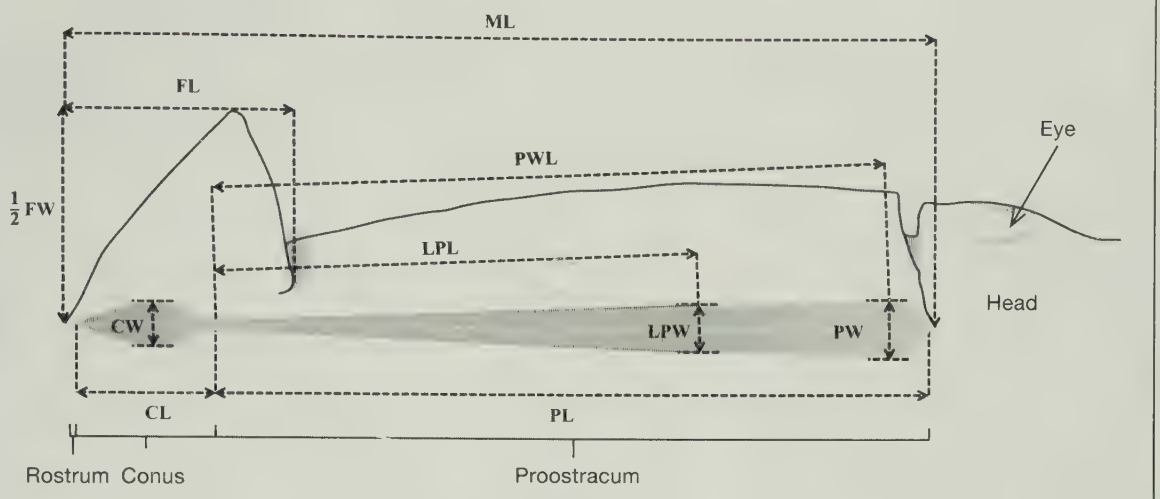

Figure 1

Morphometric measurements of the gladius and mantle recorded for jumbo squid (*Dosidicus gigas*) sampled off the Costa Rica Dome (CRD), off the Peruvian exclusive economic zone (PE), and in offshore waters of the central eastern Pacific (CEP) in 2009, 2013, and 2014 and examined in this study (measurements were taken on the basis of work by Arkhipkin et al., 2012). The measurements are mantle length (ML), conus length (CL), maximum width of conus (CW), proostracum length (PL), maximum width of prostracum (PW), length from anterior tip of conus to the widest point of proostracum (PWL), length from anterior tip of conus to proximal end of lateral plates (LPL), width between two anterior apices of lateral plates (LPW), fin length (FL), and fin width (FW). Adapted from Lorrain et al. (2011).

turity have been identified (Nigmatullin et al. 2001). It has been assumed that there is a small group that occurs in the near-equatorial waters, a medium-size group that is distributed within the entire distribution range, and a large-size group that occurs at the northern and southern peripheries of its distribution range. However, a high degree of variability in the size of the groupings was observed along the eastern Pacific Ocean (Keyl et al., 2011; Morales-Bojórquez and Pacheco-Bedoya, 2016); for example, the mantle length at first maturity was found to vary between 31.0 to 77.0 cm off Mexico (Markaida, 2006). Moreover, little genetic diversity has been found among these three groups on the basis of microsatellite loci (Sanchez et al., 2016). In contrast to this hypothetical spatial distribution, other researchers have divided *D. gigas* into northern and southern populations on the basis of genetic structure (Sandoval-Castellanos et al., 2007) or elemental signatures in the statolith (Liu et al., 2015b). In this study, not only *D. gigas* from northern and southern populations were examined, but also individuals from equatorial central eastern Pacific. For squid whose population structure is uncertain, a holistic management approach should always be considered on the assumption that it is a single population. However, if it can be unequivocally shown that separate stocks are present in the *D. gigas* population, stock-specific harvest strategies may be more effective in providing a sustainable biomass.

In *D. gigas*, the gladius, or pen, is a flexible internal structure that grows from the tail fin toward the head (Fig. 1). Morphologically, the gladius consists of a feather-shaped plate, the proostracum that tapers toward the posterior end of the gladius, becoming a funnel-shaped conus with a smallish rostrum (Arkhipkin et al, 2012). The gladius lies within the shell sac, which attaches to the fin cartilage in the vicinity of the conus and rostrum, whereas, the cartilage attaches to the fin muscles (Young and Vecchione, 1996; Arkhipkin et al, 2012). The gladius is a metabolically inert tissue that grows continuously throughout the lifetime of the species. Previous studies have shown that it is useful in age studies and can reveal ontogenetic patterns associated with changes in diet and habitat (Perez et al., 1996; Ruiz-Cooley et al., 2010; Li et al., 2017). Nonetheless, little attention has been paid to variations in gladius growth although the differences in age, growth, and population structure have often been observed (Sandoval-Castellanos et al., 2007; Chen et al., 2013; Ibáñez et al., 2016).

In this study, the morphometric characteristics of the gladius were analyzed. Our goal was to identify potential sexual dimorphism and spatial variations of gladius shape among population units within *D. gigas*. This study provides an alternative way to identify the potential geographic populations of *D. gigas* and contributes new information on the gladius of Ommastrephidae.

Materials and methods

Sampling and preparation

D. gigas samples were collected during various commercial jigging vessels operating in 2009, 2013, and 2014 in the waters of northern (off the Costa Rica Dome, [CRD]) and southern hemisphere (off the Peru Exclusive Economic Zone, [PE]) and equatorial Pacific Ocean (offshore waters of the central eastern Pacific, [CEP]) (Fig. 2). All squid were frozen on board and then transported to the Key Laboratory of Sustainable Exploitation of Oceanic Fisheries Resources at Shanghai Ocean University where they were defrosted under normal room temperature. Dorsal mantle length (ML), fin length (FL), and fin width (FW) were recorded to the nearest 1 mm, and body weight (BW) was measured to the nearest 1 g. Sex and maturity stage were determined on the basis of visual evaluation of the gonad morphometric characteristics defined by Lipiński and Underhill (1995). The gladius was extracted from its dorsomedial site in the mantle cavity and cleaned in an ultrasonic cleaner with distilled water. Gladii which appeared to be damaged were eliminated. Statoliths were extracted for age determination and the number of growth increments were counted under the assumption that the increment is deposited daily (Jackson and Forsythe, 2002).

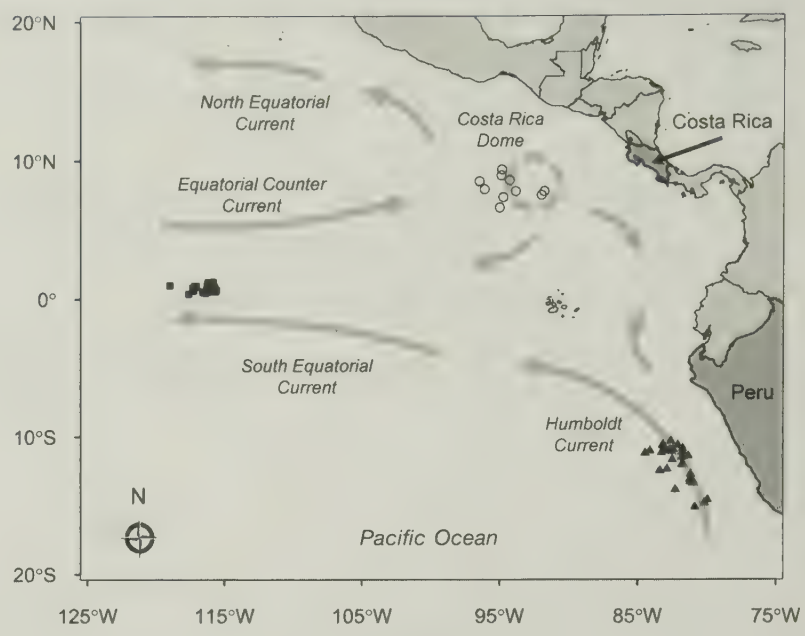

Figure 2

Map of the major surface currents (adapted from Anderson and Rodhouse, 2001) and the locations where jumbo squid (*Dosidicus gigas*) were sampled in 2009, 2013, and 2014 off the Costa Rica Dome (CRD). Sampling locations off the CRD are indicated with open circles, sampling locations off the Peruvian exclusive economic zone (PE), are indicated with black triangles, and those in offshore waters of the central eastern Pacific (CEP) are indicated with black squares. Morphological features were used to distinguish between populations in different geographic zones

Morphometric measurements

A total of 562 gladii from the three regions were used in the subsequent analyses, and detailed information on the samples can be seen in Table 1. Eight morphometric characteristics of the gladius (gladius length [GL], conus length [CL], maximum width of conus [CW], proostracum length [PL], maximum width of prostracum [PW], length from anterior tip of conus to the widest point of proostracum [PWL], length from anterior tip of conus to proximal end of lateral plates [LPL], the width between two anterior apices of lateral plates [LPW]) were measured from each sample to the nearest 1 mm (Fig. 1). All morphometric measurements were made by a single researcher throughout our study.

Statistical analyses

All morphometric data used for the analyses of sexual dimorphism and geographic variation were standardized to remove the allometric effects of body size and meet the assumptions of normality. To accomplish this, raw data were transformed by using the following formula (see Lleonart et al., 2000 for details):

$$Y_i^* = Y_i\left(\frac{ML_0}{ML_i}\right)^b, \quad (1)$$

where Y = one of the morphometric variables of the gladius;
Y_i^* = the standardized value for the individual I;
Y_i and ML_i = the observed values of Y and ML for the individual I;
ML_0 = the arithmetic mean for the study population; and
b can be predicted from the following formula:

$$\ln(Y) = \ln(a) + b\ln(ML) + \varepsilon \; \varepsilon \sim N(0,\sigma^2), \quad (2)$$

where a = a parameter to be estimated; and
σ^2 = the variance for the normally distributed unexplained errors ε.

The standardized variables are represented by subscript "S", i.e. CL_S, CW_S, PL_S, PW_S, PWL_S, LPL_S, LPW_S, FL_S and FW_S.

One-way analysis of variance (ANOVA) and stepwise discriminant analysis (SDA) were used to analyze sexual dimorphism. The SDA is a method of linear modeling to estimate the proportion of correct classification with a leave-one out stepwise jack-knife procedure. Owing to the small sample size of males, samples from off the CRD was excluded from this analysis.

Table 1

Summary information, including mean dorsal mantle length (ML) and body weight (BW) with standard deviations (SDs), for jumbo squid (*Dosidicus gigas*) sampled in 2009, 2013, and 2014 off the Costa Rica Dome (CRD), off the Peruvian exclusive economic zone (PE), and in offshore waters of the central eastern Pacific (CEP) to examine the use of morphological features to distinguish between populations in different geographic zones. *n*=number of squid in a sample

					ML (cm)				BW (g)			
Geographic population	*n* (F, M)	Sampling date	Coordinates	Maturity stage	Maximum	Minimum	Mean	SD	Maximum	Minimum	Mean	SD
CRD	105 (89, 16)	Jul. to Aug. 2009	91°48′– 99°30′W 6°36′– 9°30′N	I–IV	40.9	21.8	29.5	3.1	1907.5	252.6	737.2	256.9
PE	32 (27, 5)	Sep. to Oct. 2009	82°06′– 84°29′W 10°21– 11°17′S	I–III	44.7	26.4	32.7	4.6	2928.7	490.0	1088.2	555.4
	179 (116, 63)	Jul. to Oct. 2013	79°57′– 83°24′W 10°54′– 15°09′S	I–IV	39.6	21.8	26.8	4.3	1647.0	278.0	548.8	379.8
	71 (38, 33)	Feb. to Sep. 2014	74°57′– 83°13′W 10°26′–22°38′S	I–IV	48.5	19.1	28.1	7.3	3361.0	177.0	767.9	721.4
CEP	121 (57, 64)	Apr. to Jun. 2013	114°59′–119°00′W 0°28′N–1°00′S	I–IV	37.2	22.2	29.2	3.7	1523.0	291.0	746.7	300.7
	54 (45, 9)	Apr. to May. 2014	116°00′– 117°19′W 0°42′– 0°58′N	I–III	41.2	27.5	33.0	3.0	1849.0	608.0	1059.8	300.9

Principal component analysis (PCA) was used to determine the main morphometric variables among three population units by reducing the multidimensional data. SDA was performed on the results of PCA to identify the variables that would distinguish the geographic populations and calculate the classification rates.

Moreover, to remove the potential impacts of the disproportionate number of female *D. gigas* and different sex ratios for the three sites, PCA and SDA were repeated with female data only as an independent data set to evaluate the geographic divergence of females.

The analyses of growth rates were performed on untransformed morphometric and age data. The absolute daily growth rate (DGR, mm/day) was calculated for each 25-day interval with the following equation (Forsythe and Van Heukelem, 1987):

$$DGR = \frac{L_2 - L_1}{t_2 - t_1}, \quad (3)$$

where L = one of the morphometric variables of the gladius;

L_1 and L_2 = the observed values (mm) at the beginning (t_1) and the end (t_2) of each interval of time (day).

Multiple comparison was examined by using ANOVA with post-hoc Tukey's honestly significant difference (HSD) test. For nonnormal and ordinal data, a matched comparison with the Friedman test was applied. A P value of ≤0.05 was considered significant for all statistical tests, and statistical analyses were carried out by SPSS Statistics,[1] vers. 19.0 (IBM Corp., Armonk, NY).

Results

Gladius structure

Morphometric variables of the three geographic populations are presented in the Supplementary Table.

Regression analysis performed on the GL and ML showed strong correlations within the three geographic populations (CRD: r=0.95, ML=1.005GL+1.267; PE: r=0.98, ML=0.94GL+0.99; CEP: r=0.99, ML=1.03GL–0.63). As main morphological parts of the gladius, the ratio of CL to PL (CL/PL) showed significant differences (ANOVA, P<0.05, $F_{2, 558}$=87.30) among regions. The CL/PL values for squid off the CRD (0.22 ±0.02) were lower than those off the PE (0.24 ±0.02) and CEP squid (0.26 ±0.02). In addition, the CL showed significant positive relationships with FW (CR: r=0.77; PE: r=0.90; CEP: r=0.70) and FL (CR: r=0.82; PE: r=0.89; CEP: r=0.72).

Sexual dimorphism

When comparing morphometric characteristics between females and males, we found that only CL_S, CW_S and

[1] Mention of trade names or commercial companies is for identification purposes only and does not imply endorsement by the National Marine Fisheries Service, NOAA.

Table 2

Results of analysis of variance between sexes for standardized (S) gladius morphometric variables of jumbo squid (*Dosidicus gigas*) sampled in 2009, 2013, and 2014 off the Peruvian exclusive economic zone (PE) and in offshore waters of the central eastern Pacific (CEP). The morphometric variables are conus length (CL), maximum width of conus (CW), proostracum length (PL), maximum width of prostracum (PW), length from anterior tip of conus to the widest point of proostracum (PWL), length from anterior tip of conus to proximal end of lateral plates (LPL), and width between 2 anterior apices of lateral plates (LPW). *n*=number of samples; *F*=variance between the means of female and male values; ns=nonsignificant, probability (*P*)>0.05; *=*P*<0.05; **=*P*<0.01

	PE		CEP	
Variable	*F*	*P*	*F*	*P*
n	282		175	
CL_S	3.72	ns	38.67	**
CW_S	2.40	ns	27.06	**
PL_S	8.21	**	281.11	**
PW_S	5.93	*	89.90	**
PWL_S	26.29	**	57.87	**
LPL_S	3.07	ns	78.39	**
LPW_S	4.34	*	60.13	**

LPL_S of PE specimens were not different for the sexes (Table 2). Meanwhile, the SDA results showed that the correct cross-validated classification rates reached from 62.4 % to 94.3 % for the region off PE and within the CEP, respectively (Table 3). The results may indicate a significant difference between the sexes within each population.

Geographic variations

For all individuals, the PCA of the morphometric features of squid gladii retained two principal components (PC1 and PC2), having eigenvalues greater than 1 and accounted for 62.40 % and 14.81 % of the total variance, respectively. The main variables counting for variation in PC1 were CL_S, PL_S, PW_S, PWL_S, LPL_S, and LPW_S. Variation of PC2 was mainly influenced by CW_S. The SDA performed on all samples identified four valid gladius morphometric features (CL_S, CW_S, PL_S and PW_S) that served as discriminatory variables for the three geographic populations (Table 4). The first canonical function explained 83.9% of the total variance. Although there was considerable overlap, the final correct cross-validated classification rates among the geographic populations reached 80.0% (off the CRD), 74.8% (off the PE) and 84.0% (within the CEP), respectively (Table 5A).

The PCA performed on data sets for females detected only one principal component with eigenvalues greater than 1 and explaining 65.30% of the total variance. All morphometric features showed high contributions to the principal component analysis. The SDA selected CL_S, CW_S, PL_S, and PW_S as suitable variables to distinguish female *D. gigas* from the three regions, with a misclassification rate of 16.8% (Tables 4 and 5B).

Table 3

The percentages of cross-validated classification from stepwise discriminant analysis for each sex of 2 geographic populations of jumbo squid (*Dosidicus gigas*) sampled in 2013 and 2014 off the Peruvian exclusive economic zone (PE) and in offshore waters of the central eastern Pacific (CEP).

	PE		CEP	
	Female	Male	Female	Male
Female	62.0%	38.0%	96.1%	3.9%
Male	36.7%	63.3%	8.2%	91.8%
Total	62.4%		94.3%	
P	<0.001		<0.001	

A total of 340 statoliths from the three sites were satisfactorily prepared for age determination. In all three population units, values of DGR for PL were larger than CL during all studied periods for each sex (Friedman test, $P<0.01$, Table 6), although small sample sizes may have influenced the reliability of calculated growth rates in some age groups.

For each geographic population, the maximum DGR in CL was found from 201 to 225 days of age for female *D. gigas* (Table 6). Although the maximum DGR in PL occurred at different periods, the value for off the CRD (1.44 mm/d, 201–225 days) and off the PE (1.12 mm/d, 201–225 days) were larger but occurred later than the CEP value (1.11 mm/d, 176–200 days). For males, the maximum DGR in CL (0.41 mm/d) was reached from 201to 225 days of age for PE, wheras in the CEP the maximum is smaller (0.34 mm/d) and it is reached before, at 176–200 days. In contrast, the maximum DGR in PL was observed at 201–225 and 176–200 days for males off the PE and within the CEP (Table 6).

Discussion

Gladius structure

In *D. gigas*, a strong correlation was found between GL and ML in each geographic population. This finding indicates that the gladius can be considered a hard tissue that supports the mantle and internal organs. Similar results were reported for other ommastrephids, *Illex illecebrosus* (Perez et al., 1996) and *Ommastrephes bartramii* (Kato et al., 2016). Also, GL may be a more reliable measurement than ML when individuals are

Table 4

Function coefficients for 3 geographic populations of jumbo squid (*Dosidicus gigas*) sampled off the Costa Rica Dome (CRD), off the Peruvian exclusive economic zone (PE), and offshore waters of the central eastern Pacific (CEP) in 2009, 2013, and 2014. The morphometric features used for the examination are proostracum length (PL), conus length (CL), the maximum width of conus (CW), and the maximum width of prostracum (PW).

		CR	PE	CEP
All individuals	PL_S	19.56	20.17	23.78
	CL_S	12.02	18.08	25.72
	CW_S	31.57	29.65	32.15
	PW_S	−37.22	−31.43	−37.54
	(constant)	−392.63	−365.74	−441.60
Females	PL_S	25.07	25.63	30.48
	CL_S	42.88	47.98	62.08
	CW_S	40.57	38.26	42.58
	PW_S	−26.65	−18.64	−25.87
	(constant)	−532.33	−498.69	−629.86

stored frozen because soft tissues can be deformed during the thawing process. In this study, positive correlations were found between the CL with FL and FW in all three population units. The conus, which is located in the middle of the tail fin, is the main morphological section of the gladius (Arkhipkin et al., 2012). With their anatomical analysis, Young and Vecchione (1996) found that fin cartilage connected the fin muscles and shell sac, which secretes the conus and cone flags. Therefore, the conus could be considered a supporting structure that helps the fin resist the dynamic pressures generated during swimming (Bizikov and Arkhipkin, 1997; Arkhipkin et al., 2012). A longer conus might also provide appropriate support for the fin when the animal is experiencing high speed currents.

Sexual size dimorphism

Sexual size dimorphism is a common phenomenon that occurs in the hard structures of cephalopods (Fang et al., 2014; Liu et al., 2015a). Our results also showed that the shapes of gladii were different for the sexes within two of the populations (i.e., off the PE and within the CEP). These results are in agreement with those from Liu et al. (2015a) who observed sexual dimorphism in another hard structure, the beak of *D. gigas*, from these same two populations which are found in the waters off Peru and Ecuador, termed PE and CEP, respectively in our study. This difference in shapes was despite the fact that both populations experienced similar environmental conditions and food availability. However, sex-specific different nutritional requirements have recently been described for female and male squid and may explain the sexual dimorphism we observed (e.g. *Nototodarus gouldi*, (Steer and Jackson, 2004), *Sepioteuthis australis* (Pecl and Moltschaniwskyj, 2006) and *Illex argentines* (Lin et al., 2015)). In these cases, females and males within the population show divergent energetic needs for growth or reproduction, and one might expect this to result in squid with different growth-related parameters, which could have a potential impact on the gladius morphometric characteristics (van der Vyver et al., 2016). Additionally, there may be sexually related behavioral differences where females and males might forage on different prey items at different depths in a given habitat (Arkhipkin and Middleton, 2002).

Geographic variations

Dosidicus gigas is a species endemic to the eastern Pacific and has a complex population structure. Geographic variations in age, growth, and reproduction of this species have often been observed (Sandoval-Castellanos et al., 2007; Chen et al., 2013; Ibáñez et al., 2016). As reported by Liu et al. (2015a), spatial variations in the beak structure of *D. gigas* could be used to distinguish geographic populations. This difference was attributed to a phenotypic response resulting from distinct environmental conditions that a population experiences at a given geographic location (Liu et al., 2015a; van der Vyver et al., 2016), but further research is needed to confirm the exact relationship between a species' physiological response to variations in the environment.

In this study, the SDA revealed a high rate of correct classification of gladii shapes among geographic populations, even with the female data as an independent data set (Table 5B). When looking at the environmental conditions these populations experience,

Table 5

Results of the stepwise procedure of discriminant analysis showing the order of standardized ($_S$) morphometric variables to entry for (**A**) 3 geographic populations and (**B**) the female jumbo squid (*Dosidicus gigas*) sampled in 2009, 2013, and 2014 off the Costa Rica Dome (CRD), off the Peruvian exclusive economic zone (PE), and in offshore waters of the central eastern Pacific (CEP). Correct cross-validated classification rates are shown in bold type. The morphometric variables are proostracum length (PL), conus length (CL), the maximum width of conus (CW), and the maximum width of prostracum (PW). At each step, the variable with the largest F value that exceeds the entry criteria is added.

A

Step no.	Variable	F	df 1	df 2	P
1	PL_S	264.60	2	559.00	<0.01
2	CL_S	193.95	4	1116.00	<0.01
3	CW_S	151.85	6	1114.00	<0.01
4	PW_S	119.01	8	1112:00	<0.01

	Number and percentage of samples classified to a population			
Population	CR	PE	CEP	Total
CR	84	18	3	105
%	**80.0**	17.1	2.9	100
PE	62	211	9	282
%	22.0	**74.8**	3.2	100
CEP	14	14	147	175
%	8.0	8.0	**84.0**	100
			Total correct (%)	**78.6**

B

Step no.	Variable	F	df 1	df 2	P
1	PLs	331.32	2	372.00	<0.01
2	CLs	204.84	4	742.00	<0.01
3	CWs	165.34	6	740.00	<0.01
4	PWs	129.74	8	738.00	<0.01

	Number and percentage of samples classified to a population			
Population	CR	PE	CEP	Total
CR	72	14	3	89
%	**80.9**	15.7	3.4	100
PE	39	141	4	184
%	21.2	**76.6**	2.2	100
CEP	3	0	99	102
%	2.9	0	**97.1**	100
			Total correct (%)	**83.2**

there is reason to believe that our SDA results can be explained by these environmental differences. For example, the Costa Rica Dome (Fig. 2) is an oceanic upwelling center where the thermocline is shallow (Sasai et al., 2007), whereas the waters off Peru (PE) are primarily affected by the cold northward flowing Humboldt Current and are associated with strong upwelling of cool subsurface waters (Chavez et al., 2008). Individuals in the CEP were from an area primarily influenced by a warm Equatorial Counter Current and the cooler South Equatorial Current (Fig. 2). The differences in oceanographic conditions in each region may consequently result in morphometric variations in the gladius. For example, several studies have shown that ambient temperature has a significant influence on the growth and development of *D. gigas* (Keyl et al.,

Table 6

Absolute daily growth rates (DGR) in mm/day for conus length (CL) and proostracum lengh (PL) for female and male jumbo squid (*Dosidicus gigas*) sampled off the Costa Rica Dome (CRD), off the Peruvian exclusive economic zone (PE), and in offshore waters of the central eastern Pacific (CEP) in 2009, 2013, and 2014. *n*=number of squid in a sample. na=data not available.

Population	Sex	Age class (d)	*n*	Average CL (mm)	DGR (mm/d)	Average PL (mm)	DGR (mm/d)
CR	F	126-150	2	37.5	na	167.5	na
		151-175	15	43.1	0.22	198.0	1.22
		176-200	36	49.2	0.24	222.9	1.00
		201-225	29	57.9	0.35	259.0	1.44
		226-250	3	63.0	0.20	288.0	1.16
PE	F	126-150	8	46.0	na	188.0	na
		151-175	31	49.2	0.13	200.6	0.50
		176-200	41	51.9	0.11	211.0	0.42
		201-225	7	62.1	0.41	239.0	1.12
		226-250	2	68.5	0.26	255.5	0.66
		251-275	2	78.0	0.38	278.5	0.92
	M	126-150	6	42.5	na	186.3	na
		151-175	17	47.3	0.19	194.8	0.34
		176-200	21	49.8	0.10	204.2	0.38
		201-225	8	60.1	0.41	233.4	1.17
CEP	F	126-150	5	50.6	na	191.6	na
		151-175	6	54.7	0.16	208.3	0.67
		176-200	26	59.7	0.20	236.0	1.11
		201-225	12	65.8	0.24	250.7	0.59
		226-250	4	69.5	0.15	276.0	1.01
	M	126-150	5	45.8	na	185.0	na
		151-175	13	51.6	0.23	200.5	0.62
		176-200	27	60.1	0.34	234.7	1.37
		201-225	13	64.5	0.18	252.50	0.71
		226-250	1	67.0	0.10	268.00	0.62

2011; Staaf et al., 2011). The proostracum contributes to a large proportion of GL (>80 %) and has a higher longitudinal growth rate than conus (Table 6). With the assumption that the conus provides a supporting structure for the fin during swimming, the higher growth rate of the proostracum can be considered a structure that meets the requirements for rapid growth of squids because the gladius is a tissue that supports the growth of the mantle and internal organs (Bizikov and Arkhipkin, 1997; Arkhipkin et al., 2012). Comparisons in CL/PL values and growth rates between geographic populations show spatial variations in these two structures. The squid from CEP had higher CL/PL values than the squid from the area of the CRD and PE. We suggest that this result is possibly due to the environmental conditions experienced by the squid off the CRD and PE that are reflected in the longitudinal growth of proostracum. The Humboldt Current or upwelling (or both) supply nutrients to the waters off Peru and the CRD, while the waters of the central equatorial Pacific have lower primary productivity (Anderson and Rodhouse, 2001; Fiedler, 2002). Because food availability is considered as one of the central factors that influences *D. gigas* growth (Chen et al., 2013; Liu et al., 2013), regional differences in primary productivity may be strongly correlated with the observed differences in the growth of gladius.

Although the squid populations can be distinguished on the basis of morphological evidence, there is still considerable overlap, as shown in Table 5, A and B, which suggests that stable population substructuring is not the norm. Similar overlap has also been observed in elemental signatures in statoliths o *D. gigas* from waters off the Costa Rica Dome and Peru (Liu et al., 2015b). Indeed it was reported that a weak northern and southern hemisphere divergence was found for *D. gigas* with the use of molecular methods. Sandoval-Castellanos et al. (2010) and Staaf et al. (2010), and some of our results from CEP individuals have also indicated a close similarity to the other two jumbo squid populations. This finding would suggest that although the morphological studies reported here suggest clear spatial subpopulations, further research will reveal the stability of these populations units over time.

Acknowledgments

We thank observers who helped us with the collection and processing of samples. We also thank B. L. Liu, for providing the squid age data. Y. Gong and Y. K. Li were supported by the National Natural Science Foundation of China (#41541042), the Natural Science Foundation of Shanghai (#17ZR1413000), and the Shanghai Leading Academic Discipline Project (Fisheries Discipline). The senior author and X. Chen contributed equally to this work.

Literature cited

Alegre, A., F. Ménard, R. Tafur, P. Espinoza, J. Argüelles, V. Maehara, O. Flores, M. Simier, and A. Bertrand.
2014. Comprehensive model of jumbo squid *Dosidicus gigas* trophic ecology in the northern Humboldt Current System. PLoS ONE 9(1):e85919.

Anderson, C.I. and P. G. Rodhouse.
2001. Life cycles, oceanography and variability: ommastrephid squid in variable oceanographic environments. Fish. Res. 54:133–143.

Arkhipkin, A.I., and D. A. J. Middleton.
2002. Sexual segregation in ontogenetic migrations by the squid *Loligo gahi* around the Falkland Islands. Bull. Mar. Sci. 71:109–127.

Arkhipkin, A. I., V. A. Bizikov, and D. Fuchs.
2012. Vestigial phragmocone in the gladius points to a deepwater origin of squid (Mollusca: Cephalopoda). Deep-Sea Res., I. 61:109–122.

Arkhipkin, A., J. Argüelles, Z. Shcherbich, and C. Yamashiro.
2015. Ambient temperature influences adult size and life span in jumbo squid (*Dosidicus gigas*). Can. J. Fish. Aquat. Sci. 72:400–409.

Bizikov, V. A. and A. I. Arkhipkin.
1997. Morphology and microstructure of the gladius and statolith from the boreal Pacific giant squid *Moroteuthis robusta* (Oegopsida; Onychoteuthidae). J. Zool. 241: 475–492.

Chavez, F. P., A. Bertrand, R. Guevara-Carrasco, P. Soler, and J. Csirke.
2008. The northern Humboldt Current System: brief history, present status and a view towards the future. Prog. Oceanogr. 79:95–105.

Chen, X., J. Li, B. Liu, Y. Chen, G. Li, Z. Fang, and S. Tian.
2013. Age, growth and population structure of jumbo flying squid, *Dosidicus gigas*, off the Costa Rica Dome. J. Mar. Biol. Assoc. U.K. 93:567–573.

Crespi-Abril, A. C., E. M. Morsan, and P. J. Barón.
2010. Analysis of the ontogenetic variation in body and beak shape of the *Illex argentinus* inner shelf spawning groups by geometric morphometrics. J. Mar. Biol. Assoc. U.K. 90:547–553.

Fang, Z., B. Liu, J. Li, H. Su, and X. Chen.
2014. Stock identification of neon flying squid (*Ommastrephes bartramii*) in the North Pacific Ocean on the basis of beak and statolith morphology. Sci. Mar. 78:239–248.

FAO (Food and Agricultural Organization of the United Nations).
2016. FAO yearbook. Fishery and aquaculture statistics 2014, 78 p. FAO, Rome.

Fiedler, P. C.
2002. The annual cycle and biological effects of the Costa Rica Dome. Deep-Sea Res., I. 49:321–338.

Field, J. C., K. Baltz, A. J. Phillips, and W. A. Walker.
2007. Range expansion and trophic interactions of the jumbo squid, *Dosidicus gigas*, in the California Current. CalCOFI Rep. 48:131–146.

Forsythe, J. W. and W. F. Van Heukelem.
1987. Growth. *In* Cephalopod life cycles. Vol. II: Comparative reviews (P. R. Boyle, ed.), p. 135–156. Academic Press, London.

Ibáñez, C. M. and L. A. Cubillos.
2007. Seasonal variation in the length structure and reproductive condition of the jumbo squid *Dosidicus gigas* (d'Orbigny, 1835) off central-south Chile. Sci. Mar. 71:123–128.

Ibáñez, C.M., J. Argüelles, C. Yamashiro, R. D. Sepúlveda, M. C. Pardo-Gandarillas, and F. Keyl.
2016. Population dynamics of the squids *Dosidicus gigas* (Oegopsida: Ommastrephidae) and *Doryteuthis gahi* (Myopsida: Loliginidae) in northern Peru. Fish. Res. 173:151–158.

Jackson, G. D., and J. W. Forsythe.
2002. Statolith age validation and growth of *Loligo plei* (Cephalopoda: Loliginidae) in the north-west Gulf of Mexico during spring/summer. J. Mar. Biol. Assoc. U.K. 82:677–678.

Kato, Y., M. Sakai, H. Nishikawa, H. Igarashi, Y. Ishikawa, D. Vijai, Y. Sakurai, T. Wakabayshi, and T. Awaji.
2016. Stable isotope analysis of the gladius to investigate migration and trophic patterns of the neon flying squid (*Ommastrephes bartramii*). Fish. Res. 173:169–174.

Keyl, F., J. Argüelles, and R. Tafur.
2011. Interannual variability in size structure, age, and growth of jumbo squid (*Dosidicus gigas*) assessed by modal progression analysis. ICES J. Mar. Sci. 68:507–518.

Li, Y., Y. Gong, Y. Zhang, and X. Chen.
2017. Inter-annual variability in trophic patterns of jumbo squid (*Dosidicus gigas*) off the exclusive economic zone of Peru, implications from stable isotope values in gladius. Fish. Res. 187:22-30.

Lin, D., X. Chen, Y. Chen, and Z. Fang.
2015. Sex-specific reproductive investment of summer spawners of *Illex argentinus* in the southwest Atlantic. Invertebr. Biol. 134:203–213.

Lipiński, M. R., and L. G. Underhill.
1995. Sexual maturation in squid: quantum or continuum? S. Afr. J. Mar. Sci. 15:207–223.

Liu, B., X. Chen, Y. Chen, S. Tian, J. Li, Z. Fang, and M. Yang.
2013. Age, maturation, and population structure of the Humboldt squid *Dosidicus gigas* off the Peruvian Exclusive Economic Zones. Chin. J. Oceanol. Limnol. 31:81–91.

Liu, B., Z. Fang, X. Chen, and Y. Chen.
2015a. Spatial variations in beak structure to identify potentially geographic populations of *Dosidicus gigas* in the Eastern Pacific Ocean. Fish. Res. 164:185–192.

Liu, B. L., Y. Chen, and X. J. Chen.
2015b. Spatial difference in elemental signatures within early ontogenetic statolith for identifying jumbo flying squid natal origins. Fish. Oceanogr. 24:335–346.

Lleonart, J., J. Salat, and G. J. Torres.
2000. Removing allometric effects of body size in morphological analysis. J. Theor. Biol. 205:85-93.

Lorrain, A., J. Arguelles, A. Alegre, A. Bertrand, J. M. Munaron, P. Richard, and Y. Cherel.
2011. Sequential isotopic signature along gladius highlights contrasted individual foraging strategies of jumbo squid (*Dosidicus gigas*). PLoS ONE 6(7):e22194.

Markaida, U.
2006. Population structure and reproductive biology of jumbo squid *Dosidicus gigas* from the Gulf of California after the 1997–1998 El Niño event. Fish. Res. 79:28–37.

Morales-Bojórquez, E. and J. L. Pacheco-Bedoya.
2016. Population dynamics of jumbo squid *Dosidicus gigas* in Pacific Ecuadorian waters. J. Shellfish Res. 35:211-224.

Nesis, K. N.
1993. Population structure of oceanic ommastrephids, with particular reference to *Sthenoteuthis oualaniensis*: a review. *In* Recent advances in cephalopod fisheries biology (T. Okutani, R. K. O'Dor, and T. Kubodera, eds.), p. 375–383. Tokai Univ. Press, Tokyo, Japan.

Nigmatullin, C.M., K. N. Nesis, and A. I. Arkhipkin.
2001. A review of the biology of the jumbo squid *Dosidicus gigas* (Cephalopoda: Ommastrephidae). Fish. Res. 54:9–19.

Pecl, G.T., and N. A. Moltschaniwskyj.
2006. Life history of a short-lived squid (*Sepioteuthis australis*): resource allocation as a function of size, growth, maturation, and hatching season. ICES. J. Mar. Sci. 63:995–1004.

Perez, J. A. A., R. K. O'Dor, P. Beck, and E. G. Dawe.
1996. Evaluation of gladius dorsal surface structure for age and growth studies of the short-finned squid, *Illex illecebrosus* (Teuthoidea: Ommastrephidae). Can. J. Fish. Aquat. Sci. 53:2837–2846.

Ruiz-Cooley, R.I., E. C. Villa, and W. R. Gould.
2010. Ontogenetic variation of $\delta^{13}C$ and $\delta^{15}N$ recorded in the gladius of the jumbo squid *Dosidicus gigas*: geographic differences. Mar. Ecol. Prog. Ser. 399:187–198.

Sanchez, G., S. Tomano, C. Yamashiro, R. Fujita, T. Wakabayashi, M. Sakai, and T. Umino.
2016. Population genetics of the jumbo squid *Dosidicus gigas* (Cephalopoda: Ommastrephidae) in the northern Humboldt Current system based on mitochondrial and microsatellite DNA markers. Fish. Res. 175:1–9.

Sandoval-Castellanos, E., M. Uribe-Alcocer, and P. Díaz-Jaimes.
2007. Population genetic structure of jumbo squid (*Dosidicus gigas*) evaluated by RAPD analysis. Fish. Res. 83:113–118.
2010. Population genetic structure of the Humboldt squid (*Dosidicus gigas* d'Orbigny, 1835) inferred by mitochondrial DNA analysis. J. Exp. Mar. Biol. Ecol. 385:73–78.

Sasai, Y., H. Sasaki, K. Sasaoka, A. Ishida, and Y. Yamanaka.
2007. Marine ecosystem simulation in the eastern tropical Pacific with a global eddy resolving coupled physical-biological model. Geophys. Res. Lett. 34:208–219.

Staaf, D. J., R. I. Ruiz-Cooley, C. Elliger, Z. Lebaric, B. Campos, U. Markaida, and W. F. Gilly.
2010. Ommastrephid squids *Sthenoteuthis oualaniensis* and *Dosidicus gigas* in the eastern Pacific show convergent biogeographic breaks but contrasting population structures. Mar. Ecol. Prog. Ser. 418:165–178.

Staaf, D. J., L. D. Zeidberg, and W. F. Gilly.
2011. Effects of temperature on embryonic development of the Humboldt squid *Dosidicus gigas*. Mar. Ecol. Prog. Ser. 441:165–175.

Steer, B. L. M., and G. D. Jackson.
2004. Temporal shifts in the allocation of energy in the arrow squid, *Nototodarus gouldi*: sex-specific responses. Mar. Biol. 144:1141–1149.

van der Vyver, J. S. F., W. H. H. Sauer, N. J. McKeown, D. Yemane, P. W. Shaw, and M. R. Lipinski.
2016. Phenotypic divergence despite high gene flow in chokka squid *Loligo reynaudii* (Cephalopoda: Loliginidae): implications for fishery management. J. Mar. Biol. Assoc. U.K. 96:1507–1525.

Young, R.E. and M. Vecchione.
1996. Analysis of morphology to determine primary sister-taxon relationships within coleoid cephalopods. Am. Malacol. Bull. 12:91–112.

National Marine Fisheries Service
NOAA

Fishery Bulletin
established in 1881

Spencer F. Baird
First U.S. Commissioner of Fisheries and founder of *Fishery Bulletin*

Distinction of saffron cod (*Eleginus gracilis*) from several other gadid species by using microsatellite markers

Noel Sme[1]
Sarah Lyon[1]
Michael Canino[2]
Natalia Chernova[3]
Jason O'Bryhim[4]
Stacey Lance[4]
Kenneth Jones[5]
Franz Mueter[1]
Anthony Gharrett (contact author)[1]

Email address for contact author: a.gharrett@alaska.edu

[1] Juneau Center
College of Fisheries and Ocean Sciences
University of Alaska Fairbanks
17101 Point Lena Loop Road
Juneau, Alaska 99801

[2] Alaska Fisheries Science Center
National Marine Fisheries Service, NOAA
7600 Sand Point Way NE
Seattle, Washington 98115

[3] Zoological Institute of the Russian Academy of Sciences
Universitetskaja Naberezhnaya 1

[4] Savannah River Ecology Laboratory
University of Georgia
P.O. Drawer E
Aiken, South Carolina 29802

[5] Section of Hematology-Oncology
Department of Pediatrics
University of Colorado School of Medicine
12800 East 19th Ave, RC-1 North, Room 4129
Aurora, Colorado 80045
St. Petersburg, Russia 199034

Abstract—Nine microsatellite loci isolated in saffron cod (*Eleginus gracilis*) have potential applications for population genetics. Polymerase chain reaction products of samples of *E. gracilis* from northwestern Alaska amplified reliably, produced only one or two microsatellite bands, and had no apparent homozygote excess. A collection of *E. gracilis* sampled in the Gulf of Alaska (GOA) near Kodiak Island did not amplify reliably at one locus, and allele frequency profiles clustered distinctly (with principal component analysis [PCA]) from the northwestern Alaska collection. Northwestern Alaska and GOA *E. gracilis* collections were genetically different (on the basis of a standardized genetic differentiation measure [G'_{ST}]=0.313, chord distance [D_{chord}]=0.078, P<0.0001) and differed in expected average heterozygosities at shared loci (0.859 and 0.689, respectively). We tested the microsatellite primers on other gadid species endemic to the northern Pacific Ocean, Bering Sea, and Arctic Ocean for cross-species amplification. Not all loci amplified reliably in navaga (*E. nawaga*), Pacific tomcod (*Microgadus proximus*), Arctic cod (*Boreogadus saida*), Pacific cod (*Gadus macrocephalus*), or walleye pollock (*G. chalcogrammus*). Reliable loci varied in microsatellite size profiles and produced distinct PCA clusters and accurate genotype assignments that allowed accurate species identification. The identifications support previous morphological and genetically determined systematic classifications and distinguished the geographically separated collections of *E. gracilis*.

Manuscript submitted 20 April 2017.
Manuscript accepted 7 November 2017.
Fish. Bull. 116:60–68 (2018)
Online publication date: 13 December 2017.
doi: 10.7755/FB.116.1.6

The views and opinions expressed or implied in this article are those of the author (or authors) and do not necessarily reflect the position of the National Marine Fisheries Service, NOAA.

The saffron cod (*Eleginus gracilis*) is a gadid fish distributed from the northern Gulf of Alaska (GOA), around the Pacific Rim into the Sea of Okhotsk, and into the Arctic Ocean abutting the North Pacific Ocean (Cohen et al., 1990; Mecklenburg et al., 2016). Mature fish, which generally exceed 20 cm in fork length (FL) and may grow to more than 50 cm FL, are eaten by indigenous Alaskans and in Asia and have potential for commercial harvest in North America (Cohen et al., 1990; NPFMC[1]; Love et al.[2]). Saffron cod is also an important component of the Arctic ecosystem (Wolotira, 1985; Copeman et al., 2016; Love et al.[2]) and is a significant prey item for several marine mammals (Bluhm and Gradinger, 2008). It is thought to compete for food with Arctic cod (*Boreogadus saida*) and may have a competitive advantage as sea ice changes occur in response to climate change (Love et al.[2]). The species, especially in North Ameri-

[1] NPFMC (North Pacific Fisheries Management Council). 2009. Fishery management plan for fish resources of the Arctic management area, 76 p. NPFMC, Anchorage, AK. [Available from website.]

[2] Love, M. S., N. Elder, C. W. Mecklenburg, L. K. Thorsteinson, and T. A. Mecklenburg. 2016. Alaska Arctic marine fish species accounts: saffron cod (*Eleginus gracilis*). *In* Alaska Arctic marine fish ecology catalog. U.S. Geological Survey Sci. Invest. Rep. 2016–5038 (OCS Study, BOEM 2016-048) (L. K. Thorsteinson and M. S. Love, eds.), p. 201–208. [Available from website.]

can waters, is little studied, but its position in the food web, potential population responses to warming and reduction of sea ice in the Arctic, and proposed offshore oil and gas development make learning about this species imperative.

The distributions of several other gadid species—Arctic cod (*B. saida*), Pacific cod (*Gadus macrocephalus*), walleye pollock (*Gadus chalcogrammus*), and Pacific tomcod (*Microgadus proximus*)—overlap with that of *E. gracilis*, and furthermore navaga (*Eleginus nawaga*) from the western Arctic Ocean is a congener of *E. gracilis*. Small gadids of several species are very similar morphologically and often present challenges for identification. The morphological bases of gadiform taxonomy, including the subfamily Gadinae to which all of the species in our study belong, have been described (e.g., Schultz and Welander, 1935; Svetovidov, 1948; Cohen, 1989), as have the phylogenetic relationships among gadiform families (e.g., Roa-Varón and Ortí, 2009) and within Gadinae (Teletchea et al., 2006). However, questions remain about the relationships among *E. gracilis*, *E. nawaga*, and *M. proximus* (e.g., Carr et al., 1999; Roa-Varón and Ortí, 2009). Moreover, the modern geographic separation between *E. eleginus* and *E. nawaga*, if any exists, is unknown.

Genetic analyses of a species can provide insight into several facets of its biology, including population structure, life history (e.g., Kamin et al., 2014), and recent demographic history (e.g., Harpending et al., 1998). Information about population structure can be obtained from surveys in different geographic regions and the fish tested for genetic variation. Microsatellite data are beneficial, when compared with other classes of molecular markers, in that they are often highly polymorphic in fish species (DeWoody et al., 2000) and are relatively inexpensive to apply. Consequently, microsatellite markers were isolated from and developed for *E. gracilis*. Here we 1) examine their variability in two *E. gracilis* collections from geographically separated areas; 2) determine their cross-reactivity with other northern Pacific and Arctic ocean gadids and the ability of suites of these loci to accurately distinguish among species; and 3) evaluate differences in the allele profiles among *M. proximus*, *E. nawaga*, and the two collections of *E. gracilis*.

Materials and methods

Samples and DNA isolation

Collections of *E. gracilis* were collected from the Chuckchi Sea in 2011 and near Kodiak Island, Alaska, in 2013. Collections of *B. saida* from the Chukchi Sea were made in 2012 and collections of *E. nawaga* were collected from the Barents Sea in 2013. In 2015, *G. chalcogrammus* were collected in the southeast Bering Sea. Two collections of *M. proximus* were obtained, one from Puget Sound, Washington, between 1997 and 1999, and one from Prince William Sound, Alaska, in 2012. Two collections of *G. microcephalus* were collected in 2013, one collected from Puget Sound and the other from Unimak Pass in the northern Gulf of Alaska (see details for all collections in Table 1).

Tissue samples were preserved in a DNA preservative solution (Seutin et al., 1991) or 95% ethanol and stored in the laboratory at –20°C. Total cellular DNA was isolated with Gentra Puregene[3] or Qiagen DNeasy kits (Qiagen, Hilden, Germany) by following the manufacturer's instructions.

Discovery of microsatellites

An Illumina paired-end shotgun library (Illumina, Inc., San Diego, CA) was prepared by shearing 1 µg of DNA from a single *E. gracilis* Chukchi Sea individual with a Covaris S220 focused-ultrasonicator (**Covaris, Inc.,** Woburn, MA). The standard protocol for the TruSeq DNA library kit (Illumina, Inc.) and a multiplex identifier adaptor index were used (see e.g., Stoutamore et al., 2012). A HiSeq system (Illumina, Inc.) was used to sequence 100-base pair [bp] paired-end readings. The program PAL_FINDER, vers. 0.02.03 (Castoe et al., 2012) was used to analyze 5 million of the resulting sequences to identify readings that had di-, tri-, tetra-, penta-, and hexanucleotide repeat motifs. The data are archived in the Sequence Read Archive of the National Center for Biotechnology Information under accession number SAMN06333955. Once positive reads were identified, oligonucleotide primers were designed with the program Primer3, vers. 2.0.0 (Koressaar and Remm, 2007; Untergasser et al., 2012). To avoid issues with copy number of primer sequences in the genome, loci for which the primer sequences occurred only once or twice in the 5 million reads were selected. Forty-eight presumed loci from *E. gracilis* that met this criterion were chosen for primer design.

The 48 primer pairs were tested with DNA from 8 *E. gracilis* individuals. The polymerase chain reactions (PCRs) were conducted over two 10°C spans of annealing temperatures (65–55°C or 58–48°C) with touchdown thermal cycling profiles (Don et al., 1991). The results (not presented) were analyzed with GeneMapper, vers. 3.7 (Thermo Fisher Scientific, Waltham, MA). Eighteen primer pairs were then selected for evaluation with larger sample sizes.

Analysis of microsatellites

Target sequences of the 18 primer pairs amplified with a touchdown PCR strategy reduced nontarget bands in the product spectrum (Don et al., 1991). All reactions contained ~1 unit Taq polymerase, 1× PCR buffer (50 mM KCl_2, 10 mM Tris-HCl pH 9.0, 0.1% Triton X-100; Promega Corp., Madison, WI), 0.5 µM deoxyribonucleotide triphosphates, and 0.025 to 0.1 µg DNA

[3] Mention of trade names or commercial companies is for identification purposes only and does not imply endorsement by the National Marine Fisheries Service

Table 1

Number of samples (n), geographic regions, gear used, collector (when known) and collector's affiliation for collections of 6 gadid species sampled in this study: saffron cod (*Eleginus gracilis*), navaga (*E. nawaga*), Pacific tomcod (*Microgadus proximus*), Pacific cod (*Gadus macrocephalus*), walleye pollock (*G. chalcogrammus*), and Arctic cod (*Boreogadus saida*). Asterisks denote specimens originally identified in the field as saffron cod, but were later re-examined.

Species	Scientific name	n	Geographic region	Latitude	Longitude
Saffron cod	*Eleginus gracilis*	30	Chukchi Sea	66.91°N	162.55°W
		41	Gulf of Alaska	57.73°N	152.51°W
Nawaga	*Eleginus nawaga*	81	Barents Sea	69.04°N	57.87°E
Pacific tomcod	*Microgadus proximus*	8	Puget Sound	47.71°N	122.52°W
		15	Prince William Sound*	60.87°N	147.19°W
Pacific cod	*Gadus macrocephalus*	5	Puget Sound	48.40°N	124.41°W
		8	Unimak Pass	54.45°N	164.99°W
Walleye pollock	*Gadus chalcogrammus*	6	SE Bering Sea	55.67°N	163.33°W
Arctic cod	*Boregadus saida*	39	Chukchi Sea	66.90°N	162.59°W
		14	Chukchi Sea*	66.90°N	162.59°W

Species	Date	Gear	Collector	Affiliation
Saffron cod	9/11	jig	A. Whiting	Native Village of Kotzebue
	6/7/2013	rod and reel	E. Munk	NOAA Fisheries
Navaga	7/13	trawl	N. Chernova	Russian Academy of Sciences
Pacific tomcod	3/1997-8/1999	beach seine	M Canino	NOAA Fisheries
	7/12	beach seine	M. Arimitsu	U.S. Geological Survey
Pacific cod	3/13	beach seine	M. Canino	NOAA Fisheries
	3/13	trawl	M. Canino	NOAA Fisheries
Walleye pollock	9/15	trawl	W. Strasburger	NOAA Fisheries
Arctic cod	4/12	jig	A. Whiting	Native Village of Kotzebue
	4/12	jig	A. Whiting	Native Village of Kotzebue

template. Fluorescent primers labeled with an IRDye infrared dye (10 µg/mL; Integrated DNA Technologies, Inc., Coralville, IA) were included in the reactions. The amplification profiles for each locus were the following: denaturation at 95°C for 5 min; 20 touchdown cycles at 95°C for 30 s, annealing temperatures ranging from 62 to 52°C (touchdown) for 30 s (decreased 0.5°C per cycle), and 72°C for 30 s; then 15 cycles of 95°C for 30 s, the lowest annealing temperature (55°C) for 30 s, and 72°C for 30 s, and a final extension at 72°C for 5 minutes.

Approximately 1 µL of amplified PCR product and stop buffer (95% formamide, 0.1% bromophenol blue) was loaded onto a 0.25 mm 6% acrylamide gel (PAGE-PLUS™, Amresco, Solon, OH) and fragments were separated in 1× TBE buffer (0.09 M Tris-Borate, 2 mM EDTA, pH 8) at 1500 V with a 4300 DNA Analyzer (LI-COR, Inc., Lincoln, NE). Electrophoresis times varied from 2 to 3 hours depending on allele sizes of the PCR product. The image of the PCR product was analyzed with SAGA, vers. 3.1 (LI-COR, Inc.) software. Two individuals scored each gel separately and samples that differed in recorded allele size were genotyped a second or third time.

Analysis of data

Two collections of *E. gracilis* (one from the Chukchi Sea and another from near Kodiak Island, Alaska) were examined separately (Table 1). Collections of *B. saida* from the Chukchi Sea were combined for analysis as a single species as were collections of *M. proximus* (Prince William Sound and Puget Sound), and of *G. macrocephalus* (Puget Sound and Unimak Pass) (Table 1).

Allele frequencies and expected unbiased heterozygosities were estimated and genotype frequencies were tested for departures from Hardy–Weinberg expectations with GENEPOP, vers. 4.5.1 (Rousset, 2008). Significance of multiple tests was confirmed with sequential Bonferroni tests (Rice, 1989) and false discovery rate (FDR; Benjamini and Hochberg, 1995) corrections. Genotypes of individuals that produced deviations from Hardy–Weinberg expectations or apparent principal component analysis (PCA) outliers were reconfirmed by additional genotyping.

Two genetic distances that are not strongly influenced by the numbers of alleles at a locus, but that are based on very different algorithms, were estimated. The standardized genetic differentiation measure G'_{ST}

Table 2

Microsatellite properties of northern gadid species of the Pacific Rim and Arctic Ocean for the 9 loci designed for saffron cod (*Eleginus gracilis*) sampled in the Chukchi Sea and Gulf of Alaska (GOA) in 2011 and 2013. Number of samples for each species (n), the numbers of different allele observed (n_a), the range of allele sizes, the mean and standard error of the mean (SE) of allele sizes, expected heterozygosities (H_e), and inbreeding coefficients (F_{is}) are given. An entry of dna means the locus did not reliably amplify. Collections were made in 2013 for navaga (*E. nawaga*), during 1997–1999 for Pacific tomcod (*Microgadus proximus*), in 2013 for Pacific cod (*Gadus macrocephalus*), in 2015 for walleye pollock (*G. chalcogrammus*), and in 2012 for Arctic cod (*Boreogadus saida*).

Locus and species	n	n_a	range	mean	H_e	F_{is}
Elgr07						
Chukchi Sea *E. gracilis*	30	10	127–175	155.7 (1.2)	0.867	–0.016
GOA *E. gracilis*	41	7	151–179	160.6 (0.5)	0.683	–0.054
E. nawaga	81	14	115–183	133.7 (0.7)	0.815	–0.028
M. proximus	22	1	123	123.0 (0.0)	0.000	–
G. macrocephalus	14	2	115 and 131	128.7 (1.1)	0.286	–0.130
G. chalcogrammus	6	2	131 and 135	133.3 (0.6)	0.833	–0.667
B. saida	53	dna	–	–	–	–
Elgr11						
Chukchi Sea *E. gracilis*	30	12	208–272	222.1 (1.7)	0.833	0.043
GOA *E. gracilis*	41	8	204–260	214.0 (1.3)	0.634	–0.117
E. nawaga	81	21	240–336	274.7 (1.4)	0.877	0.043
M. proximus	22	17	248–340	285.8 (3.0)	0.727	0.230[a]
G. macrocephalus	14	18	192–204	202.9 (0.6)	0.286	–0.072
G. chalcogrammus	6	dna	–	–	–	–
B. saida	53	dna	–	–	–	–
Elgr31						
Chukchi Sea *E. gracilis*	30	6	191–211	197.1 (0.7)	0.833	–0.103
GOA *E. gracilis*	41	4	191–203	194.8 (0.5)	0.659	–0.015
E. nawaga	81	11	179–231	204.4 (0.8)	0.864	–0.052
M. proximus	22	14	215–267	240.5 (2)	0.955	–0.027
G. macrocephalus	14	18	223–299	263.3 (3.7)	1.000	–0.034
G. chalcogrammus	6	10	215–267	241.7 (4.8)	1.000	–0.035
B. saida	53	37	223–543	355.6 (7.6)	0.962	0.005
Elgr38						
Chukchi Sea *E. gracilis*	30	9	112–144	127.5 (1.1)	0.867	–0.026
GOA *E. gracilis*	41	dna	–	–	–	–
E. nawaga	81	dna	–	–	–	–
M. proximus	22	6	120–140	127.9 (0.8)	0.727	0.068
G. macrocephalus	14	6	128–160	141.9 (1.9)	0.786	0.037
G. chalcogrammus	6	7	236–276	258.0 (4.4)	0.833	0.039
B. saida	53	37	252–448	348.6 (6.3)	0.566	0.422[c]

Table continued

(Hedrick, 2005), based on ratios of heterozygosities adjusted to account for the amount of genetic variation observed at each locus, was estimated with the software program SMOGD, vers. 1.2.5 (Crawford, 2010). Estimates of chord distances (Cavalli-Sforza and Edwards, 1967), a geometric measure, were made with PHYLIP, vers. 3.6 (Felsenstein, 2005).

Principal component analysis was used to contrast the genetic compositions of species groups (SYTAT, vers. 13 software; SYSTAT Software, Inc., San Jose, CA). Correlation matrix-based PCA standardizes variables so that each variable has a similar scale; it was used to contrast the allelic compositions. Covariance matrix-based PCA applies the observed variances so that the scale of variation is included in the analysis; it was used to contrast allele-frequency profiles. Loci missing from a collection or a species did not contribute to the PCA score.

Assignment tests (GeneClass2; Piry et al., 2004) were used to evaluate the robustness of the differences among species groups. The tests removed each individual fish from the species groups before assignment. The criterion of Rannala and Mountain (1997) was applied in all tests.

Results

Only genotypes from loci that could be reliably interpreted were analyzed in for each species. Nine loci am-

Table 2 (cont.)

Locus and species	n	n_a	range	mean	H_e	F_{is}
Elgr13						
Chukchi Sea *E. gracilis*	30	12	230–286	251.1 (1.3)	0.867	0.007
GOA *E. gracilis*	41	10	226–286	254.3 (1.4)	0.805	0.006
E. nawaga	81	19	214–286	243.8 (1.3)	0.926	–0.009
M. proximus	22	19	242–338	284.5 (3.7)	0.909	0.040
G. macrocephalus	14	14	250–346	314.7 (4.3)	1.000	–0.093
G. chalcogrammus	6	dna	–	–	–	–
B. saida	53	12	206–318	250.8 (1.0)	0.830	–0.064
Elgr14						
Chukchi Sea *E. gracilis*	30	14	322–378	347.6 (1.7)	0.800	0.101
GOA *E. gracilis*	41	9	330–370	345.7 (1.1)	0.829	–0.007
E. nawaga	81	12	318–362	329.4 (0.7)	0.790	–0.010
M. proximus	22	11	326–370	340.3 (1.6)	0.682	0.217
G. macrocephalus	14	4	314–346	325.6 (0.9)	0.143	0.667[b]
G. chalcogrammus	6	10	330–418	364.7 (7.2)	1.000	–0.035
B. saida	53	19	290–366	325.5 (1.7)	0.811	0.121
Elgr44						
Chukchi Sea *E. gracilis*	30	14	212–264	240.9 (1.7)	0.867	0.057
GOA *E. gracilis*	41	7	228–272	247.1 (1.1)	0.537	0.161[a]
E. nawaga	81	14	216–268	238.4 (1.1)	0.840	0.079
M. proximus	22	dna	–	–	–	–
G. macrocephalus	14	dna	–	–	–	–
G. chalcogrammus	6	dna	–	–	–	–
B. saida	53	dna	–	–	–	–
Elgr45						
Chukchi Sea *E. gracilis*	30	13	205–265	218.8 (1.6)	0.867	0.0085
GOA *E. gracilis*	41	4	209–221	213.0 (0.4)	0.683	0.0145
E. nawaga	81	17	189–269	224.5 (1.2)	0.864	0.0471
M. proximus	22	6	197–217	204.9 (0.8)	0.955	–0.0769
G. macrocephalus	14	dna	–	–	–	–
G. chalcogrammus	6	dna	–	–	–	–
B. saida	53	dna	–	–	–	–
Elgr23						
Chukchi Sea *E. gracilis*	30	15	142–202	170.5 (1.8)	0.933	–0.027
GOA *E. gracilis*	41	4	162–190	168.1 (0.4)	0.683	–0.181
E. nawaga	81	17	138–214	168.1 (1.1)	0.926	–0.019
M. proximus	22	13	138–206	161.6 (2.4)	0.909	–0.044
G. macrocephalus	14	17	154–286	215.0 (5.0)	0.929	0.034
G. chalcogrammus	6	11	186–318	246.7 (12.6)	1.000	–0.017
B. saida	53	23	138–258	191.6 (2.3)	0.660	0.309[c]

[a]$P<0.05$; [b]$P<0.01$; [c]$P<0.001$.

plified reliably and had no apparent homozygote excess in *E. gracilis* (Table 2; Suppl. Table 1) (online only). However, not all loci that were reliable in *E. gracilis* amplified consistently and produced just 1 or 2 bands in all sets of samples. Most notably, Elgr38 did not amplify reliably in GOA samples of *E. gracilis*, nor was it reliable in *E. nawaga*. In addition, only 7 of the 9 loci worked well in *M. proximus* and only 5 in either *G. chalcogrammus* or *B. saida*. Again, Elgr38 did not amplify reliably in the GOA samples of *E. gracilis* nor was it reliable in *E. nawaga*. In addition, only 7 of the loci worked well in *M. proximus* and only 5 in each of *G. chalcogrammus* and *B. saida*. Of the loci that did not amplify reliably for a species group, several did produce bands. Only the loci that could be interpreted reliably were analyzed in each species.

Comparisons of gadid collections

Differences in ranges of allele sizes differentiated species and species groups (Table 2, Suppl. Fig. 1) (online only). For example, alleles at Elgr38 were on average much larger for *B. saida* and *G. chalcogrammus* than for the other species; alleles at Elgr31 were larger on average for *B. saida* and alleles at Elgr23 were on average larger for *G. macrocephalus* and *G. chalcogrammus*. The divergences in allele frequency size ranges were reflected in values of D_{chord} and G'_{ST} (Table 3),

all of which were significant (adjusted pairwise homogeneity tests $P<0.0001$). The estimate of G'_{ST} between the two *E. gracilis* collections was smaller than values between all other gadid pairs; whereas the estimate of D_{chord} was smaller than that of all but three of the comparisons of gadids, even though different suites of microsatellite loci were used. To provide a comparison of the extent of divergence between the two *E. gracilis* collections, values of G'_{ST} and D_{chord} were estimated for the species pair *Sebastes aleutianus* and *S. melanostictus* from data in Gharrett et al. (2005), $G'_{ST}=0.551$ and $D_{chord}=0.064$. The estimate of G'_{ST} between the *E. gracilis* pair was lower (0.313) but the estimate of D_{chord} was higher (0.078) than that between *S. aleutianus* and *S. melanostictus*, presumably because different algorithms were applied; D_{chord} has a geometric basis and G'_{ST} is based on ratios of heterozygosities adjusted to account for the amount of genetic variation observed at each locus (Hedrick, 2005).

Individual-based PCA of allelic compositions (a correlation matrix) and allele frequency profiles (a covariance matrix) produced both species- and collection-specific clusters (Fig. 1). The plot of the first and second components of the correlation-based PCA separated individual species more clearly, but separation of the two *E. gracilis* collections was not as strong. The covariance-based PCA clearly separated the two *E. gracilis* collections, but the other species were not separated quite as well. The first five components of the correlation-based analysis accounted for 10.6% and the first two components accounted for 5.1% of the overall variation in allelic composition. In contrast, the first five components of the covariance-based PCA accounted for 24.3% and the first two for 14.1% of the overall variation in allelic frequencies. Nevertheless, sufficient variation existed to separate these species and the two collections of *E. gracilis*.

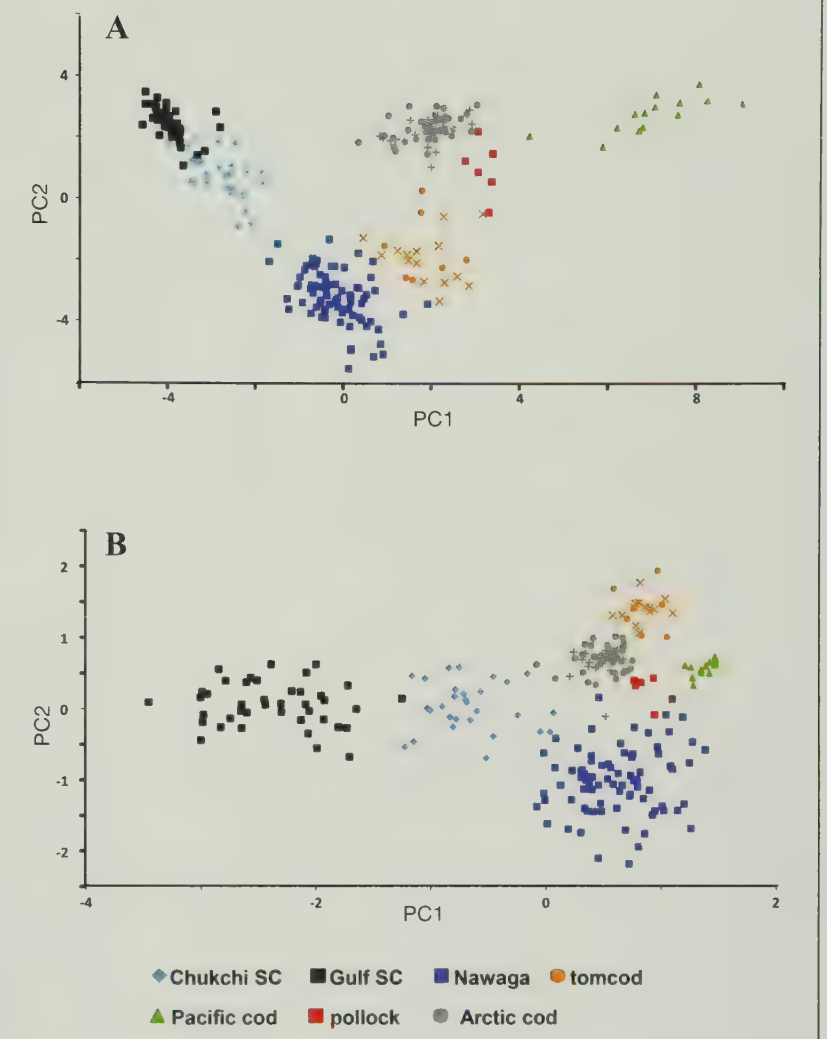

Figure 1

Results of principle component (PC) analyses. (**A**) Allele composition (a correlation matrix) and (**B**) allele frequency profiles (a covariance matrix) of microsatellite data from saffron cod (*Eleginus gracilis* [SC]) collected in the Chukchi Sea (Chukchi SC) and Gulf of Alaska (Gulf SC) in 2011 and 2013, navaga (*E. nawaga*) collected in the Barents Sea in 2013, Pacific tomcod (*Microgadus proximus*) collected in Puget Sound during 1997–1999 and in Prince William Sound in 2012, Pacific cod (*Gadus macrocephalus*) collected in Puget Sound and Unimak Pass in 2013, walleye pollock (*G. chalcogrammus*) collected in the southeastern Bering Sea in 2015, and Arctic cod (*Boreogadus saida*) collected in the Chukchi Sea in 2012. The symbols '+' and '×' denote individuals provided in saffron cod collections that were later re-identified as Arctic cod and Pacific tomcod, respectively.

A series of 4 tests was needed to estimate assignments of individuals because not all loci could be used for all species groups (Suppl. Table 2) (online only). The tests were the following: 1) all individuals were assigned on the basis of the three loci all groups had in common—Elgr14, Elgr23, and Elgr31; 2) the individuals scored in 1) as Chukchi Sea *E. gracilis* (CSC), GOA *E. gracilis* (GSC), *E. nawaga* (NAW), *M. proximus* (PTC), and *G. macrocephalus* (PCO) were assigned on the basis of Elgr7, Elgr11, Elgr13, Elgr14, Elgr23, and Elgr31; 3) the individuals scored in 2) as CSC, GSC, or NAW were tested at Elgr7, Elgr11, Elgr13, Elgr14, Elgr23, Elgr31, Elgr44, and Elgr45; and 4) the individuals scored in 1) as PTC, PCO, *G. chalcogrammus* (WPO), or *B. saida* (ACO) were tested

Table 3

Estimates of pairwise chord distances (D_{chord}; above the diagonal) and standardized genetic differentiation measure (G'_{ST}, below the diagonal) for saffron cod (*Eleginus gracilis*) sampled in the Chukchi Sea and Gulf of Alaska (GOA) in 2011 and 2013 and for navaga (*E. nawaga*), Pacific tomcod (*Microgadus proximus*), Pacific cod (*Gadus macrocephalus*), walleye pollock (*G. chalcogrammus*), and Arctic cod (*Boreogadus saida*) sampled in the Pacific Rim and Arctic Ocean during 1997–2015. All estimates were significant (adjusted probabilities: $P<0.0001$). Values of average unbiased expected heterozygosity (H_e) are indicated in italic type on the diagonal.

Collection	A	B	C	D	E	F	G
A Chukchi Sea *E. gracilis*	*0.859*	0.078[a]	0.076[a]	0.138[a]	0.189[b]	0.218[d]	0.076[d]
B GOA *E. gracilis*	0.313	*0.689*	0.130[a]	0.183[b]	0.245[b]	0.296[e]	0.095[e]
C *E. nawaga*	0.414	0.680	*0.863*	0.093[b]	0.137[c]	0.158[e]	0.069[e]
D *M. proximus*	0.603	0.779	0.565	*0.733*	0.182[b]	0.228[d]	0.088[e]
E *G. macrocephalus*	0.877	0.963	0.822	0.721	*0.633*	0.204[d]	0.092[e]
F *G. chalcogrammus*	0.868	0.893	0.739	0.582	0.449	*0.933*	0.087[e]
G *B. saida*	0.599	0.680	0.584	0.781	0.681	0.607	*0.766*

[a] 8 loci;
[b] 7 loci;
[c] 6 loci;
[d] 5 loci;
[e] 4 loci for both D_{chord} and G'_{ST} estimates.

at Elgr14, Elgr23, Elgr31, and Elgr38. The results of 3) and 4) assigned each individual to its own group, except 1 CSC (96.7% of the total) and 1 ACO (98.1% of the total) (Table 4).

Previous molecular studies have recognized *G. macrocephalus*, *G. chalcogrammmus*, and *B. saida* as distinct species (Coulson et al., 2006, Carr et al., 1999) but the systematic relationships among *E. gracilis*, *E. nawaga*, and *M. proximus* are still unresolved (Mecklenburg et al., 2016). Differences in the allele frequency profiles are easier to see in plots that include only those four groups (Table 2, Suppl. Fig. 2) (online only). The *M. proximus* and *E. nagawa* distributions clearly differ from those of the 2 *E. gracilis* collections at Elgr07 and Elgr11. The profiles for *M. proximus* and *E. nagawa* clearly differ from those for the 2 collections *of E. gracilis* at Elgr07 and Elgr11. *M. proximus* also differs at Elgr13 and Elgr31 and has a substantially higher number of large alleles. The numbers of observed alleles (Table 2) in the collection of GOA *E. gracilis* are relatively lower than those of the others and several are more abundant (Suppl. Fig. 2) (online only), which is consistent with the somewhat lower heterozygosity (Table 2) of the GOA *E. gracilis*.

Discussion

Eight of the nine microsatellites that were evaluated for two collections of *E. gracilis* and that amplified reliably were variable (heterozygosities 0.537 to 0.933) and had no apparent homozygote excess, indicating low null allele frequencies. The single exception, Elgr38, amplified reliably for the Chukchi Sea collection of *E. gracilis* but not for the GOA collection. At the other loci, the two collections had similar allele size ranges but differed substantially in allele frequencies (G'_{ST}=0.313, D_{chord}=0.078, $P<0.0001$). The observed differences were similar to those between two cryptic rockfish species that had overlapping ranges, *S. aleutianus* and *S. melanostictus*, although they were estimated with different suites of loci. In the PCA plots, individuals from the two collections of *E. gracilis* were mostly distinct from each other, particularly in the analysis of the covariance matrix, which focuses on the allele frequencies rather than allele composition. It is also notable that the PCA analyses included frequency differences of the other gadids analyzed, and differences between the 2 collections of *E. gracilis* were evident against the background variation from other species.

Assignment tests placed all but one saffron cod in the group from which it originated. Not all nine microsatellite loci amplified reliably in all of the other gadid species analyzed and some had an excess of homozygotes, most likely as a consequence of null alleles; those loci were not used for assignment tests. Nevertheless, where comparisons were possible, all the other gadids differed in microsatellite composition ($P<0.0001$) from both collections of *E. gracilis* and each other. The correlation matrix-based PCA, in particular, clustered individuals according to species or geographic groups of species. The PCA analyses turned out to be valuable in analyzing a large set of samples of putative *E. gracilis* because the analysis revealed outliers that, when compared with the clusters of other gadids, enabled detection of individuals misidentified as *E. gracilis*. Two

Table 4

Summary of results of a series of tests (Piry et al., 2004) that assigned each fish to 1 of 7 species groups: saffron cod (*Eleginus gracilis*) of the Chukchi Sea (CSC), saffron cod of the Gulf of Alaska (GSC), navaga (*E. nawaga*) (NAW), Pacific tomcod (*Microgadus proximus*) (PTC), Pacific cod (*Gadus macrocephalus*) (PCO), walleye pollock (*G. chalcogrammus*) (WPO), and Arctic cod (*Boreogadus saida*) (ACO). *n*=the number of individuals of each group. For all results from the assignment tests, see Supplementary Table 2.

		Assigned to						
n	Species group	CSC	GSC	NAW	PTC	PCO	WPO	ACO
30	CSC	29	1[a]	0	0	0	0	0
41	GSC	0	41	0	0	0	0	0
81	NAW	0	0	81	0	0	0	0
23	PTC	0	0	0	23	0	0	0
14	PCO	0	0	0	0	14	0	0
6	WPO	0	0	0	0	0	6	0
53	ACO	0	0	0	0	0	1[b]	52

[a]83% GSC/ 17% CSC.
[b]55% PCO/ 44% WPO/ 1% ACO.

notable instances were 14 aberrant genotypes included in a collection of *E. gracilis* from the Chukchi Sea and another 15 in a collection of *E. gracilis* from Prince William Sound. In both instances, it was possible to re-examine the individual specimens; the former were re-identified as *B. saida* and the latter as *M. proximus* (Table 1). Both sets of re-identified individuals were included with their correct species in the analyses presented here (designated as '+' and '×', respectively in Fig. 1). Assignment tests correctly reassigned all of the other gadids except one Arctic cod.

In these analyses, the two collections of *E. gracilis*, and the collections of *M. proximus*, and *E. nawaga* were all distinct from each other ($P<0.0001$). The degree of their divergences mostly exceeded those observed between *S. aleutianus* and *S. melanostictus* (Gharrett et al., 2005) and each of the collections clustered separately in PCAs. It is notable that misidentified individuals of Prince William Sound *M. proximus* were collected at the same site with *E. gracilis*, but were genetically distinct from them. Clearly, some field identifications, even by trained personnel, are challenging (cf. Teletchea, 2009). It is unlikely that they represent two sympatric populations of a single marine species—populations that are so strongly different genetically. Although it could be argued that the genetic differences between the collections of *E. nawaga* and *E. gracilis* could result from divergence over the large distance that separates them, the very large divergences in allele frequencies, as well as similar differences in allele size ranges at Elgr11 and Elgr14, are more consistent with their being distinct species. More complete information on the modern Arctic distributions of the two species of *Eleginus*, and the location of the historic contact zone between them, would contribute to resolving their systematic status, as would independent data, such as mitogenomic sequences of *E. nawaga* and *E. gracilis*, coupled with morphological characters (Teletchea, 2009).

Acknowledgements

Funding was provided by the U.S. Department of Interior (Bureau of Ocean Energy Management Agreements M12AC00009 and M12AC00009), the U.S. Department of the Interior (Fish and Wildlife Service Agreements 10-CIAP-010 and F12AF00188), the Department of Energy (award no. DE-FC09-07SR22506), and the Russian Federation for Fundamental Investigations (Grant15-04-02081, Gostema no. 01201351186). This article is contribution EcoFOCI-0896 to NOAA's Ecosystems and Fisheries Oceanography Coordinated Investigations program.

Literature cited

Benjamini, Y., and Y. Hochberg.
1995. Controlling the false discovery rate: a practical and powerful approach to multiple testing. J. R. Stat. Soc., B. 57:289–300.

Bluhm, B. A., and R. Gradinger.
2008. Regional variability in food availability for arctic marine mammals. Ecol. Appl. 18:S77–S96.

Castoe, T. A., A. W. Poole, A. P. J. de Koning, K. L. Jones, D. F. Tomback, S. J. Oyler-McCance, J. A. Fike, S. L. Lance, J. W. Streicher, E. N. Smith, and D. D. Pollack.
2012. Rapid microsatellite identification from Illumina paired-end genomic sequencing in two birds and a snake. PLoS ONE 7(2):e30953.

Cavalli-Sforza, L. L, and A. W. F. Edwards.
1967. Phylogenetic analysis: models and estimation procedures. Evolution 21:550–570.
Crawford, N. G.
2010. SMOGD: software for the measurement of genetic diversity. Mol. Ecol. Resour. 10:556–557.
Carr, S. M., and H. D. Marshall.
2008. Phylogeographic analysis of complete mtDNA genomes from Walleye Pollock (*Gadus chalcogrammus* Pallas, 1811) shows an ancient origin of genetic biodiversity. DNA Sequence 19:490–496.
Carr, S. M., D. S. Kivlichan, P. Pepin, and D. C. Crutcher.
1999. Molecular systematics of gadid fishes: implications for the biogeographic origins of Pacific species. Can. J. Zool. 77:19–26.
Cohen, D. M. (ed.).
1989. Papers on the systematics of gadiform fishes. Nat. Hist. Mus. Los Ang. Cty., Sci. Ser. 32, 262 p.
Cohen, D. M., T. Inada, T. Iwamoto, and N. Scialabba.
1990. FAO species catalogue, vol. 10. Gadiform fishes of the world (Order Gadiformes). An annotated and illustrated catalogue of cods, hakes, grenadiers and other gadiform fishes known to date. FAO Fisheries Synopsis 125, 442 p. FAO, Rome.
Copeman, L. A., B. J. Laurel, K. M. Boswell, A. L. Sremba, K. Klinck, R. A. Heintz, J. Vollenweider, T. E. Helser, and M. L. Spencer.
2016. Ontogenetic and spatial variability in trophic biomarkers of juvenile saffron cod (*Eleginus gracilis*) from the Beaufort, Chukchi and Bering Seas. Polar Biol. 39:1109–1126.
Coulson, M. W., H. D. Marshall, P. Pepin, and S. M. Carr.
2006. Mitochondrial genomics of gadine fishes: implications for taxonomy and biogeographic origins from whole-genome data sets. Genome 49:1115–1130.
DeWoody, J. A., and J. C. Avise.
2000. Microsatellite variation in marine, freshwater and anadromous fishes compared with other animals. J. Fish Biol. 56:461–473.
Don, R. H., P. T. Cox, B. J. Wainwright, K. Baker, and J. S. Mattick.
1991. 'Touchdown' PCR to circumvent spurious priming during gene amplification. Nucleic Acids Res. 19:4008.
Felsenstein, J.
2005. PHYLIP (Phylogeny Inference Package), vers. 3.6. Dep. Genome Sci., Univ. Washington, Seattle, WA. [Available from website.]
Gharrett, A. J., A. P. Matala, E. L. Peterson, A. K. Gray, and Z. Li.
2005. Two genetically distinct forms of rougheye rockfish are different species. Trans. Am. Fish. Soc. 134:242–260.
Harpending, H. C, M. A. Batzer, M. Gurven, L. B. Jorde, A. R. Rogers, and S. T. Sherry.
1998. Genetic traces of ancient demography. Proc. Natl. Acad. Sci. U.S.A. 95:1961–1967.
Hedrick, P. W.
2005. A standardized genetic differentiation measure. Evolution 59:1633–1638.
Kamin, L. M., K. J. Palof, J. Heifetz, and A. J. Gharrett.
2014. Interannual and spatial variation in the population genetic composition of young-of-the-year Pacific ocean perch (*Sebastes alutus*) in the Gulf of Alaska. Fish. Oceanogr. 23:1–17.
Koressaar, T., and M. Remm.
2007. Enhancements and modifications of primer design program Primer3. Bioinformatics 23:1289–1291.
Mecklenburg, C. W., T. A. Mecklenburg, B. A. Sheiko, and D. Steinke.
2016. Pacific Arctic marine fishes, 375 p. Conservation of Arctic Flora and Fauna, Akureyri, Iceland.
Piry, S., A. Alapetite, J.-M. Cornuet, D. Paetkau, L. Baudouin, and A. Estoup.
2004. GENECLASS2: A software for genetic assignment and first-generation migrant detection. J. Hered. 95:536–539.
Rannala, B., and J. L. Mountain.
1997. Detecting immigration by using multilocus genotypes. Proc. Natl. Acad. Sci. U.S.A. 94:9197–9201.
Rice, W. R.
1989. Analyzing tables of statistical tests. Evolution 43:223–225.
Roa-Varón, A., and G. Ortí.
2009. Phylogenetic relationships among families of Gadiformes (Teleostei, Paracanthopterygii) based on nuclear and mitochondrial data. Mol. Phylogen. Evol. 52:688–704.
Rousset, F.
2008. GENEPOP'007: a complete re-implementation of the GENEPOP software for Windows and Linux. Mol. Ecol. Resour. 8:103–106.
Schultz, L. P., and A. D. Welander.
1935. A review of the cods of the northeastern Pacific with comparative notes on related species. Copeia 1935:127–139.
Seutin, G., B. N. White, and P. T. Boag.
1991. Preservation of avian blood and tissue samples for DNA analysis. Can. J. Zool. 69:82–90.
Stoutamore, J. L., C. N. Love, S. L. Lance, K. L. Jones, and D. Tallmon.
2012. Development of polymorphic microsatellite markers for blue king crab (*Paralithodes platypus*). Conserv. Genet. Resour. 4:897–899.
Svetovidov, A. N.
1948. Gadiformes (Treskoobraznye). Fauna of the U.S.S.R., vol. 9, no. 4, 304 p. Israel Program Sci. Transl., Jerusalem, Israel.
Teletchea, F.
2009. Molecular identification methods of fish species: reassessment and possible applications. Rev. Fish Biol. Fish. 19:265–293.
Teletchea, F., V. Laudet, and C. Hännia.
2006. Phylogeny of the Gadidae (sensu Svetovidov, 1948) based on their morphology and two mitochondrial genes. Mol. Phylogen. Evol. 38:189–199.
Untergasser, A., I. Cutcutache, T. Koressaar, J. Ye, B. C. Faircloth, M. Remm, and S. G. Rozen.
2012. Primer3—new capabilities and interfaces. Nucleic Acids Res. 40:e115.
Wolotira, R. J., Jr.
1985. Saffron cod *(Eleginus gracilis)* in western Alaska, the resource and its potential. NOAA Tech. Memo. NMFS F/NWC-79, 119 p.

National Marine
Fisheries Service
NOAA

Fishery Bulletin
established in 1881

Spencer F. Baird
First U.S. Commissioner
of Fisheries and founder
of *Fishery Bulletin*

The forgotten need for spatial persistence in catch data from fixed-station surveys

Laura M. Lee (contact author)[1]
Jason E. Rock[2]

Email address for contact author: laura.lee@ncdenr.gov

[1] North Carolina Division of Marine Fisheries
P.O. Box 769
Morehead City, North Carolina 28557

[2] North Carolina Division of Marine Fisheries
Washington Regional Office
943 Washington Square Mall
Washington, North Carolina 27889

Abstract—Design-based estimators, which have well known statistical properties, exist for random sampling survey designs and provide unbiased estimates of the mean and variance of summary catch statistics. Although application of these estimators to fixed-station surveys is not technically valid, they can result in unbiased differences between years if the data exhibit spatial persistence A persistent system is one in which the differences in relative abundance of a population that are recorded at fixed stations are consistent from year to year (i.e., there is no interaction between station and years in a 2-way classification). In a fully persistent system, the changes in relative abundance derived from fixed stations will be unbiased. In this study, the persistence in relative abundance data collected from a fixed-station survey intended to monitor juveniles of economically important species is evaluated. The results can be used to infer those species for which changes in relative abundance estimated from fixed-station surveys will be more accurate than changes in relative abundance estimated from random surveys.

Manuscript submitted 24 July 2017.
Manuscript accepted 20 November 2017.
Fish. Bull. 116:69–74 (2018).
Online publication date: 12 December 2017.
doi: 10.7755/FB.116.1.7

The views and opinions expressed or implied in this article are those of the author (or authors) and do not necessarily reflect the position of the National Marine Fisheries Service, NOAA.

Sampling is essential for studying fish populations. The primary objective for many fisheries-independent surveys is to monitor the relative abundance of a population, which is an important input for stock assessments and management considerations. A wide variety of survey designs can be used to monitor relative abundance. The advantage of statistically designed surveys (e.g., stratified random) is they are associated with design-based estimators for which the statistical properties are well known. These design-based estimators are designed to provide unbiased estimates of the mean and variance (when the survey design is implemented properly).

What about fixed-station surveys? There are no design-based estimators associated with fixed-station sampling and therefore there are no estimators that guarantee unbiased statistics for these surveys. Random surveys are designed to provide an unbiased estimate of the mean, whereas fixed-station surveys, in general, provide a biased estimate; however, the magnitude of that bias could be anywhere from negligible to substantial. There is no way of determining the extent of this bias from the data themselves. Bias in any given year may be of little consequence if changes in relative abundance between years is accurately reflected by the changes in the index of relative abundance (Warren, 1994). This is determined through the property of persistence.

Persistence, in this study, is the constancy of differences in the patterns of relative abundance at fixed locations during sampling years (Warren, 1994). The greater the persistence, the greater the ability to detect interannual changes in relative abundance. In a fully persistent situation (Fig. 1A), changes in relative abundance from fixed-station surveys from year to year will be unbiased and more accurate than changes in relative abundance estimated from a random sampling design. In the case of a complex and changeable spatial pattern in relative abundance (i.e., where distribution pattern varies from year to year; Fig. 1B), a fixed-station design will result in biased estimates except in exceptional and unlikely circumstances (ICES[1]). A randomized design leads to unbiased

[1] ICES (International Council for the Exploration of the Sea). 1989. Report of the working group on methods of fish stock assessments (WGMG), 10–17 November 1989, Nantes, France. ICES CM 1990/Assess:15, 95 p.

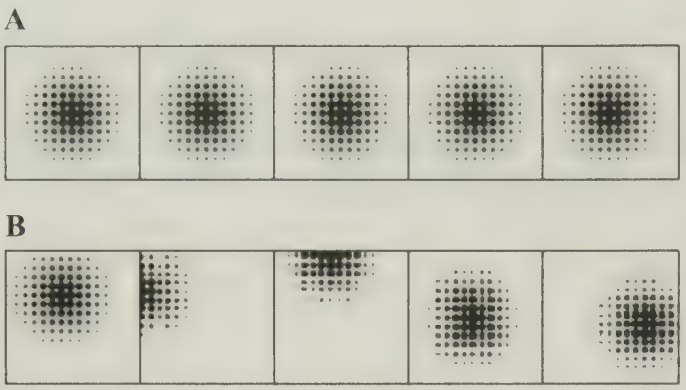

Figure 1

Simple theoretical examples of spatially (**A**) persistent and (**B**) nonpersistent catches over time. (Adapted from Houghton, 1987). Source: ICES CM 1987/D:15, 7 p. [Available from website.]

estimates even in a case of a complex and changeable spatial pattern in relative abundance.

Our objective was to evaluate the persistence of relative abundance for selected species collected from one of the fixed-station trawl surveys conducted by the North Carolina Division of Marine Fisheries (NCDMF). Relative abundance indices derived from this survey have been provided to the stock assessment work groups at the NCDMF, the Atlantic States Marine Fisheries Commission, and university researchers. The survey data have been used to characterize nursery area habitat, help designate new nursery areas, and have also been important for the federal designation of Essential Fish Habitat.

Materials and methods

Data

The NCDMF has operated the statewide Estuarine Trawl Survey, also known as Program 120, since 1971. The main objectives for the survey are to identify primary nursery areas and produce annual recruitment indices for economically important species. The survey has also been used to monitor species distribution by season and area and to evaluate environmental impact projects. The survey targets Atlantic croaker (*Micropogonias undulatus*), Atlantic menhaden (*Brevoortia tyrannus*), southern flounder (*Paralichthys lethostigma*), spot (*Leiostomus xanthurus*), summer flounder (*P. dentatus*), weakfish (*Cynoscion regalis*), blue crab (*Callinectes sapidus*), brown shrimp (*Farfantepenaeus aztecus*), pink shrimp (*F. duorarum*), and white shrimp (*Litopenaeus setiferus*).

The survey samples were collected in shallow-water areas of the Pamlico Sound system in North Carolina and waters south to the North Carolina-South Carolina border. Selection of stations was nonrandom. Major changes in sampling methods occurred in 1978 and 1989. In 1978, tow times were standardized to 1 min during daylight hours. In 1989, survey data were analyzed to determine a more efficient sampling time frame (until then sampling occurred year-round). This analysis identified a fixed set of 105 core stations and sampling was reduced to May and June only, except for July when weakfish were sampled (dropped in 1998; sampling in July was reinitiated in 2004 for spotted seatrout), and only a trawl with a 3.2-m (10.5-ft) headrope and with 6.4-mm (0.25-in) bar mesh would be used. Each station was sampled once per month.

The current sampling gear consists of a 2-seam otter trawl with a 3.2-m headrope, 6.4-mm bar mesh with body netting of 210/6-size twine, and a tailbag made of 3.2-mm Delta-style knotless nylon and with a 150-mesh circumference and 450-mesh length. Three loops of 4.8-mm (0.19-inch) chain are hung on each wing. A 4.8-mm diameter tickler chain is used and 2 floats, each 76.2-mm (3-inch)×101.6-mm (4-inch), are attached to the center of the headrope. The gear is towed for 1 min during daylight hours during similar tidal stages and covers 68.6 m (75 yards).

Environmental data are recorded during each sampling event and include depth, temperature, salinity, dissolved oxygen, wind speed, and direction. Additional habitat fields were added in 2008.

Analysis

Because not all stations were sampled in May of the first year (1978) we used data collected from 1979 through 2016 and limited the analysis to those data collected from stations within the Pamlico Sound system. Only those stations sampled in both May and June over the selected period were included—a total of 29 stations for analysis (Fig. 2).

We first calculated the frequency of occurrence for each target species based on the number of tows the species was present in out of all possible tows during 1979 through 2016 (29 stations×2 months×38 years=2204 total tows). Indices of relative abundance were then calculated for all target species to provide estimates of trends in abundance over time. The Mann–Kendall test was applied to the indices to evaluate temporal trends. The Mann–Kendall test is a nonparametric test used to evaluate a monotonic trend in time-ordered data (Gilbert, 1987). The null hypothesis is that the time series is independent (observations are not serially correlated over time) and identically distributed (i.e., there is no significant trend across time, and therefore monotonic). The Mann–Kendall test allows for missing values and accounts for tied values when present. Mann–Kendall test statistics, including *P*-values, were calculated in R statistical software, vers. 3.4.2 (R Core Team, 2017)

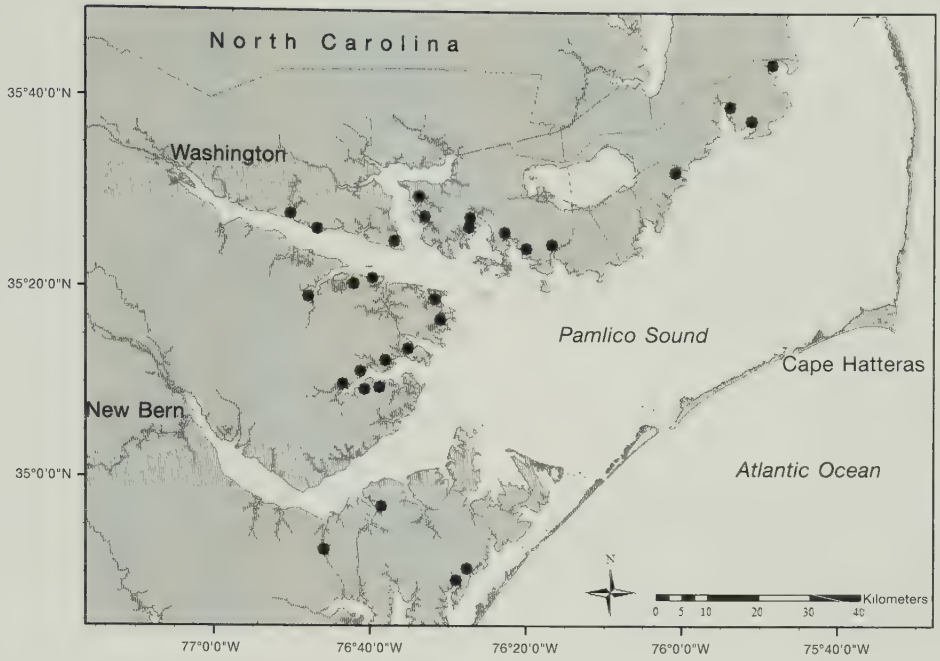

Figure 2

Map of the locations of the 29 stations (•) selected for use in the persistence analysis and sampled during 1979–2016 in the Pamlico Sound system in North Carolina as part of the Estuarine Trawl Survey of the North Carolina Division of Marine Fisheries.

and by using the mk.test function in the package trend, vers. 1.01 (Pohlert, 2017). Trends were considered significant at α=0.05.

Following Nicholson et al.[2], we applied a 2-way analysis of variance (ANOVA) to test the significance of the interaction of year and station for each target species. This analysis was conducted in R with the aov function in the stats package (R Core Team, 2017). Samples collected at the same station during May and June within the same year were considered replicates in order that the interaction term could be tested. The interaction was considered significant at α=0.05. A significant interaction indicates a lack of persistence. Main effects were also included in the ANOVA but the results are not presented here.

Results

The target species range widely in frequency of occurrence from being present in less than 2% of tows (summer flounder) to being present in over 98% of tows (for spot) (Table 1).

The indices of relative abundance exhibit considerable interannual variability for all species (Fig. 3). Statistically significant decreasing trends were detected for Atlantic croaker, Atlantic menhaden, spot, and weakfish (Table 2). Statistically significant increasing trends were found for southern flounder, brown shrimp, and white shrimp. No statistically significant trends were present in the indices of relative abundance for summer flounder, blue crab, or pink shrimp.

Table 1

Frequency of occurrence of 10 target species in 2204 trawl samples from the North Carolina Division of Marine Fisheries Estuarine Trawl Survey, 1979–2016, in the Pamlico Sound system in North Carolina.

Species	Number of tows	Occurrence (%)
Atlantic croaker	1889	85.7
Atlantic menhaden	1290	58.5
Southern flounder	1339	60.8
Spot	2162	98.1
Summer flounder	27	1.2
Weakfish	100	4.5
Blue crab	1450	65.8
Brown shrimp	1489	67.6
Pink shrimp	100	4.5
White shrimp	52	2.4

[2] Nicholson, M. D., T. K. Stokes, and A. B. Thompson. 1991. The interaction between fish distribution, survey design and analysis. ICES CM 1991/D:11, 9 p. [Available from website.]

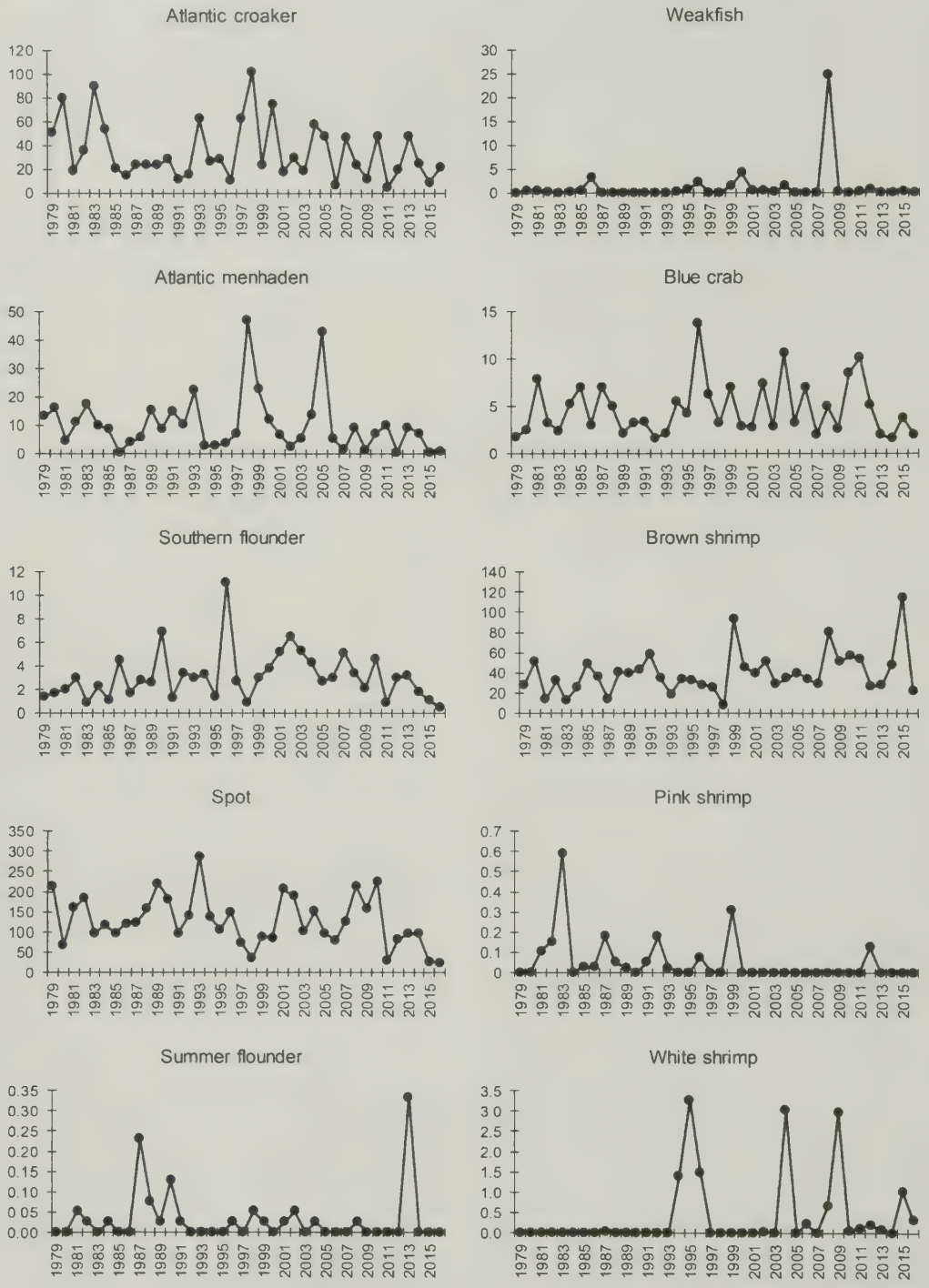

Figure 3

Indices of relative abundance (measured as the average number of individuals per tow), for 10 target species based on data from trawl surveys conducted during 1979–2016 in the Pamlico Sound system in North Carolina. The target species are Atlantic croaker (*Micropogonias undulatus*), Atlantic menhaden (*Brevoortia tyrannus*), southern flounder (*Paralichthys lethostigma*), spot (*Leiostomus xanthurus*), summer flounder (*P. dentatus*), weakfish (*Cynoscion regalis*), blue crab (*Callinectes sapidus*), brown shrimp (*Farfantepenaeus aztecus*), pink shrimp (*F. duorarum*), and white shrimp (*Litopenaeus setiferus*).

Table 2

Results of Mann–Kendall trend analyses of the relative abundance indices of 10 target species the data of which were collected from trawl surveys conducted during 1979–2016 in the Pamlico Sound system of North Carolina. *P*-values are the 2-tailed probabilities for the trend test. The arrows in the column marked "trend" indicate the direction of the trend (decrease and increase in relative abundance over time) if a statistically significant temporal trend was detected (α=0.05). NS=not significant.

Species	*P*-value	Trend
Atlantic croaker	0.0010	↓
Atlantic menhaden	<0.0001	↓
Southern flounder	0.0165	↑
Spot	0.0104	↓
Summer flounder	0.1183	NS
Weakfish	0.0197	↓
Blue crab	0.9636	NS
Brown shrimp	<0.0001	↑
Pink shrimp	0.4002	NS
White shrimp	<0.0001	↑

Table 3

Results of the 2-way analysis of variance tests for the year–station interaction (1036 degrees of freedom) for the period of 1979–2016 for target species collected during the North Carolina Division of Marine Fisheries Estuarine Trawl Survey conducted in the Pamlico Sound system in North Carolina. The *F* value measures the ratio of the variance that is caused by the interaction effect to the unexplained variance. A significant interaction (α=0.05) indicates a lack of persistence.

Species	Mean square error	*F*-value	*P*(>*F*)
Atlantic croaker	5611	1.46	<0.0001
Atlantic menhaden	6418	1.01	0.4210
Southern flounder	37.90	1.43	<0.0001
Spot	38,524	0.79	1.0000
Summer flounder	0.15	1.02	0.3930
Weakfish	194	0.97	0.6840
Blue crab	33.79	1.55	<0.0001
Brown shrimp	4859	1.26	0.0001
Pink shrimp	0.70	1.02	0.3950
White shrimp	6.47	0.93	0.8930

The results of the 2-way ANOVA tests for main interaction effects indicate a lack of persistence (i.e., of statistically significant interaction) for Atlantic croaker, southern flounder, blue crab, and brown shrimp (Table 3). The data for all other target species showed the presence of persistence over the time period and stations analyzed.

Discussion

The idea of persistence made its first appearance in the primary literature in Warren's article (1994) on sampling with partial replacement. Despite the ubiquity of fixed-station surveys, the practice of testing for persistence has largely been ignored. A cited reference search (via Web of Science Core Collection) identified 7 papers that referenced Warren (1994). Of these articles, only one evaluated persistence in a fixed-station sampling survey (Li et al., 2015). Another briefly described the idea of persistence (Kimura and Somerton, 2006). Given that bias can be introduced into a relative abundance index by a lack of persistence, it seems reasonable to recommend that persistence be routinely evaluated and documented for fixed-station surveys.

The results of this study suggest that the presence of persistence is species-specific within the NCDMF Estuarine Trawl Survey. A lack of persistence was shown for Atlantic croaker, southern flounder, blue crab, and brown shrimp and indicated that this survey may be ineffective in tracking abundance for some of its target species, at least for the time series and stations selected for our analysis. Investigation into those life history characteristics that lead to more or less persistence may be warranted. Further examination into the spatial distribution of the catches and the changes in environmental conditions may lead to an improved understanding of persistence. The selection of stations may be species specific. For example, removal of stations where species of interest are not consistently caught may lead to improved or reduced persistence. Additionally, preliminary investigations conducted in preparation for this article suggest that choice of time series and stations can have a substantial influence on whether persistence is present.

In summary, fixed-station sampling is acceptable when random sampling is impractical, so long as persistence is evaluated and is present for the species of interest. Fixed-station surveys can be easier to implement, especially if a substantial part of the target sampling area is inaccessible to the gear. Van der Meer (1997) found that fixed-station sampling could have a higher power of detecting change over time than random sampling. In another comparison of fixed and random designs, Quist et al. (2006) found that a fixed-station design can provide a more sensitive measure of temporal variation.

How the data collected from a fixed-station survey will be used should be carefully considered. If bias in annual changes is a concern, persistence should be evaluated so that the data can be examined in context. This approach is especially important if the survey is going to be used to develop a relative index of abundance for use in a stock assessment because it is currently unknown how that bias may affect stock as-

sessment results and subsequent management. Alternatively, one could use geostatistical modeling to produce unbiased estimates, thereby avoiding the pitfalls of applying design-based estimators to fixed-station survey data (e.g., Rivoirard et al., 2000).

Acknowledgments

The authors wish to thank 3 anonymous reviewers whose comments greatly improved this manuscript. The views and opinions in this article are those of the authors and do not necessarily reflect the position of the North Carolina Division of Marine Fisheries.

Literature cited

Gilbert, R. O.
1987. Statistical methods for environmental pollution monitoring, 336 p. John Wiley & Sons, Inc., New York.

Kimura, D. K., and D. A. Somerton.
2006. Review of statistical aspects of survey sampling for marine fisheries. Rev. Fish. Sci. 14:245–283..

Li, B., J. Cao, J.-H. Chang, C. Wilson, and Y. Chen.
2015. Evaluation of effectiveness of fixed-station sampling for monitoring American lobster settlement. N. Am. J. Fish. Manage. 35(5):942–957..

Pohlert, T.
2017. trend: non-parametric trend tests and change-point detection. R package, vers. 1.0.0. [Available from website, accessed October 2017.]

Quist, M. C., K. G. Gerow, M. R. Bower, and W. A. Hubert.
2006. Random versus fixed-site sampling when monitoring relative abundance of fishes in headwater streams of the upper Colorado River Basin. N. Am. J. Fish. Manage. 26:1011–1019.

R Core Team.
2017. R: a language and environment for statistical computing. R Foundation for Statistical Computing, Vienna, Austria. [Available at website, accessed October 2017.]

Rivoirard, J., J. Simmonds, K. G. Foote, P. Fernandes, and N. Bez.
2000. Geostatistics for estimating fish abundance, 216 p. Blackwell Science, Ltd, Oxford, UK.

Van der Meer, J.
1997. Sampling design of monitoring programmes for marine benthos: a comparison between the use of fixed versus randomly selected stations. J. Sea Res. 37:167–179.

Warren, W. G.
1994. The potential of sampling with partial replacement for fisheries surveys. ICES J. Mar. Sci. 51:315–324.

National Marine Fisheries Service
NOAA

Fishery Bulletin
established in 1881

Spencer F. Baird
First U.S. Commissioner of Fisheries and founder of *Fishery Bulletin*

Bias in estimates of growth when selectivity in models includes effects of gear and availability of fish

Kevin R. Piner (contact author)[1]
Hui-Hua Lee[1]
Lennon R. Thomas[2]

Email address for contact author: kevin.piner@noaa.gov

[1] Southwest Fisheries Science Center
National Marine Fisheries Service, NOAA
8901 La Jolla Shores Drive
La Jolla, California 92037

[2] Bren School of Environmental Science and Management
University of California Santa Barbara
2400 Bren Hall
Santa Barbara, California 93106

Abstract—Stock assessment models use data influenced by distribution patterns that are due to the nonrandom movement of fish, which can create bias in the assessment. For many stocks, length data are used to characterize the age structure of the population, and therefore there is a need for unbiased estimates of growth. Because of the influence of size-selective fishing gear, growth and length-based selectivity are often estimated as part of an assessment model to account for the size selection of gear. However, estimated selectivity can include not only length-based gear selection, but the biological aspects of the spatial availability of the target species. If availability to the fishing gear is a function of age, an approximation of an age-based process as a length-based one can bias growth estimates. The magnitude of the bias would be greater for fish with highly variable growth and for those with strong age-based distribution patterns.

Manuscript submitted 14 June 2017.
Manuscript accepted 7 November 2017.
Fish. Bull. 116:75–80 (2018).
Online publication date: 22 December 2017.
doi: 10.7755/FB.116.1.8

The views and opinions expressed or implied in this article are those of the author (or authors) and do not necessarily reflect the position of the National Marine Fisheries Service, NOAA.

Spatial patterns in the distribution of sizes and ages of fish (patterns due to the behavior of fish) are common. Because movement rates may be difficult to estimate as part of a population dynamics model (Lee et al., 2017a), the spatial patterns in size or age are often modeled implicitly as selectivity (Hurtado-Ferro et al., 2014; Waterhouse et al., 2014; Lee et al. 2017a). Implicit treatment of spatial patterns uses the model estimate of the selectivity process to represent both spatial availability, as well as the selectivity of the gear (Maunder et al., 2014). Gear selectivity represents the probability that a fish is captured when it encounters the gear, whereas availability is the probability that a fish will encounter the gear. It is common practice to estimate fleet selectivity as a function of fish length (Crone and Valero, 2014) because it is generally assumed that gear selectivity is related to fish size (Stewart, 1975; Yanase et al., 2007), whereas availability due to movement could be a function of size (Nøttestad et al., 1999) or age (Francis, 2016; McDaniel et al., 2016).

Length-based, age-structured modeling is used for many migratory fish stocks because routine age determination of fishery samples is not always provided. In these assessment models the length composition data are used to approximate the age structure of the catch. To use the observed lengths reliably, an unbiased estimate of the length-at-age relationship is needed. Unless properly accounted for, the processes of availability of fish and gear selectivity can cause bias in comparisons with the actual total population, which can bias estimates of growth (Piner et al., 2016; Lee et al., 2017b) and ultimately the management of catch quotas (Maunder and Piner, 2017).

Age–length data used to estimate growth must satisfy at least one of two assumptions depending on how they are used (Francis, 2016). With the random-at-age method for estimating growth, lengths are assumed to be random with respect to age. Estimates from this method can be biased without a proper accounting for length-based processes (e.g. length-based gear selectivity). Length-at-age

Table 1

Parameter values used in creating the hypothetical population of a small, migratory pelagic fish to show bias in the estimates of fish growth. Growth was estimated by using a deterministic population dynamic model in which selectivity includes effects of gear and fish availability. Sensitivity analyses in this article provided changes in the base parameter values. CV=coefficient of variation.

Parameter	Base values	Sensitivity analyses
Maximum age	10	
Total mortality (Z)	0.5/year all ages	
Asymptotic length (L_{inf})	20 cm	
Growth coefficient (K)	0.4	
Hypothetical age when average length is zero (a_0)	−1	
CV of length at age	0.15 all ages	0.1 all ages
Availability in sampling area (d_a)	5% at ages 0–3, 100% at ages 4 and older	100% at ages 0–3, 5% at ages 4 and older
Gear selectivity (s_l)	Asymptotic pattern (Fig. 1B)	Domed pattern (Fig. 3B)

can also be estimated by using random-at-length methods (Hoyle and Maunder[1]; Piner et al., 2016). Random-at-length estimation methods provide a comparison of observed and expected age distribution for a specific length with the assumption that ages are random with respect to length. Age-based processes, such as age-based movements (McDaniel et al., 2016) can lead to biased growth estimates with the use of random-at-length methods (Lee et al., 2017b).

In many studies where fish growth is estimated, the biological (e.g., movement) and observation processes (e.g., selectivity) are ignored, which, if ignored, can lead to violations of the assumptions about randomness (a review by Maunder and Piner, 2017). Estimating growth parameters simultaneously with these processes as part of an integrated model (Fournier et al., 1990; Methot and Wetzel, 2013) can account for these sources of potential bias. Proper use of the integrated model is based on the knowledge of biological and fisheries processes involved in the collection of data.

The evolution of integrated assessment modeling has generally lead to the inclusion of a greater number of factors in an attempt to reduce estimation biases. Simultaneously estimating growth and the length-based effects of gear selectivity have been thought to remove selectivity bias (Parma and Deriso, 1990; Taylor et al., 2005; Schueller et al., 2014; Piner et al., 2016). However in this study we show that a bias can be induced when estimates of mean length-at-age (random at age assumption) are derived by using a selectivity that is a combination of length-based gear and age-based availability. This is an approximation bias that is the result of approximating an age-based effect by using a length-based process. The magnitude and direction of the bias is dependent on the spatial areas sampled and variability in the length-at-age relationship.

Materials and methods

We use a deterministic population dynamics model to show the effects on growth estimates of combining both age-based availability and length-based gear selectivity, into a single length-based process. Conceptually the stock is distributed in two areas: one area is primarily a juvenile area and the other is primarily an adult area. The deterministic model approximates the spatial dynamics by using age-based availability as implicit areas in a single well-mixed area. Availability is defined as the proportion of each age class found in an area. In our study, the life history and fishery characteristics of a small migratory pelagic fish are used to create the hypothetical population (Table 1). To further simplify the example, we assume that all fishing takes place at the same time each year and therefore length-at-age can be calculated without the additional complication of within year growth.

The mean length-at-age from fishery data collected in the adult area is calculated in three ways: 1) true (used to generate population numbers at age/length), 2) observed (does not account for length-based selectivity or age-based availability), and 3) estimated (which accounts for the observed length-based selection, which is a combination of length-based gear selectivity and an approximation of age-based availability). Sensitivity of the estimates of mean length-at-age to changes in life history and fishery characteristics are illustrated as single-instance changes to the example given in Table 1. The equations governing the simulated population are given below.

The value for population proportions-at-age is given by

[1] Hoyle, S. D., and M. N. Maunder. 2005. Status of yellowfin tuna in the eastern Pacific Ocean in 2004 and outlook for 2005, 102 p. Inter-Am. Trop. Tuna Comm., La Jolla, CA. [Available from website.]

$$p(a) = \frac{e^{-aZ_a}}{\Sigma_a e^{-aZ_a}}, \quad (1)$$

where Z_a = instantaneous total mortality rate at age a.

We assume that the lengths in each age class are normally distributed around their mean length and the mean lengths at age are determined by the von Bertalanffy (1938) growth model (VBGM). The population proportions-at-age and proportions-at-length can be calculated by using

$$p_{a,l} = (P(l/a)p(a), \quad (2)$$

where conditional probability $P(l/a)$ of being in a discrete length l given age a follows a normal distribution around the predicted length-at-age (L_a) based on the VBGM:

$$L_a = L_{inf}(1 - e^{-K(a-a_0)} + \varepsilon, \quad (3)$$

where, L_{inf} = the asymptotic length;
K = the growth coefficient;
ε = the error; and
a_0 = the hypothetical age (expressed in years) when average length is zero.

The error (ε) is the variation in length at age and is assumed to be normal with a mean of 0 and a standard deviation of CV_aL_a

The observed proportions at age and length from the fleet is given by:

$$q_{a,l} = d_a s_l p_{a,l}, \quad (4)$$

where $p_{a,l}$ = the population proportion at age and length; and
$d_a s_l$ = the combined effects of age-based probability that a fish is in the area where the fleet occurs (d_a, availability) and the length-base probability that an encountered fish will be caught (s_l, gear selectivity).

The observed length-based selectivity that includes the length-based gear selectivity that is adjusted for the approximation of age-based availability is given by

$$v_l = \frac{\Sigma_a q_{a,l}}{\Sigma_a p_{a,l}}, \quad (5)$$

where $q_{a,l}$ = the observed; and
$p_{a,l}$ = the population proportions-at-age and -length.

The selectivity-adjusted proportions-at-age and proportions-at–length are given by

$$m_{a,l} = \frac{q_{a,l}}{v_l}, \quad (6)$$

where $q_{a,l}$ = the observed proportion-at-age and proportion-at-length; and

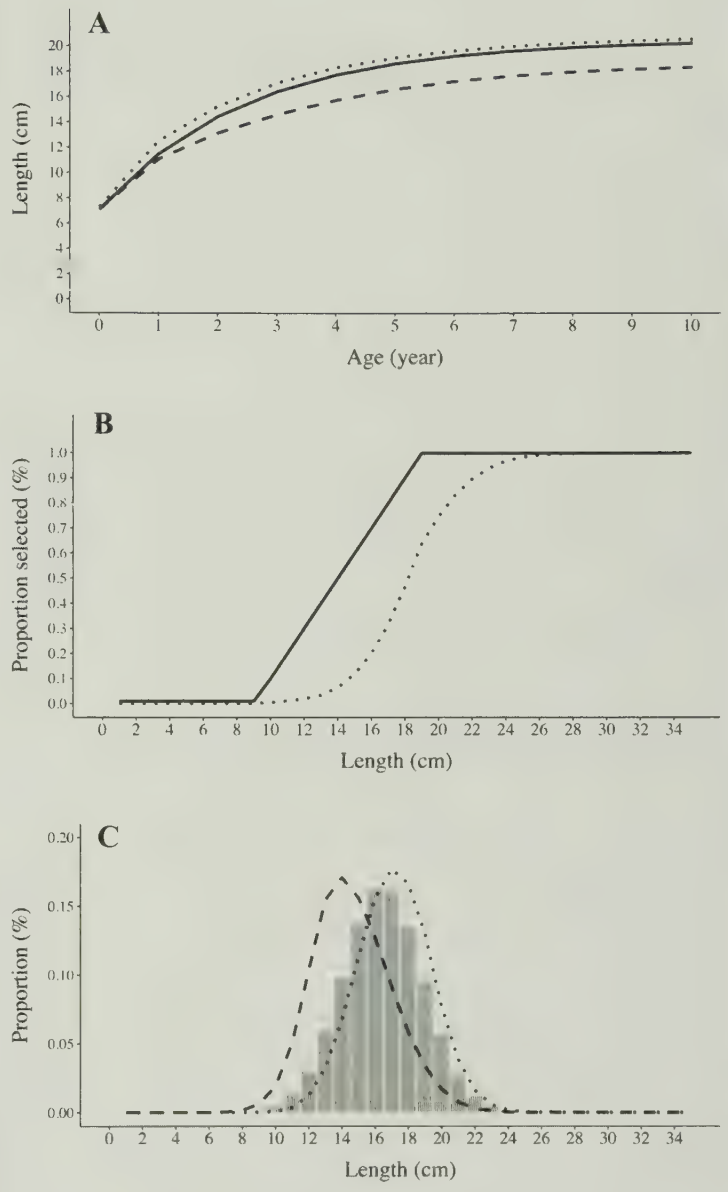

Figure 1

Results from a deterministic population dynamic model of a hypothetical population of a small, migratory pelagic fish in which selectivity includes effects of gear and availability of fish and was used in this study to examine bias in growth estimates. (**A**) Plot of true length-at-age (solid line), length-at-age observed by the fishery without accounting for selectivity effects (dotted line), and estimated length-at-age after accounting for the observed length-based selectivity that included both gear and an approximation of the age-based availability (dashed line). (**B**) Plot of the true length-based gear selectivity (solid line) and the observed length-based selectivity that included the addition of an approximation of age-based availability (dotted line). (**C**) Plot of the true length distribution of age-3 fish (gray bars), length distribution observed by the fishery (dotted line), and estimated length distribution after accounting for the observed length-based selectivity that included an approximation of age-based availability (dashed line).

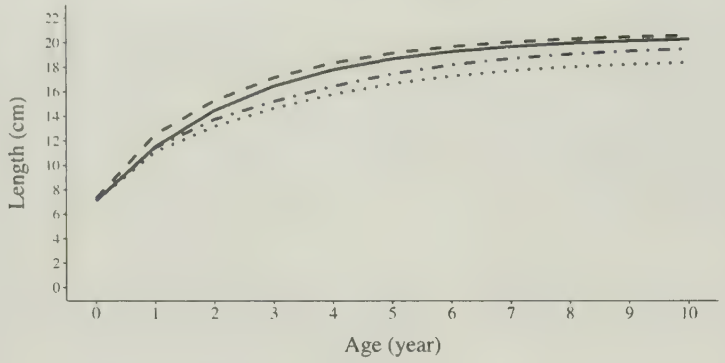

Figure 2

Plot of the true length-at-age (solid line) and estimated length-at-age accounting for the observed length-based gear selectivity that included an approximation of age-based availability of fish. The estimated lengths-at-age are from the example described in Table 1 (dotted line), from a change in the example reducing the coefficient of variation (CV) for the true length-at-age relationship to CV=0.1 (dotted and dashed line), and from a change in the example where the observations are taken from an area with 5% availability of age-4+ fish and 100% availability of fish of ages 0–3 (dashed line).

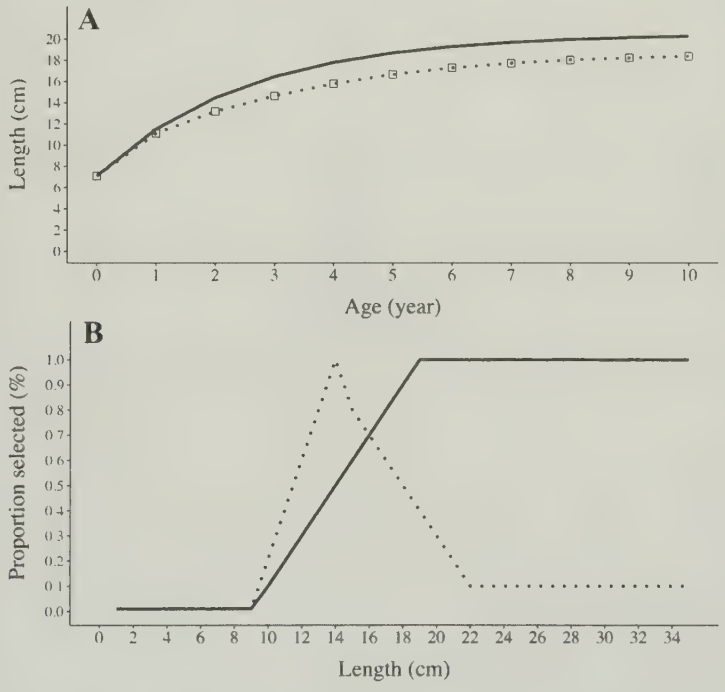

Figure 3

(**A**) Plot of true length-at-age (solid line) and the estimated length-at-age accounting for the observed length-based selectivity that included an approximation of age-based availability. Two different true length-based gear selections were used: asymptotic (dotted line) and domed shaped (open squares). (**B**) Plot of the true length-based gear selectivity without accounting for age-based availability and used in the estimation of length-at-age in plot A. The two examples depicted are asymptotic (solid line) and domed (dotted line).

v_l = the observed length-based selectivity as estimated by an integrated model.

The mean length-at-age for the true population is given by

$$\overline{L}_{a,true} = \frac{\Sigma_l p_{a,l} l}{\Sigma_l p_{a,l}}. \quad (7)$$

Similarly, we can replace $p_{a,l}$ with $q_{a,l}$ to calculate the mean length-at-age for the observed lengths-at-age from the fishery and with $m_{a,l}$ to calculate the mean length-at-age after accounting for the observed selectivity.

Results

A bias in the estimate of mean length-at-age occurs when expected lengths-at-age account for the observed selectivity (v_l) that incorporated an approximation of age-based availability in addition to the length-based gear selectivity (Fig. 1A). Incorporating the approximation results in an alteration of the true length-based process (Fig. 1B). In this example, the asymptotic true length-based gear selectivity has the well-known effect of observing larger than true fish, and this observed bias is unaffected by the age-based availability. However after accounting for the observed length selectivity that includes the additional approximation of age-based availability of fish, the selectivity over-corrects the observed lengths-at-age and results in an estimated length distribution that is shifted to smaller fish (Fig. 1C).

The magnitude and direction of the approximation bias on the estimated length-at-age is affected by several factors. The variability in the length-at-age relationship affects the magnitude of the approximation bias, and larger variability leads to larger bias in the example (Fig. 2). The magnitude and direction of the approximation bias is also affected by the pattern of age-based availability (Fig. 2), and the direction of the bias changes if the availability is reversed and young fish are fully available and older fish are largely unavailable. After the observed selectivity is accounted for, the true shape of the length-based gear selectivity does not affect the estimated mean length-at-age (Fig. 3, A and B).

Discussion

In a growing body of research, the effects of spatial structure on important model processes such as selectivity (Waterhouse et al., 2014; O'Boyle, 2016), and the reliability of

estimates of management quantities (Lee et al., 2017a) are being examined. Lee et al. (2017b) have shown the importance of accounting for age-based movement when estimating growth with random at-age methods. However, little research has shown the effects of approximating age-based processes together with length-based ones (Lee et al., 2017a). This article shows that the widespread application of estimated length-based selection in integrated assessment modeling argues that researchers are assuming unrealistic instantaneous mixing, size-based movements, or are ignoring potential approximation biases.

Our results apply even when fleet distribution covers the entire stock area because the spatial distribution of fishing mortality may not be the same as the spatial distribution of stock abundance. If spatial patterns in the stock are due to age-based movement, then the observed composition data and estimated selectivity would include age-based spatial patterns. Making matters more complicated, as spatial patterns of the stock or the fishery change, the age-based availability of fish would also change annually (Lee et. al., 2017a). Similarly, the approximation bias is not confined to the estimation of growth. Even if an unbiased growth curve is specified in the assessment model, length-based models that do not correctly model both age- and length-based processes would still contain this approximation bias.

Given the wide range of possible biotic and abiotic processes influencing fishery data, it may be difficult to provide a recipe for how best to approach the issues of estimating the growth of fish in fishery assessments. In situations with both age- and length-based processes impacting data, incorporating the relevant processes by using the correct biological units as part of the assessment model may provide the best option. Yet for length-based, age-structured assessment models, estimating growth greatly complicates the analysis. Growth estimates may be confounded by estimates from other model processes (Maunder and Piner, 2015) and therefore require dubious assumptions, such as forcing asymptotic selectivity on a fleet.

Analysts should give additional consideration to the estimation of growth when using only length-based selectivity. Modeling length-composition data is quite challenging, often requiring subjective choices about managing the inevitable misfit to these data (Francis 2011; Lee et al., 2017a). These issues may be of greater importance for stocks assessed by using length-based, age-structured assessment models because of the importance that model predictions match observed length data. Research that is focused on understanding the relative roles of length and age on many important fishery processes should be undertaken (McDaniel et al., 2016).

Acknowledgments

The authors would like to thank several reviewers for helpful comments, as well as M. Maunder for guidance on this topic.

Literature cited

Crone, P. R., and J. L. Valero.
2014. Evaluation of length- vs. age-composition data and associated selectivity assumptions used in stock assessments based on robustness of derived management quantities. Fish. Res. 158:165–171.

Fournier, D. A., J. R. Sibert, J. Majkowski, and J. Hampton.
1990. MULTIFAN a likelihood-based method for estimating growth parameters and age composition from multiple length frequency data sets illustrated using data for southern bluefin tuna (*Thunnus maccoyii*). Can. J. Fish. Aquat. Sci. 47:301–317.

Francis, R. I. C. C.
2011. Data weighting in statistical fisheries stock assessment models. Can. J. Fish. Aquat. Sci. 68:1124–1138.
2016. Growth in age-structured stock assessment models. Fish. Res. 180:77–86.

Hurtado-Ferro, F., A. E. Punt, and K. T. Hill.
2014. Use of multiple selectivity patterns as a proxy for spatial structure. Fish. Res. 158:102–115.

Lee, H.-H., K. R. Piner, M. N. Maunder, I. G. Taylor, and R. D. Methot Jr.
2017a. Evaluation of alternative modelling approaches for spatial effects due to age-based movement. Can. J. Fish. Aquat. Sci. 74:1832–1844.

Lee, H.-H., L. R. Thomas, K. R. Piner, and M. N. Maunder.
2017b. Effects of age-based movement on the estimation of growth assuming random-at-age and random-at-length data. J. Fish. Biol. 90:222–235.

Maunder, M. N., and K. R. Piner.
2015. Contemporary fisheries stock assessment: many issues still remain. ICES J. Mar. Sci. 72:7–18.
2017. Dealing with data conflicts in statistical inference of population assessment models that integrate information from multiple diverse data sets. Fish. Res. 192:16–27.

Maunder, M. N., P. R. Crone, J. L. Valero, and B. X. Semmens.
2014. Selectivity: theory, estimation, and application in fishery stock assessment models. Fish. Res. 158:1–4.

McDaniel, J., K. R. Piner, H. H. Lee, and K. Hill.
2016. Evidence that the migration of the northern subpopulation of Pacific sardine (*Sardinops sagax*) off the west coast of the United States is age-based. PLoS ONE 11(11):e0166780.

Methot, R. D., Jr., and C. R. Wetzel.
2013. Stock synthesis: a biological and statistical framework for fish stock assessment and fishery management. Fish. Res. 142:86–99.

Nøttestad, L., J. Giske, J. C. Holst, and G. Huse.
1999. A length-based hypothesis for feeding migrations in pelagic fish. Can. J. Fish. Aquat. Sci. 56(S1):26–34.

O'Boyle, R. O., M. Dean, and C. M. Legault.
2016. The influence of seasonal migrations on fishery selectivity. ICES J. Mar. Sci. 73:1774–1787.

Parma, A. M., and R. B. Deriso.
1990. Dynamics of age and size composition in a population subject to size-selective mortality: effects of phenotypic variability in growth. Can. J. Fish. Aquat. Sci. 47:274–289.

Piner, K. R., H.-H. Lee, and M. N. Maunder.
2016. Evaluation of using random-at-length observations and an equilibrium approximation of the population age structure in fitting the von Bertalanffy growth function. Fish Res. 180:128–137.

Schueller, A. M., E. H. Williams, and R. T. Cheshire.
2014. A proposed, tested, and applied adjustment to account for bias in growth parameter estimates due to selectivity. Fish. Res. 158:26–39.

Stewart, P. A. M.
1975. Catch selectivity by electrical fishing systems. ICES J. Mar. Sci. 36:106–109.

Taylor, N. G., C. J. Walters, and S. J. D. Martell.
2005. A new likelihood for simultaneously estimating von Bertalanffy growth parameters, gear selectivity, and natural and fishing mortality. Can. J. Fish. Aquat. Sci. 62:215–223.

von Bertalanffy, L.
1938. A quantitative theory of organic growth (inquiries on growth laws II). Hum. Biol. 10:181–213.

Waterhouse, L., D. B. Sampson, M. N. Maunder, and B. X. Semmens.
2014. Using areas-as-fleets selectivity to model spatial fishing: Asymptotic curves are unlikely under equilibrium conditions. Fish. Res. 158:15–25.

Yanase, K., S. Eayrs, and T. Arimoto.
2007. Influence of water temperature and fish length on the maximum swimming speed of sand flathead, *Platycephalus bassensis*: implications for trawl selectivity. Fish. Res. 84:180–188.

National Marine
Fisheries Service
NOAA

Fishery Bulletin
established in 1881

Spencer F. Baird
First U.S. Commissioner
of Fisheries and founder
of *Fishery Bulletin*

Identifying populations of the blue jack mackerel (*Trachurus picturatus*) in the Northeast Atlantic by using geometric morphometrics and otolith shape analysis

Joana Vasconcelos (contact author)[1,2,3]
Ana R. Vieira[4]
Vera Sequeira[4]
José A. González[5]
Manfred Kaufmann[3,6]
Leonel Serrano Gordo[4,7]

Email address for contact author: joana.pr.vasconcelos@madeira.gov.pt

[1] Direção de Serviços de Investigação
Direção Regional de Pescas da Região Autónoma da Madeira
Estrada da Pontinha
9004-562 Funchal, Madeira, Portugal

[2] Centro de Ciências do Mar e do Ambiente (MARE)
Quinta do Lorde Marina
Sítio da Piedade
9200-044 Caniçal, Madeira, Portugal

[3] Universidade da Madeira
Faculdade de Ciências da Vida
Campus Universitário da Penteada
Caminho da Penteada
9020-105 Funchal, Madeira, Portugal

[4] MARE
Faculdade de Ciências
Universidade de Lisboa
Rua Ernesto Vasconcelos
Campo Grande, 1749-016 Lisboa, Portugal

[5] Ecología Marina Aplicada y Pesquerías
Instituto de Estudios Ambientales y Recursos Naturales (i-UNAT)
Universidad de Las Palmas de Gran Canaria
Campus Universitario de Tafira
35017 Las Palmas de Gran Canaria, Spain

[6] Centro Interdisciplinar de Investigação Marinha e Ambiental da Madeira
Edifício Madeira Tecnopolo (Piso 0)
Caminho da Penteada
9020-105 Funchal, Madeira, Portugal

[7] Departamento de Biologia Animal
Faculdade de Ciências
Universidade de Lisboa
Rua Ernesto Vasconcelos
Edifício C2, 2°Piso
Campo Grande, 1749-016 Lisboa, Portugal

Abstract—The population structure of the blue jack mackerel (*Trachurus picturatus*, Osteichthyes, Carangidae), in the northeast Atlantic is still unknown. To identify any distinct population units, three areas were selected: waters off Madeira, Peniche (mainland Portugal), and the Canary Islands. Knowledge of population structure is an aspect of the population dynamics of a species that is essential to effectively assess the existence of stocks and manage fisheries. In this study, geometric morphometrics and otolith shape analysis were successfully applied for population identification. Multivariate analysis of variance (MANOVA) revealed no body shape differences between males and females in each area studied, and therefore the sexes were combined for the analysis. The results of the discriminant analysis showed that a low misclassification occurred among areas; 78.0% of individuals were correctly classified. MANOVA performed on the otolith normalized elliptic Fourier descriptors revealed significant areal differences, but no difference between sexes. An overall classification success of 73.3% in the canonical discriminant analysis was achieved. These results indicate the usefulness of both otolith and body shape analysis for differentiation of blue jack mackerel stocks from the northeast Atlantic and indicate the existence of at least three distinguishable populations of this species.

Manuscript submitted 28 March 2017.
Manuscript accepted 20 November 2017.
Fish. Bull. 116:81–92 (2018).
Online publication date: 13 December 2017.
doi: 10.7755/FB.116.1.9

The views and opinions expressed or implied in this article are those of the author (or authors) and do not necessarily reflect the position of the National Marine Fisheries Service, NOAA.

In fisheries management, understanding population structure is key because a stock is the basic unit in population dynamic models that are used both to determine the status of a stock and to implement management actions appropriate for ensuring the sustainability of a population (Secor, 2014). Begg and Waldman (1999) suggested a holistic approach to understanding populations of fish by using both genetic and phenotypic analyses to define stock boundaries, because this integrative approach maximizes the likelihood of correctly defining a fish stock and enables a higher degree of confidence than that generated by a single procedure.

The capacity of populations in different environmental conditions to adapt and develop as separate biological entities is counterbalanced by the shifting of individual fish among populations (Turan, 2004). However, each individual fish is characterized by a number of distinctive features that are influenced by environmental and genetic factors (Cadrin and

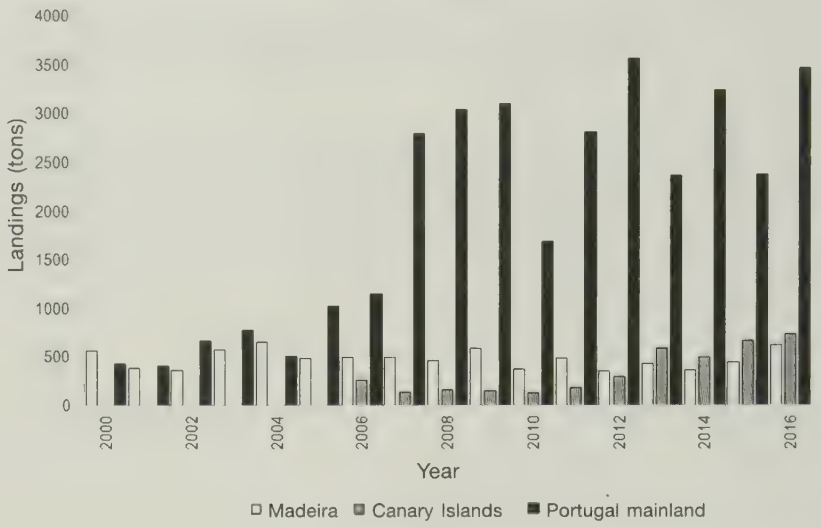

Figure 1

Landings (in metric tons) of blue jack mackerel (*Trachurus picturatus*) caught off Peniche, a city on the coast of mainland Portugal, off the Madeira archipelago, and off the Canary Islands during 2000–2016. Source: Instituto Nacional de Estatística, Portugal

Friedland, 1999). Consequently, phenotypic and genetic variation among fish within a species can occur as a result of isolation, and such variation can be seen as a basis for separation of fish into groups that can be managed as distinct populations (Turan, 2004). However, areal differentiation within a species may also arise from other factors, such as 1) countergradient variation when environmental influences reinforce the genetic differences between populations (Yamahira and Conover, 2002; Barria et al., 2014), 2) thermal reaction (Yamahira et al., 2007; Yamahira and Takeshi, 2008), and 3) local adaptation and adaptive phenotypic plasticity (Yampolsky et al., 2014).

Identification of fish stocks by using shape analysis has evolved from measuring simple linear distances to deriving geometric variables (Stransky, 2014). The development of image processing tools has facilitated the change from traditional morphometrics to more complex geometric functions (Cadrin and Friedland, 1999) and has increased the power of morphometric analysis for population discrimination (Rohlf and Bookstein, 1990; Marcus et al., 1996; Cadrin and Friedland, 1999; Cadrin et al., 2014). Geometric approaches to morphometric analysis are often classified as either "landmark methods" (Cadrin et al., 2014) or "outline methods" (Bookstein et al., 1985; Marcus et al., 1996). Landmark methods are based on anatomical points or landmarks to analyze morphometry, and outline methods are used to identify different patterns of otolith shapes.

Otolith shape is species specific, is less variable than body growth for fish (Campana and Casselman, 1993), and the appearance and shape of the otolith often vary geographically for any given species (Tuset et al., 2008). Unlike scales and bones, otoliths grow during the entire life of a fish, and re-absorption or alteration of otolith material once it has been deposited is unlikely (Campana and Neilson, 1985; Casselman, 1987). Consequently, otoliths remain unchanged during short-term changes in fish condition (e.g. starvation) (Campana and Casselman, 1993). Nevertheless, environmental and genotypic factors can induce differences in metabolism and growth that might influence otolith shape (Cardinale et al., 2004). In addition, the otolith shape can vary substantially if genetic or environmental differences persist and the populations remain partially isolated and inhabit different environments (Bird et al., 1986; Campana and Casselman, 1993; Begg and Brown, 2000; Begg et al., 2001; Smith et al., 2002).

The blue jack mackerel, *Trachurus picturatus* (Bowdich, 1825) (Osteichthyes, Carangidae) is an oceanic pelagic species ranging to depths of at least 370 m (Smith-Vaniz, 1986) (575 m in the Azores, Menezes et al., 2006) and can be found from the Bay of Biscay (France) southward to Morocco and eastward into the Mediterranean Sea (Smith-Vaniz, 1986). It is a commercially important species with highly variable landings. On the Portuguese mainland, for example, landings have doubled over the last decade (INE[1]), while landings off the Canary Islands have tripled (Castro[2]) (Fig. 1).

Apart from one very recent study of parasites in

[1] INE (Instituto Nacional de Estatística). 2013. Estatísticas da Pesca 2012, 133 p. Instituto Nacional de Estatística, I.P., Lisboa, Portugal. [Available from website.]

[2] Castro, J.J. 2017. Personal commun. Faculty of Marine Sciences, University of Las Palmas de Gran Canaria.

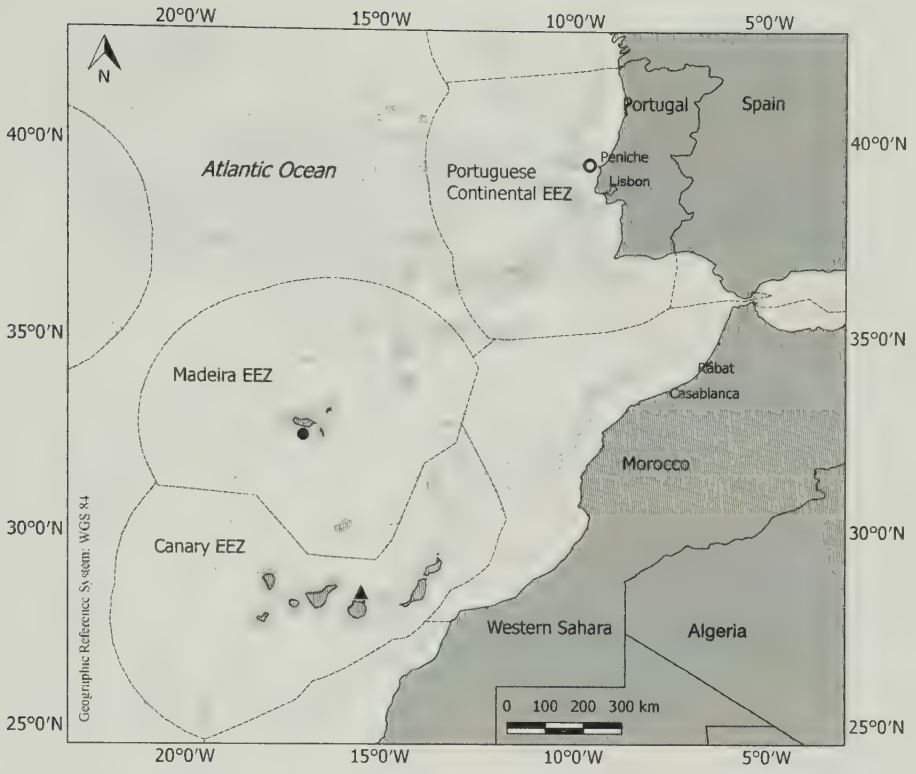

Figure 2

Map showing the 3 locations where blue jack mackerel (*Trachurus picturatus*) were sampled in 2015 for this study: off Peniche, a city on mainland Portugal (open circle), the Madeira archipelago (black circle), and the Canary Islands (black triangle). Source: Direção de Serviços de Investigação da Direção Regional de Pescas. The dashed lines indicate the exclusive economic zones (EEZs).

the blue jack mackerel, no other work has focused on the possible population structure over the distributional range of this fish (ICES[3]; Vasconcelos et al., 2017a). Interestingly, some studies on reproduction and growth from Madeira (Jesus[4]; Vasconcelos et al., 2006; Vasconcelos et al., 2017b), Azores (Isidro, 1990; Garcia et al., 2015) and the Canary Islands (Shaboneyev and Ryazantseva, 1977; Riviero[5]; Jurado-Ruzafa and Santamaría, 2013) have reported a similar reproductive season, but differences in growth and age at first maturity were observed between individuals from the Azores and those from Madeira (Jesus[4]; Vasconcelos et al., 2006) and the Canaries (Jurado-Ruzafa and Santamaría, 2013). A number of studies have successfully used parasites of *T. picturatus* as biological tags (Gaevskaya and Kovaleva, 1985; Costa et al., 2013; Vasconcelos et al., 2017a) and it may be that variation in the occurrence and infection levels of parasites may reflect the existence of different populations of *T. picturatus* in the northeast Atlantic. The goal for this study was to provide a first step toward the identification of geographical variation in blue jack mackerel body and otolith shape by using landmark-based geometric morphometrics and elliptic Fourier analysis, respectively, to determine whether variation in these parameters may have implications for fishery management.

Materials and methods

A total of 438 specimens of *T. picturatus* (135 from waters off Peniche, mainland Portugal, 155 from the Madeira archipelago and 148 from the Canary archipelago) (Fig. 2) were randomly sampled from commercial catches, per sampling period (quarter), between January and December 2015. The methods and fishing gear used to catch *T. picturatus* varied among locations:

[3] ICES. 2016. Report of the working group on southern horse mackerel, anchovy and sardine (WGHANSA), 24–29 June 2016, Lorient, France. ICES CM 2016/ACOM:17, 588 p. [Available from website.]

[4] Jesus, G. T. 1992. Study of the growth and reproduction of *Trachurus picturatus* (Bowdich, 1825) in Madeira. Doc. XIV/C/1-1991/03 (DG XIV/CE), 66 p. Direçao Regional de Pescas da Região Autónoma da Madeira, Funchal, Madeira, Portugal.

[5] Riviero, I. 2006. Biometrics of pelagic fish in Gran Canaria Island waters (Canary Islands), 17 p. Univ. Palmas-Gran Canaria, Las Palmas de Gran Canaria, Canary Islands, Spain. [Available from website.]

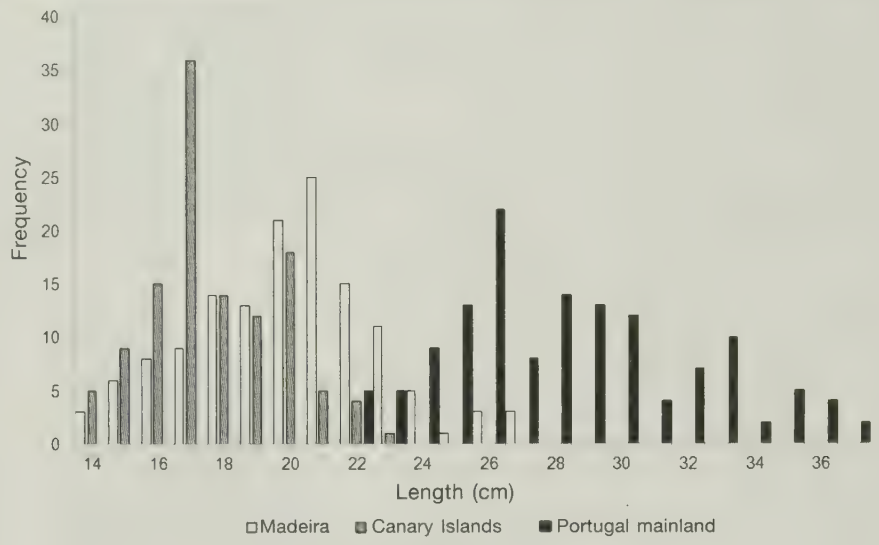

Figure 3

Length–frequency distribution per sampling area for blue jack mackerel (*Trachurus picturatus*) sampled in 2015 for this study in 3 areas: off Peniche, a city on the coast of Portugal, off the Madeira archipelago, and off the Canary Islands

purse seine fishing off both Madeira and the Canary Islands; and trawling off Peniche.

Samples from waters off Peniche and off the Canary Islands were stored frozen (–20°C) until just before they were measured at the laboratory, and all steps were taken to maintain fish shape. Fish from Madeira were analyzed fresh. From each specimen, total length was measured and, after being photographed for body shape analysis, sex was determined macroscopically. Both sagittal otoliths (hereafter referred to as otoliths) were extracted, rinsed, and stored dry in labeled vials for later otolith shape analysis.

Body shape analysis

A total of 300 fish equally distributed among the areas were sampled (Fig. 3): Peniche, 22–37 cm total length (TL), 40 females and 60 males; Madeira, 14–27 cm TL, 48 females and 52 males; Canaries, 16–23 cm TL, 46 females and 54 males.

Twelve anatomical landmarks (e.g., fin insertion point) were defined and used mainly along the left side of the body contour (Fig. 4), in order to be meaningful as systematic terms (Cadrin, 2000; Cadrin et al., 2014), and were based on the 11 anatomical landmarks selected for horse mackerel in a similar study (Murta et al., 2008a).

Each of the 100 fish was then photographed with the left side upwards, by using a Canon[6] EOS 700D digital camera (Canon, Inc., Ohta-ku, Tokyo) with a Canon EF-S 18-55 mm lens that was placed on a firm support to maintain a right angle and adequate height to stabilize and avoid image distortion. From each digital image, a digital TPS (thin-plane spline) file was generated with x and y coordinates for each homologous point with tpsDig software, vers. 2.10 (Rohlf, 2006).

Subsequent methodological procedures followed those of Sequeira et al. (2011) and Porrini et al. (2015). The tpsDig software (Rohlf, 2006) was used to acquire x and y coordinates of the landmarks previously noted, and a generalized least squares Procrustes superimposition (Rohlf, 1990) was used to adjust them. In order to calculate and eliminate the effect of size on shape (allometry), a multivariate (total) regression of the Procrustes coordinates on centroid size was carried out with MorphoJ software, vers. 1.05c (Klingenberg, 2011) and the residuals of this regression were used as 'size-free' variables. To test the null hypothesis of independence between shape and size, a permutation test with 10,000 runs was applied (Good, 1994). Possible sexual dimorphism among study areas was tested by using IBM SPSS, vers. 23 (IBM Corp., Armonk, NY) and a multivariate analysis of variance (MANOVA). To detect possible morphometric differences in the body shape of *T. picturatus* among the 3 study areas, a canonical variate analysis was performed with MorphoJ. A canonical discriminant analysis with jackknife cross-validation procedures was carried out with IBM SPSS software to calculate an unbiased estimation of classification success.

A significance level of 0.05 was set for all statistical analyses.

[6] Mention of trade names or commercial companies is for identification purposes only and does not imply endorsement by the National Marine Fisheries Service, NOAA.

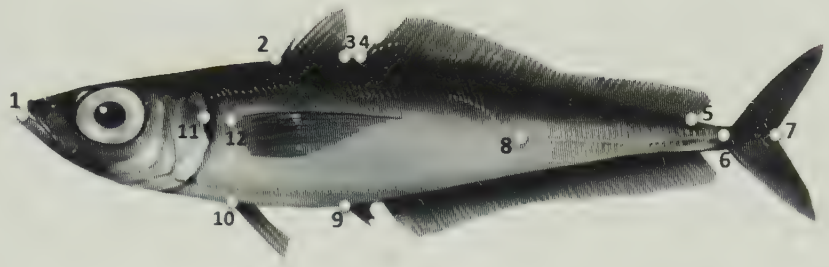

Figure 4

Illustration showing the 12 anatomical landmarks of the blue jack mackerel (*Trachurus picturatus*): 1) anterior tip of the mouth; 2) origin of the 1st dorsal fin; 3) posterior end of the 1st dorsal fin; 4) origin of the 2nd dorsal fin; 5) posterior end of the 2nd dorsal fin; 6) caudal peduncle; 7) middle point of the forked caudal fin; 8) inflection point of the lateral line; 9) origin of the anal fin; 10) origin of the pelvic fin; 11) posterior insertion of the operculum; and 12) insertion of the pectoral fin.

Otolith shape analysis

A total of 277 otoliths were analyzed (Fig. 3): 100 from waters off Peniche (22–37 cm TL, 40 females and 60 males), 100 off Madeira (15–27 cm TL, 50 females and 50 males), and 77 off the Canary Islands (14–23 cm TL, 34 females and 43 males).

The otoliths were positioned on a microscope slide and photographed with the sulcus acusticus facing down and the rostrum to the left on the horizontal plane to reduce distortion errors in the normalization process. High-contrast digital images were captured by a Leica EC3 digital camera (Leica Microsystems, Wetzlar, Germany) linked to a Leica MZ9.5 stereomicroscope that uses transmitted light and with the software Leica Application Suite X Core, vers. 4.5, that delivers dark 2-dimensional objects against a white background. The microscope magnification was adjusted to the largest otolith size to ensure the same magnification (8×) for all otoliths.

The image processing program SHAPE, vers. 1.3 (Iwata and Ukai, 2002), was used to enhance contrast of the images, transforming color or grayscale images to black-and-white silhouettes of the structure (Cadrin and Friedland, 2005). Otoliths contours were extracted as chain-codes from the digital image by means of the ChainCoder package that is part of SHAPE. The elliptic Fourier descriptors, or harmonics, were obtained from the SHAPE package Chc2Nef by using a discrete Fourier transformation of the chain-coded contour (Kuhl and Giardina, 1982; Lestrel, 1989, 1997). The four coefficients of each harmonic were normalized in relation to the first harmonic to become invariant to otolith size, rotation, and starting point (Kuhl and Giardina, 1982; Iwata and Ukai, 2002). The first three coefficients of the first harmonic were degenerated to fixed values: $a_1 \pm 1$, $b_1 = c_1 = 0$ (Tracey et al., 2006).

A random subsample of 10 otoliths for each sex and area was used to define the minimum number of harmonics needed (99% accumulated variance) for the multivariate analysis. For each otolith, 100 harmonics were generated. Possible effect of area and sex on otolith normalized elliptic Fourier descriptors (NEFDs) was tested by using MANOVA. To detect possible morphometric differences in the contour shape of otoliths from the three studied areas, a canonical discriminant analysis was performed and a jackknife cross-validation procedure was carried out with IBM SPSS software to validate similarities between groups by listing the misclassification of individuals within other areas (Neves et al., 2011; Vieira et al., 2014).

A significance level of 0.05 was set for all statistical tests used.

Results

Body shape analysis

No shape differences were found between males and females within the three areas under study (Madeira: F=0.15, P=0.72; Peniche: F=0.68, P=0.83; Canary Islands: F=0.40, P=0.59), and therefore sexes were pooled for each region.

A significant difference in the mean body shape of blue jack mackerel was found for each of the three study areas (Table 1). The overall assignment of blue jack mackerel individuals in their original sample was correctly classified for 78.0% of the total number of specimens (Table 2). In the jackknifed classification matrix of the discriminant analysis, a proportion of 33.0% of the specimens from Madeira were incorrectly assigned to the Canary Islands (23.0%) and Peniche (10.0%). Misclassifications also occurred between the

Table 1

Procrustes distances for the mean body shape of blue jack mackerel (*Trachurus picturatus*) from the 3 areas sampled in this study in 2015, off the Madeira archipelago, off Peniche on mainland Portugal, and off the Canary Islands. Corresponding *P*-values (in parentheses) obtained from a permutation test (10,000 permutation runs) are also given. The results indicate that all of the mean body shapes are statistically different between the 3 areas.

Region	Madeira	Mainland Portugal	Canary Islands
Madeira	–	0.03 (<0.0001)	0.03 (<0.0001)
Mainland Portugal	–	–	0.03 (<0.0001)

Table 2

Classification matrix from the discriminant analysis performed by using a jackknife procedure for cross-validation of the body shape of individual blue jack mackerel (*Trachurus picturatus*) sampled from 3 areas in the northeast Atlantic Ocean in 2015: off the Madeira archipelago, off mainland Portugal, and off the Canary Islands. Values are percentages of individuals sampled in the areas (given in rows) that were classified into the area given in columns (values for correct classification are presented in bold). Overall classification success was 78.0%.

Region	Madeira	Mainland Portugal	Canary Islands
Madeira	**67.0**	10.0	23.0
Mainland Portugal	13.0	**83.0**	4.0
Canaries	11.0	5.0	**84.0**

Canary Islands and Peniche (5.0%) and Madeira (11.0%), as well as between Peniche and the Canary Islands (4.0%) and Madeira (13.0%). However, the percentage of individuals incorrectly classified between the referred locations was low. The proportion of correctly classified samples off Peniche (83.0%) and the Canary Islands (84.0%) to their original group was highest, showing a clear separation from samples off Madeira (67.0%).

The 2-dimensional ordination plot (Fig. 5) showed a differentiation of stocks for the three areas studied, but with some overlapping of stocks mainly between Madeira and the two other areas; the Canary Islands and Peniche seem to be more distinct from each other. The first two canonical variate analysis accounted for 74.5% and 25.5% of the between-group variability.

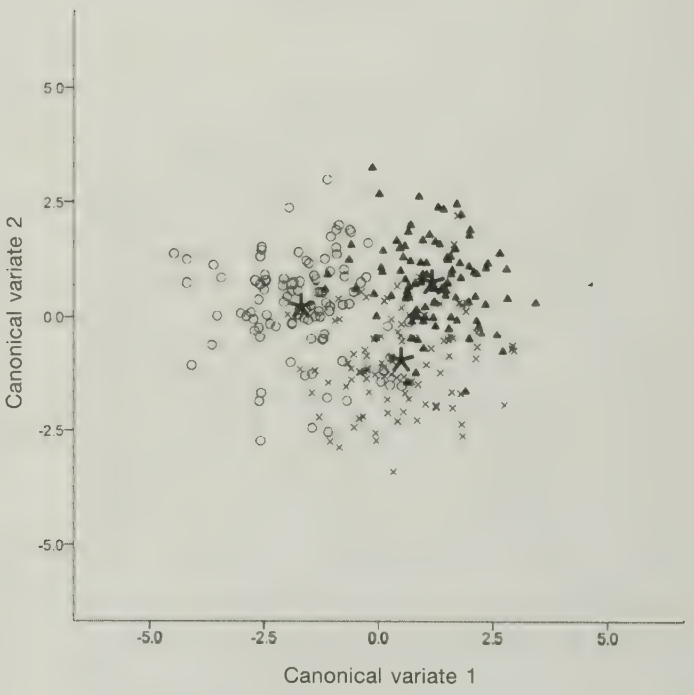

Figure 5

Two-dimensional ordination plot of the samples of blue jack mackerel (*Trachurus picturatus*), collected in 2015 from off the Madeira archipelago (black crosses), off mainland Portugal (open circles), and off the Canary Islands (black triangles), based on canonical variate analysis. Stars indicate class centroids per sampled area (each individual was allocated to the group with the nearest centroid).

Otolith shape analysis

The mean and standard deviations of the cumulative variance of the harmonics are shown in Figure 6. Only the first 15 harmonics were used for multivariate analysis because these were responsible for over 99% of the otolith shape variation.

Figure 7 represents the outlines of the mean NEFDs, by region, plotted as an overlay picture to enhance differences in average otolith shapes. Overall, the highest shape variation among areas occurred in the excisura ostii and antirostrum. Variations also occurred in the dorsal and ventral edges of the otolith.

The results of the MANOVA applied to compare the NEFDs by area and sex are shown in Table 3. Because neither differences in otolith shape between males and females within the three areas, nor interaction between area and sex, were found, all subsequent analyses were performed for sexes combined.

The variables used in the stepwise discriminant analysis are represented in Table 4. For the analysis

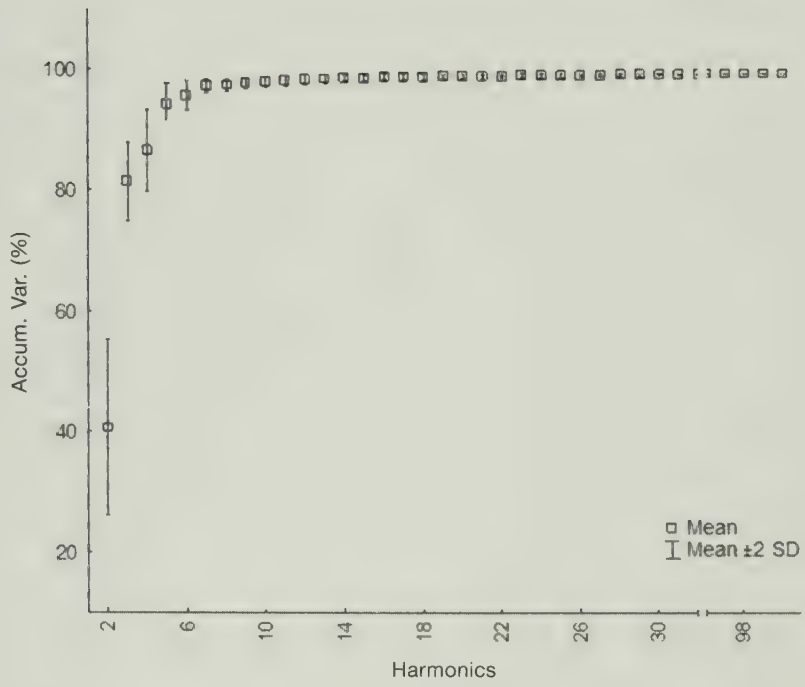

Figure 6

Mean and standard deviation (SD) of the cumulative variance of 100 harmonics for 60 randomly selected otoliths of blue jack mackerel (*Trachurus picturatus*) taken from fish sampled in 2015 in the northwest Atlantic Ocean. Mean (open squares) and standard deviation (whiskers) values represent the accumulated percentage of variance (% accum. var.) explained by the *n*th harmonic.

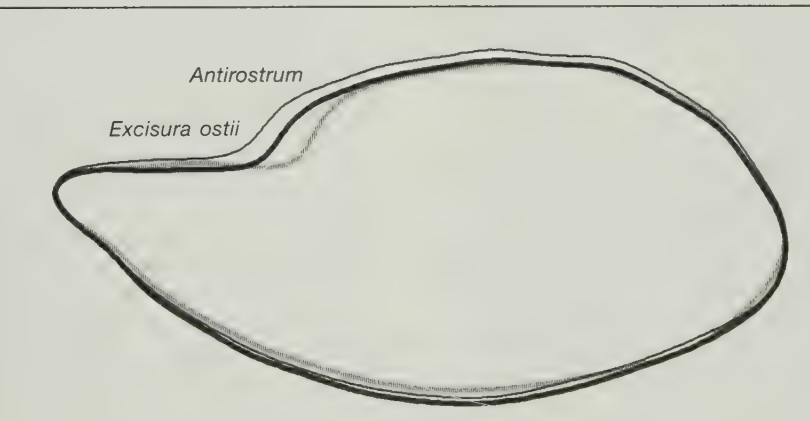

Figure 7

Mean otolith shape for blue jack mackerel (*Trachurus picturatus*) sampled in 2015 from the Madeira archipelago (solid black line), off mainland Portugal (solid dark gray line), and the Canary Islands (thin black line).

13 variables were used. The differences among the three areas shown by the MANOVA were also supported by the MANOVA performed on the otolith NEFDs. An overall successful classification rate of 73.3% in the canonical discriminant analysis was achieved for both sexes combined (Table 4). The highest classification rate was found for specimens from Peniche with 89.0% classification success, whereas specimens from the Ca-

Table 3

Summary of results from a multivariate analysis of variance (MANOVA) (n=300) on normalized elliptic Fourier descriptors for otoliths of blue jack mackerel (*Trachurus picturatus*) sampled in 2015 from the Madeira archipelago, off mainland Portugal and off the Canary Islands. Results include the test statistics Pillai's trace and Wilks' λ. df=degrees of freedom (numerator, nominator).

	Pillai's trace	Wilks' λ	df	*P*-value
Area	1.09	0.15	114.43	<0.0001
Sex	0.23	0.77	57.22	0.27
Area * sex	0.43	0.62	114.43	0.41

nary Islands showed the lowest classification success with 62.3%.

The two discriminant functions were significant and discriminated the three areas studied (f1: λ=0.26, P<0.0001; f2: λ=0.85, P<0.0001). The score plots for the first 2 discriminant functions (Fig. 8) showed a separation between the 3 areas studied, but some overlapping can be observed. The first discriminant function explained 92.6% of between-group variance.

Table 4

Classification matrix of the discriminant analysis performed by using a jackknife procedure for cross-validation of the otolith shape of individual blue jack mackerel (*Trachurus picturatus*) sampled from 3 areas in the northeast Atlantic Ocean in 2015: off the Madeira archipelago, off mainland Portugal, and off the Canary Islands. Values are percentages of individuals sampled in the areas given in rows that were then classified into the areas given in columns (values for correct classification are presented in bold). Overall classification success: 73.3%, Wilks' λ=0.26. In the discriminant analysis, 13 variables were used.

Region	Madeira	Mainland Portugal	Canary Islands
Madeira	**66.0**	10.0	24.0
Mainland Portugal	9.0	**89.0**	2.0
Canaries	31.2	6.5	**62.3**
Variables	d7, b9, c8, b8, c13, c15, d13, d12, d15, c5, a5, c14, c9		

Discussion

The blue jack mackerel population structure in the southern part of the northeast Atlantic (Peniche–Madeira–Canary Islands) was unknown before this study. The present results reveal the usefulness of anatomical geometric morphometric and otolith shape analysis in supporting the existence of three stock units of blue jack mackerel in the southern northeast Atlantic. The same holistic approach that we applied was also used to discriminate the stocks of another species of the genus *Trachurus* in the northeast Atlantic Ocean and Mediterranean Sea, the horse mackerel (*Trachurus trachurus*). The body shape (Murta et al., 2008a) and otolith shape (Stransky et al., 2008) analysis provided evidence of a consistent separation between Atlantic and Mediterranean locations, with 90% correct allocation of individuals of each stock in the otolith shape analysis (Murta et al., 2008a; Stransky et al., 2008).

Ideally, a sampling strategy should focus on a specific time scale (e.g. spawning season) and on a specific length or age range of fish. Adherence to this strategy would have enhanced our results, but different fishing methods did not allow the implementation of an ideal sampling strategy. To overcome this potential weakness, the corrections used in both analyses removed the effect of size on shape. High values of classification success (78.0% and 73.3%) were achieved in the canonical discriminant analysis used in both anatomical morphometric and otolith shape analysis, respectively, indicating three phenotypically distinct local populations. No differences between sexes were observed by using either technique.

Using both analytical techniques, we found the highest percentages of misclassification for specimens from Madeira that were classified in the Canary Islands group and vice-versa. This overlap between areas may be indicative of some degree of migration between these two populations. In general, the migratory movements of the blue jack mackerel are driven by feeding and spawning requirements (Menezes et al., 2006) and where seamounts are used as feeding areas in their preadult and adult phase, but it is likely that there are immigrants to the seamount from the island shelf areas (Menezes et al.[7]). Differences in the biological and physical environments of hatchery and nursery areas can also result in morphometric variations between these populations (Robinson et al., 1993; Chipps et al., 2004; Vila-Gispert et al., 2007). Other, nonenvironmental factors may also contribute to differences among populations. For example, a greater growth capacity in high-latitude populations reflects an adaptation that would counteract a slowing of growth rate over the growing season; otherwise a reduction in annual growth rates of individuals with increasing latitude would be expected because of the shorter growing seasons at higher latitudes that result in a reduction in body size (Conover and Present, 1990; Yamahira et al., 2007). Yamahira et al. (2007) observed that individ-

[7] Menezes, G., A. Rogers, H. Krug, A. Mendonça, B. M. Stockley, E. Isidro, M. R. Pinho, and A. Fernandes. 2001. Seasonal changes in biological and ecological traits of demersal and deep-water fish species in the Azores, 164 p. Univ. Açores, Dep. Oceanogr. (DOP), Arquivos DOP Sér. Estud. 1/2001.

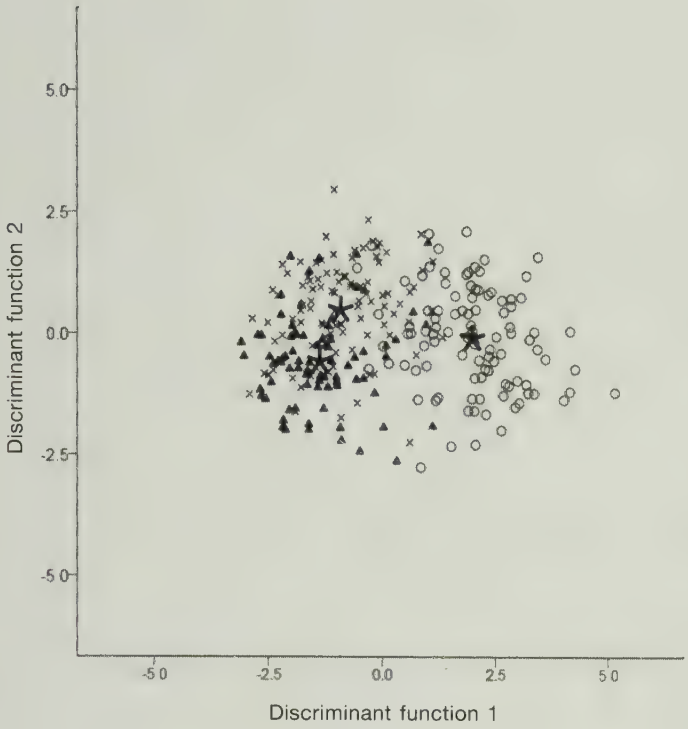

Figure 8

Plots of function scores determined with discriminant analysis, with sexes combined, for blue jack mackerel (*Trachurus picturatus*) sampled in 2015 from off the Madeira arhcipelago (black crosses), off mainland Portugal (open circles), and off the Canary Islands (black triangles). Scores were based on 57 normalized elliptical Fourier descriptor coefficients of the first 15 harmonics. Stars indicate class centroids per area sampled (each individual was allocated to the group with the nearest centroid).

uals at higher-latitudes did not only grow faster than lower-latitude individuals but also at all temperatures that they examined and suggested that populations moving to higher latitudes have developed a capacity for growth by vertically shifting the thermal reaction norms for ascendant growth rates. These thermal reactions results in an increase in the growth rates of individuals at a certain temperature (Yamahira and Takeshi, 2008). Local adaptation in its two forms (temperature adaptation and countergradient variation) may also be expected to vary within and among species (Yamahira and Conover, 2002).

The results of this study reveal a clear differentiation between Peniche and the Macaronesian archipelagos, especially between Peniche and the Canary Islands. This differentiation may be due to an adaptation of the population off mainland Portugal to high-latitude environments, and therefore to a faster growth rate than that of the Canary Islands population. Considering that the northeast Atlantic system, the Canary Islands, and the region of the Iberian Peninsula form two quite distinct subsystems (Dias, 2015), their separation is not only geographic but also a result of the unique oceanographic features of the northeast Atlantic region; the discontinuity of currents imposed by the flow of the Mediterranean Sea through the Strait of Gibraltar to the Gulf of Cadiz (Dias, 2015). These subsystems may be seen as biogeographic breaks that often result in abrupt changes in phenotypic traits among resident populations (Barria et al., 2014). This separation may explain our results that show low levels of population mixture between the Canary Islands and Peniche.

Both archipelagos, i.e. Madeira and the Canary Islands, are under the influence of the subtropical gyre of the eastern central Atlantic, which would facilitate the transport of planktonic larvae to these archipelagos from American, European, and northwest African coasts. This gyre may influence the mixing levels found between the two archipelagos in our study. In the case of the Canary Islands (relatively close to Africa—104 km from Cape Juby, Morocco), a strong mesoscale distribution of the larval community has been recently described from filaments of the upwelling system from Africa reaching the southeast of this archipelago (Rodríguez et al., 2004; Bécognée et al., 2009). This pattern in the larval community corroborates our findings and supports the distinction of the Madeira and Canary Islands stocks, although some mixing of fish from these two archipelagos exists.

The final determination of the existence of stocks of blue jack mackerel in the northeast Atlantic for assessment and ultimately the management of the fisheries must obviously be based on more than one method or single result. Clearly, the most successful way of defining stock limits is through a holistic approach, involving a combination of a broad spectrum of complementary techniques (Begg and Waldman, 1999) which will, in combination, provide considerable insight into the practical identification and delineation of individual population subunits or stocks (Elliott et al., 1995; Cadrin et al., 2005; Waldman, 2005; Waples et al., 2008). The different methods (e.g., life history parameters, tagging, otolith elemental composition, fatty acid profiles, parasites as biological tags, morphometric landmarks, morphometric outlines, and genetic analysis) that can be used to identify stocks were exhaustively compiled by Cadrin et al. (2005) and updated by Cadrin et al. (2014). Considering the existence of three possible *T. picturatus* populations as suggested by the results of the present work and in order to maintain the sustainability and genetic biodiversity (Begg and Waldman, 1999) of this resource in Madeira, the management strategy should be one in which a precautionary approach is taken (e.g., to regard the fish in the three areas studied as separate stocks) while other avenues of research are being pursued. A failure to ac-

knowledge these stocks as separate stocks may lead to flawed management actions and ultimately to overexploitation. However, the results obtained here suggest that there may be a mix (below 32% misclassification) of individuals of different stocks, namely between Madeira and the Canary Islands, which could offer a buffer against any regional overexploitation. This finding implies that, for an accurate assessment of the overall population and state of each stock, its boundaries should not only be defined but also an estimate should be made of the proportion of mixing of fish from the different population units, by location and time of year during which the mixing of stocks occurs (Murta et al., 2008b).

Acknowledgments

JV was supported by Regional Agency for the Development of Research Technology and Innovation (Programme RUMOS, PhD grant—Project 22/1080/1974). VS was supported by a grant from the 'Fundação para a Ciência e a Tecnologia' (FCT) (SFRH/BPD/108917/2015). This study had also the support of FCT, through the strategic project UID/MAR/04292/2013 granted to MARE and the Oceanic Observatory of Madeira project (M1420-01-0145-FEDER-000001—'Observatório Oceânico da Madeira'—OOM).

Literature cited

Barria, A. M., M. A. Lardies, A. P. Beckerman, and L. D. Bacigalupe.
2014. Latitude or biogeographic breaks? Determinants of phenotypic (co)variation in fitness-related traits in *Betaeus truncatus* along the Chilean coast. Mar. Biol. 161:111–118.

Bécognée, P., M. Moyano, C. Almeida, J. M. Rodríguez, E. Fraile-Nuez, A. Hernández-Guerra, and S. Hernández-León.
2009. Mesoscale distribution of clupeoid larvae in an upwelling filament trapped by a quasi-permanent cyclonic eddy off Northwest Africa. Deep-Sea Res., I 56:330–343.

Begg, G. A., and J. R. Waldman.
1999. An holistic approach to fish stock identification. Fish. Res. 43:35–44.

Begg, G. A., and R. W. Brown.
2000. Stock identification of haddock *Melanogrammus aeglefinus* on Georges Bank based on otolith shape analysis. Trans. Am. Fish. Soc. 129:935–945.

Begg, G. A., W. J. Overholtz, and N. J. Munroe.
2001. The use of internal otolith morphometrics for identification of haddock (*Melanogrammus aeglefinus*) stocks on Georges Bank. Fish. Bull. 99:1–14.

Bird, J. L., D. T. Eppler, and D. M. Checkley Jr.
1986. Comparisons of herring otoliths using Fourier series shape analysis. Can. J. Fish. Aquat. Sci. 43:1228–1234.

Bookstein, F. L., B. Chernoff, R. L. Elder, J. M. Humphries Jr., G. R. Smith, and R. E. Strauss.
1985. Morphometrics in evolutionary biology: the geometry of size and shape change, with examples from fishes. Acad. Nat. Sci. Phila. Spec. Publ. 15, 277 p.

Cadrin, S. X.
2000. Advances in morphometric identification of fishery stocks. Rev. Fish Biol. Fish. 10:91–112.

Cadrin, S. X., and K. D. Friedland.
1999. The utility of image processing techniques for morphometric analysis and stock identification. Fish. Res. 43:129–139.
2005. Morphometric outlines. *In* Stock identification methods: applications in fishery science (S. X. Cadrin, K. D. Friedland, and J. R Waldman, eds.), p. 173–183. Elsevier, Inc., Amsterdam, Netherlands.

Cadrin, S. X., K. D. Friedland, and J. R. Waldman (eds.).
2005. Stock identification methods: applications in fishery science, 719 p. Elsevier, Inc., Amsterdam, Netherlands.

Cadrin, S. X., L. A. Kerr, and S. Mariani (eds.).
2014. Stock identification methods: applications in fishery science, 566 p. Elsevier, Inc., Amsterdam, Netherlands.

Campana, S. E., and J. D. Neilson.
1985. Microstructure of fish otoliths. Can. J. Fish. Aquat. Sci. 42:1014–1032.

Campana, S. E., and J. M. Casselman.
1993. Stock discrimination using otolith shape analysis. Can. J. Fish. Aquat. Sci. 50:1062–1083.

Cardinale, M., P. Doering-Arjes, M. Kastowsky, and H. Mosegaard.
2004. Effects of sex, stock, and environment on the shape of known-age Atlantic cod (*Gadus morhua*) otoliths. Can. J. Fish. Aquat. Sci. 61:158–167.

Casselman, J. M.
1987. Determination of age and growth. *In* The biology of fish growth (A. H. Weatherley and H. S. Gill, eds.), p. 209–242. Academic Press, New York.

Chipps, S. R., J. A. Dunbar, and D. H Wahl.
2004. Phenotypic variation and vulnerability to predation in juvenile bluegill sunfish (*Lepomis macrochirus*). Oecologia 138:32–38.

Conover, D. O., and T. M. C. Present.
1990. Countergradient variation in growth rate: compensation for length of the growing season among Atlantic silversides from different latitudes. Oecologia 83:316–324.

Costa, G., M. T. Garcia Santamaria, J. Vasconcelos, C. Perera, and E. Melo-Moreira.
2013. Endoparasites of *Trachurus picturatus* (Pisces: Carangidae) from the Madeira and Canary Islands: selecting parasites for use as tags. Sci. Mar. 77:61–68

Dias, E. C.
2015. A circulação oceânica costeira de Portugal. M.S. diss., 49 p. Escola Naval, Alfeite, Portugal.

Elliott, N. G., K. Haskard, and J. A. Koslow.
1995. Morphometric analysis of orange roughy (*Hoplostethus atlanticus*) off the continental slope of southern Australia. J. Fish. Biol. 46:202–220.

Gaevskaya, A. V., and A. A. Kovaleva.
1985. The Parasite fauna of the oceanic horse-mackerel *Trachurus picturatus picturatus* and eco-geographical characteristics of its formation. Ehkol. Morya 20:80–84.

Garcia, A., J. G. Pereira, Â. Canha, D. Reis, and H. Diogo.
2015. Life history parameters of blue jack mackerel *Trachurus picturatus* (Teleostei: Carangidae) from northeast Atlantic. J. Mar. Biol. Assoc. U.K. 95:401–410.

Good, P.
1994. Permutation tests: a practical guide to resampling methods for testing hypotheses, 228 p. Springer-Verlag, New York.

Isidro, H. A.
1990. Age and growth of *Trachurus picturatus* (Bowdich, 1825) (Teleostei: Carangidae) from the Azores. Arquipélago Life Earth Sci. 8:45–54.
Iwata, H., and Y. Ukai.
2002. SHAPE: a computer program package for quantitative evaluation of biological shapes based on elliptic Fourier descriptors. J. Hered. 93:384–385.
Jurado-Ruzafa, A., and M. T. G. Santamaría.
2013. Reproductive biology of the blue jack mackerel, *Trachurus picturatus* (Bowdich, 1825), off the Canary Islands. J. Appl. Ichthyol. 29:526–531.
Klingenberg, C. P.
2011. MorphoJ: an integrated software package for geometric morphometrics. Mol. Ecol. Resour. 11:353–357.
Kuhl, F. P., and C. R. Giardina.
1982. Elliptic Fourier features of closed contour. Comput. Graph. 18:236–258.
Lestrel, P. E.
1989. Method for analysing complex two-dimensional forms: elliptical Fourier functions. Am. J. Hum. Biol. 1:149–164.
Lestrel, P. E. (ed.).
1997. Fourier descriptors and their applications in biology, 466 p. Cambridge Univ. Press, Cambridge, U.K.
Marcus, L. F., M. Corti, A. Loy, G. J. P. Naylor, and D. E. Slice (eds.).
1996. Advances in morphometrics, 588 p. Plenum Press, New York.
Menezes, G. M., M. F. Sigler, H. M. Silva, and M. R. Pinho.
2006. Structure and zonation of demersal fish assemblages off the Azores Archipelago (mid-Atlantic). Mar. Ecol. Prog. Ser. 324:241–260.
Murta, A. G., A. L. Pinto, and P. Abaunza.
2008a. Stock identification of horse mackerel (*Trachurus trachurus*) through the analysis of body shape. Fish. Res. 89:152–158.
Murta, A. G., P. Abaunza, F. Cardador, and F. Sánchez.
2008b. Ontogenic migrations of horse mackerel along the Iberian coast. Fish. Res. 89:186–195.
Neves, A., V. Sequeira, I. Farias, A. Vieira, R. Paiva, and L. S. Gordo.
2011. Discriminating bluemouth, *Helicolenus dactylopterus* (Pisces: Sebastidae), stocks in Portuguese waters by means of otolith shape analysis. J. Mar. Biol. Assoc. U.K. 91:1237–1242.
Porrini, L. P., P. J. Fernández Iriarte, C. M. Iudica, and E. Aristizabal Abud.
2015. Population genetic structure and body shape assessment of *Pagrus pagrus* (Linnaeus, 1758) (Perciformes: Sparidae) from the Buenos Aires coast of the Argentine Sea. Neotropical Ichthyol. 13:431–438.
Robinson, B. W., D. S. Wilson, A. S. Margosian, and P. T. Lotito.
1993. Ecological and morphological differentiation of pumpkinseed sunfish in lakes without bluegill sunfish. Evol. Ecol. 7:451–464.
Rodríguez, J. M., E. D. Barton, S. Hernández-León, and J. Arístegui.
2004. The influence of mesoscale physical processes on the larval fish community in the Canaries CTZ, in summer. Prog. Oceanogr. 62:171–188.
Rohlf, F. J.
1990. Rotational fit (Procrustes) methods. *In* Proceedings of the Michigan morphometrics workshop; Ann Arbor, MI, 16–28 May 1988 (F. J. Rohlf and F. L. Bookstein, eds.), p. 227–236. Univ. Michigan Mus. Zool., Ann Arbor, MI.
2006. tpsDig. [vers. 2.10.] Dep. Ecol. Evol., State Univ. New York Stony Brook, Stony Brook, New York [Available from website].
Rohlf, F. J., and F. L. Bookstein (eds.).
1990. Proceedings of the Michigan morphometrics workshop held at the University of Michigan, Ann Arbor, Michigan from May 16 through May 28, 1988, 380 p. Univ. Michigan Mus. Zool., Ann Arbor, MI.
Secor, D. H.
2014. The unit stock concept: bounded fish and fisheries. *In* Stock identification methods: applications in fishery science (S. X. Cadrin, L. A. Kerr, and S. Mariani, eds.), p. 7–28. Elsevier, Inc., Amsterdam, Netherlands.
Sequeira, V., R. Rodríguez-Mendoza, A. Neves, R. Paiva, F. Saborido-Rey, and L. Serrano Gordo.
2011. Using body geometric morphometrics to identify bluemouth, *Helicolenus dactylopterus* (Delaroche, 1809), populations in the Northeastern Atlantic. Hydrobiologia 669:133–141.
Shaboneyev, I. Y., and Y. I. Ryazantseva.
1977. Population structure of the oceanic horse mackerel (*Trachurus picturatus picturatus*). J. Ichthyol. 17:954 958.
Smith, P. J. , S. G. Robertson, P. L. Horn, B. Bull, O. F. Anderson, B. R. Stanton, and C. S. Oke.
2002. Multiple techniques for determining stock relationships between orange roughy, *Hoplostethus atlanticus*, fisheries in the eastern Tasman Sea. Fish. Res. 58:119–140.
Smith-Vaniz, W. F.
1986. Carangidae. *In* Fishes of the north-eastern Atlantic and the Mediterranean, vol. 2 (P. J. P Whitehead, M.-L. Bauchot, J.-C. Hureau, J. Nielsen, and E. Tortonese, eds.), p. 815–844. UNESCO, Paris.
Stransky, C.
2014. Morphometric outlines. *In* Stock identification methods: applications in fishery science (S. X. Cadrin, L. A. Kerr, and S. Mariano, eds.), p. 129–140. Elsevier, Inc., Amsterdam, Netherlands.
Stransky, C., A. G. Murta, J. Schlickeisen, and C. Zimmermann.
2008. Otolith shape analysis as a tool for stock separation of horse mackerel (*Trachurus trachurus*) in the Northeast Atlantic and Mediterranean. Fish. Res. 89:159–166.
Tracey, S. R., J. M. Lyle, and G. Duhamel.
2006. Application of elliptical Fourier analysis of otolith form as a tool for stock identification. Fish. Res. 77:138–147.
Turan, C.
2004. Stock identification of Mediterranean horse mackerel (*Trachurus mediterraneus*) using morphometric and meristic characters. ICES J. Mar. Sci. 61:774–781.
Tuset, V. M., A. Lombarte, and C. A. Assis.
2008. Otolith atlas for the western Mediterranean, north and central eastern Atlantic. Sci. Mar. 72(S1):7–198.
Vasconcelos, J., A. Alves, E. Gouveia, and G. Faria.
2006. Age and growth of the blue jack mackerel, *Trachurus picturatus* Bowdich, 1825 (Pisces: Teleostei) off Madeiran archipelago. Arquipélago Life Earth Sci. 23A:47–57.
Vasconcelos, J., M. Hermida, A. Saraiva, J. A. González, and L. Serrano Gordo.
2017a. The use of parasites as biological tags for stock

identification of blue jack mackerel, *Trachurus picturatus*, in the North-eastern Atlantic. Fish. Res. 193:1–6.

Vasconcelos, J., G. Faria, R. Freitas, and L. Serrano Gordo.
2017b. Fecundity regulation strategy of the blue jack mackerel, *Trachurus picturatus* (Bowdich, 1825), off Madeira Island (NE Atlantic). Fish. Res. 190:150–156.

Vieira, A. R., A. Neves, V. Sequeira, R. Paiva, and L. Serrano Gordo.
2014. Otolith shape analysis as a tool for stock discrimination of forkbeard (*Phycis phycis*) in the Northeast Atlantic. Hydrobiologia 728:103–110.

Vila-Gispert, A., M. G. Fox, L. Zamora, and R. Moreno-Amich.
2007. Morphological variation in pumpkinseed *Lepomis gibbosus* introduced into Iberian lakes and reservoirs; adaptations to habitat type and diet? J. Fish Biol. 71:163–181.

Waldman, J. R.
2005. Defining of stocks: an evolving concept. *In* Stock identification methods: applications in fishery science (S. X. Cadrin, K. D. Friedland, and J. R. Waldman, eds.), p.7–16. Elsevier, Inc., Amsterdam, Netherlands.

Waples, R. S., A. E. Punt, and J. M. Cope.
2008. Integrating genetic data into management of marine resources: how can we do it better? Fish Fish. 9:423–449.

Yamahira, K., and D. O. Conover.
2002. Intra- vs. interspecific latitudinal variation in growth: adaptation to temperature or seasonality? Ecology 83:1252–1262.

Yamahira, K., and K. Takeshi.
2008. Variation in juvenile growth rates among and within latitudinal populations of the medaka. Popul. Ecol. 50:3–8.

Yamahira, K., M. Kawajiri, K. Takeshi, and T. Irie.
2007. Inter- and intrapopulation variation in thermal reaction norms for growth rate: evolution of latitudinal compensation in ectotherms with a genetic constraint. Evolution 61:1577–1589.

Yampolsky, L. Y., T. M. M. Schaer, and D. Ebert.
2014. Adaptive phenotypic plasticity and local adaptation for temperature tolerance in freshwater zooplankton. Proc. R. Soc., B 281:20132744.

National Marine Fisheries Service
NOAA

Fishery Bulletin
established in 1881

Spencer F. Baird
First U.S. Commissioner of Fisheries and founder of *Fishery Bulletin*

Occurrence of pelagic *Sargassum* in waters of the U.S. Gulf of Mexico in response to weather-related hydrographic regimes associated with decadal and interannual variability in global climate

Guillermo Sanchez-Rubio (contact author)
Harriet Perry
James S. Franks
Donald R. Johnson

Email address for contact author: guillermo.sanchez@usm.edu

Center for Fisheries Research and Development
Gulf Coast Research Laboratory
School of Ocean Science and Technology
The University of Southern Mississippi
703 East Beach Drive
Ocean Springs, MS 39564

Abstract—Pelagic species of *Sargassum*, surface drifting macroalgae, occur in continental shelf and deep basin waters across the Gulf of Mexico (GOM). They often accumulate in mats and "windrows" to form a structured habitat that serves as a source of food and refuge for a diverse assemblage of fish and invertebrates. Long-term temporal data on the distribution and abundance of *Sargassum* species in the GOM are lacking, but there is a time series of occurrence of those species across the U.S. GOM (USGOM) associated with ichthyoplankton surveys conducted by the Southeast Area Monitoring and Assessment Program. The seasonal presence of *Sargassum* species in regions of the USGOM was compared under contrasting weather-related hydrographic regimes using nonparametric tests (Kruskal–Wallis H test, Mann–Whitney U test, Wilcoxon signed rank test). Phases of the Atlantic Multidecadal Oscillation (AMO) and North Atlantic Oscillation (NAO) along with El Niño–Southern Oscillation (ENSO) events influenced seasonal presence of *Sargassum* species across the area of study. Occurrence of *Sargassum* species was highest under the coupled warm AMO and neutral NAO phases and cold ENSO events and was associated with physical and biological processes that transported the macroalgae to the USGOM and maintained them over time.

Manuscript submitted 6 June 2017.
Manuscript accepted 1 December 2017.
Fish. Bull. 116:93–106 (2018).
Online publication date: 2 January (2018).
doi: 10.7755/FB.116.1.10

The views and opinions expressed or implied in this article are those of the author (or authors) and do not necessarily reflect the position of the National Marine Fisheries Service, NOAA.

Two holopelagic species of *Sargassum*, floating macroalgae (Phaeophyceae), co-occur in continental shelf and deep basin waters across the Gulf of Mexico (GOM): *Sargassum natans* and *S. fluitans*. These 2 species of macroalgae drift in surface waters (Deacon, 1942; Stoner, 1983) through the western Caribbean region into the GOM and exit through the Florida Straits and up the eastern seaboard of the United States in the Gulf Stream, and out into the Atlantic Ocean to the Sargasso Sea (Calder, 1995). The abundance and distribution of the 2 pelagic species of *Sargassum* in the Atlantic Ocean are highly variable over space and time (Gower and King, 2011; Gower et al., 2013). Two historical quantitative studies of the abundance of pelagic *Sargassum* species were conducted in overlapping areas within the Sargasso Sea, the first between 1933 and 1935 (Parr, 1939) and the second between 1977 and 1981 (Stoner, 1983). No differences in overall abundance of these pelagic *Sargassum* species were found with these studies. In a more recent study, Hufford et al. (2014) examined temporal and spatial variability of pelagic *Sargassum* community change over a 40-year period and noted that the distribution, abundance, or circulation patterns (or a combination of these variables) of pelagic *Sargassum* species in the Atlantic Ocean during 2010 and 2011 were highly anomalous compared with the 2003–2010 period. In the spring and summer of 2011, Franks et al. (2011) and Johnson et al. (2013) reported that unprecedented amounts of pelagic *Sargassum* washed ashore along the Caribbean Islands, and satellite observations pointed to waters north of the mouth of the Amazon River as a source region for the event (Gower et al., 2013). Johnson et al. (2013) examined data from satellite- tracked current drifters during 2010 and 2011 but were unable to connect the event to the central North Atlantic Ocean. These authors used an archived numerical circulation model (Hybrid Coordinate Ocean Model) to backtrack pelagic *Sargassum* macroalgae to the North Equatorial Recirculation Region (NERR). They sug-

gested that pelagic *Sargassum* macroalgae bloomed in the NERR, where they may have recirculated over an extended period of time, before being picked up by the North Brazil Current and transported to the eastern Caribbean region. In waters with elevated nutrients (Lapointe et al., 2014), high salinities, high light intensities (low cloud cover), and sea-surface temperatures (SSTs) between 18°C and 30°C (Hanisak and Samuel, 1987), pelagic species of *Sargassum* are capable of rapid growth (Lapointe, 1986; Hanisak and Samuel, 1987).

Climate plays a major role in setting the physical hydrographic processes (Karnauskas et al., 2015) that act to transport, aggregate, or scatter pelagic *Sargassum* species, and it affects algal productivity through its influence on the position of the Intertropical Convergence Zone (ITCZ) (Franks et al., 2011; Schneider et al., 2014; Franks et al., 2016). Climate in the Northern Hemisphere is influenced by oceanic and atmospheric modes of variability from the Atlantic Ocean (Mehta et al., 2000; Sutton and Hodson, 2005) and Pacific Ocean (Wang and Fu, 2000). The Atlantic Multidecadal Oscillation (AMO) represents below (cold AMO [AMOc]) and above (warm AMO [AMOw]) normal SST across the North Atlantic Ocean from 0°N to 70°N latitude (Enfield et al., 2001) and has a characteristic periodicity of around 65–80 years (Kerr, 2000; Gray et al., 2004). The North Atlantic Oscillation (NAO) is associated with an oscillation in the sea-level air-pressure gradient between Iceland and the Azores (Hurrell and Van Loon, 1997). The NAO displays negative (NAOn) and positive (NAOp) phases and responds to the effects of different physical processes on seasonal to multidecadal time scales (Hurrell et al., 2003). The El Niño–Southern Oscillation (ENSO) is the quasiperiodic (2–7 years) warming or cooling of the eastern equatorial Pacific Ocean (Walker, 1924; Bjerknes, 1969; Lighthill, 1969; Godfrey, 1975; McCreary, 1976) with the shift of southeast trade winds over the central and western Pacific Ocean (Krueger and Winston, 1975; Wyrtki, 1975; McPhaden, 1999). The warm phase of the ENSO (ENSOw) is referred to as El Niño and the cool phase (ENSOc) is referred to as La Niña. The phase between ENSOc and ENSOw is referred to as neutral (ENSOn). The ENSO phases are identified by the SST anomaly from the Niño 3.4 region (5°S–5°N and 120°W–170°W) in the equatorial Pacific Ocean.

Phases of the NAO (Seager et al., 2000) and ENSO (Giannini et al., 2001) contribute to the annual variability of SST and winds in the tropical Atlantic Ocean that is measured with an index called the Atlantic Meridional Mode (AMM). These weather-related hydrographic characteristics in the tropical Atlantic Ocean affect the position and strength of the thermal equator and hence the position and strength of the ITCZ with its heated, rising air. The ITCZ is an area where the northeast and southeast trade wind systems meet creating a rain band in the tropical North Atlantic Ocean (Vimont and Kossin, 2007). The position of the ITCZ directly affects hydrographic characteristics in neritic waters of West Africa, northeast Brazil, and Central America and has been associated with variability in rainfall over West Africa (Lamb, 1978; Janicot et al., 1998; Sultan and Janicot, 2000), northeast Brazil (Hastenrath and Heller, 1977; Uvo et al., 1998; Robertson et al., 2004), and Central America (Giannini et al., 2000; Taylor et al., 2002). The ITCZ is important because it affects the cross-equatorial transport of heat and salinity by upper-level ocean currents (Berger and Wefer, 1996; Maslin et al., 1997; Vink et al., 2002) and the strength of the Loop Current (LC), a northward flowing current that enters the Gulf of Mexico (GOM) from the Caribbean Sea (Nürnberg et al., 2008). The LC connects the Yucatan Channel and Straits of Florida (Hurlburt and Thompson, 1980; Oey et al., 2005) and there is a significant link between the intrusion of the LC into the GOM and the estimated transport of the Florida Current (Lin et al., 2010) at low frequencies (time scales longer than 120 days; Lin et al., 2010). The northward intrusion of the LC can extend as far as the Mississippi River Delta and the Florida continental shelf (Huh et al., 1981; Wiseman and Dinnel, 1988). This intrusion deflects Mississippi River discharge westward with hydrographic conditions in surface waters of the northeastern GOM approaching those of the Caribbean Sea (high salinity and SST) (Nürnberg et al., 2008).

Phases of the AMO and NAO affect moist-air–related wind patterns in the GOM. In the summer, under the AMOc phase, the Bermuda High is strengthened and its associated easterly and southeasterly low-level jets can extend well over the warm waters of the Caribbean region. These jets, transport moist air westward along the GOM (Wang et al., 2006; Hu and Feng, 2007). During the NAOp phases, low geopotential heights and high SST levels are set along the GOM, bringing southerly winds in winter over south Florida, and in spring over south Florida and the Florida panhandle (Hurrell and Deser, 2009).

Pelagic species of *Sargassum* often accumulate in mats and windrows (lines of floating *Sargassum* caused by wind, tide or currents) to form a structured habitat and a source of food and refuge for a rich and diverse assemblage of fish and invertebrates (Dooley, 1972; Bortone et al., 1977; Butler et al., 1983; Coston-Clements et al., 1991; Comyns et al., 2002; Wells and Rooker, 2004; Hoffmayer et al., 2005). Habitat of *Sargassum* species was declared essential fish habitat in the U.S. South Atlantic region in 2002 (SAFMC, 2002), and management measures were implemented by the National Marine Fisheries Service (NMFS) in 2003. Seasonal and yearly differences in the abundance and distribution of pelagic *Sargassum* could contribute to the variation observed in recruitment of marine fishes and other marine organisms (Butler et al., 1983). In spite of the importance of *Sargassum* as habitat, few studies have examined the effect of climate regimes on the occurrence of species of pelagic *Sargassum* over decadal and interannual time scales.

The Southeast Area Monitoring and Assessment Program (SEAMAP) is a federal and state cooperative

effort to collect, manage, and disseminate fishery-independent data and information in the southeastern United States. The SEAMAP ichthyoplankton database (Hanisko[1]) contains data on observed occurrence of pelagic *Sargassum* species in samples from surveys conducted across the USGOM. Data used for our study were prior to and lead up to the 2011 bloom in the tropical North Atlantic Ocean and are intended to provide linkage to define the relationship between yearly and seasonal *Sargassum* occurrence in the USGOM and weather-related hydrographic regimes imposed by AMO, NAO, and ENSO events. Because the SEAMAP conducts surveys each year, the relationship of recent Caribbean and South American inundation events with *Sargassum* occurrence in the USGOM can be examined in the future. Reference to *Sargassum* occurrence in the following sections is specific to the pelagic species *S. fluitans* and *S. natans*.

Material and methods

Decadal AMO and NAO phases and interannual ENSO events

Characterization of AMO and NAO phases and the individual ENSO events were adopted from Sanchez-Rubio and Perry (2015). Years not included in the latter study (2011–2013) were placed under the coupled AMOw/NAOn (slash denotes coupling of those phases) phase and the 2011 year was identified as ENSOc. The coupling of AMOc and NAOp phases was in place from 1971 through 1994 (first regime, wet); the coupling of AMOw and NAOn phases was in place from 1995 through 2013 (second regime, dry). Although the change from one phase to another is transitional, published studies cite the mid-1990s as the time when the shift occurred (Karnauskas et al., 2015). The years from 1977 to 2010 were identified as ENSOw (1977, 1982, 1986, 1987, 1991–1994, 1997, 2002, 2004, 2006, and 2009), ENSOn (1978–1981, 1985, 1989, 1990, 1995, 1996, 2001, and 2003), and ENSOc (1983, 1984, 1988, 1998-2000, 2005, 2007, 2008, 2010, and 2011) years.

Biological data

Biological data were taken from a series of ichthyoplankton surveys conducted under the state and federal SEAMAP program administered by the NMFS. Data used to determine the occurrence of species of *Sargassum* were, in part, observational and therefore dependent upon the field biologists to record the presence of *Sargassum* species in the sample or sample area. Individuals responsible for field collections were long-term employees of the NMFS thus there was continuity of personnel over the study period (personal observation and NMFS Cruise Reports, Harriet Perry). Although *Sargassum* species were not the primary focus of the surveys, their presence was recorded because they form important nursery habitat for commercially and recreationally sought fishes. Knowledge of the presence of *Sargassum* macroalgae aids in taxonomic resolution of species and provides information on the distribution of the *Sargassum* habitat. Acknowledging problems associated with the use of observational data, the surveys still offer a unique opportunity to examine the relationship between climate variables and algal presence because this data set provides the only long-term, systematic information on the occurrence of these *Sargassum* species in the GOM.

The SEAMAP ichthyoplankton database was obtained from Hanisko.[1] Data from samples in this survey program were available from 1982 to 2012. The SEAMAP sampling area encompasses the USGOM from the 10-m isobath to the U.S. Exclusive Economic Zone. The sampling gear and methods used during SEAMAP surveys have been described by Kramer et al. (1972), Smith and Richardson (1977), and Posgay and Marak (1980). Most SEAMAP survey stations were occupied at approximately 56 km (or 0.5°) intervals in a fixed, systematic grid of transects across the USGOM. Samples were taken upon arrival at each station regardless of time of day or night. Plankton surveys have been consistently conducted over 2 survey time frames (spring–early summer and late summer–early fall) since 1982 (Lyczkowski-Shultz and Hanisko, 2007) and approximately 200 stations have been targeted for sampling. In addition, numerous surveys have been periodically conducted over shorter time frames and with specific targeted species groups. For this study, the complete SEAMAP ichthyoplankton database (Hanisko[1]) was used to increase temporal and spatial resolution of the data. Data on the occurrence of *Sargassum* species were obtained from direct observations recorded in ichthyoplankton data logs during SEAMAP cruises. In addition, the occurrence of species of *Sargassum* was indirectly inferred from the presence of the Sargassumfish (*Histrio histrio*), a species endemic to *Sargassum* (Coston-Clements et al., 1991).

Ichthyoplankton samples associated with *Sargassum* macroalgae were extracted from the main SEAMAP database to form a more manageable data set. The extracted data set contained 1077 samples of which 1051 were collected in neuston net tows and 26 in bongo net tows. All months of the year and most of the years, with the exception of 1982, 1987, and 1988, were represented in the data set of ichthyoplankton samples associated with species of *Sargassum*. Of the 1077 samples associated with *Sargassum* macroalgae, 284 were collected under the coupling of AMOc and NAOp phases and 793 were collected during the coupling of AMOw and NAOn phases. *Sargassum* species occurred in samples from January to November during the coupling of AMOc and NAOp phases and from February to December during the coupling of AMOw and NAOn

[1] Hanisko, D. S. 2015. Unpubl. data. [Historical data set of ichthyoplankton collected in 1982–2012 during Southeast Area Monitoring and Assessment Program surveys.] Miss. Lab., Southeast Fish. Sci. Cent., Natl. Mar. Fish. Serv., NOAA, 3209 Frederic St., Pascagoula, MS 39568-1207.

phases. The 1077 samples were further characterized as collected after ENSOc (n=394), ENSOn (n=302), and ENSOw (n=381) events. *Sargassum* species occurred in samples from February to November after ENSOc years, from April to December after ENSOn years, and from January to November after ENSOw years.

Samples associated with species of *Sargassum* were subdivided temporally by month of collection and spatially within square degree areas of 1 degree latitude and 1 degree longitude across the USGOM. Monthly samples associated with *Sargassum* species within each square degree area were further subdivided by the weather-related hydrographic regime in place when samples were collected. Monthly samples collected during1982–1994 and 1995–2012 were classified under the influence of the couplings of AMOc and NAOp and AMOw and NAOn phases, respectively. The same monthly samples were also classified by the ENSO event (warm, neutral, or cold) that was present from May of the previous year to February of the year in which samples were collected. The final data set represented the monthly ichthyoplankton samples associated with species of *Sargassum* within square degree areas (1 degree of latitude by 1 degree of longitude) across the USGOM under the influence of the coupling of AMO and NAO phases and ENSO events.

Samples from May to July and from September to November associated with the *Sargassum* species within each square degree area and weather-related hydrographic regime were added to obtain the total number of samples associated with the *Sargassum* species within each square degree area, weather-related hydrographic regime, and summer and fall seasons. Samples associated with species of *Sargassum* within each square degree area, weather-related hydrographic regime, and season were added, multiplied by 100, and then divided by the total number of SEAMAP ichthyoplankton samples collected within each square degree area, weather-related hydrographic regime, and season. If the number of samples collected was fewer than 8 per square degree area, the percentage of seasonal samples associated with *Sargassum* species was not calculated. The calculated values represented the percentage of seasonal SEAMAP samples associated with species of *Sargassum* within each square degree area across the USGOM, weather-related hydrographic regime, and season. Percentages were used because differences in sampling effort (total number of samples and sampling years) existed among hydrographic regimes. The number of samples collected was 7768 (summer) and 5939 (fall) during the coupling of AMOc/NAOp phases, 7910 (summer) and 9196 (fall) samples during the coupling of AMOw/NAOn phases, 6532 (summer) and 5820 (fall) samples after ENSOw events, 4389 (summer) and 4396 (fall) samples after ENSOn events, and 4757 (summer) and 4919 (fall) samples after ENSOc events. The number of samples collected under the AMO and NAO phases and after ENSO events were 15,678 (summer) and 15,135 (fall). After spatially comparing the seasonal occurrences of pelagic species of *Sargassum*, analysis was restricted to data calculated from more than 9 square degree areas per regime. Because the ichthyoplankton surveys did not specifically target areas with *Sargassum* macroalgae, the percentage of samples associated with species of *Sargassum* was considered a measure of occurrence across the USGOM.

Data analysis was limited spatially to survey areas between 81°W to 97°W and 24°N to 29°N and an area that extended from 86°W to 88°W and 30°N. The 90th parallel west divided the general area into western and eastern regions. The study area was also divided into deep basin and continental shelf waters. The deep basin was limited spatially to survey areas between 85°W to 95°W and 24°N to 26°N and an area that extended from 86°W to 88°W and 27°N. To statistically compare the seasonal occurrence of *Sargassum* species within square degree areas in USGOM regions between 2 or more contrasting weather-related hydrographic regimes, 3 nonparametric tests were performed by using SPSS Statistics[2] software, vers. 20.0 (IBM Corp., Armonk, NY). Using the Kruskal–Wallis H test, we compared seasonal occurrences of pelagic species of *Sargassum* in USGOM regions among 3 contrasting weather-related hydrographic regimes associated with ENSO events. With the Mann–Whitney U test, we compared seasonal occurrences of pelagic species of *Sargassum* in USGOM regions between 2 contrasting weather-related hydrographic regimes associated with the coupling of AMO and NAO phases and ENSO events. With the Wilcoxon signed rank test, we compared seasonal occurrences of *Sargassum* species from identical square degree areas in USGOM regions between 2 contrasting weather-related hydrographic regimes associated with the couplings of AMO and NAO phases and ENSO events.

Environmental data

The AMM index was downloaded as monthly values from 1981 through 2009 from the NOAA Earth System Research Laboratory (data available from website, accessed October 2015). This index represents the variations in SST and sea level pressure between the tropical Atlantic Ocean north and south of the ITCZ. The ITCZ is an area where the northeast and southeast trade wind systems meet, creating a rain band in the tropical North Atlantic Ocean (Vimont and Kossin, 2007). Monthly data for Amazon River discharge were downloaded from SO HYBAM (streamflow data available from website, accessed December 2015). The data from 1982 through 2013 were limited to the months (from April to August) of highest river discharge. Wind speed and direction data were downloaded from the NOAA National Data Buoy Center (data available from website, accessed October 2015). These data were recorded hourly at the western (buoy 42002: 1978–2011), central (buoy 42001:1979–2011), and eastern (buoy

[2] Mention of trade names or commercial companies is for identification purposes only and does not imply endorsement by the National Marine Fisheries Service, NOAA.

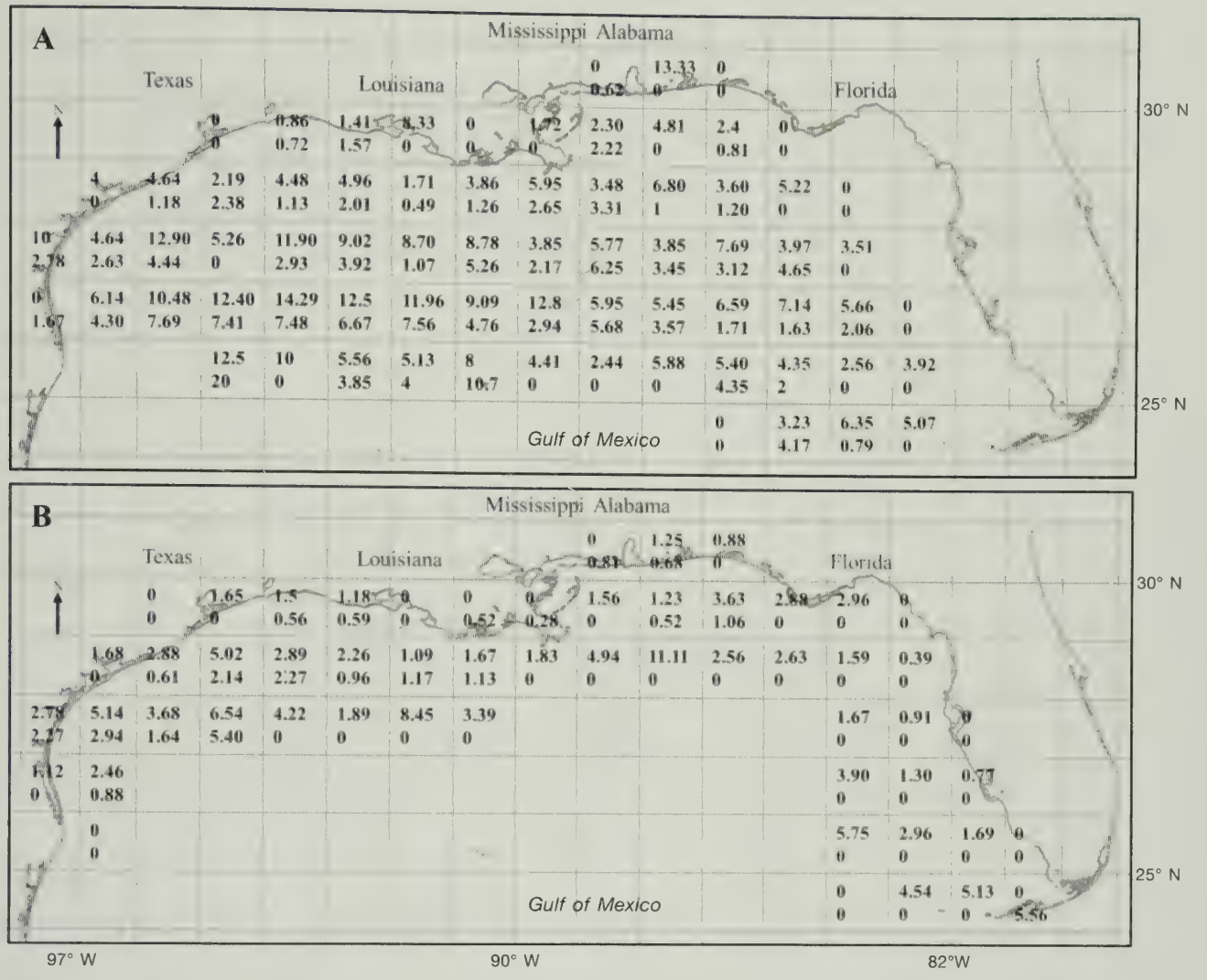

Figure 1

Occurrence of pelagic *Sargassum* macroalgae in (**A**) summer (May–July) and (**B**) fall (September–November) across the U.S. Gulf of Mexico during the coupling of phases of the Atlantic Multidecadal Oscillation (AMO) and North Atlantic Oscillation (NAO) from 1982 through 2012. Values within each square degree area (1 degree of latitude by 1 degree of longitude) represent the percentages of samples associated with species of *Sargassum* during the coupling of AMO warm and NAO negative phases (top values) and AMO cold and NAO positive phases (bottom values).

42003: 1979–2011) GOM regions. The wind data were limited to those months in which more than 400 hours were recorded. The hourly data for each of the buoys were grouped according to the direction of the wind (northern wind: 337.6–22.5°, northeastern wind: 22.6–67.5°, eastern wind: 67.6–112.5°, southeastern wind: 112.6–157.5°, southern wind: 157.6–202.5°, southwestern wind: 202.6–247.5°, western wind: 247.6–292.5°, and northwestern wind: 292.6–337.5°). These data were then divided by season (fall: September–November, winter: December–February, spring: March–May, and summer: June–August). The seasonal average wind speed (meters per second) was calculated for each direction of the wind for each buoy. Using these data, we calculated seasonal wind stress (T) in newtons per square meter:

$$T = \rho \times CD \times U_{10}^2, \quad (1)$$

where ρ = the density of air at 1.225 kg/m^3;
U_{10}, = wind speed in meters per second at 10 m above the water surface; and
CD = the drag coefficient (Hellerman, 1965).

Smith (1980) proposed a formula to calculate CD:

$$1000\ CD = 0.44 + (0.063 \times U_{10}). \quad (2)$$

Seasonal data of wind stress were then transformed to wind momentum (newton-second [Ns] per square meter) by multiplying the wind stress by the average number of seconds per hour that the wind blows for each of the directions. The index of wind momentum represents the direction and flux of water driven by the seasonal winds in the 3 GOM regions. Monthly

Table 1

Mean seasonal occurrence, with 95% confidence intervals, of pelagic species of *Sargassum* across the U.S. Gulf of Mexico and by western and eastern regions during the coupling of phases of the Atlantic Multidecadal Oscillation (AMO) and North Atlantic Oscillation (NAO) from 1982 through 2012. Occurrence represents the percentage of ichthyoplankton samples associated with pelagic *Sargassum*. *n*= the total number of square degree areas (1 degree latitude by 1 degree longitude) that were compared. Numbers in parentheses are the number of square degree areas (1 degree latitude, 1 degree longitude) with higher percentages of *Sargassum* species occurrence during the coupling of AMO and NAO phases. NS=nonsignificant.

Season	U.S. Gulf of Mexico	*n*	Cold AMO, positive NAO phases	Warm AMO, negative NAO phases	
Summer (May–Jul)	Whole	71	2.54 ±0.75% (9)	5.51 ±0.90% (55)	P_1= 0
	Western	33	3.63 ±1.39% (5)	6.84 ±1.46% (26)	P_1<0.0001
	Eastern	38	1.59 ±0.58% (4)	4.35 ±0.96% (29)	P_1=0
Fall (Sep–Nov)	Whole	55	0.58 ±0.31% (5)	0.96 ±0.52% (2)	P_1=0
	Western	24	0.96 ±0.52% (2)	2.56 ±0.85% (19)	P_1<0.0001
	Eastern	31	0.29 ±0.36% (3)	2.20 ±0.83% (24)	P_1<0.0001
Summer (May-Jul)	Western	33	3.63 ±1.39%	6.84 ±1.46%	
	Eastern	38	1.59 ±0.58%	4.35 ±0.96%	
			P_2=0.0060	P_2=0.0075	
Fall (Sep-Nov)	Western	24	0.96±0.52%	—	
	Eastern	31	0.29±0.36%	—	
			P_2=0.0036	P_2=NS	

P_1-values given by the Wilcoxon signed rank test for the analysis between AMO and NAO phases.
P_2-values given by the Mann–Whitney U test for the analysis within AMO and NAO phases.

hurricane tracks during the Atlantic Ocean hurricane season (June to November) for each of the 2 AMO-NAO phases were downloaded as maps from 1980 through 2009 (NOAA National Ocean Service, data available from website, accessed October 2015). A hurricane is a tropical cyclone with maximum sustained (1-min) 10-m winds of 33 m/s (65 kt) or greater. The number of hurricanes that occurred from June to November in the NERR and GOM were enumerated for the periods 1980–1994 (AMOc and NAOp phases) and 1995–2009 (AMOw and NAOn phases). Hurricanes were included only when sustained wind speed during at least part of their track in the NERR and GOM was classified as a hurricane. A historical list of monthly shedding of LC's spin-off eddies was obtained from Vukovich (2012). The spin-off eddies were enumerated for the periods 1979–1994 (AMOc and NAOp phases) and 1995–2010 (AMOw and NAOn phases).

To statistically compare monthly and seasonal values of the AMM and wind momentum among weather-related hydrographic regimes imposed by the coupling of AMO and NAO phases and ENSO events, 2 nonparametric rank-sum tests were carried out with SPSS Statistics software. A nonparametric multiple samples test (Kruskal–Wallis H test) was performed to compare the values of the indices among 3 contrasting weather-related hydrographic regimes associated with ENSOw, ENSOn, and ENSOc events. A nonparametric 2-sample test (Mann–Whitney U test) was performed to compare values of the indices between 2 contrasting weather-related hydrographic regimes associated with the couplings of AMOc and NAOp and AMOw and NAOn phases, ENSOw and ENSOn events, ENSOw and ENSOc events, and ENSOn and ENSOc events. To adjust the *P*-values for multiple comparisons, the α level of each individual test was adjusted downward by using the Bonferroni correction method (Bonferroni, 1935). No statistical test was used to compare the number of years with above or below Amazon River discharge in the NERR, the total number of hurricanes in the NERR and GOM, and LC's spin-off eddies in the GOM waters between the coupling of AMO and NAO phases.

Results

Variability of seasonal occurrence of pelagic Sargassum in USGOM regions in response to the coupling of AMO and NAO phases and ENSO events

Occurrence of species of *Sargassum* differed by season, region, water depth, and climate (Tables 1–4). High-

Table 2

Mean summer (May–July) occurrence, with 95% confidence intervals, of pelagic species of *Sargassum* in waters over the continental shelf and deep basin of the U.S. Gulf of Mexico and the western and eastern regions during phases of the coupling of the Atlantic Multidecadal Oscillation (AMO) and North Atlantic Oscillation (NAO) from 1982 through 2012. Occurrence represents the percentage of ichthyoplankton samples associated with pelagic *Sargassum*. *n*=the total number of square degree areas (1 degree latitude by 1 degree longitude) that were compared. Numbers in parentheses represent the number of square degree areas (1 degree latitude, 1 degree longitude) with higher percentages of occurrence of *Sargassum* species during the coupling of AMO and NAO phases.

U.S. Gulf of Mexico	Water depth	*n*	Cold AMO, positive NAO phases	Warm AMO, negative NAO phases	
Whole	Continental shelf	45	1.36 ±0.44% (5)	4.41 ±1.03% (34)	P_1=0
	Deep basin	26	4.58 ±1.64% (4)	7.42 ±1.43% (21)	P_1=0.0005
Western	Continental shelf	22	1.81 ±0.67% (3)	5.17 ±1.62% (17)	P_1=0.0002
	Deep basin	11	7.28 ±2.99% (2)	10.2 ±1.76% (9)	P_1=0.0375
Eastern	Continental shelf	23	0.93 ±0.53% (2)	3.67 ±1.24% (17)	P_1=0.0002
	Deep basin	15	2.59 ±1.04% (2)	5.40 ±1.43% (12)	P_1=0.0021
Whole	Continental shelf	45	1.36 ±0.44%	4.41 ±1.03%	
	Deep basin	26	4.58 ±1.64%	7.42 ±1.43%	
			P_2<0.0001	P_2=0.0005	
Western	Continental shelf	22	1.81 ±0.67%	5.17 ±1.62%	
	Deep basin	11	7.28 ±2.99%	10.2 ±1.76%	
			P_2=0.0002	P_2=0.0006	
Eastern	Continental shelf	23	0.93 ±0.53%	3.67 ±1.24%	
	Deep basin	15	2.59 ±1.04%	5.40 ±1.43%	
			P_2=0.0099	P_2=0.0183	

P_1-values given by the Wilcoxon signed rank test for the analysis between AMO and NAO phases.
P_2-values given by the Mann–Whitney U test for the analysis within AMO and NAO phases.

est percentages of positive samples (*Sargassum* species present) occurred under the coupling of AMOw and NAOn phases regardless of region and season (Fig. 1, Table 1). Regionally, higher percentages of positive samples occurred in the western GOM, regardless of season and climate regime (Table 1). Comparing the presence of *Sargassum* species over the continental shelf and deep basin during the summer, we found that occurrences were higher under the coupling of AMOw and NAOn phases regardless of region and water depth (Table 2). Occurrences were also higher over the deep basin regardless of region and climate phase (Table 2).

Occurrence of species of *Sargassum* by ENSO event, region, continental shelf or deep basin waters during the summer is shown in Table 3. Presence of *Sargassum* species by region and over the deep basin was not significantly different among ENSO events. Presence of *Sargassum* species was higher in the continental shelf after ENSOc than after ENSOn events. Presence of species of *Sargassum* was higher in the western GOM after ENSOc and ENSOw events and in the deep basin regardless of an ENSO event. Occurrence of *Sargassum* species by ENSO events and regions during the fall is shown in Table 4. Higher values for presence of *Sargassum* species were noted in the western GOM regardless of an ENSO event. Highest, intermediate, and lowest values for the presence of *Sargassum* species were observed after ENSOc, ENSOn, and ENSOw years, respectively, regardless of region.

Variability of weather-related hydrographic characteristics in the NERR and GOM in response to the coupling of AMO and NAO phases and ENSO events

Monthly and seasonal weather-related hydrographic characteristics in the NERR and GOM showed mathematically significant differences between the 2 AMO/NAO phases (Table 5). During the coupled AMOw/NAOn phase, higher values were found for the AMM index, the number of hurricanes, and the above average annual discharge of the Amazon River in the NERR and the number of LC spin-off eddies, num-

Table 3

Mean summer (May–July) occurrence, with 95% confidence intervals, of pelagic species of *Sargassum* across the U.S. Gulf of Mexico and in the western and eastern regions, continental shelf, and deep basin after El Niño–Southern Oscillation (ENSO) events from 1982 through 2012. Occurrence represents the percentages of ichthyoplankton samples associated with pelagic *Sargassum* at the time of their collection. Numbers in parentheses represent the total number of square degree areas (1 degree latitude by 1 degree longitude) that were compared. Numbers in brackets represent the number of square degree areas with higher percentages of *Sargassum* species occurrence after ENSO events. NS=nonsignificant.

U.S. Gulf of Mexico	Cold ENSO	Neutral ENSO	Warm ENSO	
Whole	—	—	—	P_1=NS
Western	—	—	—	P_1=NS
Eastern	—	—	—	P_1=NS
Continental shelf	3.43 ±0.91% (48)	2.02 ±0.77% (48)	2.52 ±0.66% (48)	P_1=0.0424
Deep basin	—	—	—	P_1=NS
Continental shelf	3.31 ±0.92% (48) [24]	2.02 ±0.77% (48) [11]		P_2=0.0022
	—		—	P_2=NS
		—	—	P_2=NS
Western	4.64±1.10% (31)	—	5.28±1.53% (32)	
Eastern	3.62±1.29% (40)	—	2.51±0.74% (40)	
	P_3=0.0455	P_3=NS	P_3=0.0020	
Continental shelf	3.43±0.91% (48)	2.02±0.77% (48)	2.52±0.66% (48)	
Deep basin	5.38±1.83% (23)	7.79±2.38% (24)	6.19±1.85% (24)	
	P_3=0.0188	P_3<0.00001	P_3=0.0002	

P_1-values given by the Kruskal–Wallis H test for the analysis among ENSO events.
P_2-values given by the Wilcoxon signed rank test for the analysis between ENSO events.
P_3-values given by the Mann–Whitney U test for the analysis within ENSO events.

ber of hurricanes and the south and southeast wind momentums in the GOM. A seasonal weather-related hydrographic characteristic in the GOM was also significantly different under ENSO events. Higher values of south wind momentum were detected at the western region in spring during ENSOc events (22.09 ±14.31 Ns/m^2) than during ENSOw events (6.02 ±2.93 Ns/m^2; P=0.007). Higher values of north and northwest wind momentum were found at the central region in spring during ENSOw events (N: 15.88 ±4.41 Ns/m^2; NW: 11.15 ±4.72 Ns/m^2) than during ENSOn events (N: 7.97 ±3.29 Ns/m^2; NW: 2.49 ±1.29 Ns/m^2; P<0.006).

Discussion

Sargassum macroalgae in the western Atlantic Ocean are home to a diverse and unique community of small invertebrates and fish species. Despite the designation of *Sargassum* species as essential fish habitat, long-term data on the distribution and abundance of species of *Sargassum* in the GOM are lacking. The time frame of the SEAMAP ichthyoplankton surveys provided a unique opportunity to examine occurrence of *Sargassum* species under differing decadal and interannual regimes of global climate.

The GOM is part of a broader western Atlantic Ocean region of *Sargassum* occurrence. Historically, the recognized route of floating *Sargassum* macroalgae was through the Caribbean Sea, into the GOM, up the eastern seaboard of the United States within the Gulf Stream, and into the Sargasso Sea (Calder, 1995). A new source area for *Sargassum* species in the tropical North Atlantic Ocean (NERR) was recently discovered (Franks et al., 2011; Gower et al., 2013; Johnson et al., 2013) and provides another route of entry for the macroalgae to the greater Caribbean region and GOM. This newly defined route (NERR) has been cited as the source of the *Sargassum* species currently inundating the Caribbean region, and weather-related hydrographic characteristics (nutrient input, position and strength of the ITCZ) have been identified as contributors to the massive accumulation of the macroalgae (Franks et al., 2011; Franks et al., 2016). Weather-related hydrographic characteristics associated with the NERR (AMM, ITCZ, Amazon River discharge), as well as factors unique to the GOM (LC spin-off eddies) may help to explain differences in abundance of *Sargassum* species across the USGOM in response to shifts in climate regimes.

Table 4

Mean fall (September–November) occurrence, with 95% confidence intervals, of pelagic species of *Sargassum* over the continental shelf across the U.S. Gulf of Mexico and in the western and eastern regions after El Niño–Southern Oscillation (ENSO) events from 1982 through 2012. Occurrence represents the percentage of ichthyoplankton samples associated with pelagic *Sargassum*. The numbers in parentheses represent the total number of square degree areas (1 degree latitude by 1 degree longitude) that were compared. Numbers in brackets represent the number of square degree areas (1 degree latitude, 1 degree longitude) with higher percentages of *Sargassum* species after ENSO events. NS=nonsignificant.

U.S. Gulf of Mexico	Cold ENSO	Neutral ENSO	Warm ENSO	
Whole	2.72 ±0.69% (53)	1.84 ±0.69% (49)	0.87 ±0.38% (53)	P_1=0.0001
Western	2.97 ±1.10% (24)	2.70 ±1.21% (22)	0.96 ±0.53% (24)	P_1=0.0077
Eastern	2.51 ±0.88% (29)	1.13 ±0.69% (27)	0.80 ±0.55% (29)	P_1=0.0022
	P_2=NS	P_2=0.0087	P_2=NS	
Whole	2.63 ±0.67% (49) [29]	1.84 ±0.69% (49) [15]		P_3=0.0075
	2.72 ±0.69% (53) [40]		0.87 ±0.38% (53) [4]	P_3=0
		1.70 ±0.65% (48) [26]	0.92 ±0.41% (48) [10]	P_3=0.0084
Western	—	—		P_3=NS
	2.97 ±1.10% (24) [18]		0.96 ±0.53% (24) [2]	P_3=0.0008
		2.70 ±1.21% (22) [15]	1.05 ±0.57% (22) [4]	P_3=0.0049
Eastern	2.14 ±0.77% (27) [18]	1.13 ±0.69% (27) [6]		P_3=0.0055
	2.51 ±0.88% (29) [22]		0.80 ±0.55% (29) [2]	P_3=0.0001
		—	—	P_3=NS

P_1-values given by the Kruskal–Wallis H test for the analysis among ENSO events.
P_2-values given by the Mann–Whitney U test for the analysis within ENSO events.
P_3-values given by the Wilcoxon signed rank test for the analysis between ENSO events.

Two different decadal regimes of weather-related hydrographic characteristics associated with the coupling of AMO and NAO phases occurred over the time period represented in the SEAMAP samples. Overall percentages of samples with species of *Sargassum* across the USGOM under the coupled AMOc/NAOp and coupled AMOw/NAOn phases were 2.95% and 7.28%, respectively. Factors affecting the occurrence of *Sargassum* species under both regimes are those that influence growth (e.g., temperature, nutrient input), fragmentation (reproduction) and dispersion (e.g., hurricane and eddies), and containment within a region (e.g., wind momentum and eddies).

Productivity in the USGOM is strongly influenced by river flows from the Mississippi and Atchafalaya rivers. Sanchez-Rubio et al. (2011) found the AMO and NAO to be important drivers of climate-related features influencing long-term hydrological conditions across coastal Louisiana and Mississippi. In their study, high river discharge occurred under the coupling of AMOc/NAOp phases and lower volumes were associated with the coupled AMOw/NAOn phase. Low river discharge and a lowered nitrogen:phosphorus ratio (Sanchez-Rubio and Perry, 2015), conditions less favorable for *Sargassum* productivity, characterized the regime with greater *Sargassum* species occurrence; this finding indicates that factors associated with transport and retention may have played a greater role than growth in facilitating the occurrence of *Sargassum* species. Although physical processes associated with the dry regime undoubtedly played a major role in moving and maintaining the occurrence of *Sargassum* species, biological processes may also have contributed to maintenance of the macroalgae in the western GOM. Lapointe et al. (2014) reported that the excretion of ammonium and soluble reactive phosphorus by high abundances of fishes associated with *Sargassum* macroalgae (filefishes and carangids) provides nutrients that help to sustain growth and biomass. They noted that new production of *Sargassum* macroalgae may occur in neritic waters of the western Atlantic Ocean and GOM as a result of this mutualistic association. Thus, both physical and biological processes may facilitate occurrence.

Hurricane activity was higher in the North Atlantic Ocean, Caribbean region (Goldenberg et al., 2001), NERR, and GOM (this study), and the AMM index was higher and positive (this study) for the years after the mid 1990s climate shift. Vimont and Kossin (2007) found that the AMM was strongly related to hurricane activity on both decadal and interannual time frames and noted that the influence of the AMO on hurricane activity was manifested through the AMM. The influ-

Table 5

Monthly mean values, with 95% confidence intervals, of environmental factors from the North Equatorial Recirculation Region (NERR) and Gulf of Mexico (GOM) during the coupling of phases of the Atlantic Multidecadal Oscillation (AMO) and North Atlantic Oscillation (NAO). The numbers in parentheses and *n* represent the total number of values or features that were compared; *P*-values are those given by the Mann–Whitney U test for the analysis of values between AMO and NAO phases. AMM=Atlantic Meridional Mode.

Variables	Region	Month	Wind direction	*P*	Cold AMO, positive NAO phases	Warm AMO, negative NAO phases
AMM	NERR	Aug–Mar		0	−1.56 ±0.81 (13)	1.52 ±0.85 (15)
Wind momentum	Western GOM	Sep–Nov	NW	0.031	4.27 ±2.50 (12)	7.65 ±3.19 (14)
		Dec–Feb	SE	0.005	46.61 ±9.37 (15)	67.64 ±22.89 (10)
		Mar–May	SE	0.030	82.66 ±21.59 (13)	109.80 ±34.02 (12)
	Central GOM	Sep–Nov	S	0.017	6.78 ±1.94 (12)	10.95 ±3.08 (15)
		Jun–Aug	W	0.022	1.03 ±0.48 (7)	1.89 ±0.53 (15)
	Eastern GOM	Sep–Nov	S	0.010	4.18 ±1.74 (9)	9.76 ±3.77 (13)
		Sep–Nov	SW	0.003	1.05 ±0.42 (8)	4.23 ±1.65 (12)
Hurricanes	GOM	Jun–Nov			*n*=23	*n*=38
	NERR	Jun–Nov			*n*=3	*n*=12
Loop Current eddies	GOM	Jan–Dec			*n*=17	*n*=23
Amazon River discharge	NERR	Apr–Aug			Below average (7/13)	Above average (14/19)

ence of hurricanes on abundance of *Sargassum* species is largely undocumented, but biotic characteristics of the macroalgae (such as fragmentation) and its position in the water column (i.e., in surface waters) would cause the species to be responsive to physical processes associated with the passing of tropical storms. Water turbulence associated with hurricanes may positively affect abundances through increased dispersion, transport, upwelling, and fragmentation. Pelagic *Sargassum* species reproduce asexually by fragmentation (Fritsch, 1965; Round, 1981; Awasthi, 2007; Rogers, 2011) when younger parts of the thallus separate from the older parts or when there is physical injury to any part of the plant (Hanisak and Samuel, 1987). Separated parts of the plant have the potential to mature into fully formed organisms (Hanisak and Samuel, 1987). In addition to fragmentation of individual plants, mats of *Sargassum* species could be broken apart and more widely dispersed.

For species of *Sargassum*, the eastern region of the GOM is generally regarded as a zone of transport that serves to move the macroalgae into the GOM via the Yucatan Current and out via the Florida Current. The western zone is considered an area of residence and growth where LC spin-off eddies decay and deposit *Sargassum* macroalgae. Circulation in the eastern GOM is dominated by the LC, a fast-moving current that can reach maximum flow speeds of 1.5 to 1.8 m/s (Gordon, 1967). Degree of northward penetration of the LC into the GOM varies as does the time and number of eddies shed. Eddies are usually mesoscale circulation features but can measure 200-400 km in diameter and extend to a depth of 1000 m (Mooers, 1998). They are shed randomly every 3 to 17 months (Sturges and Leben, 2000) and the majority of them drift to the western GOM where they may persist for weeks (Oey et al., 2005). Species of *Sargassum* can be readily entrained in fronts formed by convergent surface currents associated with large spin-off eddies that appear in satellite images (Gower et al., 2006) as long curving lines. The balance of forces in eddy motions favors entrapment of *Sargassum* around the periphery of anticyclonic (counterclockwise in the Northern Hemisphere) eddies and in the center of cyclonic eddies owing to sea-surface height gradients and frictional processes. More complex patterns, however, are formed by stepwise convergent fronts across the surface of mesoscale eddies and associated lines of *Sargassum* (Zhong et al., 2012) within both cyclonic and anticyclonic eddies.

The higher numbers of eddies shed under the coupled AMOw/NAOn phases and the relatively long period associated with eddy decay may have contributed to the greater incidence of *Sargassum* species observed in the western USGOM in our study. Regional occurrence was 8.46% in the western USGOM and 6.47% in the eastern USGOM under the coupled AMOw/NAOn phases and 3.41% and 2.69% in the western and eastern regions under the coupled AMOc/NAOp phases, respectively. Highest percentages of positive samples (*Sargassum* species present) occurred over the deep basin in the western region irrespective of climate regime: coupled AMOw/NAOn phases (10.2%), coupled AMOc/NAOp phases (7.28%). Gower et al. (2006), using satellite imagery, observed that most *Sargassum* macroalgae were found in the western GOM and noted that in areas where surface waters circulate in slowly rotating gyres, the macroalgae would be expected to accumulate. Wind momentum, a measure of the transport of surface water, also favored retention of species of *Sargassum*. South and southeast wind momentum was

higher along the USGOM under the coupled AMOw/NAOn phases. These wind conditions would facilitate retention of *Sargassum* mats within the study region and the transport of new mats of *Sargassum* species from the southern GOM.

Operating within the decadal regimes are weather-related hydrographic characteristics imposed by interannual ENSO events. Higher occurrences of *Sargassum* species in the USGOM were associated with the ENSOc phase. Under ENSOc years, hydrographic characteristics in the NERR, Caribbean Sea, and GOM generally favor production, growth, and dispersion of the macroalgae. During ENSOc years, the ITCZ shifts south of its mean location (Saravanan and Chang, 2000), creating a lower vertical shear over the regions of hurricane genesis and development of the tropical Atlantic Ocean (Gray, 1984; Goldenberg et al., 2001; Vitart and Anderson, 2001). The decrease in vertical shearing enhances the growth of prehurricane disturbances in the Atlantic Ocean and increases the number of hurricane landings on the continental United States (Elsner et al., 2001). The turbulence associated with hurricanes would enhance fragmentation and dispersion of mats of pelagic *Sargassum* species along their paths of circulation. During the ENSOc years, the westward influence of south and southeast winds along the USGOM (Smith et al., 1998) and south wind momentum in spring (March–May) in the western USGOM region (this study) were enhanced and therefore reduced the frequency of cold wind outbreaks, off-shelf water flow (Nowlin and Parker, 1974), and coastal upwelling (Dagg, 1988). These wind conditions would favor retention of *Sargassum* mats in this region. Highest percentages of positive samples (*Sargassum* species present) occurred over the deep basin in the western region after ENSO events. Distributional results were consistent with traditional observations that the eastern region is a zone of transport and the western region is a zone of accumulation for *Sargassum* in the USGOM.

Acknowledgments

The authors would like to thank the anonymous reviewers who provided constructive comments that strengthened the manuscript. This research was funded by NMFS 2014 Marine Fisheries Initiative grant NA14NMF433022, for the project titled, "The effect of changing climate regimes on ephemeral nursery habitats: influence on selected reef fish populations in national marine sanctuaries and habitat areas of particular concern in the northern Gulf of Mexico."

Literature cited

Awasthi, D. K.
2007. Cryptogams: algae, Bryophyta and Pteridophyta, 448 p. Krishna Prakashan Media, Ltd., Meerut, India.

Berger, W. H., and G. Wefer.
1996. Central themes of South Atlantic circulation. *In* The South Atlantic: present and past circulation (G. Wefer, W. H. Berger, G. Siedler, D. J. Webb, eds.), p. 1–11. Springer-Verlag, Berlin, Germany.

Bjerknes, J.
1969. Atmospheric teleconnections from the equatorial Pacific. Mon. Weather Rev. 97:163–172.

Bonferroni, C. E.
1935. Il calcolo delle assicurazioni su gruppi di teste. *In* Studi in onore del professore Salvatore Ortu Carboni, p. 13–60. Bardi, Rome.

Bortone, S. A., P. A. Hastings, and S. B. Collard.
1977. The pelagic *Sargassum* ichthyofauna of the eastern Gulf of Mexico. Northeast Gulf Sci. 1:60–67.

Butler, J. N., B. F. Morris, J. Cadwallader, and A. W. Stoner.
1983. Studies of *Sargassum* and the *Sargassum* community. Bermuda Biol. Stat. Spec. Publ. 22, 307 p.

Calder, D. R.
1995. Hydroid assemblages on holopelagic *Sargassum* from the Sargasso Sea at Bermuda. Bull. Mar. Sci. 56:537–546.

Comyns, B. H., N. M. Crochet, J. S. Franks, J. R. Hendon, and R. S. Waller.
2002. Preliminary assessment of the association of larval fishes with pelagic *Sargassum* habitat and convergence zones in the northcentral Gulf of Mexico. *In* Proceedings of the fifty-third Gulf and Caribbean Fisheries Institute; Biloxi, MS, 6–10 November 2000 (R. L. Creswell, ed.), p. 636–645. Gulf Caribb. Fish. Inst., Fort Pierce, FL.

Coston-Clements, L., L. R. Settle, D. E. Hoss, and F. A. Cross.
1991. Utilization of the *Sargassum* habitat by marine invertebrates and vertebrates: a review. NOAA Tech. Memo. NMFS-SEFSC-296, 32 p.

Dagg, M. J.
1988. Physical and biological responses to the passage of a winter storm in the coastal and inner shelf waters of the northern Gulf of Mexico. Cont. Shelf Res. 8:167–178.

Deacon, G. E. R.
1942. The Sargasso Sea. Geogr. J. 99:16–28.

Dooley, J. K.
1972. Fishes associated with the pelagic *Sargassum* complex with a discussion of the *Sargassum* community. Contrib. Mar. Sci. 16:1–32.

Elsner, J. B., B. H. Bossak, and X.-F. Niu.
2001. Secular changes to the ENSO-U.S. hurricane relationship. Geophys. Res. Lett. 28:4123–4126.

Enfield, D. B., A. M. Mestas-Nuñez, and P. J. Trimble.
2001. The Atlantic Multidecadal Oscillation and its relation to rainfall and river flows in the continental U.S. Geophys. Res. Lett. 28:2077–2080.

Franks, J. S., D. R. Johnson, D.-S. Ko, G. Sanchez-Rubio, J. R. Hendon, and M. Lay.
2011. Unprecedented influx of pelagic *Sargassum* along Caribbean island coastlines during summer 2011. *In* Proceedings of the 64th Gulf and Caribbean Fisheries Institute; Puerto Morelos, Mexico, October 31–November 4, p. 6–8. Gulf Carib. Fish. Inst., Marathon, FL.

Franks, J. S., D. R. Johnson and D. S. Ko.
2016. Pelagic *Sargassum* in the tropical North Atlantic. Gulf Carib. Res. 27(1):SC6-SC11.

Fritsch, F. E.
1965. The structure and reproduction of algae, vol. II, 939 p. Cambridge Univ. Press, Cambridge, UK.

Giannini, A., Y. Kushnir, and M. A. Cane.
2000. Interannual variability of Caribbean rainfall, ENSO, and the Atlantic Ocean. J. Clim. 13:297–311.

Giannini, A., M. A. Cane, and Y. Kushnir.
2001. Interdecadal changes in the ENSO teleconnection to the Caribbean region and the North Atlantic Oscillation. J. Clim. 14:2867–2879.

Godfrey, J. S.
1975. On ocean spindown I: a linear experiment. J. Phys. Oceanogr. 5:399–409.

Goldenberg, S. B., C. W. Landsea, A. M. Mestas-Nuñez, and W. M. Gray.
2001. The recent increase in Atlantic hurricane activity: causes and implications. Science 293:474–479.

Gordon, A. L.
1967. Circulation of the Caribbean Sea. J. Geophys. Res. 72:6207–6223.

Gower, J. F. R., and S. A. King.
2011. Distribution of floating *Sargassum* in the Gulf of Mexico and the Atlantic Ocean mapped using MERIS. Int. J. Remote Sens. 32:1917–1929.

Gower, J., C. Hu, G. Borstad, and S. King.
2006. Ocean color satellites show extensive lines of floating *Sargassum* in the Gulf of Mexico. IEEE Trans. Geosci. Remote Sens. 44:3619–3625.

Gower, J. F. R., E. Young, and S. King.
2013. Satellite images suggest a new *Sargassum* source region in 2011. Remote Sens. Lett. 4:764–773.

Gray, W. M.
1984. Atlantic seasonal hurricane frequency. Part I: El Niño and 30 mb quasi-biennial oscillation influences. Mon. Weather Rev. 112:1649–1668.

Gray, S. T., L. J. Graumlich, J. L. Betancourt, and G. T. Pederson.
2004. A tree-ring based reconstruction of the Atlantic Multidecadal Oscillation since 1567 A.D. Geophys. Res. Lett. 31:L12205.

Hanisak, M. D., and M. A. Samuel.
1987. Growth rates in culture of several species of *Sargassum* from Florida, USA. Hydrobiologia 151–152: 399–404.

Hastenrath, S., and L. Heller.
1977. Dynamics of climate hazards in northeast Brazil. Quart. J. Roy. Meteor. Soc. 103:77–92.

Hellerman, S.
1965. Computations of wind stress fields over the Atlantic Ocean. Mon. Weather Rev. 93(4):239–244.

Hoffmayer, E. R., J. S. Franks, B. H. Comyns, J. R. Hendon, and R. S. Waller.
2005. Larval and juvenile fishes associated with pelagic *Sargassum* in the northcentral Gulf of Mexico. *In* Proceedings of the 56th Gulf and Caribbean Fisheries Institute; Tortola, British Virgin Islands, 10–14 November 2003, p. 259–269. Gulf Caribb. Fish. Inst., Fort Pierce, FL.

Hu, Q., and S. Feng.
2007. Decadal variation of the southwest U.S. summer monsoon circulation and rainfall in a regional model. J. Clim. 20:4702–4716.

Huh, O. K., W. J. Wiseman Jr., and L. J. Rouse Jr.
1981. Intrusion of Loop Current waters onto the west Florida continental shelf. J. Geophys. Res. 86:4186–4192.

Huffard, C. L., S. von Thun, A. D. Sherman, K. Sealey, and K. L. Smith, Jr.
2014. Pelagic *Sargassum* community change over a 40-year period: temporal and spatial variability. Mar. Biol. 161:2735–2751.

Hurlburt, H. E., and J. D. Thompson.
1980. A numerical study of Loop Current intrusions and eddy shedding. J. Phys. Oceanogr. 10:1611–1651.

Hurrell, J. W., and H. van Loon.
1997. Decadal variations in climate associated with the North Atlantic Oscillation. Clim. Change 36:301–326.

Hurrell, J. W., and C. Deser.
2009. North Atlantic climate variability: the role of the North Atlantic Oscillation. J. Mar. Syst. 78:28–41.

Hurrell, J. W., Y. Kushnir, G. Ottersen, and M. Visbeck.
2003. An overview of the North Atlantic Oscillation. *In* The North Atlantic Oscillation: climatic significance and environmental impact. Geophys Monogr. 134 (J. W. Hurrell, Y. Kushnir, G. Ottersen, and M. Visbeck, eds.), p. 1–35. Am. Geophys. Union, Washington, DC.

Janicot, S., A. Harzallah, B. Fontaine, and V. Moron.
1998. West African monsoon dynamics and eastern equatorial Atlantic and Pacific SST anomalies (1970–88). J. Clim. 11:1874–1882.

Johnson, D. R., D. S. Ko, J. S. Franks, P. Moreno, and G. Sanchez-Rubio.
2013. The *Sargassum* invasion of the eastern Caribbean and dynamics of the equatorial North Atlantic. *In* Proceedings of the 65th Gulf and Caribbean Fisheries Institute; Santa Marta, Colombia, 5–9 November 2012, p 102–103. Gulf Caribb. Fish. Inst., Marathon, FL.

Karnauskas, M., M. J. Schirripa, J. K. Craig, G. S. Cook, C. R. Kelble, J. J. Agar, B. A. Black, D. B. Enfield, D. Lindo-Atichati, B. A. Muhling, et al.
2015. Evidence of climate-driven ecosystem reorganization in the Gulf of Mexico. Global Change Biol. 21:2554–2568.

Kerr, R. A.
2000. A North Atlantic climate pacemaker for the centuries. Science 288:1984–1985

Kramer D., M. J. Kalin, E. G. Stevens, J. R. Thrailkill, and J. R. Zweifel.
1972. Collecting and processing data on fish eggs and larvae in the California Current region. NOAA Tech. Rep. NMFS Circ. 370, 38 p.

Krueger, A. F., and J. S. Winston.
1975. Large-scale circulation anomalies over the tropics during 1971–72. Mon. Weather Rev. 103:465–473.

Lamb, P. J.
1978. Large-scale tropical Atlantic surface circulation patterns associated with Subsaharan weather anomalies. Tellus 30:240–251.

Lapointe, B. E.
1986. Phosphorus-limited photosynthesis and growth of *Sargassum natans* and *Sargassum fluitans* (Phaeophyceae) in the western North Atlantic. Deep-Sea Res. Oceanogr., A 33:391–399.

Lapointe, B. E., L. E. West, T. T. Sutton, and C. Hu.
2014. Ryther revisited: nutrient excretions by fishes enhance productivity of pelagic *Sargassum* in the western North Atlantic Ocean. J. Exp. Mar. Biol. Ecol. 458:46–56.

Lighthill, M. J.
1969. Dynamic response of the Indian Ocean to onset of the Southwest Monsoon. Philos. Trans. R. Soc. Lond., A, 265:45–92.
Lin, Y., R. J. Greatbatch, and J. Sheng.
2010. The influence of Gulf of Mexico Loop Current intrusion on the transport of the Florida Current. Ocean Dyn. 60:1075–1084.
Lyczkowski-Shultz, J., and D. S. Hanisko.
2007. A time series of observations on red snapper larvae from SEAMAP surveys, 1982–2003: seasonal occurrence, distribution, abundance, and size. Am. Fish. Soc. Symp. 60:3–23.
Maslin, M., S. Burns, H. Erlenkeuser, and C. Hohnemann.
1997. Stable isotope records from sites 932 and 933. Proc. Ocean Drilling Prog., Sci. Results 155:305–318.
McCreary, J.
1976. Eastern tropical ocean response to changing wind systems: with application to El Niño. J. Phys. Oceanogr. 6:632–645.
McPhaden, M. J.
1999. Genesis and evolution of the 1997–98 El Niño. Science. 283:950–954.
Mehta, V. M., M. J. Suarez, J. V. Manganello, and T. L. Delworth.
2000. Oceanic influence on the North Atlantic Oscillation and associated northern hemisphere climate variations: 1959–1993. Geophys. Res. Lett. 27:121–124.
Mooers, C. N. K., and G. A. Maul.
1998. Intra-Americas circulation. *In* The sea, vol. 11. The global coastal ocean: regional studies and syntheses (A. R. Robinson and K. Brink, eds.), p. 183–208. John Wiley & Sons, New York.
Nowlin, W. D., Jr., and C. A. Parker.
1974. Effects of a cold-air outbreak on shelf waters of the Gulf of Mexico. J. Phys. Oceanogr. 4:467–486.
Nürnberg, D., M. Ziegler, C. Karas, R. Tiedemann, and M. W. Schmidt.
2008. Interacting Loop Current variability and Mississippi River discharge over the past 400 kyr. Earth Planet. Sci. Lett. 272:278–289.
Oey, L.-Y., Jr., T. Ezer, and H.-C. Lee.
2005. Loop Current, rings and related circulation in the Gulf of Mexico: a review of numerical models and future challenges. *In* Circulation in the Gulf of Mexico: observations and models). Geophys. Monogr. 161 (W. Sturges and A. Lugo-Fernandez, eds.), p. 31–56. Am. Geophys. Union, Washington, DC.
Parr, A. E.
1939. Quantitative observations on the pelagic sargassum vegetation of the western North Atlantic. With preliminary discussion of morphology and relationships. Bull. Bingham Oceanogr. Collect. 6:1–94.
Posgay, J. A., and R. R. Marak.
1980. The MARMAP bongo zooplankton samplers. J. Northwest Atl. Fish. Sci. 1:91–99.
Robertson, A. W., S. Kirshner, and P. Smyth.
2004. Downscaling of daily rainfall occurrence over northeast Brazil using a hidden Markov model. J. Climate. 17:4407–4424.
Rogers, K. (ed.).
2011. Fungi, algae, and protists, 232 p. Britannica Educational Publishing, New York.
Round, F. E.
1981. The ecology of algae, 653 p. Cambridge Univ. Press, New York.
SAFMC (South Atlantic Fishery Management Council).
2002. Fishery management plan for pelagic *Sargassum* habitat of the South Atlantic region: including a final environmental impact statement, initial regulatory flexibility analysis, regulatory impact review, and social impact assessment/fishery impact statement, 153 p. SAFMC, Charleston, SC. [Available from website.]
Sanchez-Rubio, G., and H. Perry.
2015. Climate-related meteorological and hydrological regimes and their influence on recruitment of Gulf menhaden (*Brevoortia patronus*) in the northern Gulf of Mexico. Fish. Bull. 113:391–406.
Sanchez-Rubio, G., H. M. Perry, P. M. Biesiot, D. R. Johnson, R. N. Lipcius.
2011. Oceanic–atmospheric modes of variability and their influence on riverine input to coastal Louisiana and Mississippi. J. Hydrol. 396:72–81.
Saravanan, R., and P. Chang.
2000. Interaction between tropical Atlantic variability and El Nino–Southern Oscillation. J. Clim. 13:2177–2194.
Schneider, T., T. Bischoff, and G. H. Haug.
2014. Migrations and dynamics of the intertropical convergence zone. Nature 513:45–53.
Seager, R., Y. Kushnir, M. Visbeck, N. Naik, J. Miller, G. Krahmann, and H. Cullen.
2000. Causes of Atlantic Ocean climate variability between 1958 and 1998. J. Clim. 13:2845–2862.
Smith, S. D.
1980. Wind stress and heat flux over the ocean in gale force winds. J. Phys. Oceanogr. 10:709–726.
Smith, P. E., and S. L. Richardson.
1977. Standard techniques for pelagic fish egg and larva surveys. FAO Fish. Tech. Pap. 175, 100 p.
Smith, S. R., P. M. Green, A. P. Leonardi, and J. J. O'Brien.
1998. Role of multiple-level tropospheric circulations in forcing ENSO winter precipitation anomalies. Mon. Weather Rev. 126:3102–3116.
Stoner, A. W.
1983. Pelagic *Sargassum*: evidence for a major decrease in biomass. Deep-Sea Res. Oceanogr., A 30:469–474.
Sturges, W., and R. Leben
2000. Frequency of ring separations from the Loop Current in the Gulf of Mexico: a revised estimate. J. Phys. Oceanogr. 30:1814–1819.
Sultan, B., and S. Janicot.
2000. Abrupt shift of the ITCZ over West Africa and intraseasonal variability. Geophys. Res. Lett. 27:3353–3356.
Sutton R. T., and D. L. R. Hodson.
2005. Atlantic Ocean forcing of North American and European summer climate. Science 309:115–118.
Taylor, M. A., D. B. Enfield, and A. A. Chen.
2002. Influence of the tropical Atlantic versus the tropical Pacific on Caribbean rainfall. J. Geophys. Res. 107(C9):3127.
Uvo, C. B., C. A. Repelli, S. E. Zebiak, and Y. Kushnir.
1998. The relationships between tropical Pacific and Atlantic SST and northeast Brazil monthly precipitation. J. Clim. 11:551–562.
Vimont, D. J., and J. P. Kossin.
2007. The Atlantic Meridional Mode and hurricane activity. Geophys. Res. Lett. 34:L07709.

Vink, A., A. Brune, C. Höll, K. A. F. Zonneveld, and H. Willems.
2002. On the response of calcareous dinoflagellates to oligotrophy and stratification of the upper water column in the equatorial Atlantic Ocean. Palaeogeogr. Palaeoclim. Palaeoecol. 178:53–66.

Vitart, F., and J. L. Anderson.
2001. Sensitivity of Atlantic tropical storm frequency to ENSO and interdecadal variability of SSTs in an ensemble of AGCM integrations. J. Clim. 14:533–545.

Vukovich, F. M.
2012. Changes in the Loop Current's eddy shedding in the period 2001–2010. Int. J. Oceanogr. vol. 2012, ID 439042, 18 p.

Walker, G. T.
1924. Correlation in seasonal variations of weather, IX. A further study of world weather. Mem. India Meteorol. Dep. 24:275–332.

Wang, H., and R. Fu.
2000. Influence of ENSO SST anomalies and water stormtracks on the interannual variability of the upper-tropospheric water vapor over the Northern Hemisphere extratropics. J. Clim. 13:59–73.

Wang, C., D. B. Enfield, S. K. Lee, and C. W. Landsea.
2006. Influences of the Atlantic warm pool on Western Hemisphere summer rainfall and Atlantic hurricanes. J. Clim. 19:3011–3028.

Wells, R. J. D., and J. R. Rooker.
2004. Spatial and temporal patterns of habitat use by fishes associated with *Sargassum* mats in the northwestern Gulf of Mexico. Bull. Mar. Sci. 74:81–99.

Wiseman, W. J., Jr., and S. P. Dinnel.
1988. Shelf currents near the mouth of the Mississippi River. J. Phys. Oceanogr. 18:1287–1291.

Wyrtki, K.
1975. Fluctuations of the dynamic topography in the Pacific Ocean. J. Phys. Oceanogr. 5:450–459.

Zhong, Y., A. Bracco, and T. A. Villareal.
2012. Pattern formation at the ocean surface: *Sargassum* distribution and the role of the eddy field. Limnol. Oceanogr. 2:12–27.

Fishery Bulletin

Guidelines for authors

Contributions published in *Fishery Bulletin* describe original research in marine fishery science, fishery engineering and economics, as well as the areas of marine environmental and ecological sciences (including modeling). Preference will be given to manuscripts that examine processes and underlying patterns. Descriptive reports, surveys, and observational papers may occasionally be published but should appeal to an audience outside the locale in which the study was conducted.

Although all contributions are subject to peer review, responsibility for the contents of papers rests upon the authors and not on the editor or publisher. *Submission of an article implies that the article is original and is not being considered for publication elsewhere.*

Plagiarism and double publication are considered serious breaches of publication ethics. To verify the originality of the research in papers and to identify possible previous publication, manuscripts may be screened with plagiarism-detection software.

Manuscripts must be written in English; authors whose native language is not English are strongly advised to have their manuscripts checked by English-speaking colleagues before submission.

Once a paper has been accepted for publication, online publication takes approximately 3 weeks.

There is no cost for publication in *Fishery Bulletin.*

Types of manuscripts accepted by the journal

Articles generally range from 20 to 30 double-spaced typed pages (12-point font) and describe an original contribution to fisheries science, engineering, or economics. Tables and figures are not included in this page count, but the number of figures should not exceed one figure for every four pages of text. Articles contain the following divisions: abstract, introduction, methods, results, and discussion.

Short contributions are generally less than 15 double spaced typed pages (12-point font) and, like articles, describe an original contribution to fisheries science. They follow the same format as that for articles: abstract, introduction, results and discussion, but the results and discussion sections may be combined. They are distinguished from full articles in that they report a noteworthy new observation or discovery—such as the first report of a new species, a unique finding, condition, or event that expands our knowledge of fisheries science, engineering or economics—and do not require a lengthy discussion.

Companion articles are presented together and published together as a scientific contribution. Both articles address a closely related topic and may be articles that result from a workshop or conference. They must be submitted to the journal at the same time.

Review articles generally range from 40 to 60 double-spaced typed pages (12-point font) and address a timely topic that is relevant to all aspects of fisheries science. They should be forward thinking and address novel views or interpretations of information that encourage new avenues of research. They can be reviews based on the outcome from thematic workshops, or contributions by groups of authors who want to focus on a particular topic, or a contribution by an individual who chooses to review a research theme of broad interest to the fisheries science community. A review article will include an abstract, but the format of the article per se will be up to the authors. Please contact the Scientific Editor to discuss your ideas regarding a review article before embarking on such a project.

Preparation of manuscript

Title page should include authors' full names, mailing addresses, and the senior author's e-mail address.

Abstract should be limited to 200 words (one-half typed page), state the main scope of the research, and emphasize the authors conclusions and relevant findings. Do not review the methods of the study or list the contents of the paper. Because abstracts are circulated by abstracting agencies, it is important that they represent the research clearly and concisely.

General text must be typed in 12-point Times New Roman font throughout. A brief introduction should convey the broad significance of the paper; the remainder of the paper should be divided into the following sections: Materials and methods, Results, Discussion, and Acknowledgments. Headings within each section must be short, reflect a logical sequence, and follow the rules of subdivision (i.e., there can be no subdivision without at least two subheadings). The entire text should be intelligible to interdisciplinary readers; therefore, all acronyms, abbreviations, and technical terms should be written out in full the first time they are mentioned. Abbreviations should be used sparingly because they are not carried over to indexing databases and slow readability for those readers outside a discipline. They should never be used for the main subject (species, method) of a paper.

For general style, follow the U.S. *Government Printing Office Style Manual* (2008) [available at website] and *Scientific Style and Format: the CSE Manual for Authors, Editors, and Publishers* (2014, 8th ed.) published by the Council of Science Editors. For scientific nomenclature, use the current edition of the American Fisheries Society's *Common and Scientific Names of*

Fishes from the United States, Canada, and Mexico and its companion volumes (*Decapod Crustaceans, Mollusks, Cnidaria and Ctenophora*, and *World Fishes Important to North Americans*). For species not found in the above mentioned AFS publications and for more recent changes in nomenclature, use the Integrated Taxonomic Information System (ITIS) (available at website), or, secondarily, the California Academy of Sciences *Catalog of Fishes* (available at website) for species names not included in ITIS. Common (vernacular) names of species should be lowercase. Citations must be given of taxonomic references used for the identification of specimens. For example, "Fishes were identified according to Collette and Klein-MacPhee (2002); sponges were identified according to Stone et al. (2011)."

Dates should be written as follows: 11 November 2000. Measurements should be expressed in metric units, e.g., 58 metric tons (t); if other units of measurement are used, please make this fact explicit to the reader. Use numerals, not words, to express whole and decimal numbers in the general text, tables, and figure captions (except at the beginning of a sentence). For example: We considered 3 hypotheses. We collected 7 samples in this location. Use American spelling. Refrain from using the shorthand slash (/), an ambiguous symbol, in the general text.

Word usage and grammar that may be useful are the following:

- *Aging*
  For our journal, the word *aging* is used to mean both age determination and the aging process (senescence). Authors should make clear which meaning is intended where ambiguity may arise.

- *Fish and fishes*
  The plural of the word fish (a collective noun that implies individuals without regard to species) is *fish*.
  Example: The *fish* were collected by trawl net.
  Example: The numbers of *fish* collected that season were less than the numbers from previous years.

  The plural for *fish species* is *fishes* (a contrived plural used by taxonomists to mean several or more *fish species*) or one can use *fish species* (which is preferred in this journal for clarity across disciplines).
  Example: The *fishes* of Puget Sound [biodiversity is implied] or
  The *fish species* of Puget Sound [preferred plural for clarity across disciplines].

- *Crab and crabs, squid and squids, etc.*
  The plural of the word *crab* (i.e., many individuals without regard to species) is *crab*.
  Example: The crab were sorted by weight.
  Example: Many red king *crab* were dying [Many individuals of one species of crab.]

  The plural of *crab species* is *crabs* (a word used by taxonomists) or *crab species* (the latter is preferred in this journal for clarity).
  Example: These *crabs* were selected for treatment. [Different crab species are implied.]
  These *crab species* were selected for treatment. [Preferred word choice for clarity of meaning.]
  Example: Snow *crabs* are found throughout the North Pacific Ocean and Bering Sea. [There are 2 species of snow crab and therefore the word *crabs* can be used here.]
  Two species of snow *crab* are found throughout the North Pacific Ocean and Bering Sea. [Preferred usage for clarity.]
  Example: Three crabs were selected for treatment. [3 species of crab are implied.]
  Three crab species were selected for treatment. [Preferred word choice for clarity.]

- *The definite article with common names of species*
  When the singular common name of a species represents the entire class or group to which it belongs, use the definite article.
  Example: Only one species of the genus Salmo is found in the Atlantic Ocean—*the* Atlantic salmon (*Salmo salar*).
  Example: The sonic emissions of *the* bottlenose dolphin are complex.

  For plural common names, this rule does not apply.
  Example: Chinook salmon are found throughout the Pacific Ocean.
  Example: Bottlenose dolphins are found in temperate and tropical waters.

- *Sex* For the meaning of male and female, use the word *sex*, not *gender*.

- *Participles* As adjectives, participles must modify a specific noun or pronoun.
  Example: Using mark-recapture methods, these scientists determined the size of the population. [Correct. The participle *using* modifies the word *scientists*.]
  Example: These scientists, based on the collected data, concluded that the mortality rate of these fish had increased. [Incorrect. The scientists were not based on the collected data.]
  These scientists concluded, on the basis of collected data, that the mortality rate of these fish had increased. [Correct. The offending participle has been eliminated and an adverbial phrase modifies the verb *concluded*.]

Equations and mathematical symbols should be set from a standard mathematical program (MathType or Equation Editor). Equations formatted in LaTex are not acceptable. For mathematical symbols in the general text (α, χ^2, π, $\pm$, etc.), use the symbols provided by the MS Word program and italicize all variables, except those variables represented by Greek letters. Do not use photo mode when creating these symbols in the general text and do NOT CUT and PASTE equations, letters, or symbols from a different software program.

Number equations (if there are more than 1) for future reference by scientists; place the number within parentheses at the end of the first line of the equation.

Literature cited section comprises published works and those accepted for publication in peer-reviewed journals (in press). Follow the name and year system for citation format in the "Literature cited" section (that is to say, citations should be listed alphabetically by the authors' last names, and then by year if there is more than one citation with the same authorship. A list of abbreviations for citing journal names can be found at this website.

Authors are responsible for the accuracy and completeness of all citations. Literature citation format: Author (last name, followed by first-name initials). Year. Title of article. Abbreviated title of the journal in which it was published. Always include number of pages. For a sequence of citations in the general text, list chronologically: (Smith, 1932: Green. 1947; Smith and Jones, 1985).

Acknowledgments should be no more than 6 lines of text. Only those who have contributed in an outstanding way should be acknowledged by name. For recognition of other persons or groups, use a general term, such as "crew," "observers," "research coordinators," and do not include names with these terms.

Digital object identifier (doi) code ensures that a publication has a permanent location online. Doi code should be included at the end of citations of published literature. Authors are responsible for submitting accurate doi codes. Faulty codes will be deleted at the page-proof stage.

Cite all software, special equipment, and chemical solutions used in the study within parentheses in the general text: e.g., SAS, vers. 6.03 (SAS Inst., Inc., Cary, NC).

Footnotes are used for all documents that have not been formally peer reviewed and for observations and personal communications. These types of references should be cited sparingly in manuscripts submitted to the journal.

All reference documents, administrative reports, internal reports, progress reports, project reports, contract reports, personal observations, personal communications, unpublished data, manuscripts in review, and council meeting notes are footnoted in 9 pt font and placed at the bottom of the page on which they are first cited. Footnote format is the same as that for formal literature citations. A link to the online source (e.g., [http://www/..... , accessed July 2007.]), or the mailing address of the agency or department holding the document, should be provided so that readers may obtain a copy of the document.

Tables are often overused in scientific papers; it is seldom necessary to present all the data associated with a study. Tables should not be excessive in size and must be cited in numerical order in the text. Headings should be short but ample enough to allow the table to be intelligible on its own.

All abbreviations and unusual symbols must be explained in the table legend. Other incidental comments may be footnoted with italic numeral footnote markers. Use asterisks only to indicate significance in statistical data. Do not type table legends on a separate page; place them above the table data. *Do not submit tables in photo mode.*

- Note probability with a capital, italic *P*.
- Provide a zero before all decimal points for values less than one (e.g., 0.07).
- Round all values to 2 decimal points.
- Use a comma in numbers of five digits or more (e.g., 13,000 but 3000).

Figures must be cited in numerical order in the text. Graphics should aid in the comprehension of the text, but they should be limited to presenting patterns rather than raw data. Figures should not exceed one figure for every four pages of text and must be labeled with the number of the figure. Place labels **A, B, C,** etc. within the upper left area of graphs and photos. Avoid placing labels vertically (except for the y axis).

Figure legends should explain all symbols and abbreviations seen in the figure and should be double-spaced on a separate page at the end of the manuscript.

Line art and halftone figures should be saved at a resolution of >800 dpi (dots per inch) and >300 dpi, respectively. Color is allowed in figures to show morphological differences among species (i.e., for species identification), to show stain reactions, and to show gradations, such as those of temperature and salinity within maps. Color is discouraged in graphs. For the few instances where color is allowed, the use of color will be determined by the Managing Editor. Figures approved for color should be saved in CMYK format.

All figures must be submitted as either PDF of EPS files.

- Capitalize the first letter of the first word in all labels within figures.

- Do not use overly large font sizes in maps and for axis labels in graphs.
- Do not use bold fonts or bold lines in figures.
- Do not place outline rules around graphs.
- Place a North arrow and label degrees latitude and longitude (e.g., 170°E) in all maps.
- Use symbols, shadings, or patterns (not clip art) in maps and graphs.

Supplementary materials that are considered essential, but are too large or impractical for inclusion in a paper (e.g., metadata, figures, tables, videos, websites), may be provided at the end of an article. These materials are subject to the editorial standards of the journal. A URL to the supplementary material and a brief explanation for including such material should be sent at the time of initial submission of the paper to the journal.

- **Metadata, figures, and tables** should be submitted in standard digital format (Word docx) and should be cited in the general text as (Suppl. Table, Suppl. Fig., etc.).
- **Websites** should be cited as (Suppl. website) in the general text and be made available with doi code (if possible) at the end of the article.
- **Videos** must not be larger than 30 MB to allow a swift technical response for viewing the video. Authors should consider whether a short video uniquely captures what text alone cannot capture for the understanding of a process or behavior under examination in the article. Supply an online link to the location of the video.

Copyright law does not apply to *Fishery Bulletin,* which falls within the public domain. However, if an author reproduces any part of an article from *Fishery Bulletin*, reference to source is considered correct form (e.g., Source: Fish. Bull. 97:105).

Failure to follow these guidelines and failure to correspond with editors in a timely manner will delay publication of a manuscript.

Submission of manuscript

Submit manuscript online at the ScholarOne website. Commerce Department authors should submit papers under a completed NOAA Form 25-700. For further details on electronic submission, please contact the Associate Editor, Kathryn Dennis, at

kathryn.dennis@noaa.gov

When requested, the text and tables should be submitted in Word format. Figures should be sent as separate PDF or EPS files. Send a copy of figures in the original software if conversion to any of these formats yields a degraded version of the figure.

Questions? If you have questions regarding these guidelines, please contact the Managing Editor, Sharyn Matriotti, at

sharyn.matriotti@noaa.gov

Questions regarding manuscripts under review should be addressed to Kathryn Dennis, Associate Editor.

Fishery Bulletin

Subscription form

Superintendent of Documents **Publications** Order Form

*5178

☐ YES, please send me the following publications:

____ Subscriptions to *Fishery Bulletin*
for $32.00 per year ($44.80 foreign)

The total cost of my order is $ _____ . Prices include regular domestic postage and handling and are subject to change.

_____
(Company or Personal Name) (Please type or print)

_____
(Additional address/attention line)

_____
(Street address)

_____
(City, State, ZIP Code)

_____
(Daytime phone including area code)

_____
(Purchase Order No.)

Charge your order. IT'S EASY!

VISA

MasterCard

Please Choose Method of Payment:

☐ Check payable to the Superintendent of Documents
☐ GPO Deposit Account ☐☐☐☐☐☐☐–☐
☐ VISA or MasterCard Account
☐☐☐☐☐☐☐☐☐☐☐☐☐☐☐☐
☐☐☐☐ (Credit card expiration date)

To fax your orders (202) 512-2104

_____
(Authorizing Signature)

Mail to: Superintendent of Documents
P.O. Box 979050, St. Louis, Missouri 63197
Tel. no. (U.S. callers): 866-512-1800
Tel. no. (International callers): 1-202-512-1800

Thank you for your order!

Also available online at
http://bookstore.gpo.gov/actions/GetPublication.do?stocknumber=703-023-00000-2
email: ContactCenter@gpo.gov